Norwegian University of Life Sciences
Department of Plant Sciences

Philosophiae Doctor (PhD)
Thesis 2019:100

Sensitivity of plants exposed to gamma radiation. A physiological and molecular study

Følsomhet hos planter eksponert for gammastråling. En fysiologisk og molekylær studie

Dajana Blagojevic

Sensitivity of plants exposed to gamma radiation.

A physiological and molecular study.

Følsomhet hos planter eksponert for gammastråling.

En fysiologisk og molekylær studie.

Philosophiae Doctor (PhD) Thesis

Dajana Blagojevic

Department of Plant Sciences

Norwegian University of Life Sciences

Ås 2019

Thesis number 2019:100
ISSN 1894-6402
ISBN 978-82-575-1664-2

Table of contents

Abstract

Sessile organisms such as plants need to cope with a range of changing environmental conditions and stressors, including ionizing radiation like gamma, beta or alpha radiation and non-ionizing radiation (UV-A and UV-B radiation, visible light, infrared radiation). In the environment, gamma-, beta- or alpha emitting radionuclides originate from natural radioactive sources (NORM) such as uranium or thorium containing bedrocks, sediments and soils as well as anthropogenic sources due to releases from the nuclear weapons and fuel cycles. Ionizing radiation can trigger different physical, chemical and biochemical responses in an organism and potentially result in effects such as oxidative stress, DNA damage, reproduction failure and even transgenerational effects.

The present PhD study aimed to investigate radiosensitivity in different plant species; the ecologically important coniferous woody species Norway spruce (*Picea abies*) and Scots pine (*Pinus sylvestris*) as well as the herbaceous model plant *Arabidopsis thaliana*, by investigating different molecular, physiological and morphological parameters. To do so, a set of studies have been performed, including a comparative study involving all three species and more detailed studies of the conifers. In these, interactive effects of UV-B and gamma radiation were investigated and early molecular events in response to gamma radiation were assessed using an RNA sequencing approach.

Previous studies, among other observations after the Chernobyl nuclear power accident, have shown that Scots pine and Norway spruce are among the most radiosensitive plant species and that *Arabidopsis thaliana* is less sensitive. However, information about radiosensitivity from systematic comparisons under standardized conditions is very limited. Aiming at investigating growth, cellular and DNA parameters in response to gamma radiation and post-irradiation, all three species were exposed simultaneously to dose rates of 1-540 mGy h^{-1} from a ^{60}Co gamma source for144 h, as well as a prolonged 360 h exposure for *A. thaliana*. The experiments were done under controlled environmental conditions. The results showed induction of adverse effects in the conifers manifested as reduced plant lengths with increasing gamma dose rate ≥40 mGy h^{-1}. During the post- irradiation period, decrease in formation and elongation of needles and roots as well as visible damage and mortality were observed in plants exposed to ≥40 mGy h^{-1}, and these effects were accompanied by increasingly disorganized apical meristems with increasing dose rate.

Although *A. thaliana* exhibited delayed development of lateral roots after 144 h and 360 h gamma exposure, no visible or histological damage or mortality were observed at any of the dose rates. Post-irradiation, the development of flower buds and inflorescence stems were slightly delayed at ≥400 mGy h^{-1}.

In all three species the COMET assay results showed persistent DNA damage following exposure to ≥1-10 mGy h^{-1}, indicating induction of genomic instability. Whether there was significant increase in DNA damage at 1 or 10 mGy h^{-1} varied between experiments and measurement time points (at the end of the irradiation or during the post-irradiation period). Persistent DNA damage (genomic instability) in all three species, but strong growth-inhibition, visible and histological damage as well as mortality in the conifer species only, may indicate that the conifers are more sensitive to gamma radiation-induced DNA damage than *A. thaliana.* Although significant effects were induced by gamma radiation on gene expression in selected gene orthologs related to cell-cycle-control, DNA repair, antioxidants and general defence in the different species (qPCR analyses), there were no obvious findings that could help to explain the differences in sensitivity observed between the conifers and *A. thaliana*.

Ambient UV-B levels have been suggested to prime protective responses towards various stressors in plants. In this work it was tested whether UV-B exposure could prime acclimatisation mechanisms contributing to tolerance to low-moderate gamma radiation levels in Scots pine seedlings, and concurrently whether simultaneous UV-B and gamma exposure may have a cumulative negative effect on seedlings. Therefore, Scots pine seedlings were exposed to simultaneous UV-B (0.35 W m^{-2}) and gamma radiation (10.2-125 mGy h^{-1}) for 6 days with and without UV-B pre-exposure (0.35 W m^{-2} or 0.52 W m^{-2}) for 4 days. The results showed increased formation of reactive oxygen species and reduced shoot length at ≥42.9 mGy h^{-1}, and reduced root length at 125 mGy h^{-1}, regardless of UV-B presence, and no additional effect on growth in response to UV-B. In all experiments, a gamma dose-rate dependent increase in DNA damage was observed at ≥10.8 mGy h^{-1}, generally with additional UV-B-induced damage although there was no effect of UV-B on growth. Forty-four days post-irradiation, the seedlings exhibited gamma-induced growth inhibition and gamma- and UV-B-induced DNA damage even at 20.7 mGy h^{-1}, but this was not visible after 8 months and the growth was then normalised.

Furthermore, by employing RNA sequencing, the goal was also to assess the early molecular mechanisms and to establish a dose response connection to adverse phenotypic effects in response to gamma radiation in radiosensitive conifers using *P. abies* (exposed for 48 h) as a model plant. Gene ontology enrichment and KEGG pathway analyses as well as manual inspection of differentially expressed genes (DEGs) (gamma radiation of 1, 10, 40 and 100 mGy h^{-1} versus unexposed control; about 5300 DEGs in total) revealed that in spite of increased DNA damage at lower dose rates, only 40 mGy h^{-1} and in particular 100 mGy h^{-1} resulted in comprehensively altered gene expression with overall up-regulation of genes related to energy-metabolism, protein degradation, DNA repair and specific antioxidants and down-regulation of genes associated with biosynthesis/signalling/transport of growth-promoting hormones, cell division control, lipid biosynthesis and photosynthesis.

In conclusion, this PhD work has provided systematic, comparative data about the effects of gamma radiation on a range of endpoints across various levels of organisation (organismal, cell, and DNA) in the radiosensitive conifers Norway spruce and Scots pine, which generally showed similar responses, as well as the less sensitive *A. thaliana*. Detailed transcriptomic data for Norway spruce revealed that massive gene expression changes occurred at 40 and 100 mGy h^{-1} dose rates that resulted in substantial DNA damage and growth inhibition but not at lower dose rates. Furthermore, the work revealed no evidence of a protective or cumulative negative effect of UV-B on growth inhibition induced by gamma radiation in Scots pine.

Sammendrag

Ikke-mobile organismer som planter må håndtere en rekke endrede miljøforhold og stressorer, inkludert elektromagnetiske strålingstyper som ioniserende stråling (gamma-, alfa-, betastråling) og ikke-ioniserende stråling (UV-A og UV-B-stråling, synlig lys og infrarød stråling). I naturen kommer ioniserende stråling fra kosmisk stråling, radionuklider som uran og thorium i berggrunnen, sedimenter og jord og utslipp fra menneskeskapte kilder som kjernefysiske våpen og kjernekraftverk. Slik stråling kan utløse forskjellige fysiske, kjemiske og biokjemiske responser i en organisme og gi opphav til effekter som oksidativt stress, DNA-skade, reproduksjonssvikt og til og med transgenerasjonelle effekter.

Dette doktorgradsarbeidet tok sikte på å undersøke radiosensitivitet i forskjellige plantearter; de økologisk viktige bartreartene gran (*Picea abies*) og furu (*Pinus sylvestris*) og den urteaktige modellplanten vårskrinneblom (*Arabidopsis thaliana*). For å forstå forskjell i radiosensitivitet ble ulike molekylære, fysiologiske og morfologiske parametere sammenlignet for alle de tre artene. I tillegg ble mer detaljerte studier av bartrærne gjort. I disse studiene ble interaktive effekter av UV-B og gammastråling undersøkt og tidlige molekylære endringer i respons på gammastråling ble undersøkt ved hjelp av RNA-sekvensering.

Tidligere studier, blant annet observasjoner etter Tsjernobyl-atomkraftulykken, har vist at furu og gran er blant de mest radiofølsomme planteartene og at vårskrinneblom er mindre følsom. Kunnskap om radiosensitivitet fra systematisk sammenligning under standardiserte forhold er imidlertid begrenset. For å undersøke effekter på vekst-, celle- og DNA-parametere under og etter gammabestråling ble alle tre arter utsatt for gammadoserate fra 1-540 mGy t^{-1} fra en ^{60}Co-gammakilde i 144 timer, samt en forlenget 360 timers eksponering for vårskrinneblom. Forsøkene ble utført under kontrollerte miljøforhold. Resultatene viste negative effekter i bartrær umiddelbart etter bestråling med redusert plantelengde med økende gamma doserate fra ≥40 mGy h^{-1}. I perioden etter bestrålingen ble det observert redusert dannelse og strekningsvekst av nåler og røtter, samt synlig skade og dødelighet i planter utsatt for ≥40 mGy h^{-1}. Dette var forbundet med stadig mer uorganiserte apikale meristemer med økende doserate. Selv om *A. thaliana* viste forsinket utvikling av laterale røtter etter 144 timer og 360 timer med gammaeksponering, medførte det ingen synlig eller histologisk skade eller dødelighet. I perioden etter

gammabestrålingen ble det imidlertid observert noe forsinket dannelse av blomsterknopper og blomsterstandutvikling ved ≥ 400 mGy h^{-1}.

I alle tre arter viste COMET-analyse-resultatene vedvarende DNA-skade etter eksponering for gammadoserater ≥1-10 mGy h^{-1}. Dette indikerer at gammastrålingen resulterte i genomisk ustabilitet. Om det var signifikant økning i DNA-skade ved 1 eller 10 mGy h^{-1}, varierte mellom eksperimenter og måletidspunkter (rett etter bestrålingen eller i perioden etter avsluttet bestråling). Vedvarende DNA-skade (genomisk ustabilitet) i alle tre arter, men sterk veksthemming, synlig og histologisk skade og dødelighet bare i bartreartene, kan tyde på at disse er mer sensitive overfor gammastrålingsindusert DNA-skade enn vårskrinneblom. Selv om det ble observert signifikante effekter av gammabestrålingen på uttrykket av utvalgte ortologer av gener relatert til cellesyklus-kontroll, DNA-reparasjon, antioksidanter og generelt forsvar (qPCR-analyse) i de ulike artene, var det ingen konsistente forskjeller som kunne bidra til å forklare ulik gammasensitivitet i bartrær og vårskrinneblom.

Det har vært foreslått at normale UV-B-nivåer i miljøet kan sette i gang planteresponser som kan beskytte mot forskjellige typer stress. I dette arbeidet ble det testet om UV-B-eksponering kan føre til akklimatiseringsmekanismer som bidrar til toleranse for lave gammastrålingsnivåer i frøplanter av furu. Samtidig ble det testet om kombinert UV-B- og gamma eksponering kan ha en kumulativ negativ effekt på slike frøplanter. Furufrøplanter ble derfor utsatt for både UV-B (0.35 W m^{-2}) og gammastråling (10.2-125 mGy h^{-1}) i 6 dager med og uten pre-eksponering for UV-B (0.35 W m^{-2}) i 4 dager. Resultatene viste økt dannelse av reaktive oksygenradikaler og redusert skuddlengde ved ≥42.9 mGy h^{-1} og redusert rotlengde ved 125 mGy h^{-1}, uavhengig av UV-B-tilstedeværelse og UV-B ga ingen tilleggseffekt på strekningsveksten. I alle eksperimenter ble det observert en gammadoserate-avhengig økning i DNA-skade ved doserater ≥10.8 mGy h^{-1}, generelt med ytterligere UV-B-indusert skade. Gamma-indusert vekstinhibering og gamma- og UV-B-indusert DNA-skade var fortsatt synlig 44 dager etter bestråling, selv ved 20.7 mGy h^{-1}, men 8 måneder senere ble DNA skaden ikke lenger observert og veksten var da normalisert.

For å oppnå økt kunnskap om de tidlige molekylære mekanismene og etablere en dose-respons-sammenheng med negative fenotypiske effekter i respons på gammastråling i radiosensitive bartrær ble RNA sekvensering gjort ved bruk av gran som modellplante. Gen-ontologi- og KEGG-analyser samt manuell inspeksjon av differensielt uttrykte gener (DEGs) (gamma doseratene 1, 10,

40 and 100 mGy h^{-1} versus ikke-eksponert kontroll; ca 5300 DEGs totalt) viste at tross økt DNA-skade ved lavere doserater, resulterte bare 40 mGy h^{-1} og spesielt 100 mGy h^{-1} i omfattende endringer i genekspresjon med hovedsakelig oppregulering av gener relatert til energimetabolisme, proteindegradering, DNA-reparasjon og spesifikke antioksidanter og nedregulering av gener assosiert med biosyntese/signalering/transport av vekstfremmende plantehormoner, celledelingskontroll, lipidbiosyntese og fotosyntese.

Dette PhD-arbeidet har bidratt med systematiske, komparative data for effekt av gammastråling på en rekke endepunkter på organisme-, celle- og DNA-nivå i de radiosensitive bartreartene gran og furu som generelt viste lignende responser, samt den mindre sensitive, vårskrinneblom. Detaljerte transkriptomdata for gran viste at massive endringer i genekspresjon i slike bartrær skjedde ved doserater som resulterte i betydelig DNA-skade og veksthemming, men ikke ved lavere doserater. Arbeidet tydet ikke på at UV-B kan beskytte mot gamma-indusert veksthemming i furu og viste heller ingen kumulativ negativ effekt av UV-B i denne sammenheng.

Acknowledgments

The PhD project was financed by the Norwegian University of Life Science (NMBU) and the Research Council of Norway through its Centre of excellence funding scheme (Grant 223268/F50) to Centre of Environmental Radioactivity (CERAD).

I would like to specially thank my main supervisor Professor Jorunn E. Olsen for her guidance, encouragement, patience and support throughout the study. I am very grateful for all the knowledge you taught me, both concerning writing and experiments. Also, many thanks to my co-supervisors Dr. YeonKyeong Lee, Associate professor Ole Christian Lind and Dr. Dag Anders Brede for all our discussions, knowledge and feedbacks concerning writing articles. Thanks are also due to all the other co-authors of the different papers for providing their knowledge and essential input and feedback. I am also grateful to Professor Brit Salbu who provided the opportunity to participate in CERAD and has provided valuable input to the work in this PhD thesis.

I would like to thank Tone Melby for helping me at the Plant Cell Laboratory, as well as Linda Ripel. Also, many thanks to Silje, Marit, Ida and Gry for helping with taking care of hundreds of plants.

I would especially like to thank all my friends and colleagues at NMBU for support, help and advices.

A final thanks goes to my parents Milena and Branislav, and to my brother Milan for all their encouragement.

List of papers

Paper I

Comparative sensitivity to gamma radiation at the organismal, cell and DNA level in young plants of Norway spruce, Scots pine and *Arabidopsis thaliana*.

Dajana Blagojevic, YeonKyeong Lee, Dag A. Brede, Ole Christian Lind, Igor Yakovlev, Knut Asbjørn Solhaug, Carl Gunnar Fossdal, Brit Salbu, Jorunn E. Olsen

Paper II

No evidence of a protective or cumulative negative effect of UV-B on growth inhibition induced by gamma radiation in Scots pine (*Pinus sylvestris*) seedlings.

Dajana Blagojevic, YeonKyeong Lee, Li Xie, Dag A Brede, Line Nybakken, Ole Christian Lind, Knut Erik Tollefsen, Brit Salbu, Knut Asbjørn Solhaug, Jorunn E. Olsen

Paper III

Transcriptomic responses associated with gamma radiation damage in seedlings of the radiosensitive conifer species Norway spruce.

Dajana Blagojevic, Payel Bhattacharjee, YeonKyeong Lee, Lars Grønvold, Gareth Benjamin Gillard, Torgeir Rhoden Hvidsten, Simen Rød Sandve, Brit Salbu, Dag Anders Brede, Jorunn Elisabeth Olsen

Abbreviations

BER-base excision repair

MMR-mismatch repair

NER-nucleotide excision repair

HR-homologous recombination

NHEJ-non-homologous end joining

IR-ionizing radiation

dsDNA-double strand DNA

ssDNA-single strand DNA

GO-gene ontology

KEGG- Kyoto encyclopedia of genes and genomes

SOD-superoxide dismutase

POD-peroxidase

CAT-catalase

SPX- syringaldazine peroxidase

GPX-glutathione peroxidase

ROS-reactive oxygen species

CPDs-cyclobutane pyrimidine dimers

JA-jasmonic acid

ET- ethylene

ABA- abscisic acid

AUX-auxin

BR-brassinosteroid

GA-gibberellin

SA-salicylic acid

CK-cytokinins

1. Introduction

1.1 Background of this study

Plants are constantly exposed to different environmental conditions and stressors including ionizing radiation such as gamma, beta and alpha radiation and non-ionizing radiation such as ultraviolet (UV) radiation (UV-A and UV-B), visible light and infra-red radiation. In the environment, ionizing radiation arises from natural sources including radionuclides in bedrock, sediments and soils and cosmic radiation as well as anthropogenic sources such as nuclear weapon tests, nuclear power plants, nuclear testing, and radionuclides used for medical diagnostics and therapeutic procedures (UNSCEAR 2010; UNSCEAR 2017). Such radiation can trigger different physical, biochemical and molecular responses in an organism and give rise to somatic effects (cell damage or cell death) and genetic transgenerational effects (effects in subsequent generations) (Choppin et al. 2013).

Among different ionising radiation types, effects of external gamma radiation have been most studied in living organisms (Van Hoeck et al. 2015), and results from long-term studies showed that low levels of ionizing radiation can have adverse effects and induce mutations in plants (Real et al. 2005). So far it has been suggested that woody conifer plants (Gymnosperms) are among the most radiosensitive plant species, and that pine trees showed the highest radiosensitivity after the Chernobyl and Fukushima nuclear power plant accidents in 1986 and 2011 (Yoschenko et al. 2018). Although there have been major field and laboratory studies on impact of ionizing radiation on plants, the understanding of biological processes and oxidative stress responses across various levels of organisation (molecular, cell and organism level) in plants caused by low to moderate levels of gamma radiation is still limited. Particularly, there is limited information from comparative experiments under standardised exposure conditions.

Furthermore, although high levels of UV-B radiation may be detrimental to plants, there is evidence that ambient UV-B levels rather has an important role in adaptation to stress by inducing protective mechanisms and modulating growth and development (Dotto & Casati 2017; Jansen et al. 1998; Jansen & Bornman 2012; Jansen 2017; Robson et al. 2015b; Rozema et al. 1997). Despite that moderate UV-B levels have been suggested to prime protection mechanisms contributing to tolerance towards different stressors (Jansen 2017 and references therein), there has been no data available on whether such UV-B levels can prime protection against low to moderate gamma levels

or whether UV-B can contribute to extra stress when plants receive UV-B and gamma radiation simultaneously.

1.2 Ionizing radiation

Ionizing radiation includes alpha (He-cores), beta (electron/positron), and gamma radiation (electromagnetic radiation, Fig 1). Upon interaction with matter, molecules are exited or ionized, forming free radicals. Recombination of free radicals would produce reactive oxidative species (ROS). In living organisms, splitting of water molecules and the production of for instance H_2O_2 internally in cells could bring about damages to the cell structure as well as damages to biomolecules such as DNA. The activity of a radioactive source is measured in becquerel (Bq), which denotes the number of disintegrations per unit of time (UNSCEAR 2010). The energy (dose) absorbed by a living organism is given by the unit of gray (Gy) where (1 Gy = 1 J kg^{-1}). Sievert (Si) is a risk unit which takes into account the stochastic effects and the risk of developing negative health effects such as cancer in humans. Thus, this unit is not used for organism such as plants. Largely based on health consequences, low gamma doses and dose rates are currently defined as ≤100 mGy and ≤6 mGy h^{-1}, respectively (Averbeck et al. 2018; UNSCEAR 2017). The global mean natural background dose rate has been estimated to be 2.5 mGy $year^{-1}$, corresponding to about 0.29 µGy h^{-1} (Caplin & Willey 2018). Examples of areas with naturally elevated ionizing radiation are Ihla Grande in Brazil, Ramsar in Iran and the Fen field in Norway, with reported dose rates of 14-15 µGy h^{-1}, 4,4 µGy h^{-1} and 8 µGy h^{-1} (Caplin & Willey 2018; Freitas & Alencar 2004; Mrdakovic Popic et al. 2012).

1.3 Non-ionizing radiation

Non-ionizing radiation has sufficient energy for excitation but not for ionization of molecules or atoms. The non-ionizing spectrum includes UV radiation, visible light, infrared radiation, microwaves, and radio waves (Figure 1). Non-ionizing radiation originates from both natural sources such as sunlight or lightning discharges, and man-made sources seen in wireless communications, industrial, scientific and medical applications.

There are three types of non-ionizing UV radiation in the solar spectrum, classified by their wavelengths: UV-A (315-400 nm), UV-B (290-315 nm) and UV-C (100-280 nm) (Gill et al. 2015; Jansen 2017). Due to its short wavelengths, UV-C is the most damaging type of UV radiation, though it is entirely absorbed by the ozone layer and therefore does not reach the Earth's surface. In comparison to UV-C, UV-B radiation comprises longer wavelengths that can reach the Earth's surface and is therefore the most high-energy type of UV radiation of significance to organisms on the Earth's surface. Although UV-B radiation makes up less than 1% of the total solar energy, it is a highly active component of the solar radiation and can potentially cause plant genome damage by inducing oxidative damage (pyrimidine dimers most common) and crosslinks (both DNA protein and DNA-DNA), at least under high UV-B levels or high UV-B : PAR ratios or in plants with weak UV-B protection mechanisms (Ganguly & Duker 1991; Gill et al. 2015; Rastogi et al. 2010). UV-B are influenced by several abiotic factors, such as the thickness of the ozone layer, geographical area, season, altitude, latitude, cloud cover, and time of the day (Jansen 2017).

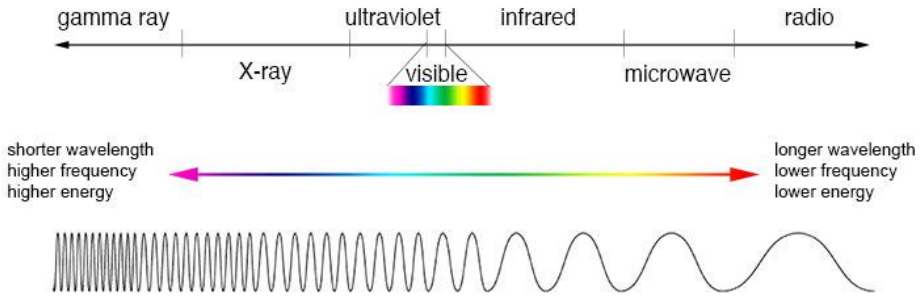

Figure 1. The electromagnetic spectrum showing relative frequency, wavelength and energy (NASA 2019).

1.4 Effects of gamma radiation on plant growth and development

Well known examples of nuclear power plant accidents are the Chernobyl accident in 1986 and the Fukushima accident in 2011. In both accidents, most of the radioactivity released was composed of volatile radionuclides (noble gases, I^{131}, Cs^{137} etc.). However, the amount of refractory elements (including actinides) emitted in the course of the Chernobyl accident was

approximately four orders of magnitude higher than during the Fukushima accident (Steinhauser et al. 2014).

Several field studies, including in Chernobyl and Fukushima, have indicated that particularly conifer species are vulnerable to gamma radiation (Arkhipov et al. 1995; Watanabe et al. 2015; Woodwell 1962; Woodwell & Rebuck 1967; Yoschenko et al. 2018). In the initial period after the Chernobyl accident death of sprouts, dying needles, necrosis of growth points, reduced reproductive capacity, chromosomal aberrations and mutations in enzyme loci were observed in Scots pine (*Pinus sylvestris*) trees, and the area of dead pine trees is known as the red forest (Kozubov & Taskaev 2002; Kozubov & Taskaev 2007; Steinhauser et al. 2014; Zelena et al. 2005). Studies of Norway spruce (*Picea abie*s) also showed changes in a wide range of characters, such as morphological abnormalities (Kozubov & Taskaev 1994; Sorochinsky & Zelena 2003), and similar changes have been reported in other plant species in the Chernobyl zone (Fesenko et al. 2005; Geras'kin et al. 2003; Geras'kin et al. 2008; Geras'kin & Volkova 2014; Kalchenko et al. 1993; Shevchenko et al. 1996; Shevchenko & Grinikh 1995). Abnormalities were shown to be present also in pine seeds collected near the Chernobyl accident site compared to seeds from control sites (Kal'chenko & Fedotov 2001). More recent studies have shown that increased mutations in chronically irradiated pines were significantly associated with the levels of radiation exposure (Geras'kin & Volkova 2014; Geras'kin et al. 2011; Makarenko et al. 2016). Such observations provide evidence for long-term effects of ionizing radiation.

A previous study testing effects of different gamma dose rates (81-2336 µGy h^{-1} for 24-54 days) on *A. thaliana* induced negative growth effect but no obvious effect on oxidative stress pathways (Vandenhove et al. 2010). However, increased photosystem II (PSII) efficiency (at gamma doses of 3.9 and 6.7 Gy) and maximum electron transport rate (ETRmax; at gamma doses of 3.9, 6.7 and 14.8 Gy) were observed in leaves of this species (Vanhoudt et al. 2014). Difference in gene expression has also been observed in *A. thaliana* exposed to acute gamma irradiation (external ^{60}Co exposure; 90 000 mGy h^{-1} for 40 sec; total dose 1 Gy) and chronic gamma irradiation (internal ^{137}CsCl (about 24% of the total radiation) and external ^{60}Co (about 76%) exposure; 2 mGy h^{-1} for 21 days; total dose 0.93 Gy) (Kovalchuk et al. 2007).

Gamma rays cause dose-dependent changes in growth and development in plants by inducing production of harmful free radicals in cells, leading to damage to nucleic acids, proteins, and membrane-lipids (Kovacs & Keresztes 2002).

1.5 Characteristics and biology of conifer species and Arabidopsis thaliana

Conifers are the most widely distributed group of gymnosperms, with 600 to 630 species in 69 genera, which cover an estimated 39% of the world's forests (Armenise et al. 2012; De La Torre et al. 2014; Wang & Ran 2014). Conifer species are characterized by a long juvenile period, high heterozygosity, long life span, are wind pollinated and dominate the temperate zone forests in the northern hemisphere (De La Torre et al. 2014; Mackay et al. 2012). The Norway spruce genome was recently sequenced and was estimated to have a genome size of 19.6 Gbp (Nystedt et al. 2013). However, due to the large genome size, the knowledge about the number of genes and full-length sequences are still incomplete (De La Torre et al. 2014; Nystedt et al. 2013). Among pine species, the loblolly pine (*Pinus taeda*) 20.1 Gbp genome was the first to be sequenced (Neale et al. 2014; Zimin et al. 2014) whereas the genome sequence of Scots pine (possibly about 23 Mbp) remains to be published. Both these conifers have 24 chromosomes (2n) (NCBI 2019). Compared to Norway spruce, Scots pine can grow in drier areas, has deeper roots and as mentioned above, conifers are considered highly radiosensitive species (Caplin & Willey 2018; Watanabe et al. 2015; Woodwell & Rebuck 1967; Yoschenko et al. 2018). *A. thaliana*, on the other hand, is a small annual or winter annual (biannual) flowering plant, which belongs to the mustard family and is distributed worldwide (TAIR 2019). The genome size is approximately 135 Mbp with 25 498 genes (2n = 10 chromosomes) (The Arabidopsis Genome 2000). Although not systematically compared under standardized conditions, compared to the conifer species, *A. thaliana* is considered a radio-resistant plant species (Caplin & Willey 2018).

1.6 DNA damage

DNA of living organisms normally suffers damage which may arise endogenously or can be induced by a variety of external genotoxic agents including UV radiation, ionizing radiation, and chemical mutagens (Manova & Gruszka 2015). At shown in humans, nuclear DNA is less sensitive to oxidative stress than mitochondrial DNA because of the absence of chromatin organization in mitochondria and lower mitochondrial DNA repair activities (Yakes & Van Houten 1997).

Overproduction of reactive oxygen species (ROS), as by-products of the metabolism or as a result of abiotic stress may lead to DNA damage. This includes single strand DNA (ssDNA) or double strand DNA (dsDNA) breaks, loss of a base to form an abasic site, chemical modification of a base to form a miscoding or noncoding lesion, and sugar-phosphate backbone breakage (Figure 2) (Manova & Gruszka 2015; Singh et al. 2010; Vonarx et al. 1998). The accumulation of mutations caused by such damages (unrecognized and unrepaired DNA damage) may result in plant genome instability, reduced growth, and productivity and also threaten the organism's immediate survival (Biedermann et al. 2011; Gill & Tuteja 2010; Singh et al. 2010; Tuteja et al. 2001; Waterworth et al. 2011). Therefore, effective detection of DNA damage, removal of damaged nucleotides, replacement with undamaged nucleotides via DNA synthesis, and repair of DNA damage are essential to eliminate the chance of permanent genetic alterations and hence to ensure the stability of the plant genome (Gill & Tuteja 2010; Roy et al. 2009; Waterworth et al. 2011). The most common DNA photoproducts induced by exposure to UV radiation are cyclobutane-type pyrimidine dimers and the pyrimidine (6,4) pyrimidone dimers (Hutchinson et al. 1988), while 8-oxoguanine (8-Oxo-G), 6-O-methylquanine (O^6meG) and N3-methyladenine (N^3MeA) get induced by gamma radiation. Besides, DNA protein cross-links, DNA strand breaks and deletion or insertion of base pairs can be induced both by UV exposure and gamma radiation (Esnault et al. 2010; Kim et al. 2004; Kovacs & Keresztes 2002; Kovalchuk et al. 2007; Manova & Gruszka 2015; Vandenhove et al. 2010; Wi et al. 2005).

1.7 DNA repair

The choice and action of a repair system depends mainly on the type of the cell, its proliferation status, the phase of the cell cycle, the type of lesion and its genomic context (Britt 1999; Manova & Gruszka 2015). Repair mechanisms involved in dsDNA breaks are non-homologous end joining (NHEJ) and homologous repair (HR), while different deletions and insertions of base pairs are regulated by mismatch repair (MMR), base excision repair (BER) and nucleotide excision repair (NER) (Figure 2). An overview of the genes involved in different DNA repair pathways is represented in figure 3. Furthermore, *Arabidopsis thaliana* ataxia telangiectasia (*atm*) mutants are sensitive to double strand break-inducing factors, whereas ataxia telangiectasia Rad3-related (*atr*) mutant plants are sensitive to replication stress, that may result in a stalled replication fork (Culligan et al. 2004; Culligan et al. 2006; Garcia et al. 2003). A role of the ATR and ATM proteins in DNA damage repair signalling in plants was validated by the fact that histone 2AX (H2AX) phosphorylation in response to irradiation-induced double strand breaks is dependent on ATM (Friesner et al. 2005). The *KU70* and *KU80* genes as well as the *DNA LIGASE IV* (*LIGIV*), *BREAST CANCER 1* (*BRCA1*) and *HOMOLOG OF X-RAY REPAIR CROSS COMPLEMENTING* 4 (*XRCC4*) genes, which encode proteins required for the initiation and completion of NHEJ, all showed upregulation in *A. thaliana* after exposure to gamma radiation (Bleuyard et al. 2005; Doutriaux et al. 1998; Lafarge & Montané 2003; Tamura et al. 2002; West et al. 2000). Transcripts of genes encoding proteins involved in HR, such as *BRCA1*, *BRCA2*, *RAD51*-like, *RAD51B*, *RAD5C*, *XRCC2*, *XRCC3*, *MEIOTIC RECOMBINATION 11*(*MRE11*) and the regulatory proteins *BRCA1* and *BRCA2* were also shown to be induced in specific species after exposure to gamma rays (Bleuyard et al. 2005; McIlwraith et al. 2000). Similar gamma-induction of DNA repair has also been described in the woody angiosperm species *Populus nigra* where expression of *RAD51*, *LIG4*, *KU70*, *XRCC4* and *PROLIFERATING CELLULAR NUCLEAR ANTIGEN* (*PCNA*) were increased by gamma rays.

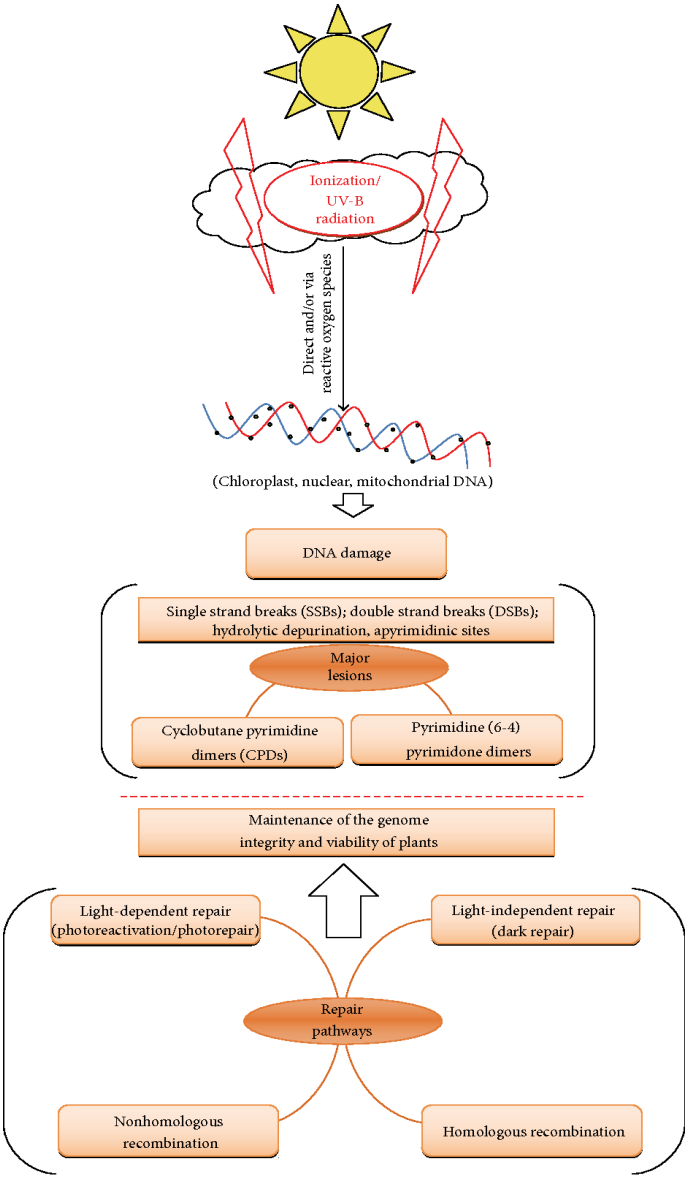

Figure 2. Major DNA lesions induced by ionizing radiation and UV-B, and the different types of DNA repair mechanisms after (Gill et al. 2015) .

1.8 Cell cycle control related to DNA damage repair

DNA damage also causes biochemical signals to activate checkpoints that are accountable for a delay in the progress of the cell cycle. The checkpoints in the G1/S and S stages stop replication of damaged DNA and the checkpoint in the G2/M stage stop chromosome segregation (Belli et al. 2002). The Ataxia telangiectasia Rad3-related (ATR) protein plays a central role in the cell's response to DNA damage by activating cell-cycle checkpoints, induce cell cycle arrest to allow time for proper DNA repair and as such is required for the G2-phase checkpoint (Culligan et al. 2004). Another protein, SUPPRESSOR OF GAMMA RADIATION 1 (SOG1), suggested to be a central transcription factor in genomic stress and to be comparable to the animal p53 protein (even though the protein`s amino acid sequence is unrelated), plays a major role in inducing cell cycle check point genes (Yoshiyama et al. 2009; Yoshiyama et al. 2013). Plant-specific B1-type CDKs (CDKB1s) and the class of B1-type cyclins (CYCB1s) are suggested to be major regulators of HR in plants and the genes encoding them are directly regulated by SOG1 (Weimer et al. 2016). For example, *CYCB1;1* showed upregulation during treatments with DNA damage-inducing agents (Adachi et al. 2011; Chen et al. 2003; Culligan et al. 2004; Culligan et al. 2006; Ricaud et al. 2007). Additionally, the *WEE1 KINASE HOMOLOG* (*WEE1*) gene, encoding a protein involved together with SOG1 in cell cycle arrest, was shown to be upregulated in *A. thaliana* after exposure to gamma radiation (De Schutter et al. 2007).

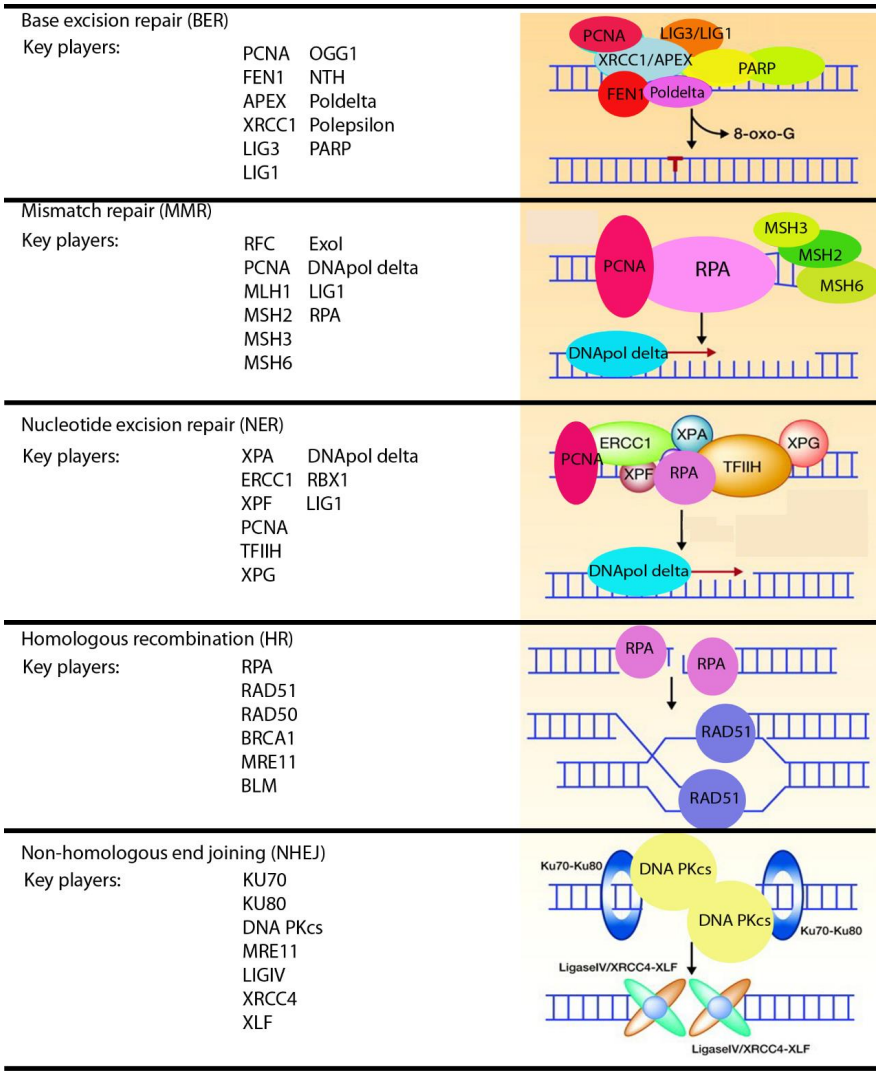

Figure 3. Key proteins involved in different DNA repair pathways, modified after (Jalal et al. 2011). The listed genes refer to *A. thaliana* genes exported from KEGG pathways (https://www.genome.jp/kegg/ 2019).

1.9 Endoreduplication

Although the genome is replicated during the synthesis (S) stage and is subsequently halved during the final step of the mitosis (M) stage, the cell cycle may continue without chromosome separation and cytokinesis (cell division) after DNA replication, leading to polyploid cells (De Schutter et al. 2007; De Veylder et al. 2011). This process, known as endoreduplication, is well known to occur in specific plant tissues and there is evidence that endoreduplication is a prominent reaction to stressful circumstances, such as pathogen attack and DNA damage (Adachi et al. 2011; De Veylder et al. 2011; Lee et al. 2009). Increased ploidy level was observed at a dose rate of 1500 mGy h^{-1} in *Lemna minor* (Van Hoeck et al. 2017). Endoreduplication in *A. thaliana* was shown to be induced by dsDNA breaks after gamma radiation from a ^{137}Cs source at a dose rate 45 times greater, 1.1 Gy min^{-1} (66 000 mGy h^{-1}) (Adachi et al. 2011). Although endoreduplication is much more prevalent in angiosperms, the phenomenon has been described in meristematic cambium cells of gymnosperms such as *Pinu*s and *Ginko* (Lev-Yadun & Sederoff 2000; Scholes & Paige 2014).

1.10 ROS scavengers

Oxidative stress happens when a severe imbalance exists between ROS production and antioxidant defence (Ahmad et al. 2010). Radiation causes water radiolysis in the cell leading to the production of ROS such as hydrogen peroxide (H_2O_2), superoxide anion (O_2^-), hydroxyl radicals (OH•), and singlet oxygen ($^1O_2$) (Kovacs & Keresztes 2002; Luckey 2006; Miller & Miller 1987; Quintiliani 1986). Low concentrations of ROS are generated when crops are exposed to low levels of UV-B radiation, which can help activate UV-acclimation reactions. By comparison, disruptions of cellular metabolism can happen when plants are exposed to elevated doses of UV-B owing to the concomitant increase of ROS concentrations (Jansen 2017). Plants have evolved various approaches to reverse, excise or tolerate the existence of DNA damage products to protect themselves. Superoxide dismutase (SOD) performs a defensive function when a plant is subjected to gamma radiation by turning superoxide into hydrogen peroxide (H_2O_2) (Gill & Tuteja 2010). Catalase (CAT) and peroxidase (POD) also play major roles in cell detoxification of H_2O_2 and thus protect cellular components such as proteins and lipids from oxidation (Wi et al. 2007). Previous studies showed POD induction in gamma-exposed pumpkin cells, and *A. thaliana*

showed POD, ascorbate peroxidase (APX), CAT and SOD induction (Kim et al. 2011; Van Hoeck et al. 2015). Another study of *A. thaliana* showed increased capacities of SOD and APX in roots of gamma irradiated plants but decreased activities of CAT, syringaldazine peroxidase (SPX) and guaiacol peroxidase (GPX), while leaves showed only enhanced level of GPX (Vanhoudt et al. 2014).

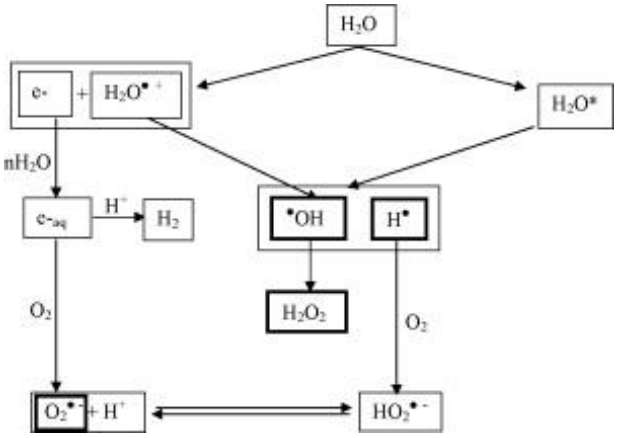

Figure 2. Primary and secondary reactive oxygen species produced by ionizing radiation after (Esnault et al. 2010).

1.11 Hormones in growth regulation and stress responses

Plant hormones (phytohormones) play a key role in controlling developmental processes and signalling plant response networks to a broad spectrum of biotic and abiotic stresses. The phytohormones salicylic acid (SA), jasmonic acid (JA), ethylene (ET) and abscisic acid (ABA) are known to play a significant role in regulating the response of plant defence to multiple pathogens and abiotic stresses such as wounding, drought, frost and ozone exposure (Verma et al. 2016). Other phytohormones such as auxin (AUX), gibberellins (GAs) and brassinosteroids (BR) are best known as growth regulators along longitudinal axes and influence the stature and organ size of plants. Cytokinins (CKs) mainly affect plant cell differentiation, leaf senescence and other important developmental processes, but it is also known that elevated cytokinin levels cause drought tolerance (Reguera et al. 2013; Sakakibara 2006).

2. Objectives of this study

The main objective of this study was to improve the understanding of how gamma radiation affects seedlings of different plant species a the organismal, cellular and molecular level.

The specific objectives and hypotheses were:

- To compare the sensitivity to gamma radiation on the organismal, cellular and molecular level in Norway spruce, Scots pine and *A. thaliana* under standardized exposure conditions (Paper I). In this respect the following hypothesis was tested: Differential radiosensitivity depends on difference in DNA repair capacity or differences in systems for DNA damage protection.

- To investigate whether effects of gamma irradiation may be modified by UV-B radiation in a radiosensitive conifer species, using Scots pine as a model system (Paper II). In this respect the following hypotheses were tested:
    - Pre-exposure to UV-B may prime defence mechanisms contributing to enhanced tolerance to gamma radiation.
    - Simultaneous UV-B and gamma exposure may have a cumulative negative effect.

- To investigate the molecular mechanisms behind the response to gamma radiation and to establish a dose response connection to adverse phenotypic effects in seedlings of a radiosensitive conifer species, using Norway spruce as a model species (Paper III). This work aimed at testing the hypothesis that the radiosensitivity is reflected in transcriptome changes in response to different gamma radiation levels in the sense that such a radiosensitive conifer species does not mobilize protective and repair systems very efficiently.

3. Materials and methods

Pre-growing conditions

Norway spruce, Scots pine and *A. thaliana* were sterilized and sown on ½ MS medium in Petri dishes. Thereafter, the seeds were germinated for 6 days at 20°C under a photon flux density of 30 μmol m^{-2} s^{-1} at 400-700 nm (TL-D 58W/840 lamps, Phillips, Eindhoven, The Netherlands) in a 16 h photoperiod (See paper I, II and III). The irradiance was measured at the top of the Petri dishes with a Li-Cor Quantum/Radiometer/Photometer (model LI-250, LI-COR, Lincoln, NE, USA).

Exposure of the seedlings to gamma radiation from a ^{60}Co source

Six days old seedlings of Norway spruce, Scots pine, and *A. thaliana* were exposed to gamma radiation with different gamma dose rates ranging from 1 to 540 mGy h^{-1}, using the FIGARO low dose gamma irradiation facility (^{60}Co; 1173.2 and 1332.5 keV γ-rays) at Norwegian University of Life Sciences (Lind et al. 2018). Scots pine and Norway spruce seedlings were exposed to gamma radiation for 144 h (Paper I and II), while *A. thaliana* seedlings got 144 h or 360 h of exposure (Paper I). In another study (Paper III) Norway spruce seedlings were exposed to gamma radiation for 48 h. The seedlings were grown in the Petri dishes during the entire gamma exposure period, and to reduce dose variability between irradiated samples, the Petri dishes were rotated 180° in the middle of each experiment. Petri dishes with unexposed control seedlings were placed outside the radiation sector behind gamma radiation-shielding lead walls. The room temperature was set at 20˚C±1°C with a 12 h photoperiod with a photon flux density of 55 μmol m^{-2} s^{-1} (400-700 nm, red:far (R:FR) ratio 3.5) provided by high pressure metal halide lamps (HPI-T Plus 250W lamps, Phillips) mounted above the Petri dishes (paper I and III). In the work in Paper II, Petri dishes with Scots pine seedlings were kept in growth chambers at 20˚C under a 12 h photoperiod with a photon flux density of 200 μmol m^{-2} s^{-1} and a R:FR ratio of 1.9 using white LED lights (PCB1E, Evolys, Oslo, Norway) and incandescent lamps (Osram, Munich, Germany). One growth chamber with Petri dishes was placed in front of the collimator with the ^{60}Co source and another growth chamber with Petri dishes was placed outside the radiation sector behind the lead shields. The growth chambers, which were manufactured by Norwegian University of Life Sciences (Ås, Norway), did not have metal in the front and side walls. In all experiments, the irradiance of the photosynthetic

active light was measured as described above and the R:FR ratio was measured using a 660/730 nm sensor (Sky Instruments, Powys, Wales, UK).

Experiments with UV-B and gamma exposure with or without UV-B pre-treatment

In Paper II, Scots pine seedlings were co-exposed to UV-B and gamma radiation in one experimental series, and in another series of experiments the seedlings were pre-treated with UV-B prior to the combined gamma and UV-B exposure. In the experiments without UV-B pre-treatment, 6 days old seedlings were exposed to gamma radiation for 6 days (144 h) with gamma dose rates of 20.7, 42.9 and 125 mGy h^{-1} with or without 10 h of daily UV-B exposure at an irradiance of 0.35 W m^{-2} in the middle of a 12 h photoperiod. The gamma radiation was provided using the FIGARO UV and low dose rate gamma irradiation facility (described above). The UV-B irradiation was obtained from UV-B fluorescent tubes (UVB-313, Q-Panel Co., Cleveland, OH, USA). To block UV-wavelengths shorter than 290 nm, cellulose diacetate foil (0.13 mm, Jürgen Rachow, Hamburg, Germany) was placed on top of half of the petri dishes in each growth chamber. UV-blocking polycarbonate filters were placed on top of the rest of the petri dishes to provide non-UV-B-exposed controls.

In the experiments including UV-B pre-treatment, the exposure conditions were the same as in the experiments with combined UV-B and gamma exposure without UV-B pre-treatments, except that the gamma dose rates were 10.8, 20.7 and 42.9 mGy h^{-1} and the 6 days old seedlings were pre-treated for 4 days with UV-B at an irradiance of 0.35 or 0.52 W m^{-2}. Both types of experiments were conducted in the growth chambers with the conditions described above.

Post-irradiation growing conditions

After the gamma exposure, seedlings were transferred to pots with fertilized peat (7.5 cm diameter and 7 cm height for *A. thaliana*; 5 cm diameter and 5 cm height for Norway spruce and Scots pine) and cultivated in growth chambers (manufactured by Norwegian University of Life Sciences). In paper I experiments, four plants of *A. thaliana* and two plants of Norway spruce and Scots pine were cultivated per pot, whereas in the experiments with Scots pine in paper II and Norway spruce in paper III, one plant per pot was used. The temperature was set to 20˚C and the relative air humidity (RH) was adjusted to 78%. For *A. thaliana*, the daily light period was initially 12 h with

an initial photon irradiance of 50 µmol m^{-2} s^{-1} (HPI-T Plus 250W, Phillips), increasing to 100 µmol m^{-2} s^{-1} within 7 days. The R:FR-ratio was adjusted to 1.7 with incandescent lamps (Osram, Munich, Germany). Thereafter the photoperiod was reduced to 8 h to slow down the reproductive development, aiming at making it easier to distinguish differences between the gamma treatments. In one of the experiments, *A. thaliana* plants were cultivated in a different type of growth chambers (Conviron growth chambers, Controlled Environments Ltd., Winnipeg, Canada) with a different type of main light (fluorescent light tubes (60W lamps, Phillips) and incandescent lamps) as compared to the experiments mentioned above. Norway spruce and Scots pine plants were cultivated in separate chambers of the same type mentioned above, but under a 24 h photoperiod with a 12 h main light period (metal halide HPI-T Plus, Phillips and incandescent lamps), followed by 12 h day extension with low-intensity light from incandescence lamps. The irradiance of the main light period was gradually increased from 50 m^{-2} s^{-1} to 180 µmol m^{-2} s^{-1} during 7 days. These light parameters were provided to ensure sustained growth after the first period following germination when they are less sensitive to photoperiod and irradiance. In experiments with UV-B pre-treatment prior to combined UV-B and gamma irradiation, Scots pine plants were transferred to a greenhouse compartment at NMBU, Ås, Norway (59°39´N.10°47´E) two months after the irradiation and grown for additional 5-6 months. The temperature was set to 21°C and RH to 75%, and in addition to the natural light, supplementary light at 165 µmol m^{-2} s^{-1} provided 16 h a day from HQI (Powerstar HQI-T 400 W, Osram, Munich, Germany) and high-pressure sodium (HPS 400 W Master PIA, Phillips) lamps (1:1 ratio).

Growth parameter recordings and histological studies

After the irradiation treatments, shoot and root lengths of Norway spruce and Scots pine (scanned on transparent sheaths with a scale) were measured using the Image J software (US National Institutes of Health, Bethesda, MD, USA; http:/imagej.nih.gov/ij/) (Paper I, II, III). In *A. thaliana*, the number of lateral roots were counted at the end of the gamma exposure (Paper I). At this stage the conifer species did not have any lateral roots, but the number of lateral roots were counted during the post-irradiation period (Paper I). In *A. thaliana* the fragile root system did not allow counting of lateral roots during the post-irradiation growing period. During the post-irradiation period the number of needles was counted and the plant height, and plant diameter were recorded in time courses in Norway spruce and Scots pine (Paper I, II, III). Plant height was measured with

a ruler from the rim of the pot to the shoot apical meristem (SAM) and the cumulative growth calculated. Shoot diameter from needle tip to needle tip across the plant at the shoot apex was calculated from two perpendicular measurements per plant. In *A. thaliana* plants (Paper I), the number of rosette leaves before appearance of flower buds and the number of plants with visible flower buds were recorded during the post-irradiation period. The percentage of plants with flower buds and elongating inflorescence stem were then calculated. In the comparative study of all three species (Paper I), the number of dead plants of Norway spruce and Scots pine was counted, whereas in *A. thaliana* no mortality was observed.

To evaluate effects of gamma and UV-B irradiation on the histology, histological studies of shoot and root apical meristems and leaves/needles were performed according to Lee et al. 2017 (Paper I, II and III). Materials of shoot and root tips and leaves fixed in 4% formaldehyde and 0.025% glutaraldehyde in sodium phosphate buffer (PBS, pH 7.0) were embedded in LR White resin (London Resin Company, London, UK) and sectioned using a microtome, followed by staining with toluidine blue O and inspection by light microscopy.

Analyses of DNA damage by the COMET assay

In all the studies the DNA damage (single and double strand breaks) after the gamma exposure was measured using the COMET assay performed according to Gichner et al. 2003 with some modifications (Gichner et al. 2003). The principle of the analyses is that damaged DNA moves out the cell nuclei during electrophoresis of lysed cells/cell nuclei in an agarose gel, and visualisation of the DNA is done by fluorescence microscopy. Nuclei with DNA damage then get elongated (COMET-like) in contrast to nuclei with undamaged DNA that retain a circular appearance. The intensity and length of the elongated cell nuclei (COMETS) due to the DNA damage is quantified relative to the head.

Analyses of gene expression by qPCR and RNA sequencing

To investigate the effect of gamma irradiation on transcript levels of specific genes related to DNA repair, antioxidants, cell cycle control and defence, shoots of young seedlings of Norway spruce, Scots pine and *A. thaliana* were harvested after 144 h of gamma exposure. As described in paper I, total RNA was extracted from each sample and transcript levels were analysed using qPCR.

To investigate the early molecular events (transcriptomic changes) in response to gamma irradiation in seedlings of a radiosensitive conifer using Norway spruce as a model species, shoot samples for RNA sequencing was harvested after 48 h of gamma radiation (Paper III). The total RNA was extracted, and RNA sequencing performed as described in Paper III. Further analyses including estimation of the transcript abundances, differential expression analyses and gene ontology (GO) term enrichment and KEGG pathway analysis were done as described in Paper III. In addition, due to the relatively poorly characterised Norway spruce genome (Nystedt et al. 2013), a comprehensive manual inspection of genes in specific groups were performed. These gene groups were selected on basis of the results of the GO term and KEGG analysis as well as the seedling phenotype and knowledge from other studies.

ROS measurements and analyses of flavonoids and total antioxidant capacity

In the work in Paper II, ROS production (H_2O_2) was assessed in Scots pine seedlings after gamma and UV-B irradiation, using 2′,7′-dichlorofluorescein diacetate (H2DCFDA) that upon oxidation is de-esterified to the highly fluorescent 2′,7-dichlorofluorescein (H2DCFD) (Razinger et al. 2010). The fluorescent signal for each of the samples was measured by a microplate reader (Fluoroskan Ascent FL, Thermo, Vantaa, Finland) with excitation and emission wavelengths of 480 nm and 530 nm, respectively.

Analyses of phenolic compounds were performed as described in Paper II. This included extraction in MeOH and analyses by HPLC using a 50 × 4.6 mm ODS Hypersil column (Thermo Fisher Scientific Inc., Waltham, MA, USA). The samples were eluted at a flow rate of 2 ml min^{-1} using a MeOH: water gradient according to Nybakken et al. (2012) (Nybakken et al. 2012).

Total antioxidant capacity was analysed using the OxiSelect Ferric Reducing Antioxidant Power (FRAP) Assay Kit (Cell Biolabs, San Diego, USA) according to the manufacturer`s instructions (Paper II).

Photosynthesis-related measurement

Twenty-eight days after gamma irradiation, *A. thaliana* plants were placed in the dark for 15 min. Thereby, to measure the optimal PSII efficiency, a modulated fluorometer (PAM-2000, Walz, Effeltrich, Germany) was used and Fv/Fm was calculated by $F_v/F_m = (F_m - F_o)/F_m$ (Paper I).

Statistical analyses

For the different growth and developmental parameters, DNA damage, relative transcript levels, ROS (H_2O_2) levels, contents of different phenolic compounds and total antioxidant capacity the effect of gamma radiation was assessed by analyses of variance (ANOVA; one-way for gamma only experiments (Paper I and III) and two-way for UV-B and gamma experiments (Paper II)) in the general linear model mode and by regression analysis using the Minitab statistical software Minitab statistical software (Minitab 18, Minitab Inc., PA, USA) ($p \leq 0.05$). For the post-irradiation growth parameters, the results from the final time point when the differences between the treatments were the largest were analysed. To test for differences between means, Tukey's post hoc test was used. When results from repeated experiments were available, the final statistical analyses included all these results. These individual experiments were first analysed separately to confirm equal responses.

Statistical analysis for the RNAseq analysis (Paper III) involved estimation of transcript abundances by using Salmon read mapping software. Differential expression was done using DESeq2 (version 1.18.1). Samples from different dose rates were compared to the control samples and genes were classified as differentially expressed genes if the False Discovery Rate adjusted p-values were < 0.05. Functional annotations were downloaded from ftp://plantgenie.org/Data/ConGenIE/Picea_abies/v1.0/Annotation/ database and gene ontology (GO) was obtained from the file Pabies1.0-gene_go_concat and *A. thaliana* orthologs to Norway spruce genes from the file piabi_artha_BEST_DIAMOND. Enrichment of GO and KEGG terms was performed using topGO (version 2.34.0) and limma package (version 3.38.2).

4. Main results and discussion

Previous studies have demonstrated that ionising radiation such as gamma radiation may cause adverse changes in plant growth and development, damage to DNA and other macromolecules, as well as altered metabolism (Esnault et al. 2010; Hamideldin & Hussien 2013; Kim et al. 2004; Kovacs & Keresztes 2002; Kovalchuk et al. 2007; Vandenhove et al. 2010; Wi et al. 2005). Furthermore, plant responses to gamma irradiation may differ between species and may depend on cultivar, developmental stage, tissue architecture, genome organisation and exposure scenario (De Micco et al. 2011). Interaction of ionizing radiation with other kinds of stressors and environmental factors in nature should also be taken into consideration, such as UV-radiation, particularly UV-B due to its short wavelengths, temperature, humidity, salt stress, pathogens etc. So far, effects on plants exposed to acute high doses have been best understood based on; (a) controlled field experiments b) field studies immediately after nuclear accidents, and (c) controlled laboratory experiments (Caplin & Willey 2018). However, few controlled experiments that examined the impacts on plants of low doses have been reported (UNSCEAR 1996). Also, there is limited information about differences in radiosensitivity from systematic comparisons of different plant species under standardized conditions.

In the present thesis, sensitivity to gamma radiation at the organismal, cellular and molecular level in the two conifers Norway spruce and Scots pine and the herbaceous *A. thaliana* was compared under controlled conditions (Paper I). Also, interactive effects of gamma and UV-B radiation were investigated in the radiosensitive Scots pine (Paper II). Furthermore, molecular mechanisms behind the response to gamma radiation in the similarly radiosensitive conifer species Norway spruce was studied using an RNA sequencing approach (Paper III). Norway spruce was used in this study since this species has the best developed molecular resources of the two conifers, which both have very large genomes. Although knowledge about full-length sequences and the number of genes is still incomplete, a genome sequence of Norway spruce has been published (Nystedt et al. 2013) in contrast to Scots pine.

4.1 Effects of gamma radiation on plant growth and development, histology and mortality

Young Norway spruce and Scots pine seedlings showed a dose-rate dependent growth inhibition after exposure to 144 h of gamma radiation 7-12 days after sowing, with reduced shoot and root lengths at dose rates ≥ 40 mGy h^{-1}, representing total doses ≥ 5.8 Gy (Paper I and Paper II). It could be noted that while Norway spruce showed reduced elongation growth at 40 mGy h^{-1} (paper I), there was variation in the response of Scots pine to this rate (paper I and II).

In one experimental series in the study in Paper II, significantly reduced shoot length was observed in response to 42.9 mGy h^{-1}, while there was no effect of 40 and 42.9 mGy h^{-1} in the study in Paper I and another experimental series in Paper II, respectively. The reason for this variation remains elusive. Gamma irradiation of Norway spruce seedlings for 48 h from day 7 after sowing also resulted in reduced shoot growth at the highest tested dose rates of 100 and 290 mGy h^{-1} (total doses 4.8 and 13.9 Gy), but root growth was not affected (Paper III).

The growth inhibition in response to the 144 h of gamma irradiation persisted post-irradiation with reduced shoot elongation, shoot diameter (i.e. length of needles) and number of needles in both Norway spruce and Scots pine at dose rates ≥ 40 mGy h^{-1} (Paper I) and ≥ 20 mGy h^{-1} when tested in Scots pine (Paper II). It could be noted that although the plant length in Scots pine was not in all cases affected at the end of the irradiation with 40 or 42.9 mGy h^{-1}, growth inhibition (for at least some growth parameters) was then generally observed post-irradiation (recorded up to day 44). Also, although no effect of 20.7 mGy h^{-1} on growth in Scots pine was observed at the end of the gamma irradiation, growth inhibition was observed post-irradiation at least for some of the growth parameters in each of the two experimental series performed in the work in Paper II. The delay in growth inhibition implies that the negative effect of such gamma dose rates may take some time to be manifested. Like at the end of the gamma irradiation, there was also some variation in the post-irradiation growth responses, with e.g. Norway spruce showing significantly reduced number of needles but not reduced shoot diameter at a dose rate of 40 mGy h^{-1}.

A possible explanation of the variation in the responses between experiments/experimental series may be genetic variation since population materials were used. Also, it may be speculated that different types of DNA damage had occurred to slightly different extents in different experiments and that these involve different types of DNA repair mechanisms. Difference in PAR during the gamma irradiation between the work in Paper I (55 µmol m^{-2} s^{-1}) and Paper II (200 µmol m^{-2} s^{-1})

may be another reason for differences in growth responses at the same dose rate for Scots pine. On the other hand, although we used the same PAR in the two series of experiments in Paper II, the growth responses varied for the same dose rate.

In the experiment with 48 h of gamma irradiation of Norway spruce seedlings, growth inhibition persisted post-irradiation with reduction of shoot diameter and number of needles at the same dose rates that affected growth at the end of the irradiation, i.e. 100 mGy h^{-1} and 290 mGy h^{-1} (highest tested dose rates). In these plants, no changes in the shoot elongation was then observed post-irradation (recorded for 58 days; Paper III).

Since shoot elongation and needle formation and growth depend on cell division and cell elongation in the shoot apical meristem (SAM)/shoot tips/leaf initials, it follows that the gamma irradiation affected these (either or both) basic growth processes (discussed further below). It could be noted that the growth inhibition in response to 144 h of gamma radiation was no longer visible 7-8 months post-irradiance when Scots pine seedlings exposed to up to 40 mGy h^{-1} were cultivated further, indicating that cell division and cell elongation then had been normalised (Paper II).

Although the conifer seedlings did not have any lateral roots at the end of the 144 h of gamma irradiation, the post-irradiation results showed reduced number of lateral roots and reduced total root length at dose rates 40 mGy h^{-1} and 100 mGy h^{-1} for Scots pine and Norway spruce, respectively (at day 44; Paper I). Reduced number of lateral roots post-irradiation was probably associated with a negative effect of the gamma irradiation on cell division activity in the pericycle that is the origin of lateral roots. Similarly, the reduced total root length might have been due to a negative effect of the gamma radiation on cell division in the shoot apical meristem and/or reduced cell elongation.

Cancelation of the apical dominance in young Scots pine trees in Chernobyl, and in Japanese red pine and Japanese fir in the Fukushima zone was observed under chronic radiation conditions (Yoschenko et al. 2018). However, no such impact in the gamma-exposed Scots pine and Norway spruce seedlings was noted in the current work (Paper I, II, III). Also, abnormally long needles were observed in Scots pine after the Chernobyl accident (Goltsova et al. 1991). Furthermore, some studies, have reported growth stimulation in crops exposed to low-doses of ionizing radiation; increased callus fresh weight and dry weight in carrot (*Daucus carota)* and increased fruit yield weight in tomato (*Lycopersicon esculentum*) (Al-Safadi & Simon 1990; Sidrak & Suess

1973). The seedlings of Norway spruce and Scots pine in the current study did not exhibit any increase in needle size in response to the gamma dose rates from 1-540 mGy h^{-1} for either 144 h (Paper I and II) or 48 h (Paper II). Factors such as different environmental conditions under the exposure to ionizing radiation, different exposure durations and different developmental stages in these field studies and our study under controlled conditions may possibly explain why such effects of gamma radiation on young conifer plants were not observed in our study. On the other hand, a recent study showed that current external and internal dose rates of 0.1-40 μGy h^{-1} and 0.1–274 μGy h^{-1}, respectively, in the Chernobyl exclusion zone did not affect the symmetry and size of birch leaves and Scots pine needles (Kashparova et al. 2018).

Furthermore, gamma exposure studies on *Pinus pinea* and *Pinus halpenis* showed the shoot apical meristem (SAM) cells to be radiosensitive (Donini 1967). Consistent with the reduced growth in response to dose rates ≥ 40 mGy h^{-1}, our histology studies showed a slight tendency of less well-developed SAM at ≥ 40 mGy h^{-1} in Norway spruce and Scots pine at the end of the gamma irradiation (Paper I). Similarly, in the study of Scots pine seedlings in Paper II slightly impaired SAM development was observed at 125 mGy h^{-1}, which resulted in growth inhibition. This is similar to results in previous work where increased frequency of necrotic needles with increased radiation exposure levels was observed on older Scots pine plants exposed to annual doses from 1.3 to 130 mGy $year^{-1}$ in the Russian region of Bryansk, contaminated by the Chernobyl accident (Makarenko et al. 2016). In contrast, Norway spruce seedlings exposed for 48 h showed no changes in SAM in spite of reduced shoot length at 100 and 290 mGy h^{-1} (Paper III). Post-irradiation results (44 days post-irradiation, 144 h gamma irradiation) showed aberrant cells or absent apical dome in SAM at dose rates ≥ 100 mGy h^{-1} in Paper I, while SAM in Scots pine in Paper II appeared normal without changes at this stage at 125 mGy h^{-1}. It may be speculated whether the higher PAR level applied (200 μmol m^{-2} s^{-1}) during the gamma irradiation in this study as compared to the 55 μmol m^{-2} s^{-1} used in the work in paper I, may have influenced the response to gamma radiation in Scots pine exposed for144 h.

On the other hand, when comparing *A. thaliana* with the conifer species (Paper I), only minor effects were seen, including decrease in lateral root number and elongation at the end of the irradiation as well as delayed flower bud formation and elongation of the inflorescence stem during the post-irradiation period (Paper I). A previous study on *A. thaliana* showed reduced plant height

with 5.2% and 11.7% at the vegetative and reproductive stages, respectively, reduction of shoot growth > 200 Gy, as well as mortality at 800 Gy (Kim et al 2011). In the current study, histological studies showed no SAM damage in *A. thaliana* right after or at the post-irradiation period as compared to the conifers (Paper I). Greater radiosensitivity of the *A. thaliana* roots relative to the leaves was previously described by other authors, and may be due to greater incidence of water radiolysis in the roots and/or antioxidant protection of leaf cells from photooxidant harm (Vanhoudt et al. 2014). In the current study, the aqueous agar growth media during the gamma exposure may possibly also have contributed to more water radiolysis in the roots, since water molecules are direct target molecules of ionizing radiation (Esnault et al. 2010). Furthermore, *A. thaliana* seedlings exposed to gamma dose rates from 81 to 2339 μGy h^{-1} for 24-54 days showed induction of negative growth effects (leaf, stem fresh weight, total plant fresh and growth) (Vandenhove et al. 2010). Another study showed increased fresh weight of shoots and roots in response to gamma radiation exposed for 14 days to dose rates from 22 to 86 mGy h^{-1} and total dose from 7 to 29 Gy (van de Walle et al. 2016). (Wi et al. 2007) found that *A. thaliana* plants exposed to low-dose gamma rays (1-5 Gy) developed normally as compared to the control, while the growth of seedlings irradiated 50 Gy showed inhibition. In Paper I, consistent with normal SAM development after gamma radiation, no consistent effects on shoot size in *A. thaliana* was observed. Importantly, unlike the conifers, *A. thaliana* showed no effects on histology, mortality or visible damage after gamma irradiation (Paper I).

4.2 Effect of gamma radiation on DNA damage and DNA repair genes

DNA damage is well known to occur in response to ionizing radiation, and it has been proposed that acute high doses in the range of 10–1000 Gy may be lethal to plants (UNSCEAR 1996). DNA repair mechanisms play a crucial role in reversing oxidative adducts and other chemical changes (Hu et al. 2016). Also, different DNA repair pathways are active at different cell cycle stages, enabling the cells to repair the DNA damage (Chatterjee & Walker 2017). However, DNA repair processes are less well described in most plant species as compared to *A. thaliana* and a range of other organisms. Nevertheless, although the radiosensitivity differs between plant species, it is well known that plant cells in general are more resistant to development of dsDNA breaks and repair them faster than animal cells (Hu et al. 2016; Yokota et al. 2005). In our study, to check the radiosensitivity of the DNA, the COMET assay was used to assess the DNA damage in seedlings

of Scots pine and Norway spruce as well as *A. thaliana* at the end of the gamma irradiation and post-irradiation. Although conifers showed greater radiosensitivity with respect to growth inhibition relative to *A. thaliana*, dose-rate dependent DNA damage was present in all three species both immediately after the irradiation and 44 days post-irradiation (Paper I, II and III). Norway spruce showed significantly increased DNA damage from 10 to 400 mGy h^{-1}, and Scots pine from 1 to 540 mGy h^{-1} gamma dose rate, respectively (Paper I and II). However, Norway spruce exposed to gamma radiation for 48 h (Paper III), showed increased level of DNA damage already from 1 mGy h^{-1}. In Paper II, although UV-B did not affect elongation growth in Scots pine, additionally increased DNA damage was observed in response to UV-B in both series of experiments as compared to the only gamma irradiated seedlings. Although a correlation between growth and DNA damage could be expected, the results showed tolerance to some degree DNA damage as also happens in circumstances other than those that affect growth.

The post-irradiation results (day 44) showed similar % of DNA damage. Norway spruce shoot tips then exhibited significantly increased level of DNA damage ≥ 1 mGy h^{-1} and Scots pine ≥ 10 mGy h^{-1}, respectively, which was lower dose rates than those affecting growth negatively (≥ 40 mGy h^{-1}). However, the level of DNA damage in roots in Norway spruce was not observed among the different dose rates, while Scots pine roots exhibited DNA damage at dose rates of 40 and 100 mGy h^{-1} (Paper I). Similarly, in Paper II, clear gamma dose-response-relationships with increased levels of DNA damage at all tested dose rates were observed in both series of experiments (with and without UV-B), immediately after irradiation and post-irradiation. However, consistent with normalised growth 7 and 8 months after irradiation, the DNA damage level was then almost or not present in any of treatments (as compared to the control) (Paper II). *A. thaliana* exposed to gamma radiation for 144 h showed significantly increased DNA damage from 10 to 540 mGy h^{-1}, while *A. thaliana* exposed for 360 h exhibited DNA damage from 1 to 400 mGy h^{-1}, immediately after irradiation (Paper I). The post-irradiation results day 44 after exposure to 360 h of gamma radiation revealed that *A. thaliana* leaves then had increased % DNA tail from 1 to 400 mGy h^{-1} (Paper I).

Since all three plant species tested showed DNA damage for an extended period of time, substantial genomic instability induced by gamma irradiance may be present. Another assumption may be that DNA repair was unable to counteract the persistent DNA damage effects or that stem cells continued to produce damaged daughter cells, which survived and grew. There is evidence of

radiation-induced genomic instability in animal cells, but such information is limited in plants (Hurem et al. 2017; Morgan et al. 1996; Morgan 2003; Mothersill & Seymour 1998). Nevertheless, gamma irradiated tobacco cells showed constant micronuclei formation in offspring of various generations after the initial insult, giving direct evidence of manifestations of radiation-induced genomic instability in higher plant cells (Yokota et al. 2010). In prior studies, *A. thaliana* exposed to acute irradiation (1 Gy in 1 day) showed activation of DNA repair genes, oxidative stress response genes and signal transduction genes, but expression of DNA repair and antioxidant genes was not altered when exposed to more chronic irradiation (1 Gy in 21 days) (Ali et al. 2015; Kovalchuk et al. 2007).

Transcript levels of the DNA repair-related genes, *RAD51* and *SOG1*, were quantified in gamma-exposed Scots pine, Norway spruce and *A. thaliana* using qPCR (Paper I). Although Norway spruce and Scots pine had similar overall radiosensitivity with respect to growth and development, DNA damage (COMET) and mortality and *A. thaliana* was far less affected and showed no damage or mortality, induction of *RAD51* and *SOG1* was only observed in Scots pine and *A. thaliana* (Paper I). However, our RNAseq Norway spruce data (48 h gamma irradiation) showed upregulation of DNA repair genes such as *SOG1*, *DNA LIGASE 4* (*LIGIV*), *ATP-DEPENDENT DNA HELICASE 2 SUBUNIT KU80* (*KU80*), *XRCC2*, *XRCC3*and *GR1* along with *WEE1*, which is also involved in the arrest of the cell cycle (Paper III). This is similar to earlier studies of *A. thaliana* that also showed upregulation of the *SOG1* and *WEE1* genes (De Schutter et al. 2007). Possible reasons why there was a lack of correlation between qPCR and RNAseq results may be e.g. normalisation bias in RNAseq analysis, bias in library preparation, PCR and specificity of qPCR primers for the candidate gene. It could also be noted that the qPCR study was performed after 6 days gamma exposure, whereas the RNA seq study was done after 48 h of gamma irradiation.

As investigated in Scots pine seedlings 7- or 8-months post-irradiation (Paper II), DNA damage was then either present to a very low degree only or no longer present. The reason for this may be that the DNA damage had been repaired via different DNA repair mechanisms or that the instability of the genome was no longer present.

4.3 Effect of gamma radiation on ROS formation, ROS-scavenging-related genes, antioxidant capacity and phenolic compounds

Upon exposure to ionizing radiation like gamma radiation, DNA damage can be caused either by direct ionisation or by induction of excess ROS that may damage DNA and other macromolecules. ROS has a strong ability to cause oxidative harm to single bases of DNA but can also introduce single or double strand breaks in DNA (Biedermann et al. 2011). In addition to ROS production in response to different stressors, ROS production including hydrogen peroxide (H_2O_2) production is well known to occur as a by-product of the metabolism, particularly in the chloroplasts, but also in the peroxisomes and mitochondria. Because H_2O_2 is the most stable ROS, it also plays a crucial role in multiple physiological processes as a signalling molecule, but when overproduced it becomes poisonous in plants cells unless the production of antioxidants is sufficiently induced. Although not measured in Norway spruce and *A. thaliana*, assessment of the H_2O_2 level in Scots pine seedlings in Paper II, revealed a significant dose-rate-dependent induction after gamma radiation at $\geq$ 40 mGy h^{-1}, consistent with the observed dose-rate dependent growth inhibition and DNA damage.

Consistent with (possible) antioxidant induction in response to gamma radiation, the qPCR analyses in Paper I showed increased expression level of the peroxidase gene *PX3* in Norway spruce at 180 and 400 mGy h^{-1} and Scots pine at 40 mGy h^{-1} (144 h gamma), whereas no such induction was observed in *A. thaliana*. However, increased *CAT* and *SOD* were not detected in Scots pine and *A.thaliana*, but these antioxidant genes showed increased expression in Norway spruce at 180 and 100 mGy h^{-1}, respectively. Furthermore, various genes associated with ROS scavenging and signal transduction pathways were noted in the RNA sequencing analysis of gamma-irradiated Norway spruce seedlings (48 h) in Paper III. These findings indicate upregulation of genes encoding ascorbate peroxidase (APX), while different genes encoding glutathione S-transferases (GST) and PX showed up and down-regulation (9 upregulated and 1 downregulated *GST* genes, 4 upregulated and 11 downregulated *PX* genes). Upregulation of some *PX* genes at 100 mGy h^{-1} is consistent with the results from Paper I showing upregulation of *PX3* although 180 and 400 mGy h^{-1} were not tested in the RNAseq analyses. Different *GST* genes were mostly upregulated from 10 to 100 mGy h^{-1}. However, one *SOD* gene was found in the RNAseq analyses but it did not exhibit any significant differences compared to the untreated control. Yet

the *SOD* gene analysed in Paper I showed increased expression level at 100 mGy h^{-1}. (Kovalchuk et al. 2007) detected that gamma radiation induced upregulation genes related to oxidative stress genes in *A. thaliana*; most notably those encoding the P450 cytochromes, peroxidases, and glutathione transferase. Similar results were observed in *L. minor* and *N. tabacum* (Cho et al. 2000; Van Hoeck et al. 2017). Some studies of *A. thaliana* exposed to gamma irradiation showed no major changes in antioxidative enzyme capacities (Vandenhove et al., 2010; Vanhoudt et al., 2010, 2011), but Vanhoudt et al 2014 showed increased activities of SOD and APX in roots at 58.8 Gy. However, no alterations were then observed in SOD, CAT and SPX capacities in the leaves, but GPX showed increased level at the lowest dose of 3.9 Gy, and reduction at the highest doses, 6.7-58.8 Gy. Also, Kim et al. 2011 showed increased POD activity at the vegetative and reproductive stage from 0-800 Gy, whereas CAT showed reduction at 100 Gy but increased level at the 800 Gy treatment, at both stages. APX activity was increased at the vegetative stage and increased from 0-800 Gy and reduced at the reproductive stage from 0 to 800 Gy. SOD was increased from 0 to 800 Gy at the reproductive stage but SOD levels of irradiated plants were lower than non-irradiated plants at the vegetative stage (Kim et al. 2011).

4.4. Effect of gamma radiation on the transcriptome in the radiosensitive conifer species Norway spruce

Of the 66 069 predicted genes in Norway spruce, 5326 (8.1%) were differentially expressed genes (DEGs) in the RNAseq analysis of gamma exposed seedlings (48 h exposure) as compared to unexposed control plants. It could be noted that although the genome is characterised to a certain extent, the information is still limited and only 13040 of the 66 069 predicted genes (20%) have a GO annotation. Main upregulated pathways in response to gamma irradiation were linked to DNA repair, the endomembrane system function, the cell cycle regulation, energy metabolism, protein syntheis and lipid degradation (beta oxidation) at 40 and 100 mGy h^{-1}. In contrast, downregulated pathways were linked to the photosynthesis and growth hormones but mostly at the dose rate of 100 mGy h^{-1}. An earlier study employing microarray analyses in *A. thaliana* exposed to very high total doses showed 496 upregulated and 1 042 downregulated genes of a total of 20 993 genes (Kim et al. 2014). In this studythe most abundant differentially expressed genes were involved in catalytic activity, the endomembrane system function, and metabolism, especially between 100–2000 Gy over 24 h.

Consistent with reduced growth at 100 mGy h^{-1} but not at lower dose rates after 48 h gamma exposure (including post-irradiation) (Paper III), genes related to photosynthesis and nitrogen metabolism were massively downregulated at 100 mGy h^{-1} but not at lower dose rates. Also, a multitude of genes related to growth-promotion showed differential expression (DE), such as auxin-response genes that were predominately downregulated at 40 mGy h^{-1} and even more commonly so at 100 mGy h^{-1} (Paper III). Simultaneously, a range of auxin transport genes were downregulated at 100 mGy h^{-1}. Additionally, gibberellin-regulated genes were downregulated in response to 100 mGy h^{-1}, while a brassinosteroid biosynthesis-related gene was downregulated and a brassinosteroid inactivation gene upregulated. Furthermore, several genes related to biosynthesis and response of the cell division-stimulating hormone cytokinin were downregulated in response to gamma irradiation at 100 mGy h^{-1}. These changes are consistent with the gamma radiation-induced growth inhibition and indicate that the hormone content and response is actively regulated by this stressor. A transcriptomic study of *Lemna minor* exposed for 7 days to gamma doses from 53 to 423 mGy h^{-1} also showed differentially expressed genes related to hormones (Van Hoeck et al. 2017). Genes related to plant hormones involved in growth inhibition and defence were also affected by the gamma exposure, but only at 100 mGy h^{-1} (paper III). Among such genes, an ABA receptor gene was upregulated, and an ABA catabolism gene was downregulated, suggesting increased ABA content and response in response to gamma radiation, consistent with reduced growth. On the other hand, downregulation of ethylene-response related genes responsible for senescence of vegetative tissues and defence signalling and the jasmonate related gene *JRG21* at 100 mGy h^{-1}, as well as lack of regulation of salicylic acid-related genes may suggest that the defence signalling pathways mediated by these hormones was not enhanced by the gamma radiation exposure.

4.5 Effect of gamma radiation on cell division

Consistent with growth reduction, Norway spruce and Scots pine showed slightly less developed SAM $\geq$ 40 mGy h^{-1} right after the gamma irradiation. However, progressive damage of SAM was observed 44 days after the gamma irradiation $\geq$ 100 mGy h^{-1}, resulting in aberrant cells and malformed or virtually absent apical dome (Paper I). In contrast, although growth inhibition was observed in Scots pine at the highest dose rates tested in Paper II (42.9 and 125 mGy h^{-1}), the SAM appeared normal 44 days post-irradiation. Also, Norway spruce showed no visible difference

between any of the dose rates and the control right after gamma irradiation for 48 h (Paper III). The qPCR analyses in Paper I showed upregulated transcript level of *CYCB1;2* in the Scots pine seedlings at 10 and 40 mGy h^{-1}, whereas the Norway spruce seedlings showed no difference in transcript level among the different gamma dose rates. However, *A. thaliana* seedlings showed increased transcription level of *CYCB1;2* at 40 mGy h^{-1} and higher dose rates as compared to the unexposed control, 1 and 10 mGy h^{-1}. *CDKB1;2* showed no increased transcription level among different gamma dose rates in any of the species. *CYCD3;1* showed increased level only at 1 mGy h^{-1} in Norway spruce as compared to the unexposed control, while no significant differences in Scots pine and *A. thaliana* were observed. Yet, the RNAseq results of Norway spruce seedlings in Paper III (48 h gamma) showed enrichment of GO terms (upregulation) related to the cell cycle and protein synthesis, i.e. anaphase, regulation of G2/M transition of the mitotic cell cycle, DNA replication initiation, regulation of DNA replication, DNA endoreduplication and translation at 40 mGy h^{-1} only, while the GO terms cell proliferation and DNA replication showed enrichment (upregulation) at both 40 and 100 mGy h^{-1}. In contrast to Paper I, this study showed both *CYCB1;1* and *CYCB1;2* downregulation at 100 mGy h^{-1}, and upregulation of *CDKB2;2* at 40 mGy h^{-1}.

4.6 Effect of UV-B on growth and development of gamma-irradiated plants

Although elevated levels UV-B can induce DNA damage, modifications in the membrane, protein cross links and formation of reactive oxygen species (ROS) in plants, there is evidence that ambient UV-B levels rather has an adaptive function. In this respect, it has been suggested that UV-B may prime defence against various stressors through induction of compounds protecting against ROS (Alexieva et al. 2001; Nogués & Baker 2000; Ouhibi et al. 2014; Stratmann 2003). Induction of cross-tolerance to stressors such as drought, cold, salt stress, wounding and pathogens has been shown to be induced by UV-B (Alexieva et al. 2001; Chalker-Scott & Scott 2004; Manetas et al. 1997; Nogués & Baker 2000; Ouhibi et al. 2014; Poulson et al. 2006; Robson et al. 2015a; Schmidt et al. 2000; Stratmann 2003).However, information about interactive effects of UV-B and low to moderate gamma radiation levels is very limited. In the current work such interactive effects were investigated in the radiosensitive conifer Scots pine (Paper II). In this respect it was investigated whether effects of gamma irradiation may be modified by UV-B radiation in the radiosensitive conifer species (Paper II) by testing whether pre-exposure to UV-B (0.35 and 0.52 W m^{-2}) may prime defence mechanisms contributing to enhanced tolerance to gamma radiation and whether

simultaneous UV-B and gamma exposure may have a cumulative negative effect. There was no additional negative impact of UV-B at 0.35 W m^{-2} on shoot and root growth in the gamma exposed seedlings (Paper II), possibly due to the efficient UV-B screening in the epidermis in such conifer species (Laakso & Huttunen 1998) Pre-treatment with UV-B before the UV-B and gamma co-exposure did not make any difference since no significant effect of UV-B on root and shoot length was then observed. Thus, UV-B did apparently not induce any protective systems that could help preventing the gamma-induced growth inhibition at the highest tested dose rates (42.9 and 125 mGy h^{-1}). Shoot apical meristem cells also showed no difference between different UV-B and gamma combined treatments (Paper II).

4.7 Effect of UV-B on DNA damage in gamma-irradiated plants

UV-B can directly harm DNA and cause various kinds of DNA damage, where cyclobutane pyrimidine dimers (CPD) and pyrimidine (6-4) pyrimidinone dimers (6—4PP) are major lesions (Britt & Fiscus 2003; Jansen 2017). Other DNA lesions caused by UV-B include oxidized or hydrated bases, single-strand breaks, and others (Ballaré et al. 2001; Gill et al. 2015; Takahashi et al. 2011). In the current study, UV-B resulted in additional DNA-damage when combined with gamma dose rates at 42.9 and 125 mGy h^{-1} for 144 h. This was the case also when the plants were pre-treated with 4 days of UV-B prior to the UV-B and gamma exposure (Paper II). However, when comparing growth inhibition and DNA damage, no additional DNA damage caused by UV-B was observed. Forty-four days post-irradiation, similar DNA damage as observed after the 6 days of irradiation was still present in several treatments with UV-B at gamma dose rates of 42.9 and 125 mGy h^{-1} in shoots and 20.7 and 125 mGy h^{-1} in roots. However, 7 and 8 months after the exposure DNA damage was decreased and almost no significant difference between different treatments were observed (Paper II). Such DNA damage reduction may be a result of different DNA repair mechanisms, which are activated to maintain genome integrity (Biedermann et al. 2011).

4.8 ROS, antioxidants and flavonoids levels in UV-B and gamma-irradiated plants

Low levels of ROS are most likely to be generated and may lead to activation of UV-acclimation reactions when plants are exposed to low levels of UV-B. In contrast, high levels of UV-B radiation can trigger cellular metabolism disruptions that can lead to elevated levels of ROS production (Jansen 2017). The responses of plants to UV-B presence, may be induction of phenolic compounds and flavonoids which act as ROS scavengers, which can neutralize free radicals (Jansen & Bornman 2012; Løvdal et al. 2010). Also, gamma radiation can induce ROS production, including H_2O_2 which can result in lipid, protein and DNA damage (Biedermann et al. 2011; Gill & Tuteja 2010). Induction of certain antioxidant enzymes such as catalase (CAT), glutathione reductase (GR), ascorbate peroxidase (APOD), syringaldazine peroxidase SPOD and guaiacol peroxidase (GPOD) are induced in plants in order to decrease elevated concentrations of singlet oxygen ($^1O_2$), superoxide radical (O_2^-) and H_2O_2 (Apel & Hirt 2004; Van Hoeck et al. 2015). Regardless of UV-B pre-treatment, our study did not demonstrate any additional impact of UV-B at 0.35 W m^{-2} on ROS (H_2O_2) contents in the gamma exposed seedlings (Paper II). However, increased levels of H_2O_2 were observed in response to gamma radiation at 42.9 and 125 mGy h^{-1}, which correlates with reduced growth. Furthermore, the levels of specific phenolic compounds were induced by UV-B, most notably the flavonoids kaempferol glycosides, but in some cases also methanol-soluble tannins, while no effect of gamma irradiation on such compounds were observed (paper II). Thus, there are no indications from this study that such phenolic compounds were induced by gamma radiation exposure in Scots pine seedlings. On the other hand, in the RNA seq study of Norway spruce seedlings (Paper III), GO enrichment analyses showed upregulation of genes related to regulation of flavonoid biosynthetic process at 100 mG h^{-1}. Van Hoeck et al. 2017. also showed that transcription levels of a significant number of genes related to flavonoid biosynthesis and lignin biosynthesis in *L. minor* showed upregulation up to a dose rate of 232 mGy h^{-1}.

4.9 Uncertainties

It is important to highlight that variability, questionable assumptions, gaps in knowledge, extrapolations and poor conceptual model structures, can contribute to large uncertainties which can often be neglected or poorly described (Salbu 2016). According to Salbu 2016, sources of

uncertainties can be categorised as input-, interpolation and extrapolation-, algorithm- and structural uncertainties as well as parameter uncertainty and variability.

In the present thesis the different environmental factors used during the gamma radiation exposure and subsequent growth, i.e. factors such as temperature, light and air humidity may be possible factors causing uncertainties and variability. E.g. in paper II, growth chambers were used during the gamma exposure, and this allowed the use of higher irradiances of visible light (PAR) than when growth chambers were not used in the studies in paper I and III (due to testing of a larger range of dose rates in these). It cannot be excluded that the irradiation of the PAR light may affect the response to at least relatively low dose rates/doses of gamma radiation since higher irradiance normally results in higher photosynthesis rate. Furthermore, population materials were used, and genetic variation may have contributed to the variation in the results for specific parameters (e.g. DNA damage and growth parameters) between experiments. Furthermore, since the seedlings were exposed to gamma radiation in Petri dishes of 5 cm diameter, there was some variation in exposure among individual seedlings. This may have contributed to the variation, although the Petri dishes were rotated in the middle of the gamma exposure period in all experiments. It should also be noted that sampling is an important issue which contributes to uncertainties. In general, the sample number was relatively limited due to the costs of analysis and available time for analyses. Thus, time courses during the gamma exposure were not analysed. This may contribute to e.g. the differences between the qPCR and RNA seq results for specific genes, since the samples for these analyses were harvested at one time point only. The harvest of the samples after 144 h (qPCR) and 48 h (RNA seq) of gamma exposure for these gene expression studies, also contributes to uncertainties regarding the effect of gamma radiation on expression of specific genes. Thus, to get a better complete picture of the effects on gamma radiation on the dynamics of gene expression during gamma irradiation, time courses should be analysed.

5. Conclusions

The first part of this thesis (paper I) aimed to shed the light on physiological, molecular and morphological mechanisms caused by gamma radiation in three different species, *Picea abies*, *Pinus sylvestris* and *Arabidopsis thaliana*. The results showed that despite persistent DNA damage in all three species after gamma irradiation, higher sensitivity at the organismal and cellular level in Scots pine and Norway spruce indicate significantly lower tolerance to DNA-damage than in *A. thaliana*.

The second part of the study (paper II) showed no protective effects of UV-B on gamma-induced growth inhibition and DNA damage in the radiosensitive Scots pine. Also, no cumulative negative effect of gamma and UV-B radiation on growth in spite of that additional UV-B-induced DNA damage was present.

Paper III investigated transcription of genes, DNA damage and growth in a radiosensitive conifer species using Norway spruce as a model species to gamma radiation. The results showed that a profound transcriptomic change occurred at dose rate $\geq$ 40 mGy h^{-1}, most notably so at 100 mGy h^{-1} (highest tested dose rate), but not at lower dose rates, where only few genes were affected. Differential expression at 40 and 100 mGy h^{-1} was particularly linked to upregulation of energy metabolism, and plant defence systems, including DNA repair, cell cycle arrest, synthesis of specific antioxidants and flavonoids. Also, the differentially expressed genes were associated with response to increased DNA damage and eventually reduced shoot growth, as well as reduced growth hormone signalling and photosynthesis. The fact that a range of defence-related genes were upregulated and a multitude of growth-related genes were down-regulated in response to gamma irradiation, suggests that repair and defence systems are activated at the expense of growth. On the other hand, very few differentially expressed genes at the lowest tested dose rates of 1 and 10 mGy h^{-1} may suggest that it takes considerable gamma radiation stress for the Norway spruce seedlings to respond.

6. Further perspectives

The results of this study added further knowledge about radiosensitivity in different plant species. The results in this thesis show that the conifer species Norway spruce and Scots pine exhibit far higher sensitivity at the organismal and cellular level compared to the *A. thaliana*. Yet, dose-rate dependent DNA damage occurred in all three species right after the irradiation and remained similar 44 days after gamma irradiation. To compare the gene expression response to gamma radiation in the radiosensitive conifer species Norway spruce (Paper III) with the situation in the radioresistant *A. thaliana*, it would also be necessary to perform a transcriptomic study of *A. thaliana*. In addition, it has been hypothesised that endoreduplication plays a major role in radioresistance of plants. Thus, it would be interesting to test this hypothesis by use of flow cytometry of apical meristem cells from gamma-exposed cells of the species studied in this thesis, i.e. employing equal exposure conditions. This could lead to a better understanding of the significance of cell ploidy-level (specially in meristem cells).

7. References

Adachi, S., Minamisawa, K., Okushima, Y., Inagaki, S., Yoshiyama, K., Kondou, Y., Kaminuma, E., Kawashima, M., Toyoda, T., Matsui, M., et al. (2011). Programmed induction of endoreduplication by DNA double-strand breaks in Arabidopsis. *Proceedings of the National Academy of Sciences of the United States of America*, 108 (24): 10004-10009.

Ahmad, P., Jaleel, C. A., Salem, M. A., Nabi, G. & Sharma, S. (2010). Roles of enzymatic and nonenzymatic antioxidants in plants during abiotic stress. *Critical Reviews in Biotechnology*, 30 (3): 161-175.

Al-Safadi, B. & Simon, P. W. (1990). The effects of gamma irradiation on the growth and cytology of carrot (Daucus carota L.) tissue culture. *Environmental and Experimental Botany*, 30 (3): 361-371.

Alexieva, V., Sergiev, I., Mapelli, S. & Karanov, E. (2001). The effect of drought and ultraviolet radiation on growth and stress markers in pea and wheat. *Plant, Cell & Environment*, 24 (12): 1337-1344.

Ali, H., Ghori, Z., Sheikh, S. & Gul, A. (2015). Effects of gamma radiation on crop production. In Hakeem, K. R. (ed.) *Crop Production and Global Environmental Issues*, pp. 27-78. Cham: Springer International Publishing.

Apel, K. & Hirt, H. (2004). Reactive oxygen species: Metabolism, oxidative stress, and signal transduction. *Annual Review of Plant Biology*, 55 (1): 373-399.

Arkhipov, N. P., Kuchma, N. D., Askbrant, S., Pasternak, P. S. & Musica, V. V. (1995). *Acute and long-term effects of irradiation on pine (Pinus silvestris) stands post-Chernobyl*, vol. 157. 383-6 pp.

Armenise, L., Simeone, M., Piredda, R. & Schirone, B. (2012). Validation of DNA barcoding as an efficient tool for taxon identification and detection of species diversity in Italian conifers. *European Journal of Forest Research*, 131.

Averbeck, D., Salomaa, S., Bouffler, S., Ottolenghi, A., Smyth, V. & Sabatier, L. (2018). Progress in low dose health risk research: Novel effects and new concepts in low dose radiobiology. *Mutation Research/Reviews in Mutation Research*, 776: 46-69.

Ballaré, C. L., Cecilia Rousseaux, M., Searles, P. S., Zaller, J. G., Giordano, C. V., Matthew Robson, T., Caldwell, M. M., Sala, O. E. & Scopel, A. L. (2001). Impacts of solar ultraviolet-B radiation on terrestrial ecosystems of Tierra del Fuego (southern Argentina): An overview of recent progress. *Journal of Photochemistry and Photobiology B: Biology*, 62 (1): 67-77.

Belli, M., Sapora, O. & Tabocchini, M. A. (2002). Molecular targets in cellular response to ionizing radiation and implications in space radiation protection. *J Radiat Res*, 43 Suppl: S13-9.

Biedermann, S., Mooney, S. & Hellmann, H. (2011). *Recognition and Repair Pathways of Damaged DNA in Higher Plants*. 201-237 pp.

Bleuyard, J.-Y., Gallego, M. E., Savigny, F. & White, C. I. (2005). Differing requirements for the *Arabidopsis* Rad51 paralogs in meiosis and DNA repair. *The Plant Journal*, 41 (4): 533-545.

Britt, A. & Fiscus, E. L. (2003). Growth responses of *Arabidopsis* DNA repair mutants to solar irradiation. 118 (2): 183-192.

Britt, A. B. (1999). Molecular genetics of DNA repair in higher plants. *Trends in Plant Science*, 4 (1): 20-25.

Caplin, N. & Willey, N. (2018). Ionizing radiation, higher plants, and radioprotection: From acute high doses to chronic low doses. *Frontiers in Plant Science*, 9.

Chalker-Scott, L. & Scott, J. D. (2004). Elevated Ultraviolet-B Radiation Induces Cross-protection to Cold in Leaves of Rhododendron Under Field Conditions. 79 (2): 199-204.

Chatterjee, N. & Walker, G. C. (2017). Mechanisms of DNA damage, repair, and mutagenesis. *Environmental and molecular mutagenesis*, 58 (5): 235-263.

Chen, I.-P., Haehnel, U., Altschmied, L., Schubert, I. & Puchta, H. (2003). The transcriptional response of Arabidopsis to genotoxic stress – a high-density colony array study (HDCA). 35 (6): 771-786.

Cho, H. S., Lee, H. S. & Pai, H.-s. (2000). Expression patterns of diverse genes in response to gamma irradiation in *Nicotiana tabacum*. *Journal of Plant Biology*, 43 (2): 82-87.

Choppin, G., Liljenzin, J. O., Rydberg, J. & Ekberg, C. (2013). *Radiochemistry and nuclear chemistry*: Elsevier.

Culligan, K., Tissier, A. & Britt, A. (2004). ATR regulates a G2-phase cell-cycle checkpoint in *Arabidopsis thaliana*. *The Plant Cell*, 16 (5): 1091.

Culligan, K. M., Robertson, C. E., Foreman, J., Doerner, P. & Britt, A. B. (2006). ATR and ATM play both distinct and additive roles in response to ionizing radiation. *The Plant Journal*, 48 (6): 947-961.

De La Torre, A. R., Birol, I., Bousquet, J., Ingvarsson, P. K., Jansson, S., Jones, S. J. M., Keeling, C. I., MacKay, J., Nilsson, O., Ritland, K., et al. (2014). Insights into conifer giga-genomes. *Plant physiology*, 166 (4): 1724-1732.

De Micco, V., Arena, C., Pignalosa, D. & Durante, M. (2011). Effects of sparsely and densely ionizing radiation on plants. *Radiation and Environmental Biophysics*, 50 (1): 1-19.

De Schutter, K., Joubès, J., Cools, T., Verkest, A., Corellou, F., Babiychuk, E., Van Der Schueren, E., Beeckman, T., Kushnir, S., Inzé, D., et al. (2007). *Arabidopsis* WEE1 kinase controls cell cycle arrest in response to activation of the DNA integrity checkpoint. *The Plant Cell*, 19 (1): 211-225.

De Veylder, L., Larkin, J. C. & Schnittger, A. (2011). Molecular control and function of endoreplication in development and physiology. *Trends in Plant Science*, 16 (11): 624-634.

Donini, B. (1967). Effects of chronic gamma-irradiation on Pinus pinea and Pinus halepensis. *Radiation Botany*, 7 (3): 183-192.

Dotto, M. & Casati, P. (2017). Developmental reprogramming by UV-B radiation in plants. *Plant Science*, 264: 96-101.

Doutriaux, M.-P., Couteau, F., Bergounioux, C. & White, C. (1998). Isolation and characterisation of the RAD51 and DMC1 homologs from Arabidopsis thaliana. *Molecular and General Genetics MGG*, 257 (3): 283-291.

Esnault, M.-A., Legue, F. & Chenal, C. (2010). Ionizing radiation: Advances in plant response. *Environmental and Experimental Botany*, 68 (3): 231-237.

Fesenko, S. V., Alexakhin, R. M., Geras'kin, S. A., Sanzharova, N. I., Spirin, Y. V., Spiridonov, S. I., Gontarenko, I. A. & Strand, P. (2005). Comparative radiation impact on biota and man in the area affected by the accident at the Chernobyl nuclear power plant. *Journal of Environmental Radioactivity*, 80 (1): 1-25.

Freitas, A. C. & Alencar, A. S. (2004). Gamma dose rates and distribution of natural radionuclides in sand beaches—Ilha Grande, Southeastern Brazil. *Journal of Environmental Radioactivity*, 75 (2): 211-223.

Friesner, J. D., Liu, B., Culligan, K. & Britt, A. B. (2005). Ionizing radiation-dependent gamma-H2AX focus formation requires ataxia telangiectasia mutated and ataxia telangiectasia mutated and Rad3-related. *Molecular biology of the cell*, 16 (5): 2566-2576.

Ganguly, T. & Duker, N. J. (1991). Stability of DNA thymine hydrates. *Nucleic acids research*, 19 (12): 3319-3323.

Garcia, V., Bruchet, H., Camescasse, D., Granier, F., Bouchez, D. & Tissier, A. (2003). AtATM is essential for meiosis and the somatic response to DNA damage in plants. *The Plant Cell*, 15 (1): 119-132.

Geras'kin, S., Zimina, L. M., Dikarev, V. G., Dikareva, N. S., Zimin, V. L., Vasiliyev, D., Udalova, A., Blinova, L. D. & Alexakhin, R. M. (2003). Bioindication of the anthropogenic effects on micropopulations of *Pinus sylvestris*, L. in the vicinity of a plant for the storage and processing of radioactive waste and in the Chernobyl NPP zone. *J Environ Radioact.* , 66 (1-2): 171-80.

Geras'kin, S., Fesenko, S. & M Alexakhin, R. (2008). Effects of non-human species irradiation after the Chernobyl NPP accident. *Environment International*, 34 (6): 880-97.

Geras'kin, S. A. & Volkova, P. Y. (2014). Genetic diversity in Scots pine populations along a radiation exposure gradient. *Science of The Total Environment*, 496: 317-327.

Geras'kin, S., Oudalova, A., Dikareva, N., Spiridonov, S., Hinton, T., Chernonog, E. & Garnier-Laplace, J. (2011). Effects of radioactive contamination on Scots pines in the remote period after the Chernobyl accident. *Ecotoxicology*, 20 (6): 1195-1208.

Gichner, T., Patková, Z. & Kim, J. K. (2003). DNA Damage Measured by the Comet Assay in Eight Agronomic Plants. *Biologia Plantarum*, 47 (2): 185-188.

Gill, S. S. & Tuteja, N. (2010). Reactive oxygen species and antioxidant machinery in abiotic stress tolerance in crop plants. *Plant Physiology and Biochemistry*, 48 (12): 909-930.

Gill, S. S., Anjum, N. A., Gill, R., Jha, M. & Tuteja, N. (2015). DNA Damage and repair in plants under ultraviolet and ionizing radiations. *The Scientific World Journal*, 2015: 11.

Goltsova, N., Abaturov, Y., Abaturov, A., Melankholin, P., Girbasova, A. & Rostova, N. (1991). Chernobyl radionuclide accident: Effects on the shoot structure of Pinus sylvestris. *Annales Botanici Fennici*, 28 (1): 1-13.

Hamideldin, N. & Hussien, O. S. (2013). Morphological, physiological and molecular changes in *Solanum tuberosum* L. in response to pre-sowing tuber irradiation by gamma rays. *American Journal of Food Science and Technology*, 1 (3): 36-41.

https://www.genome.jp/kegg/. (2019).

Hu, Z., Cools, T. & De Veylder, L. (2016). Mechanisms used by plants to cope with DNA damage. *Annual Review of Plant Biology*, 67 (1): 439-462.

Hurem, S., Gomes, T., Brede, D. A., Lindbo Hansen, E., Mutoloki, S., Fernandez, C., Mothersill, C., Salbu, B., Kassaye, Y. A., Olsen, A.-K., et al. (2017). Parental gamma irradiation induces reprotoxic effects accompanied by genomic instability in zebrafish (*Danio rerio*) embryos. *Environmental Research*, 159: 564-578.

Hutchinson, F., Yamamoto, K., Stein, J. & Wood, R. D. (1988). Effect of photoreactivation on mutagenesis of lambda phage by ultraviolet light. *Journal of Molecular Biology*, 202 (3): 593-601.

Jalal, S., Earley, J. N. & Turchi, J. J. (2011). DNA repair: from genome maintenance to biomarker and therapeutic target. *Clinical cancer research : an official journal of the American Association for Cancer Research*, 17 (22): 6973-6984.

Jansen, M. A. K., Gaba, V. & Greenberg, B. M. (1998). Higher plants and UV-B radiation: balancing damage, repair and acclimation. *Trends in Plant Science*, 3 (4): 131-135.

Jansen, M. A. K. & Bornman, J. F. (2012). UV-B radiation: from generic stressor to specific regulator. *Physiologia Plantarum*, 145 (4): 501-504.

Jansen, M. A. K. (2017). *Ultraviolet-B radiation:Stressor and regulatory signal*. Pondicherry, India. 253-278 pp.

Kal'chenko, V. A. & Fedotov, I. S. (2001). Genetic effects of acute and chronic ionizing irradiation on *Pinus sylvestris* L. inhabiting the Chernobyl meltdown area. *Russian Journal of Genetics*, 37 (4): 341-350.

Kalchenko, V. A., Rubanovich, A., Fedotov, I. S. & Arkhipov, N. P. (1993). Genetical effects in gametes of *Pinus silvestris* L. induced in the Chernobyl accident. *Genetika*, 29 (7): 1205-1212.

Kashparova, E., Levchuk, S., Morozova, V. & Kashparov, V. (2018). A dose rate causes no fluctuating asymmetry indexes changes in silver birch (*Betula pendula* (L.) Roth.) leaves and Scots pine (*Pinus sylvestris* L.) needles in the Chernobyl Exclusion Zone. *Journal of Environmental Radioactivity*: 105731.

Kim, D. S., Kim, J.-B., Goh, E. J., Kim, W.-J., Kim, S. H., Seo, Y. W., Jang, C. S. & Kang, S.-Y. (2011). Antioxidant response of *Arabidopsis* plants to gamma irradiation: Genome-wide expression profiling of the ROS scavenging and signal transduction pathways. *Journal of Plant Physiology*, 168 (16): 1960-1971.

Kim, J.-B., Kim, S. H., Ha, B.-K., Kang, S.-Y., Jang, C. S., Seo, Y. W. & Kim, D. S. J. M. B. R. (2014). Differentially expressed genes in response to gamma-irradiation during the vegetative stage in *Arabidopsis thaliana*. 41 (4): 2229-2241.

Kim, J.-H., Baek, M.-H., Chung, B. Y., Wi, S. G. & Kim, J.-S. (2004). Alterations in the photosynthetic pigments and antioxidant machineries of red pepper (Capsicum annuum L.) seedlings from gamma-irradiated seeds. *Journal of Plant Biology*, 47 (4): 314-321.

Kovacs, E. & Keresztes, A. (2002). Effect of gamma and UV-B/C radiation on plant cells. *Micron*, 33: 199-210.

Kovalchuk, I., Molinier, J., Yao, Y., Arkhipov, A. & Kovalchuk, O. (2007). Transcriptome analysis reveals fundamental differences in plant response to acute and chronic exposure to ionizing radiation. *Mutation Research/Fundamental and Molecular Mechanisms of Mutagenesis*, 624 (1–2): 101-113.

Kozubov, G. M. & Taskaev, A. I. (1994). Radiobiological and radioecological studies of arboreous plants. *St. Pt. Nauka* 167-190.

Kozubov, G. M. & Taskaev, A. I. (2002). Radiobiology investigations of conifers in region of the Chernobyl disaster. *Moscow: PPC;* .

Kozubov, M. G. & Taskaev, I. A. (2007). *[Characteristics of morphogenesis and growth processes of conifers in the Chernobyl nuclear accident zone]*, vol. 47. 204-23 pp.

Laakso, K. & Huttunen, S. (1998). Effects of the ultraviolet-B radiation (UV-B) on conifers: a review. *Environmental Pollution*, 99 (3): 319-328.

Lafarge, S. & Montané, M. H. (2003). Characterization of *Arabidopsis thaliana* ortholog of the human breast cancer susceptibility gene 1: AtBRCA1, strongly induced by gamma rays. *Nucleic acids research*, 31 (4): 1148-1155.

Lee, H. O., Davidson, J. M. & Duronio, R. J. (2009). Endoreplication: polyploidy with purpose. *Genes & Development*, 23 (21): 2461-2477.

Lev-Yadun, S. & Sederoff, R. (2000). Pines as model gymnosperms to study evolution, wood formation, and perennial growth. *Journal of Plant Growth Regulation*, 19 (3): 290-305.

Lind, O. C., Helen Oughton, D. & Salbu, B. (2018). The NMBU FIGARO low dose irradiation facility. *International Journal of Radiation Biology*: 1-6.

Luckey, T. D. (2006). Radiation hormesis: the good, the bad, and the ugly. *Dose-response : a publication of International Hormesis Society*, 4 (3): 169-190.

Løvdal, T., Olsen, K. M., Slimestad, R., Verheul, M. & Lillo, C. (2010). Synergetic effects of nitrogen depletion, temperature, and light on the content of phenolic compounds and gene expression in leaves of tomato. *Phytochemistry*, 71 (5): 605-613.

Mackay, J., Dean, J. F. D., Plomion, C., Peterson, D. G., Cánovas, F. M., Pavy, N., Ingvarsson, P. K., Savolainen, O., Guevara, M. Á., Fluch, S., et al. (2012). Towards decoding the conifer giga-genome. *Plant Molecular Biology*, 80 (6): 555-569.

Makarenko, E. S., Oudalova, A. A. & Geras'kin, S. A. (2016). Study of needle morphometric indices in Scots pine in the remote period after the Chernobyl accident. *Radioprotection*, 51 (1): 19-23.

Manetas, Y., Petropoulou, Y., Stamatakis, K., Nikolopoulos, D., Levizou, E., Psaras, G. & Karabourniotis, G. (1997). Beneficial effects of enhanced UV-B radiation under field conditions: improvement of needle water relations and survival capacity of *Pinus pinea* L. seedlings during the dry mediterranean summer. In Rozema, J., Gieskes, W. W. C., Van De Geijn, S. C., Nolan, C. & De Boois, H. (eds) *UV-B and Biosphere*, pp. 100-108. Dordrecht: Springer Netherlands.

Manova, V. & Gruszka, D. (2015). DNA damage and repair in plants – from models to crops. *Frontiers in Plant Science*, 6: 885.

McIlwraith, M. J., Van Dyck, E., Masson, J.-Y., Stasiak, A. Z., Stasiak, A. & West, S. C. (2000). Reconstitution of the strand invasion step of double-strand break repair using human Rad51 Rad52 and RPA proteins11. *Journal of Molecular Biology*, 304 (2): 151-164.

Miller, M. W. & Miller, W. M. (1987). Radiation hormesis in plants. *Health Phys.* , 52 (5): 607-616.

Morgan, W. F., Day, J. P., Kaplan, M. I., McGhee, E. M. & Limoli, C. L. (1996). Genomic instability induced by ionizing radiation. *Radiation Research*, 146 (3): 247-258.

Morgan, W. F. (2003). Non-targeted and delayed effects of exposure to ionizing radiation: I. Radiation-induced genomic instability and bystander effects in vitro. *Radiation research* 5(159): 567-580.

Mothersill, C. & Seymour, C. B. (1998). Mechanisms and implications of genomic instability and other delayed effects of ionizing radiation exposure. *Mutagenesis*, 13 (5): 421-426.

Mrdakovic Popic, J., Raj Bhatt, C., Salbu, B. & Skipperud, L. (2012). Outdoor 220Rn, 222Rn and terrestrial gamma radiation levels: investigation study in the thorium rich Fen Complex, Norway. *Journal of Environmental Monitoring*, 14 (1): 193-201.

NASA. (2019). *The eelectromagnetic spectrum*.

NCBI. (2019). https://www.ncbi.nlm.nih.gov/. In *National Center for Biotechnology Information*.

Neale, D. B., Wegrzyn, J. L., Stevens, K. A., Zimin, A. V., Puiu, D., Crepeau, M. W., Cardeno, C., Koriabine, M., Holtz-Morris, A. E., Liechty, J. D., et al. (2014). Decoding the massive genome of loblolly pine using haploid DNA and novel assembly strategies. *Genome Biology*, 15 (3): R59.

Nogués, S. & Baker, N. R. (2000). Effects of drought on photosynthesis in mediterranean plants grown under enhanced UV-B radiation. *Journal of Experimental Botany*, 51 (348): 1309-1317.

Nybakken, L., Hörkkä, R. & Julkunen-Tiitto, R. (2012). Combined enhancements of temperature and UVB influence growth and phenolics in clones of the sexually dimorphic Salix myrsinifolia. 145 (4): 551-564.

Nystedt, B., Street, N. R., Wetterbom, A., Zuccolo, A., Lin, Y.-C., Scofield, D. G., Vezzi, F., Delhomme, N., Giacomello, S., Alexeyenko, A., et al. (2013). The Norway spruce genome sequence and conifer genome evolution. *Nature*, 497: 579.

Ouhibi, C., Attia, H., Rebah, F., Msilini, N., Chebbi, M., Aarrouf, J., Urban, L. & Lachaal, M. (2014). Salt stress mitigation by seed priming with UV-C in lettuce plants: Growth, antioxidant activity and phenolic compounds. *Plant Physiology and Biochemistry*, 83: 126-133.

Poulson, M. E., Boeger, M. R. T. & Donahue, R. A. (2006). Response of photosynthesis to high light and drought for Arabidopsis thaliana grown under a UV-B enhanced light regime. *Photosynthesis Research*, 90 (1): 79.

Quintiliani, M. (1986). The oxygen effect in radiation inactivation of DNA and enzymes. *International Journal of Radiation Biology and Related Studies in Physics, Chemistry and Medicine*, 50 (4): 573-594.

Rastogi, R. P., Richa, Kumar, A., Tyagi, M. B. & Sinha, R. P. (2010). Molecular mechanisms of ultraviolet radiation-induced DNA damage and repair. *Journal of nucleic acids*, 2010: 592980-592980.

Razinger, J., Drinovec, L. & Zrimec, A. (2010). Real-time visualization of oxidative stress in a floating macrophyte *Lemna minor* L. exposed to cadmium, copper, menadione, and AAPH. *Environmental Toxicology*, 25 (6): 573-580.

Real, A., Sundell-Bergman, S., F Knowles, J., S Woodhead, D. & Zinger, I. (2005). Effects of ionizing radiation exposure on plants, fish and mammals: Relevant data for environmental radiation protection. *Journal of Radiological Protection*, 24 (4): A123-37.

Reguera, M., Peleg, Z., Abdel-Tawab, Y. M., Tumimbang, E. B., Delatorre, C. A. & Blumwald, E. (2013). Stress-induced cytokinin synthesis increases drought tolerance through the coordinated regulation of carbon and nitrogen assimilation in rice. *Plant physiology*, 163 (4): 1609-1622.

Ricaud, L., Proux, C., Renou, J.-P., Pichon, O., Fochesato, S., Ortet, P. & Montané, M.-H. (2007). ATM-mediated transcriptional and developmental responses to gamma-rays in *Arabidopsis*. *PloS one*, 2 (5): e430-e430.

Robson, T. M., Hartikainen, S. M. & Aphalo, P. J. (2015a). How does solar ultraviolet-B radiation improve drought tolerance of silver birch (*Betula pendula* Roth.) seedlings? , 38 (5): 953-967.

Robson, T. M., Klem, K., Urban, O. & Jansen, M. A. K. (2015b). Re-interpreting plant morphological responses to UV-B radiation. *Plant, Cell & Environment*, 38 (5): 856-866.

Roy, S., Singh, S. K., Choudhury, S. R. & Sengupta, D. N. (2009). An insight into the biological functions of family X-DNA polymerase in DNA replication and repair of plant genome. *Plant signaling & behavior*, 4 (7): 678-681.

Rozema, J., van de Staaij, J., Björn, L. O. & Caldwell, M. (1997). UV-B as an environmental factor in plant life: stress and regulation. *Trends in Ecology & Evolution*, 12 (1): 22-28.

Sakakibara, H. (2006). *Cytokinins: Activity, biosynthesis, and translocation. Annu Rev Plant Biol*, vol. 57. 431-49 pp.

Salbu, B. (2016). Environmental impact and risk assessments and key factors contributing to the overall uncertainties. *Journal of Environmental Radioactivity*, 151: 352-360.

Schmidt, A.-M., Ormrod, D. P., Livingston, N. J. & Misra, S. (2000). The interaction of ultraviolet-B radiation and water deficit in two *Arabidopsis thaliana* genotypes. *Annals of Botany*, 85 (4): 571-575.

Scholes, R. D. & Paige, K. (2014). Plasticity in ploidy: A generalized response to stress. *Trends in Plant Biology*, 20 (3).

Shevchenko, V. A., Abramov, V. I., Kal'chenko, V. A., Fedotov, I. S. & Rubanovich, A. V. (1996). The genetic sequelae for plant populations of radioactive environmental pollution in connection with the Chernobyl accident. *Radiats Biol Radioecol.*, 36 (4): 531-545.

Shevchenko, V. V. & Grinikh, I. L. (1995). *[The cytogenetic effects in Crepis tectorum populations growing in Bryansk Province observed in the 7th year after the accident at the Chernobyl Atomic Electric Power Station]*, vol. 35. 720-5 pp.

Sidrak, G. H. & Suess, A. (1973). Effects of low doses of gamma radiation on the growth and yield of two varieties of tomato. *Radiation Botany*, 13 (6): 309-314.

Singh, S. K., Roy, S., Choudhury, S. R. & Sengupta, D. N. (2010). DNA repair and recombination in higher plants: insights from comparative genomics of Arabidopsis and rice. *BMC genomics*, 11: 443-443.

Sorochinsky, B. & Zelena, L. (2003). Is the cytoskeleton involved in the irradiation-induced abnormal morphogenesis of coniferous plants? *Cell Biol. Int.*, 27 (3): 275-277.

Steinhauser, G., Brandl, A. & Johnson, T. E. (2014). Comparison of the Chernobyl and Fukushima nuclear accidents: A review of the environmental impacts. *Science of The Total Environment*, 470-471: 800-817.

Stratmann, J. (2003). Ultraviolet-B radiation co-opts defense signaling pathways. *Trends in Plant Science*, 8 (11): 526-533.

TAIR. (2019). https://www.arabidopsis.org/portals/education/aboutarabidopsis.jsp. In *The Arabidopsis Information Resource*.

Takahashi, M., Teranishi, M., Ishida, H., Kawasaki, J., Takeuchi, A., Yamaya, T., Watanabe, M., Makino, A. & Hidema, J. (2011). Cyclobutane pyrimidine dimer (CPD) photolyase repairs ultraviolet-B-induced CPDs in rice chloroplast and mitochondrial DNA. 66 (3): 433-442.

Tamura, K., Adachi, Y., Chiba, K., Oguchi, K. & Takahashi, H. (2002). Identification of Ku70 and Ku80 homologues in *Arabidopsis thaliana*: evidence for a role in the repair of DNA double-strand breaks. 29 (6): 771-781.

The Arabidopsis Genome, I. (2000). Analysis of the genome sequence of the flowering plant Arabidopsis thaliana. *Nature*, 408 (6814): 796-815.

Tuteja, N., Singh, M. B., Misra, M. K., Bhalla, P. L. & Tuteja, R. (2001). Molecular mechanisms of DNA damage and repair: Progress in plants. *Critical Reviews in Biochemistry and Molecular Biology*, 36 (4): 337-397.

UNSCEAR. (1996). Sources and effects of ionizing radiation. *United Nations Scientific Commitee on the Effects of Atomic Radiation*.

UNSCEAR. (2010). Summary of low-dose radiation effects on health. New York. 1-14 pp.

UNSCEAR. (2017). Sources, effects and risks of ionizing radiation. *New York*. 184 pp.

Van Hoeck, A., Horemans, N., Van Hees, M., Nauts, R., Knapen, D., Vandenhove, H. & Blust, R. (2015). Characterizing dose response relationships: Chronic gamma radiation in *Lemna minor* induces oxidative stress and altered polyploidy level. *Journal of Environmental Radioactivity*, 150: 195-202.

Van Hoeck, A., Horemans, N., Nauts, R., Van Hees, M., Vandenhove, H. & Blust, R. (2017). *Lemna minor* plants chronically exposed to ionising radiation: RNA-seq analysis indicates a dose rate dependent shift from acclimation to survival strategies. *Plant Science*, 257: 84-95.

Vandenhove, H., Vanhoudt, N., Cuypers, A., van Hees, M., Wannijn, J. & Horemans, N. (2010). Life-cycle chronic gamma exposure of *Arabidopsis thaliana* induces growth effects but no discernable effects on oxidative stress pathways. *Plant Physiology and Biochemistry*, 48 (9): 778-786.

Vanhoudt, N., Horemans, N., Wannijn, J., Nauts, R., Van Hees, M. & Vandenhove, H. (2014). Primary stress responses in *Arabidopsis thaliana* exposed to gamma radiation. *Journal of Environmental Radioactivity*, 129: 1-6.

Verma, V., Ravindran, P. & Kumar, P. P. (2016). Plant hormone-mediated regulation of stress responses. *BMC Plant Biology*, 16 (1): 86.

Vonarx, J. E., Mitchell, L. H., Karthikeyan, R., Chatterjee, I. & Kunz, B. (1998). *DNA repair in higher plants*, vol. 400. 187-200 pp.

Wang, X.-Q. & Ran, J.-H. (2014). Evolution and biogeography of gymnosperms. *Molecular Phylogenetics and Evolution*, 75: 24-40.

Watanabe, Y., Ichikawa, S. e., Kubota, M., Hoshino, J., Kubota, Y., Maruyama, K., Fuma, S., Kawaguchi, I., Yoschenko, V. I. & Yoshida, S. (2015). Morphological defects in native Japanese fir trees around the Fukushima Daiichi Nuclear Power Plant. *Scientific Reports*, 5: 1-7.

Waterworth, W. M., Drury, G. E., Bray, C. M. & West, C. E. (2011). Repairing breaks in the plant genome: the importance of keeping it together. *New Phytologist*, 192 (4): 805-822.

Weimer, A. K., Biedermann, S., Harashima, H., Roodbarkelari, F., Takahashi, N., Foreman, J., Guan, Y., Pochon, G., Heese, M., Van Damme, D., et al. (2016). The plant-specific CDKB1-CYCB1 complex mediates homologous recombination repair in Arabidopsis. *The EMBO Journal*, 35 (19): 2068-2086.

West, C. E., Waterworth, W. M., Jiang, Q. & Bray, C. M. (2000). *Arabidopsis* DNA ligase IV is induced by γ-irradiation and interacts with an *Arabidopsis* homologue of the double strand break repair protein XRCC4. *The Plant Journal*, 24 (1): 67-78.

Wi, S. G., Chung, B. Y., Kim, J.-H., Baek, M.-H., Yang, D. H., Lee, J.-W. & Kim, J.-S. (2005). Ultrastructural changes of cell organelles in *Arabidopsis* stems after gamma irradation. *Journal of Plant Biology*, 48 (2): 195-200.

Wi, S. G., Chung, B. Y., Kim, J.-S., Kim, J.-H., Baek, M.-H., Lee, J.-W. & Kim, Y. S. (2007). Effects of gamma irradiation on morphological changes and biological responses in plants. *Micron*, 38 (6): 553-564.

Woodwell, G. M. (1962). Effects of ionizing radiation on terrestrial ecosystems. *Science*, 138 (3540): 572-577.

Woodwell, G. M. & Rebuck, A. L. (1967). Effects of chronic gamma radiation on the structure and diversity of an oak-pine forest. *Ecological Monographs*, 37 (1): 53-69.

Yakes, F. M. & Van Houten, B. (1997). Mitochondrial DNA damage is more extensive and persists longer than nuclear DNA damage in human cells following oxidative stress. *Proceedings of the National Academy of Sciences of the United States of America*, 94 (2): 514-519.

Yokota, Y., Shikazono, N., Tanaka, A., Hase, Y., Funayama, T., Wada, S. & Inoue, M. (2005). Comparative Radiation Tolerance Based on the Induction of DNA Double-Strand Breaks in Tobacco BY-2 Cells and CHO-K1 Cells Irradiated with Gamma Rays. *Radiation Research*, 163 (5): 520-525.

Yokota, Y., Funayama, T., Hase, Y., Hamada, N., Kobayashi, Y., Tanaka, A. & Narumi, I. (2010). Enhanced micronucleus formation in the descendants of γ-ray-irradiated tobacco cells: Evidence for radiation-induced genomic instability in plant cells. *Mutation Research/Fundamental and Molecular Mechanisms of Mutagenesis*, 691 (1): 41-46.

Yoschenko, V., Ohkubo, T. & Kashparov, V. (2018). Radioactive contaminated forests in Fukushima and Chernobyl. *Journal of Forest Research*, 23 (1): 3-14.

Yoshiyama, K., Conklin, P. A., Huefner, N. D. & Britt, A. B. (2009). Suppressor of gamma response 1 (SOG1) encodes a putative transcription factor governing multiple responses to DNA damage. *Proceedings of the National Academy of Sciences of the United States of America*, 106 (31): 12843-12848.

Yoshiyama, K. O., Kobayashi, J., Ogita, N., Ueda, M., Kimura, S., Maki, H. & Umeda, M. (2013). ATM-mediated phosphorylation of SOG1 is essential for the DNA damage response in *Arabidopsis*. *EMBO Reports*, 14 (9): 817-822.

Zelena, L., Sorochinsky, B., von Arnold, S., van Zyl, L. & Clapham, D. H. (2005). Indications of limited altered gene expression in Pinus sylvestris trees from the Chernobyl region. *Journal of Environmental Radioactivity*, 84 (3): 363-373.

Zimin, A., Stevens, K. A., Crepeau, M. W., Holtz-Morris, A., Koriabine, M., Marçais, G., Puiu, D., Roberts, M., Wegrzyn, J. L., de Jong, P. J., et al. (2014). Sequencing and Assembly of the 22-Gb Loblolly Pine Genome. *Genetics*, 196 (3): 875.

Paper I

Planta (2019) 250:1567–1590
https://doi.org/10.1007/s00425-019-03250-y

ORIGINAL ARTICLE

Comparative sensitivity to gamma radiation at the organismal, cell and DNA level in young plants of Norway spruce, Scots pine and *Arabidopsis thaliana*

Dajana Blagojevic[1,2] · YeonKyeong Lee[1,2] · Dag A. Brede[2,3] · Ole Christian Lind[2,3] · Igor Yakovlev[4] · Knut Asbjørn Solhaug[2,3] · Carl Gunnar Fossdal[4] · Brit Salbu[2,3] · Jorunn E. Olsen[1,2]

Received: 21 December 2018 / Accepted: 25 July 2019 / Published online: 1 August 2019

Abstract

Main conclusion **Persistent DNA damage in gamma-exposed Norway spruce, Scots pine and *Arabidopsis thaliana*, but persistent adverse effects at the organismal and cellular level in the conifers only.**

Gamma radiation emitted from natural and anthropogenic sources may have strong negative impact on plants, especially at high dose rates. Although previous studies implied different sensitivity among species, information from comparative studies under standardized conditions is scarce. In this study, sensitivity to gamma radiation was compared in young seedlings of the conifers Scots pine and Norway spruce and the herbaceous *Arabidopsis thaliana* by exposure to ^{60}Co gamma dose rates of 1–540 mGy h^{-1} for 144 h, as well as 360 h for *A. thaliana*. Consistent with slightly less prominent shoot apical meristem, in the conifers growth was significantly inhibited with increasing dose rate ≥ 40 mGy h^{-1}. Post-irradiation, the conifers showed dose-rate-dependent inhibition of needle and root development consistent with increasingly disorganized apical meristems with increasing dose rate, visible damage and mortality after exposure to ≥ 40 mGy h^{-1}. Regardless of gamma duration, *A. thaliana* showed no visible or histological damage or mortality, only delayed lateral root development after ≥ 100 mGy h^{-1} and slightly, but transiently delayed post-irradiation reproductive development after ≥ 400 mGy h^{-1}. In all species dose-rate-dependent DNA damage occurred following ≥ 1–10 mGy h^{-1} and was still at a similar level at day 44 post-irradiation. In conclusion, the persistent DNA damage (possible genomic instability) following gamma exposure in all species may suggest that DNA repair is not necessarily mobilized more extensively in *A. thaliana* than in Norway spruce and Scots pine, and the far higher sensitivity at the organismal and cellular level in the conifers indicates lower tolerance to DNA damage than in *A. thaliana*.

Keywords DNA damage · Development · Growth · Ionizing radiation · *Picea abies* · *Pinus sylvestris*

Introduction

Living organisms like plants are exposed to a variety of environmental stressors, including ionizing radiation from natural sources such as cosmic radiation and naturally occurring radioactive materials (NORM) such as uranium, thorium and their progenies contained in bedrocks, sediments and soils (Paschoa 1998). The current global mean background dose rate is 2.5 mGy $year^{-1}$, which corresponds to about 0.29 μGy h^{-1}, but there are also specific areas with naturally elevated ionizing radiation level such as 4–5 or 14–15 μGy h^{-1} (Caplin and Willey 2018). Increased doses of radiation in the environment are also due to releases of radionuclides from anthropogenic activities, such as those related to the nuclear weapons and fuel cycles. Based on

Electronic supplementary material The online version of this article (https://doi.org/10.1007/s00425-019-03250-y) contains supplementary material, which is available to authorized users.

✉ Jorunn E. Olsen
jorunn.olsen@nmbu.no

[1] Department of Plant Sciences, Faculty of Biosciences, Norwegian University of Life Sciences, P.O. Box 5003, 1432 Ås, Norway

[2] Centre of Environmental Radioactivity (CERAD), Norwegian University of Life Sciences, P.O. Box 5003, 1432 Ås, Norway

[3] Faculty of Environmental Sciences and Natural Resource Management, Norwegian University of Life Sciences, P.O. Box 5003, 1432 Ås, Norway

[4] Norwegian Institute of Bioeconomy Research, 1431 Ås, Norway

results from experiments and observations after accidents, it has been noted that acute high doses of ionizing radiation between 10 and 1000 Gy can be lethal to plants, and that < 10 mGy day^{-1} (about 0.42 mGy h^{-1}) does probably not result in damage to terrestrial plants in the field (UNSCEAR 1996; Caplin and Willey 2018). Largely based on health consequences, low doses and dose rates of ionizing radiation such as gamma radiation are currently defined as ≤ 100 mGy and ≤ 6 mGy h^{-1}, respectively (UNSCEAR 2017; Averbeck et al. 2018). Of the different types of electromagnetic radiation, gamma radiation has the highest energy and accordingly high penetration power (Caplin and Wiley 2018).

Exposure to gamma radiation can result in biological responses such as DNA damage, oxidative stress, growth reduction, reproduction impairment and morphological alterations (Reisz et al. 2014; Caplin and Willey 2018). These can arise either through direct ionization of DNA or other biomolecules, or indirectly via ionization and excitation of water molecules, resulting in production of free radicals, followed by recombination to reactive oxygen species (ROS). Being highly reactive, ROS may rapidly injure and interfere with the function of macromolecules such as proteins, lipids, and nucleic acids (Woodwell and Rebuck 1967; Azzam et al. 2012; Esnault et al. 2010; Caplin and Willey 2018).

The responses of organisms including plants towards gamma irradiation may vary between species and may depend on cultivar, stage of development, tissue architecture and genome organization as well as exposure scenario (De Micco et al. 2011). Previous studies have demonstrated great morphological and functional variation for plants upon exposure to acute, semi-chronic and chronic high doses of gamma radiation (Woodwell 1962; Kawai and Inoshita 1965; Killion and Constantin 1972; Wi et al. 2007). Following the Chernobyl nuclear power plant accident, conifer trees were strongly affected by acute irradiation. Especially Scots pine (*Pinus sylvestris*), which is a dominating tree species in this region, experienced high mortality close to the power plant zone (Yoschenko et al. 2017; Tulik 2001; Zelena et al. 2005). Recently, it was reported that the calculated absorbed gamma dose in dead pine trees in the Chernobyl area was 80–100 Gy (Kashparova et al. 2018). Previously, it was estimated that conifers during the first 2 weeks after the power plant accident received a dose close to 3.7 Gy (Fesenko et al. 2005). Under high-dose chronic irradiation, cancelling of the apical dominance occurred in young populations of Scots pine in the Chernobyl exclusion zone as well as in Japanese red pine (*Pinus densiflora*) and Japanese fir (*Abies firma*) in the Fukushima power plant accident zone (Watanabe et al. 2015; Goltsova et al. 1991). In a field study of an oak–pine forest in central Long Island, New York, which was chronically exposed to gamma radiation of 9.500 Ci from ^{137}Cs (corresponding to $3.52. \times 10^8$ MBq) during 4 years, *P. sylvestris* displayed mortality, whereas all plants of the herbaceous *Carex pensylvanica* and *Ericaceous* shrubs survived (Woodwell and Rebuck 1967; Woodwell 1962; Amiro and Sheppard 1994). Another field gamma irradiation study showed that long-term exposure (14 years) exacerbates the effects on the coniferous trees and revealed that pine trees were affected at ≥ 0.1 mGy h^{-1} (Amiro and Sheppard 1994). Additionally, high mortality of oak and pine species in later studies demonstrated high radiosensitivity in such woody species (Stalter and Kincaid 2009). In plants of the short-lived herbaceous species *Arabidopsis thaliana*, low chronic gamma exposure (81–2339 μGy h^{-1} for 24–54 days) induced negative growth effects (Nagata et al. 1999; Vandenhove et al. 2010). Other studies of this species have shown growth inhibition and ultrastructural changes after 50 Gy as well as increased leaf trichome formation after massive acute doses of 1–3 kGy from an external ^{60}Co source (Wi et al. 2005; Nagata et al. 1999).

Plants possess DNA damage response systems to sense DNA damage, arrest the cell cycle, repair DNA lesions and induce programmed cell death (Yoshiyama et al. 2013). Still, depending on the duration and level of the exposure, plants exhibit differences in gene expression responses depending on whether plants were acutely or chronically irradiated (Kovalchuk et al. 1999, 2007). However, DNA damage triggers biochemical signals that activate DNA repair mechanisms, playing a crucial role in recovering DNA strands from damage. The *RADIATION 51* (*RAD51*) gene, which is involved in homologous recombination, were induced following gamma exposure (Yoshiyama et al. 2013). Furthermore, several genes in the DNA repair pathways are modulated through SUPPRESSOR OF GAMMA RESPONSE 1 (SOG1), which consecutively activate canonical pathways involved in DNA repair, apoptosis and endoreplication (Yoshiyama et al. 2013).

Furthermore, checkpoints responsible for delay in cell cycle progression are essential for plants to accommodate time for sufficient DNA repair. If DNA damage cannot be repaired, checkpoints aim to induce permanent cell cycle arrest or cell death (apoptosis) in an attempt to eliminate such severely damaged cells. This is achieved by activation of cell cycle checkpoints that target the cyclin (CYC)/cyclin-dependent kinase (CDK)-complex that normally promotes cell cycle progression (Deckbar et al. 2011). However, *A. thaliana* exposed to gamma radiation, showed induction of specific cell cycle genes such as *CYCB1;1* and suppression of *CDKB2;1* 1.5 h after 100 Gy (2 days of irradiation) (Culligan et al. 2006; Yoshiyama et al. 2009).

To counteract ROS-induced oxidative stress, plants can modulate their antioxidative defence systems, which include ROS scavenging enzymes and non-enzymatic

antioxidant metabolites. By this, cellular damage can be avoided, while still allowing ROS-dependent signalling known to be an integrated part of defence responses (Mittler et al. 2004; Gill and Tuteja 2010; Ahmad et al. 2010). Different antioxidant enzymes such as catalase (CAT), glutathione reductase (GR), superoxide dismutase (SOD), ascorbate peroxidase (APOD), syringaldazine peroxidase (SPOD) and guaiacol peroxidase (GPOD) and metabolites like glutathione, flavonoids, phenolic compounds and carotenoids are typically induced to reduce elevated concentrations of singlet oxygen ($^1O_2$), superoxide radical (O_2^-), hydrogen peroxide (H_2O_2) or hydroxyl radical (HO·) in plant cells (Apel and Hirt 2004). Such enzyme activities have been well studied in *A. thaliana* (Barescut et al. 2012; Kim et al. 2011) and a range of other plant species, such as *Capsicum annuum*, *Lemna minor*, *Stipa capillata*, *Rosmarinus officinalis* and *Raphanus sativus L.* (Kim et al. 2005).

Plants possess stem cells in their shoot apical meristem (SAM) and root apical meristem (RAM), which are crucial in plant development and growth. In gamma irradiation experiments, histological analyses of *Pinus pinea* and *Pinus halepensis* suggested different radiosensitivity of different meristematic cells of the SAM. Cells of the apical initial zone and the central mother zone, which have low mitotic rates, showed greater radiosensitivity than the cells of the rib meristem and the peripheral tissue zone, which have higher mitotic rates (Donini 1967).

Although a wide range of studies have addressed effects of high doses or dose rates of gamma radiation particularly in field-grown plants, and the responses may differ between species, detailed information about cross-species sensitivity to gamma irradiation under standardized conditions is limited, particularly in the low-to-medium dose rate and dose area. Also, information about gamma sensitivity in young conifer seedlings is scarce. The aims of this study were to systematically compare the organismal, cellular and DNA level sensitivity of young plants of the ecologically and economically important conifers Norway spruce and Scots pine and the herbaceous model plant *A. thaliana*, all species with partly overlapping distribution range, to gamma irradiation under standardized conditions.

Materials and methods

Plant materials and pre-growing conditions

Seeds of the Landsberg *erecta* (L*er*) accession of *Arabidopsis thaliana* (L). Heyhn, were surface sterilized for 3 min in a solution consisting of 9 mL of 70% ethanol and one droplet of Tween 20, rinsed five times in distilled water, followed by a quick rinse in 96% ethanol before air drying. Seeds of Scots pine (*Pinus sylvestris* L.) and Norway spruce (*Picea abies* L. H. Karst), both from the provenance CØ1 from Halden (59°N latitude), Norway (seed lots 5632 and 98,063, respectively, Skogfrøverket, Hamar, Norway (www.skogfroverket.no)) were surface sterilized in 1% sodium hypochlorite for 5 min, rinsed five times in distilled water and placed on a filter paper for drying. Since these conifer seeds were harvested in the field a more efficient sterilization agent than ethanol was required, and it could also be noted that the vitality of these seeds was seriously decreased (high mortality) by ethanol treatment so ethanol could not be used. All seeds were evenly sown on ½ MS medium ((Murashige and Skoog 1962); Duchefa Biochemie, Haarlem, Netherlands) with 0.8% agar (Plant agar, Sigma-Aldrich, St. Louis, MO, USA) in Petri dishes of 5 cm diameter. The *A. thaliana* seeds were stratified in darkness for 4 days at 4 °C. The conifer seeds were not stratified since their germination was sufficient even without stratification. All seeds were germinated for 6 days at 20 °C under a photon flux density of 30 µmol m^{-2} s^{-1} at 400–700 nm (TL-D 58 W/840 lamps, Philips, Eindhoven, The Netherlands) in a 16-h photoperiod.

Gamma irradiation of plants using a ^{60}Co source and growing conditions during the exposure

Six-day-old seedlings of Norway spruce, Scots pine, and *A. thaliana* were exposed to gamma radiation with gamma dose rates ranging from 1 to 540 mGy h^{-1} (Tables 1, 2), using the FIGARO low-dose gamma irradiation facility (^{60}Co; 1173.2 and 1332.5 keV γ-rays) at the Norwegian University of Life Sciences (Lind et al. 2018). The Petri dishes with seedlings were placed in two rows with columns of four Petri dishes in front of the collimator. Scots pine and Norway spruce seedlings were exposed for 144 h at day 7–12 after sowing, while *A. thaliana* seedlings got 144 h or 360 h of exposure at day 7–12 and 7–21 after sowing, respectively (Tables 1, 2) since previous studies indicated high tolerance to ionizing radiation in this species. During the gamma irradiation, the room temperature was set at 20 °C ± 1 °C with a 12-h photoperiod with a photon flux density of 55 µmol m^{-2} s^{-1} provided by high-pressure metal halide lamps (HPI-T Plus 250 W lamps, Philips, Eindhoven, The Netherlands). The irradiance was measured at the top of the Petri dishes with a Li-Cor Quantum/Radiometer/Photometer (model LI-250, LI-COR, Lincoln, NE, USA). The red:far red (R:FR) ratio was 3.5, as measured by a 660/730 nm sensor (Skye Instruments, Powys, Wales, UK).

Table 1 The gamma radiation treatments applied in the different experiments with exposure of young seedlings of Norway spruce, Scots pine and *Arabidopsis thaliana* for 144 h or *A. thaliana* for 360 h using a ^{60}Co source

Dose rate (mGy h^{-1})	Dose rate interval (mGy h^{-1})		Total dose (Gy) after 144-h exposure	Total dose interval 144-h exposure (Gy)		Total dose (Gy) after 360-h exposure	Total dose interval 360-h exposure (Gy)	
	Minimum	Maximum		Minimum	Maximum		Minimum	Maximum
540	475	605	77.8	68	87	194.4	171	218
430	378	482	61.9	54	69	154.8	136	173
400	352	448	57.6	51	65	144	127	161
350	308	392	50.4	44	56	–	–	–
290	255	325	41.8	37	47	–	–	–
180	158	202	25.9	23	29	64.8	57	73
100	88	112	14.4	13	16	36.0	32	40
40	35	45	5.8	5.1	6.5	14.4	13	16
10	8.8	11.2	1.4	1.2	1.6	3.6	3.2	4.0
1	0.88	1.12	0.14	0.12	0.16	0.36	0.32	0.40

To ensure more even irradiance and gamma radiation, in the middle of each experiment the Petri dishes were rotated 180° and the two upper and two lower dishes were interchanged. At termination of the gamma exposure there were no signs of different pigmentation or any other visible differences between the plants of any of the species in the different positions in the Petri dish columns. Control samples not exposed to gamma radiation were positioned outside the radiation sector, shielded by lead walls, in the same room and under light and temperature conditions and in columns as described for the gamma radiated seedlings.

For Scots pine and Norway spruce totally three and two repeated experiments were performed, respectively (144-h gamma exposure), whereas for *A. thaliana* three and two repeated experiments were performed for 144-h and 360-h gamma exposure, respectively.

Dosimetry of the exposed plant followed an established protocol (Hansen et al. 2019). Petri dishes with plants were positioned at distances from the gamma source corresponding to the nominal dose rates, dose rate intervals, total doses and total dose intervals presented in Table 1. Field dosimetry (air kerma rates measured with an ionization chamber) was traceable to the Norwegian Secondary Standard Dosimetry Laboratory (Norwegian Radiation Protection Authority, NRPA, Oslo, Norway). Dose rates to water in the centre of the Petri dishes were estimated according to Hansen et al. (2019) and used as a proxy for dose rates to the plants. To confirm calculated dose rates at the various positions, actual air kerma rates were measured for selected representative exposure set-ups using an Optically Stimulated Luminescence (OSL) based dosimetry system from Landauer, i.e. nanoDots dosimeters and InLight microSTAR reader (Landauer, Greenwood, IL, USA). Uncertainties ($K=2$) for nanoDot measurements are ~ 5%. Total doses were calculated from estimated absorbed dose rates to water (mGy h^{-1}), multiplied by total exposure time (h). Dose rate and dose intervals were estimated based on the highest exposure variation ($<\pm12\%$) that the plants could experience between the front (closest to the gamma source) and back of Petri dishes.

Post-irradiation growing conditions

After termination of the gamma treatment, plants were transferred to pots (7.5 cm diameter and 7 cm height for *A. thaliana*; 5 cm diameter and 5 cm height for Norway spruce and Scots pine) filled with S-soil (45% low moist peat, 25% high moist peat, 25% perlite and 5% sand; Hasselfors Garden AS, Örebro, Sweden). Four plants per pot of *A. thaliana* and two plants per pot of Scots pine and Norway spruce were cultivated in growth chambers (manufactured by Norwegian University of Life Sciences). Temperature was set at 20 °C and the relative air humidity (RH) was adjusted to 78%, corresponding to 0.5 kPa water vapour pressure deficiency. The main light phase was provided by high-pressure metal halide lamps (HPI-T Plus 250 W, Phillips) with the R:FR ratio adjusted to 1.7 with incandescent lamps (Osram, Munich, Germany).

For *A. thaliana* a 12-h photoperiod was provided with an initial photon flux intensity of 50 µmol m^{-2} s^{-1} which was gradually increased to 100 µmol m^{-2} s^{-1} during 7 days. The photoperiod was then reduced to 8 h since a reduced photoperiod resulting in slower induction of flowering, might make it easier to distinguish differences between treatments in this respect. Similar irradiance and photoperiod have previously been used in a large number of studies addressing the timing of reproductive development in *A. thaliana*. Temperature, R:FR ratio and RH remained the same. In one experiment with 144-h gamma exposure of *A. thaliana*, a different type of growth chamber with another type of main light than in the other experiments, was used (Conviron

Table 2 Overview of the gamma exposure experiments of different species and recorded parameters/analyses performed

Duration of gamma exposure (h)	Species	Number of repeated experiments	Age of plants during exposure	Dose rates (mGy h^{-1})
Gamma exposure details				
144	Scot spine	3	7–12 days after sowing	1, 10, 40, 100, 180, 290, 350, 400, 430, 540
	Norway spruce	2		
	Arabidopsis	3		
360	*Arabidopsis*	2	7–21 days after sowing	1, 10, 40, 100, 180, 290, 400, 430, 540

Time point	Parameter	Species	Number of experiments	Number of replicates treatment^{-1} experiment^{-1}	Total number of replicates treatment^{-1}	Figures
Details for different analyses						
At the end of the irradiation	Shoot and root length	Scots pine, Norway spruce	2	4–6	8–12 (some dose rates 4–6)	1a, b
	Lateral root growth	*Arabidopsis*	144 h: 2 360 h: 1	10–15 25	20–30 (some dose rates 10–15) 25	2b, c
	Histology	All species (Conifers 144 h, *Arabidopsis* 360 h)	1	6	6	1c, 2a
	DNA damage	All species (144 h and 360 h)	1	3 (3:3 or 5)	3	3
	Transcripts	All species (144 h)	1	4 (2–4: 4–10)	4	4, 5
Post-irradiation, 44 days (time course for growth)	Shoot diameter, root growth	Scots pine, Norway spruce	2	10–20	20–40	6c, d, 7
	Number of leaves	All species (144 h and 360 h)	2	10–20	20–40	6a, b, 9a
	Floral development	*Arabidopsis*	144 h: 3 360 h: 2	10–20 10–20	30–60 20–40	9d–g
	Histology	All species (SAM conifers 144 h, leaf *Arabidopsis* 360 h)	1	6	6	8, 9c
	F_v/F_m	*Arabidopsis* 144 h	1	35	35	9b
	DNA damage	All species; (conifers 144 h, *Arabidopsis* 360 h)	1	3 (3:3,5 or 10)	3 (3:3)	10

For growth measurements the number of plants per treatment is shown. For other parameters the number of samples per treatment is shown with the first number in brackets referring to number of technical replicates and the second number to the number of pooled plants per sample. For DNA damage analysis (gels) 50–100 cell nuclei were scored per technical replicate (gel)

growth chambers, Controlled Environments Ltd., Winnipeg, Canada). This chamber was equipped with fluorescent light tubes (60 W lamps, Phillips) and incandescent lamps. Except the different spectral distribution provided by fluorescent lamps compared to metal halide lamps, all other growing conditions were adjusted as described above.

For Norway spruce and Scots pine, a 24-h photoperiod was given with the 12-h main light period provided by the metal halide and incandescent lamps, followed by 12-h day extension with low-intensity light from incandescent lamps only (8–10 µmol m^{-2} s^{-1}). For these species, the irradiance during the main light phase was gradually increased from 50 to 180 µmol m^{-2} s^{-1} during 7 days. These light parameters were given to ensure sustained growth of the northern latitudinal ecotypes of the conifers used in this study. Such woody species show increased sensitivity to photoperiod after the first period following germination, and then requires long days at a certain irradiance to prevent growth cessation and formation of a terminal bud (Olsen 2010).

Growth parameter recordings

At termination of the gamma irradiation, the total plant length of Norway spruce and Scots pine seedlings was

measured by use of Image J in 4–6 plants per treatment in each of two experiments for each species. In *A. thaliana* the number of lateral roots was counted in 10–15 plants per treatment in each of two experiments after exposure to 144 h of gamma radiation, and in 25 plants per treatment in another experiment with 360 h of gamma. An overview of the measured growth parameters and the other analysed parameters (described below) directly after the radiation and post-irradiation, is shown in Table 2.

Post-irradiation, in *A. thaliana*, the number of rosette leaves before appearance of flower buds was counted in 20 plants per treatment in a time course in each of two experiments for each gamma exposure duration. In 20 plants per treatment in each of the three and two experiments with 144-h and 360-h gamma radiation, respectively, the number of plants with visible flower buds was recorded in a time course, and the percentage of plants with flower buds at the different time points calculated. The percentage of plants with elongating inflorescence at the different time points was also calculated for each dose rate.

Post-irradiation, in Norway spruce and Scots pine, the number of needles was recorded, and plant height was measured from the rim of the pot to the apical meristem and the cumulative growth calculated in 10–20 plants per gamma treatment in time courses in each of two experiments. Plant diameter from needle tip to needle tip across the plant at the shoot apex was calculated from two perpendicular measurements for each of 10–20 plants per treatment in two experiments. The length of the longest root and the number of lateral roots were recorded in 4 plants per gamma treatment 44 days after termination of the exposure in one experiment in Norway spruce and in each of two experiments with Scots pine. The number of dead plants without any green tissue was registered in each of two experiments per species at day 36 after termination of the gamma exposure.

RNA extraction and analyses of transcript levels

For studies of relative transcript levels at the termination of the gamma exposure, per dose rate four biological replicates (samples), each consisting of 10 and 4 pooled shoots, respectively, of *A. thaliana* and conifer seedlings (i.e. Norway spruce and Scot pine separately) were harvested in liquid nitrogen after 144-h gamma exposure and stored at − 80 °C until analyses. Total RNA was extracted using the Masterpure Complete DNA and RNA Purification Kit (Epicenter, Madison, WI, USA) following the manufacturer's instructions except that 0.5% polyvinylpyrrolidone (PVP), mw 360 000, Sigma-Aldrich, Steinheim, Germany) was added to the extraction buffer and that 3 µl beta-mercaptoethanol per sample replaced the 1,4-dithiothreitol (DTT) in the manufacturer's protocol. RNA quality was assessed using an Agilent 2100 Bioanalyzer with an RNA 144,000 NanoKit (Agilent technologies, Palo Alto, CA, USA) and the quantity of isolated RNA was measured by a NanoDrop ND-1000 Spectrophotometer (Thermo Scientific, Wilmington, DE, USA). cDNA was synthesized from 2 µl RNA in a 20-µl reaction using reverse transcriptase 10xVILO (Invitrogen, Carlsbad, CA, US). The synthesized cDNA was diluted 1:5 and used for RT-quantitative PCR.

In Norway spruce and *A. thaliana, ACTIN (ACT)* and *ELONGATION FACTOR 1-α* (*EF1-α*) were used as reference genes while in Scots pine *ACT* and *GLYCERALDEHYDE-3-PHOSPHATE DEHYDROGENASE* (*GAPDH*) were used as reference genes for quantification of the relative transcript levels of *CYCLIN B1;2* (*CYCB1;2*), *CYCLIN-DEPENDENT KINASE B1;2* (*CDKB1;2*), *CYCLIN D3;1 (CYCD3;1), RADIATION 51 (RAD51)*, *SUPPRESSOR OF GAMMA RESPONSE 1* (*SOG1), PEROXIDASE (PX3), CATALASE (CAT), SUPEROXIDE DISMUTASE (SOD), PHENYLALANINE AMMONIA-LYASE (PAL)* and Class *IV CHITINASE (CHI4*) in the respective species (Supplementary Table S1, S2, S3). These genes were selected partly on basis of previous publications showing effect of gamma radiation of these genes in at least one of the three plant species (Culligan et al. 2006; Yoshiyama et al. 2013; Deflorio et al. 2011; De Veylder et al. 2011; Yoshiyama et al. 2009). The specific genes in the different species were selected on basis of maximum sequence similarity as compared to other genes within the specific gene family.

Gene-specific primers (Supplementary Table S1, S2, S3) were designed using the Primer3 software (Rozen and Skaletsky 2000) with default parameters and amendments according to the following criteria: melting temperature around 60 °C and product size between 100 and 150 bp. All primers were tested for their product base pair length on 1% agarose gel (Agar, Sigma-Aldrich, Steinheim, Germany). The amplifications were performed with a 7500 Fast Real-time PCR system (Applied Biosystems, Foster city, USA) with 20 µl of Platinum Quantitative PCR Supermix-UDG and SYBRGreen (Thermo Fisher, Carlsbad, CA, US) using 2 µl diluted cDNA, 10 µl SYBR Green, 7 µl RNase-free H_2O and 0.5 µl of each primer. The following program was used for amplification: 95 °C for 2 min, followed by 45 cycles of 95 °C for 15 s and 60 °C for 35 s. A non-template control was run for each primer pair.

In order to investigate the relative transcript levels and to compare the samples from different gamma treatments with the unexposed no gamma control (for each species; 0 mGy h^{-1}), the comparative Ct (Cycle threshold) method (ΔΔCt method) was used. The Ct values were calculated for the gamma-treated samples ($Ct_{\text{target gene-treated sample}} - Ct_{\text{reference gene-treated sample}}$) and the control samples not exposed to gamma ($Ct_{\text{target gene control sample}} - Ct_{\text{reference gene control sample}}$). Furthermore, the ΔΔCt value was calculated for each of the gamma-treated samples

($\Delta\Delta Ct_{treated\ sample} = \Delta Ct_{treated\ sample} - \Delta Ct_{calibrator\ (control)\ sample}$). The relative transcript levels of specific genes in the different gamma-treated samples were presented as fold difference in log^2 scale: fold difference $= log^2\ (RQ) = -\Delta\Delta Ct$. For all gamma dose rates, including the unexposed controls, 4 repeated samples consisting of 4 plants each were analysed using 2–4 technical replicates.

Plant tissue preparation and histological studies

Histological studies in Norway spruce, Scots pine (both 144-h gamma radiation) and *A. thaliana* plants (360-h gamma radiation) were performed according to Lee et al. (2017). At the termination of the gamma exposure and 44 days thereafter, 3 mm of shoot tips (all species, except *A. thaliana* at day 44) and 3 mm of root tips (only conifers at day 44 day only) from each of 6 individual plants per species per treatment were harvested for these analyses. Since all *A. thaliana* plants had inflorescences 44 days after termination of the exposure and accordingly no vegetative shoot apical meristems, shoot apices were not harvested, but 3 rosette leaves from the top of the leaf rosette (the 3 topmost leaves in the rosette) from each of 6 plants were used per treatment. The plant materials were immediately fixed in 4% formaldehyde solution and 0.025% glutaraldehyde in sodium phosphate buffer (PBS, pH 7.0) and vacuum infiltrated at room temperature for 1 h and thereafter kept at 4 °C overnight. The fixed samples were then washed with PBS, and dehydrated in a graded ethanol series. Infiltration was performed with a progressively increasing ratio of LR White resin (London Resin Company, London, UK) to ethanol, followed by embedding in the resin.

The embedded plant materials were sectioned in 1-µm sections using an Ultracut Leica EM UC6 microtome (Leica, Mannheim, Germany), and stained with toluidine blue O to visualize the cells (Sigma-Aldrich, St. Louis, MO, USA). The stained sections were examined using a Leica DM6B light microscope (Leica).

COMET assay for analysis of DNA damage

To quantify DNA damage (single and double strand breaks) after the gamma exposure, the COMET assay was performed according to Gichner et al. (2003) with some modifications. Three biological replicates, each consisting of 3–4 mm of the shoot tip of 3 plants of Scots pine and Norway spruce, were investigated individually for DNA damage per dose rate after 144 h of gamma radiation. For *A. thaliana*, three biological replicates, each consisting of 5 seedling shoots, were analysed in each case after 144 h or 360 h of gamma exposure. DNA damage was also assessed 44 days post-irradiation. For Scots pine and Norway spruce (144-h gamma) 3 shoot tip samples were then analysed per gamma dose rate with each sample consisting of 3–4 mm of the shoot tip from each of 3 plants with attached needle initials/unexpanded needles. For these species, 3 root tip samples, each consisting of 10 mm of each of 5 root tips were also analysed per treatment. Since all *A. thaliana* plants had inflorescence stems 44 days post-irradiation, and accordingly no vegetative shoot meristems, shoot tips were then not analysed, but 3 leaf samples, each consisting of 10 rosette leaves from the top of the leaf rosette (the topmost leaves in the rosette) were analysed per gamma dose rate (360 h of gamma irradiation).

The COMET assay was performed under in actinic red light to avoid light-induced DNA damage. Approximately 200 mg plant material per treatment was placed in a 90-mm Petri dish and 400 µl cold extraction buffer (PBS, pH 7.0 and 200 mM EDTA) was added. Isolation of cell nuclei was performed by chopping the plant materials vigorously for 30 s using a razor blade. The nuclei solution without plant debris was then collected. The nuclear suspension (75 µl) and 1% low melting point agarose (50 µl) (NuSieve GTG Agarose, Lonza, Basel, Switzerland) prepared in distilled water at 40 °C, were gently mixed and 10 µl aliquots placed on microscope slides, which were pre-coated with 1% low melting point agarose. The slides were placed on ice for 1 min, and then placed for 10 min in a horizontal gel electrophoresis tank containing freshly prepared cold electrophoresis buffer (1 mM Na_2EDTA and 300 mM NaOH, pH 13) in order to unwind DNA prior to electrophoresis. Electrophoresis was performed at 20 V (300 mA) for 5 min at 4 °C. After electrophoresis, the slides were washed briefly with distilled water and neutralized in PBS buffer for 10 min. The slides were then washed with distilled water, fixed in 95% ethanol and dried overnight. The dried slides were stained with SYBR Gold (Life Technologies Ltd, Paisley, UK; dilution 1:5000) for 20 min and washed in distilled water 3 times for 5 min each.

For scoring "COMETS" (elongated cell nuclei due to damaged DNA), we used Comet IV (Perceptive Instruments Ltd, Bury St. Edmunds, UK) and an Olympus BX51 fluorescence microscope with a CCD camera (Olympus, Tokyo, Japan). For each of the three biological replicates, three technical replicates were performed for the COMET analysis per gamma treatment. In each of the technical replicates 500–100 nuclei were scored. As recommended by Koppen et al. (2017), the median value for each biological replicate was calculated, followed by calculation of the average of these values for the three biological replicates.

Chlorophyll fluorescence measurement

Since *A. thaliana* did not show any visible damage even at the highest dose rates tested, the effect of gamma radiation on optimal photosystem II (PSII) efficiency (F_v/F_m) was also assessed in this species. 28 days post-irradiation (144-h gamma exposure) plants (grown in pots in a growth chamber equipped with fluorescent light tubes and incandescent lamps as described above) were dark-adapted for 15 min. Minimal fluorescence (F_o) in minimal modulated light and maximal fluorescence (F_m) during a saturating pulse of 0.8 s was measured with a modulated fluorometer (PAM-2000, Walz, Effeltrich, Germany) on a rosette leaf at the top of the rosette in 35 plants from each gamma treatment. Thereafter, F_v/F_m was calculated according to $F_v/F_m = (F_m - F_o)/F_m$ (Maxwell and Johnson 2000).

Statistical analyses

For the recorded growth and developmental parameters, analyses of DNA damage, analyses of relative transcript levels and F_v/F_m, the effect of gamma radiation was assessed by one-way analyses of variance (ANOVA) in the general linear model mode and by regression analysis using the Minitab statistical software (Minitab 18, Minitab Inc, PA, USA) ($p \leq 0.05$). To test for differences between means, Tukey's post hoc test was used. For the post-irradiation growth parameters in the conifers (number of needles, shoot diameter), only the results for the final time point were analysed.

Results

Developmental effects and histology after 144-h or 360-h gamma exposure

To compare cross-species sensitivity of developmental parameters to different gamma radiation doses or dose rates, seedlings of Norway spruce, Scots pine and *A. thaliana* were exposed to gamma radiation dose rates ranging from 1 to 540 mGy h^{-1} for 144 h. In Norway spruce and Scots pine the total plant length was reduced with increasing gamma dose rate (Fig. 1a, b). As compared to the unexposed control plants, the Norway spruce seedlings were significantly shorter at dose rates ≥ 40 mGy h^{-1} ($p \leq 0.05$) with 29% and

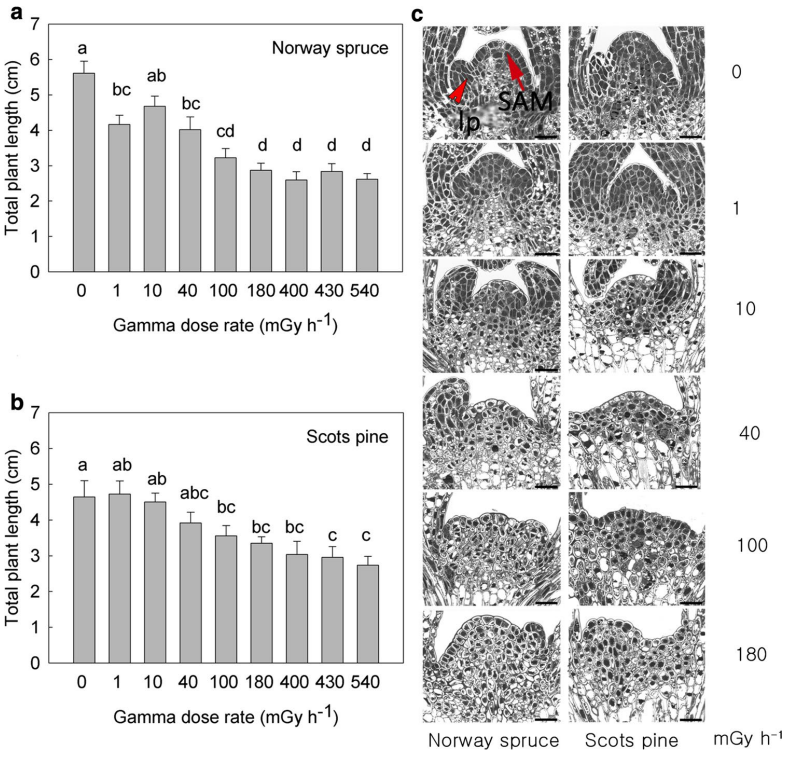

Fig. 1 Effects of exposure to gamma radiation for 144 h 7–12 days after sowing on the length of seedlings of **a** Norway spruce and **b** Scots pine. For the dose rates 0–100 mGy h^{-1}, the results are mean ± SE of 4–6 plants per treatment in each of two experiments (totally $n = 8$–12), whereas for 180 and 400 mGy h^{-1} and for 430 and 540 mGy h^{-1} the results are from each of the two individual experiments ($n = 4$–6). Different letters within each species indicate significant differences ($p \leq 0.05$) based on analysis of variance followed by Tukey's test. Regression analyses: Scots pine $R^2 = 0.96$, Norway spruce $R^2 = 0.84$. **c** Histology of shoot apical meristems after 144-h gamma. Scale bars: 50 µm. *SAM* shoot apical meristem, *lp* leaf primordia. Six plants were investigated per treatment

54% reduced seedling length at 40 and 540 mGy h^{-1}, respectively. Scots pine responded similarly with 23% and 41% reduced seedling length at 100 and 540 mGy h^{-1}, respectively ($p \leq 0.05$). Although no clear cellular damage could be observed in any of these species at this stage, the apical dome in the SAM appeared slightly less prominent at dose rates ≥ 40 mGy h^{-1} as compared to lower dose rates and the unexposed control (Fig. 1c). In both species, the shoot as well as root length were reduced with increased gamma dose rate (results not shown). Lateral roots were not yet present in any of these species including the unexposed controls.

In *A. thaliana,* no visible effect of gamma radiation on leaf rosette size and no signs of damage to the shoot could be detected at any of the dose rates after 144-h or 360-h gamma radiation (results not shown). Light microscopy revealed normal SAM histology at all dose rates (360-h duration) (Fig. 2a). However, as compared to the unexposed controls, the number of lateral roots was significantly reduced by 73–79% at the highest dose rates (430 and 540 mGy h^{-1}) after 144 h (Fig. 2b). After 360 h of gamma exposure, the number of lateral roots was significantly reduced by 48% at 100 mGy h^{-1} and was further significantly reduced by 93% at 290 and 430 mGy h^{-1}, and at 540 mGy h^{-1} no lateral roots were present in any of the plants (Fig. 2c). The effect of gamma radiation on lateral root development was also reflected in reduced length of lateral roots at high gamma dose rates (Fig. 2d; 144-h gamma exposure shown).

DNA damage after 144-h or 360-h gamma exposure

To assess dose-dependent DNA damage in Norway spruce, Scots pine and *A. thaliana*, the COMET assay was performed after 144-h (all species) and 360-h (*A. thaliana*) gamma exposure. A significant dose-rate-dependent

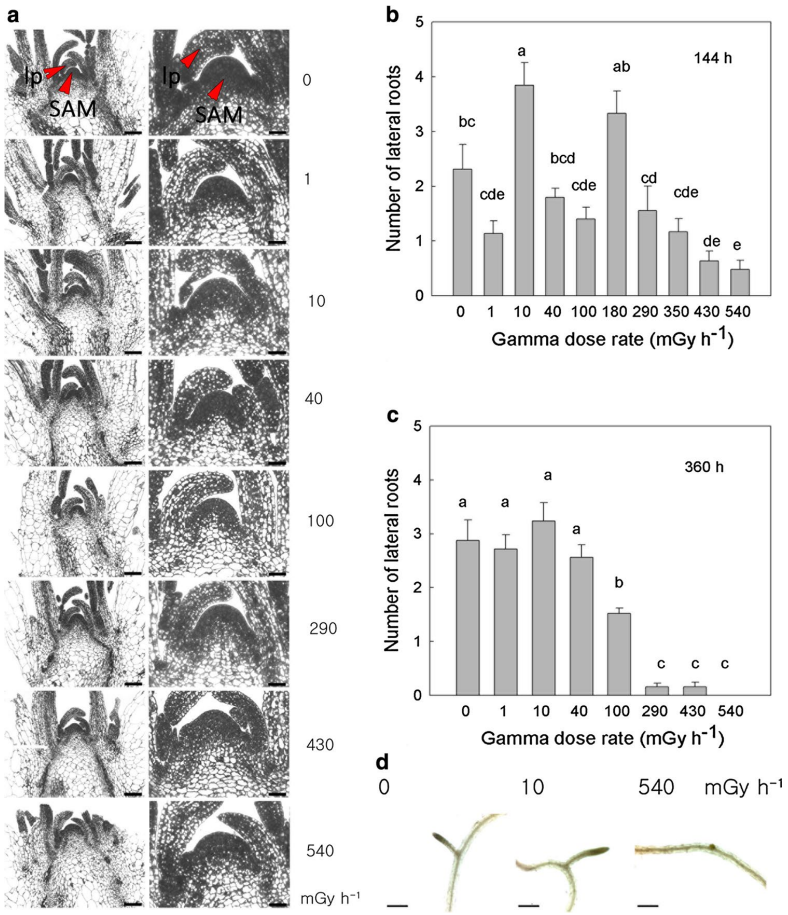

Fig. 2 Effects of gamma radiation on seedlings of *Arabidopsis thaliana*. **a** Histology of shoot apical meristems after 360 h of gamma exposure 7–21 days after sowing. Scale bars: 75 µm (left panel) and 25 µm (right panel; larger magnification of the apical dome region in sections to the left). *SAM* shoot apical meristem, *lp* leaf primordia. Six plants were investigated per treatment. Number of lateral roots after **b** 144 h of gamma irradiation 7–12 days after sowing and **c** after 360-h gamma. For 144-h exposure, the results are mean ± SE of 10–15 plants per dose rate in each of two repeated experiments (totally $n = 20–30$), except for 350 and 180 mGy h^{-1} and 100, 40 and 1 mGy h^{-1} where the results are from each of the two individual experiments ($n = 10–15$). For 360-h gamma $n = 25$. Different letters within each gamma duration indicate significant differences ($p \leq 0.05$) based on analysis of variance followed by Tukey's test. Regression analyses: 144 h $R^2 = 0.33$, 360 h $R^2 = 0.84$. **d** Close-up of representative primary roots with lateral roots after 144-h gamma. Scale bars: 200 µm

increase in DNA damage measured as % COMET tail intensity, was observed. As compared to the unexposed controls, which had 0.05% tail DNA, gamma-exposed Norway spruce seedlings exhibited significantly increased DNA damage with on average 2% tail DNA at 10 mGy h^{-1} with increasing damage up to 18% tail DNA at the highest dose rate analysed for this species, i.e. 400 mGy h^{-1} (Fig. 3a). Also, Scots pine showed significantly higher DNA damage after gamma exposure with 9% tail DNA at 1 mGy h^{-1} and significantly increasing DNA damage up to 34% and 54% tail DNA at 430 and 540 mGy h^{-1}, respectively (Fig. 3b). In comparison, the control had 2.4% tail DNA. *A. thaliana* exposed to gamma for 144 h exhibited significantly DNA damage as compared to the control (0.58% tail DNA) after 10 mGy h^{-1} with 3% tail DNA and increasing damage up to 18% tail DNA at 540 mGy h^{-1} (Fig. 3c). After exposure to gamma for 360 h, *A. thaliana* showed significantly increased DNA damage already at 1 and 10 mGy h^{-1} with 3% tail DNA for both dose rates, with damage increasing up to 14% tail DNA at 400 mGy h^{-1} (highest dose rate used) (Fig. 3d). In comparison the control had 0.68% tail DNA.

Transcript levels of genes related to cell division control, DNA repair, antioxidants and general defence reactions after 144-h gamma exposure

To evaluate the effect of gamma irradiation on genes involved in control of cell division, transcript levels of *CYCB1;2*, *CDKB1;2* and *CYCD3;1* were analysed (Fig. 4). *CYCB1;2* showed significantly higher transcript levels in Scots pine at 10 and 40 mGy h^{-1} compared to the unexposed control, with 6- to 7-fold higher transcript levels. However, in Norway spruce no significant difference among the different dose rates was observed. In *A. thaliana* seedlings significantly higher *CYCB1;2* transcript levels were observed at 40 mGy h^{-1} and higher dose rates (2.2- to 2.6-fold) as compared to 1 and 10 mGy h^{-1} and the unexposed control plants. The *CDKB1;2* transcript levels did not show any significant differences in any species. *CYCD3;1* exhibited significantly higher transcript levels in Norway spruce at 1 mGy h^{-1} (about threefold) compared to the unexposed control plants, but in Scots pine and *A. thaliana* no significant differences were observed.

The DNA repair genes *RAD51* and *SOG1* were also investigated for their transcript levels in response to gamma radiation (Fig. 4). *RAD51* in Scots pine showed significantly increased transcript level (2.2-fold) at 10 mGy h^{-1} compared to the control, and in *A. thaliana* at the two highest dose

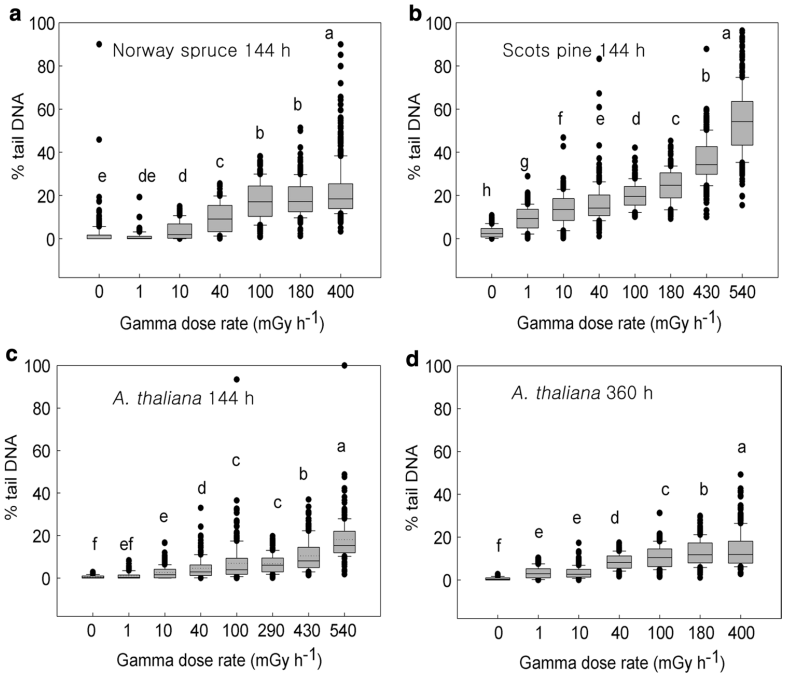

Fig. 3 Effect of gamma radiation on DNA damage analysed by the COMET assay in seedlings of **a** Norway spruce, **b** Scots pine and **c** *Arabidopsis thaliana* after 144 h of gamma exposure 7–12 days after sowing, and **d** *A. thaliana* after 360 h of gamma irradiation 7–21 days after sowing. The results are mean ± SE of the median values for 3 biological replicates per dose rate with 3 technical replicates (gels) for each which 50–100 nuclei scored in each gel. Different letters within each species or exposure duration indicate significant differences ($p \leq 0.05$) based on analyses of variance followed by Tukey's test. Regression analyses: Norway spruce $R^2 = 0.91$, Scots pine $R^2 = 0.88$, *A. thaliana* 144 h $R^2 = 0.87$, *A. thaliana* 360 h $R^2 = 0.97$

rates analysed; 180 and 400 mGy h^{-1} (1.9 and 2.1-fold). No significant differences in *RAD51* transcript level in Norway spruce among different gamma dose rates were observed. *SOG1* did not exhibit any significant increase in transcript level in response to gamma irradiation compared to the unexposed control seedlings in any of the species.

Effect of gamma irradiation on specific representatives of the *PEROXIDASE*, *CATALASE* and *SUPEROXIDE DISMUTASE* families of antioxidant genes were also investigated (Fig. 5). The transcript level of the peroxidase *PX3* was significantly increased by about 20- to 25-fold in Norway spruce at 400 and 180 mGy h^{-1} as well as 4.8-fold in Scots pine at 40 mGy h^{-1}. In *A. thaliana* no significant differences in *PX3* transcript levels among the different dose rates were observed. *CAT* showed significantly higher (2.7-fold) transcript level in Norway spruce at 180 mGy h^{-1} as compared to the unexposed control plants, but no significant difference among different gamma dose treatments in Scots pine. In *A. thaliana* no increase in *CAT* transcript level was observed at any dose rate, only significant reduction for 10, 40 and 180 mGy h^{-1} as compared to the control. *SOD* exhibited only significantly increased transcript levels (2.3-fold) in Norway spruce at 100 mGy h^{-1} compared to the unexposed control, whereas no significant differences were observed in the two other species.

Effect of gamma exposure on *PAL* (involved in biosynthesis of lignin in cell walls and other secondary metabolites) and *CHI4* (involved in general defence) was also investigated (Fig. 5). No significant differences in transcript levels of *PAL* were observed in any of the species. *CHI4* transcript level did not differ significantly between dose rates in the conifers, whereas significantly higher transcript level (4.7-fold) was observed in *A. thaliana* at 180 mGy h^{-1} only as compared to the unexposed control.

Post-irradiation effects of gamma radiation on growth and development, mortality and histology

Post-irradiation effects on growth and developmental responses were also investigated in all species. The number of needles in the Norway spruce and Scots pine seedlings exposed to 1 and 10 mGy h^{-1} gamma, did not differ significantly from the unexposed control plants 36 days after 144-h gamma radiation (Fig. 6a, b). By contrast, after 40 mGy h^{-1} both species then had significant reduction in the number of needles (by 37% and 34% in Norway spruce and Scots pine, respectively) (Fig. 6a, b, Table 3). After higher dose rates, generally no or only a few needles had developed and commonly only the pre-existing cotyledons (initiated during the embryogenesis) were present. Shoot diameter at the shoot apex (from needle tip to needle tip across the plant) was significantly reduced by about 17% after 100 mGy h^{-1} and 40–45% after exposure to 430 and 180 mGy h^{-1} in Norway spruce and 20%, 35% and 40% after 40, 100 and 180 mGy h^{-1} in Scots pine as compared to the unexposed control plants (Fig. 6c, d, Table 3). Shoot elongation was also significantly reduced with increasing dose rate $\geq$ 40 mGy h^{-1} (results not shown). Photos from 44 days after the termination of gamma exposure clearly show reduced plant size with reduced plant height, number of needles and reduced needle length for both conifer species following exposure to 40 and 100 mGy h^{-1} as well as higher dose rates (Fig. 6e–f; Supplementary Fig. S1).

At this time point the number of lateral roots and total length of the root system (length of the longest root) were significantly, and severely reduced from 100 mGy h^{-1} in Norway spruce and 40 mGy h^{-1} in Scots pine, and no significant differences were observed between these and the higher dose rates (Fig. 7a, b). In Norway spruce, the length of the root system was reduced by 88% after 100 mGy h^{-1} (on average 0.9 cm) as compared to the unexposed control (on average 7.5 cm) and the average number of lateral roots from 3.8 in the control to 0 at 100 mGy h^{-1}. In plants exposed to higher dose rates no lateral roots were present. In Scots pine, the 40 mGy h^{-1} and 100 mGy h^{-1} treatments reduced the length of the root system by 59% and 75%, respectively, compared to the control. The average number of lateral roots was reduced from 10.5 (control) to 2 in the 40 mGy h^{-1} treatment. No significant difference in number of lateral roots were observed between this dose rate and 100 and 180 mGy h^{-1}, whereas in plants exposed to 430 mGy h^{-1}, no lateral roots were present.

At 36 days post-irradiation, no mortality was observed in Norway spruce plants exposed to $\leq$ 40 mGy h^{-1} (Fig. 7c). In contrast, at higher dose rates mortality increased gradually up to 70% in 400 mGy h^{-1} treated plants. In Scots pine there was no mortality after 1 and 10 mGy h^{-1}, whereas after 40 mGy h^{-1} and 100 mGy h^{-1} 20% mortality was observed (Fig. 7d). The mortality increased to 60% after 180–400 mGy h^{-1}. At the highest dose rates a high proportion of the plants that were still alive at this time point were unable to remove their seed coat and growth was completely impaired, despite being viable with green hypocotyl and cotyledons (results not shown; Examples of dead plants that had not shed their seed coats before dying, are shown in Supplementary Fig. S1).

As assessed in Norway spruce and Scots pine plants which were viable and still green also at the highest dose rates 44 days post-irradiation, progressive damage of the SAM (Fig. 8) and the root apical meristem (results not shown) was observed with increasing gamma dose rate from 100 mGy h^{-1}. At the highest dose rates (430 and 540 mGy h^{-1}, and 180 mGy h^{-1} in Norway sprue), the apical dome was malformed or virtually absent and seemingly empty cells (possible cell death or at least

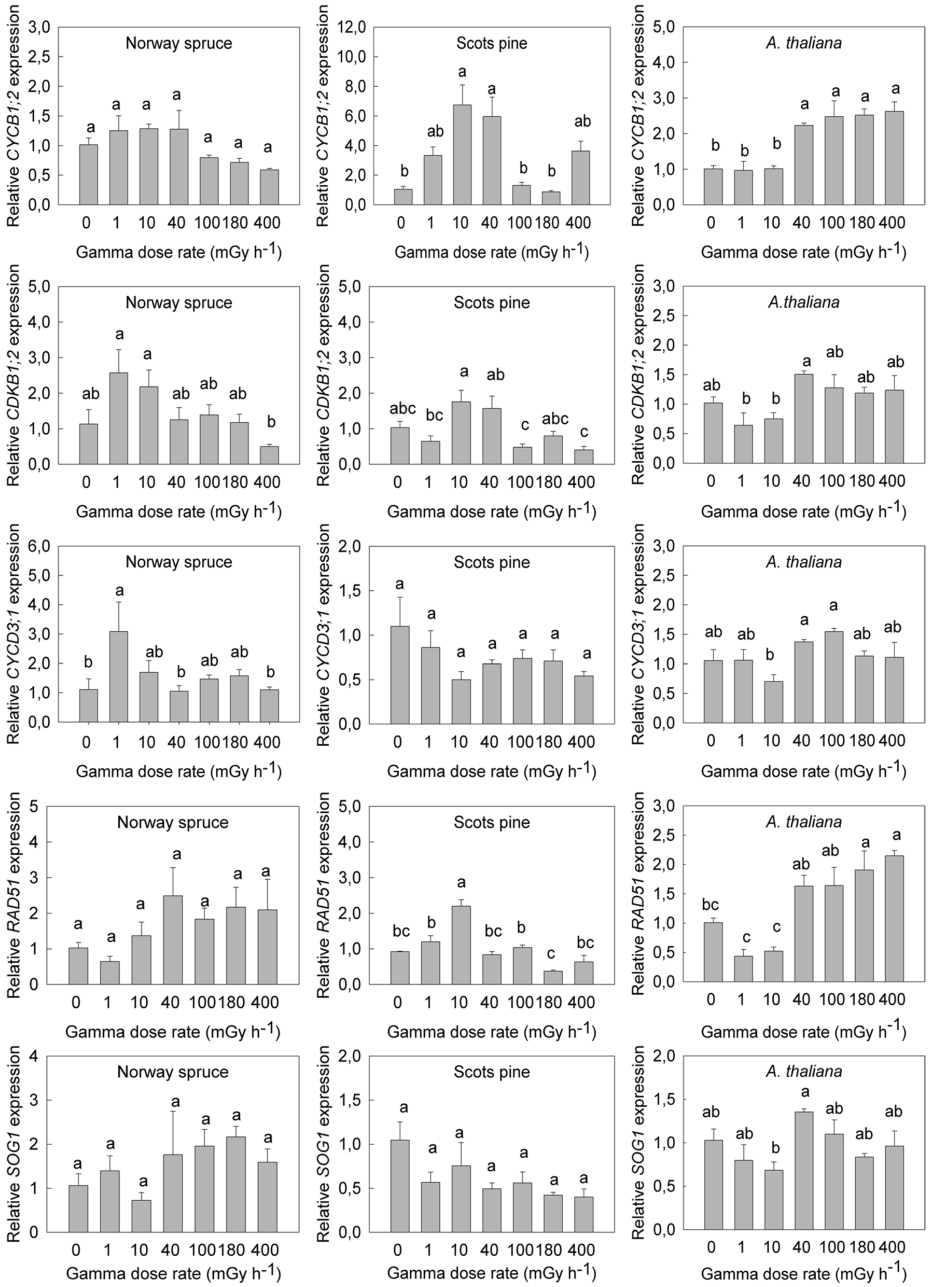

highly vacuolated cells) were observed. In plants exposed to ≤ 100 mGy h^{-1}, the cells of the SAM appeared normal.

In *A. thaliana*, no mortality or visible damage was observed for any gamma treatment. Also, no significant difference in the number of rosette leaves between any of the gamma treatments and the unexposed control was observed prior to the start of reproductive development (Fig. 9a for 144-h gamma, results for 360 h not shown). Furthermore,

◂**Fig. 4** Effect of 144 h of gamma irradiation day 7–12 after sowing on relative transcript levels of specific cell division controlling genes (*CYC*=*CYCLIN*, *CDK*=*CYCLIN-DEPENDENT KINASE*) and DNA repair genes (*RADIATION 51* (*RAD51*), *SUPPRESSOR OF GAMMA RESPONSE 1* (*SOG1*)) in shoots of Norway spruce, Scots pine and *A. thaliana*. The transcript levels were normalized against *ACTIN* (*ACT*) and *ELONGATION FACTOR 1-α* (*EF1-α*) for Norway spruce and *A. thaliana*, and *ACT* and *GLYCERALDEHYDE-3-PHOSPHATE DEHYDROGENASE* (*GAPDH*) for Scots pine and shown relative to the unexposed controls. The results are mean ± SE of 4 biological replicates ($n=4$) with 2–4 technical replicates. Different letters within each gene within a species indicate significant differences ($p \leq 0.05$) based on analysis of variance followed by Tukey's test

chlorophyll fluorescence (F_v/F_m) measured 28 days after 144-h gamma exposure, did not differ between any of the dose rates (180–540 mGy h^{-1}), as compared to the unexposed control plants (Fig. 9b). Histological studies of rosette leaves of *A. thaliana* at day 44 post-irradiation after 144-h gamma exposure, did not reveal any cellular changes after any gamma dose rate, all leaves appeared normal as analysed by light microscopy (Fig. 9c).

In contrast, differences in reproductive development among dose rates were observed in this species (Fig. 9d, e). Plants exposed to 290, 430 and 540 mGy h^{-1} for 144 h showed delayed flower bud appearance, compared to lower gamma dose rates and the unexposed control plants (Fig. 9d). At day 15 post-irradiation, the largest difference among gamma treatments was observed with 95% of the control plants having flower buds, but only 60, 45 and 30% of the plants exposed to 180, 430 and 540 mGy h^{-1}. Although smaller, a difference between the two highest dose rates and the control and the other dose rates still was observed at day 36. However, at day 43 all plants had developed flower buds. Also, *A. thaliana* plants exposed to 400 mGy h^{-1} of gamma radiation for 360 h exhibited delayed flower bud formation (Fig. 9e). At day 13 post-irradiation, these plants had no flower buds whereas 30% of the control plants had flower buds. At day 31, only 15% of the plants exposed to 400 mGy h^{-1} for 360 h had flower buds, whereas 65% of the unexposed control plants had visible flower buds. At day 52, only small differences between different gamma dose treatments were observed, and at day 56 all plants had developed flower buds.

Furthermore, at day 30 after 144-h gamma radiation, when all control plants had visible elongated/elongating inflorescence stems, the percentage of plants with an inflorescence stem was significantly reduced at 100 mGy h^{-1} and higher dose rates (Fig. 9f). At this time point, 55% of the plants exposed to 100 mGy h^{-1} and only 15% of those exposed to 540 mGy h^{-1} had a visible inflorescence stem. Such differences were no longer observed at day 36. Furthermore, at day 30, when all the control plants exposed to 360 h of gamma radiation had inflorescence stems, significantly reduced percentage of plants with inflorescence stem was observed at 400 mGy h^{-1} (38%) and this was still the case at day 36 (Fig. 9g). However, although inflorescences were present in all plants 44 days after the gamma treatment, the elongation of the inflorescence was then still delayed at 400 mGy h^{-1} (Fig. 9h).

Persistent post-irradiation DNA damage

To evaluate the persistence of the gamma-induced DNA damage, the COMET assay was performed 44 days post-irradiation for Norway spruce and Scots pine plants irradiated for 144 h for gamma dose rates up to 100 mGy h^{-1} (not higher due to high mortality and lack of growth at higher dose rates) and for *A. thaliana* plants exposed to up to 400 mGy h^{-1} for 360 h. In all three species, a significant dose rate-dependent % tail DNA values was then observed (Fig. 10). Norway spruce shoot tips then exhibited significantly increased DNA damage as compared to the control (2%) already at 1 mGy h^{-1} with 9% tail DNA (Fig. 10a). At 100 mGy h^{-1} 23% tail DNA was observed. In comparison, Norway spruce root tips showed no significant differences in DNA damage among the different gamma dose rates (Fig. 10b). Scots pine shoot tips also showed significantly higher DNA damage as compared to the control (2%) from 10 mGy h^{-1} with 7%, and 40% tail DNA at 10 and 100 mGy h^{-1}, respectively (Fig. 10c). In contrast to Norway spruce root tips, Scots pine root tips showed significant DNA damage at 40 and 100 mGy h^{-1} with 6% and 32% tail DNA as compared to 1 mGy h^{-1} and control (both 1% tail DNA) (Fig. 10d). Furthermore, *A. thaliana* leaves showed significantly increased DNA damage from 1 mGy h^{-1} with 5% tail DNA as compared to the control (1%) (Fig. 10e). At the highest dose rates of 100, 180 and 400 mGy h^{-1}, 9%, 12% and 19% DNA in the comet tail, respectively, were observed.

Discussion

Although a range of adverse effects of acute and chronic irradiation has been observed after nuclear accidents like in Chernobyl and in laboratory studies (Yoschenko et al. 2017; Tulik 2001; Zelena et al. 2005), detailed information about sensitivity to gamma irradiation among plant species under standardized exposure conditions is limited, particularly in the low-to-medium dose area. In this study we compared sensitivity to gamma radiation from a ^{60}Co source in young plants of the ecologically and economically important gymnosperms Scots pine and Norway spruce as well as the evolutionary distant herbaceous angiosperm, *A. thaliana*. We observed significantly different effects at the organismal, cell and DNA level in response to gamma dose rates within the range 1–540 mGy h^{-1}, provided during 7–12 (total doses 0.14–77.8 Gy; all species) or 7–21 (total doses

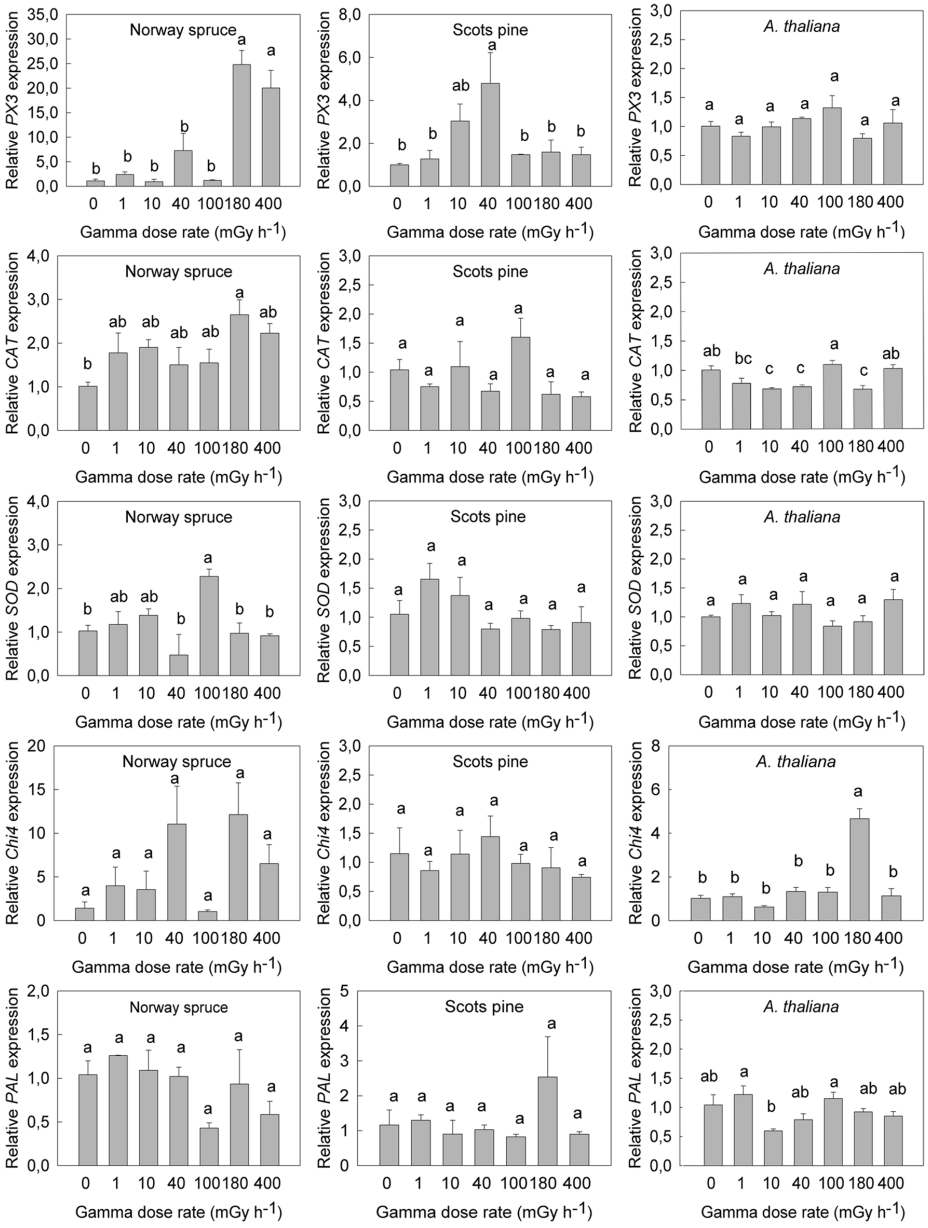

Fig. 5 Effect of 144 h of gamma irradiation day 7–12 after sowing on relative transcript levels of antioxidant genes (*PX3* = *PEROXIDASE 3*, *CAT* = *CATALASE*, *SOD* = *SUPEROXIDE DISMUTASE*) and defence-related genes (*PHENYLALANINE AMMONIA-LYASE* (*PAL*) *and IV CHITINASE* (*CHI4*)) in shoots of Norway spruce, Scots pine and *A. thaliana* seedlings. The transcript levels were normalized against *ACTIN (ACT)* and *ELONGATION FACTOR 1-α* (*EF1-α*) for Norway spruce and *A. thaliana*, and *ACT* and *GLYCERALDEHYDE-3-PHOSPHATE DEHYDROGENASE* (*GAPDH*) for Scots pine and shown relative to the unexposed controls. The results are mean ± SE of 4 biological replicates ($n = 4$) with 2–4 technical replicates. Different letters within each gene within a species indicate significant differences ($p \leq 0.05$) based on analysis of variance followed by Tukey's test

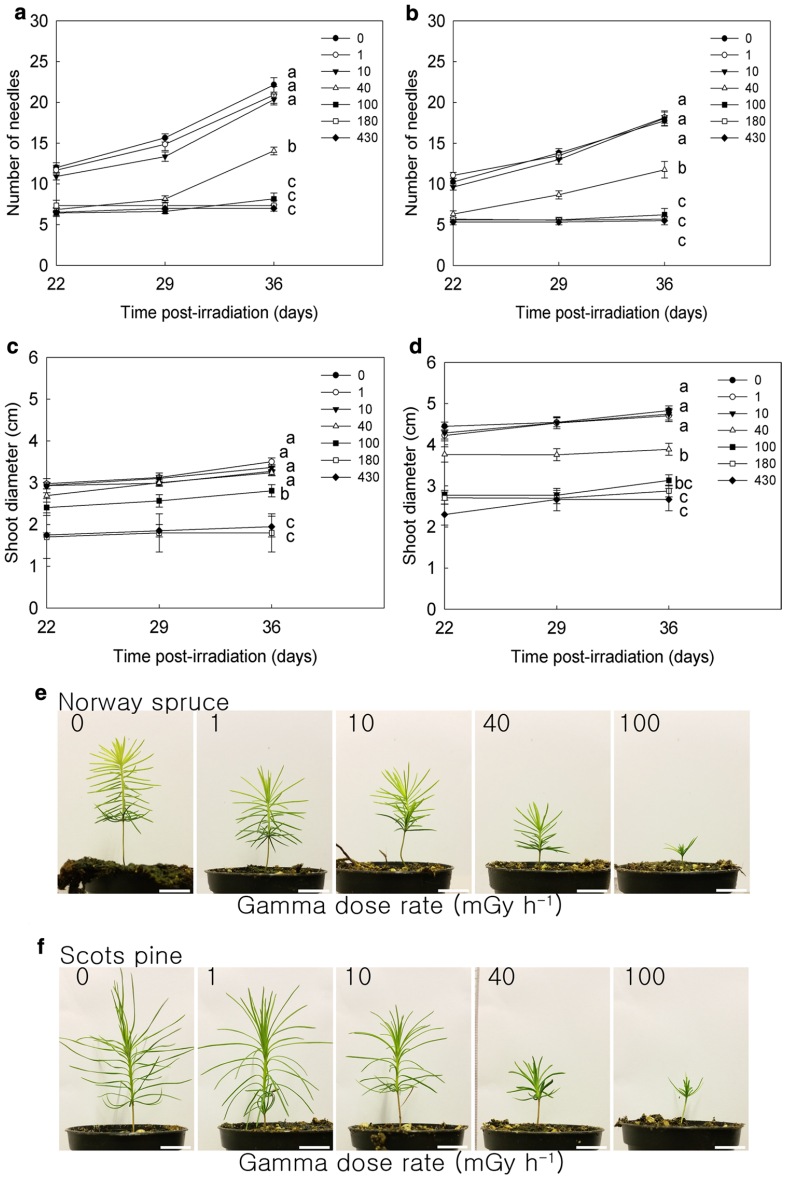

Fig. 6 Post-irradiation effects of different dose rates (mGy h^{-1}) of 144 h exposure to gamma radiation 7–12 days after sowing in seedlings of Norway spruce and Scots pine. Number of needles in **a** Norway spruce and **b** Scots pine. Shoot diameter from needle tip to needle tip in **c** Norway spruce and **d** Scots pine. The results (34–48 days after sowing) are mean ± SE of 10–20 plants per dose rate in each of two experiments ($n = 20–40$). Different letters within each growth parameter for each species indicate significant differences at the end of the experiment ($p \leq 0.05$) based on analysis of variance followed by Tukey's test. Phenotype of **e** Norway spruce and **f** Scots pine plants 44 days post-irradiation (56 days after sowing). Scale bars: 3 cm

Table 3 Regression analyses (R^2) for post-irradiation effects on growth parameters in Norway spruce and Scots pine at day 44 after gamma irradiation for 144 h

Species	Parameter	Figure	Gamma dose rate (mGy h^{-1})/R^2 values						
			0	1	10	40	100	180	430
Norway spruce	Number of needles	6a	0.95	0.97	0.93	0.88	0.83	0.74	0.75
	Shoot diameter	6c	0.99	0.94	0.98	0.99	0.99	0.74	0.75
Scots pine	Number of needles	6b	0.99	0.99	0.99	0.99	0.74	0.74	0.74
	Shoot diameter	6d	0.92	0.92	0.92	0.71	0.75	0.72	0.75

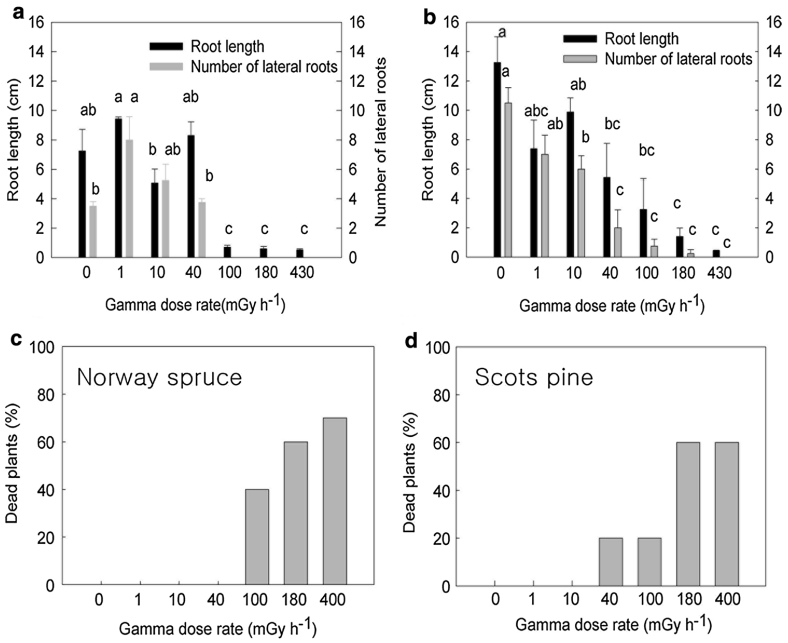

Fig. 7 Post-irradiation effects at day 44 (56 days after sowing) after 144-h exposure to gamma radiation day 7–12 after sowing on the length of the longest root and the number of lateral roots in **a** Norway spruce and **b** Scots pine, and dead plants (%) 36 days post-irradiation (48 days after sowing) in **c** Norway spruce and **d** Scots pine. The results are mean ± SE of 10–20 plants per dose rate in each of two experiments (n = 20–40). Different letters indicate significant differences within each growth parameter for each species ($p \leq 0.05$), based on analysis of variance followed by Tukey's test. Regression analyses: Norway spruce root length $R^2 = 0.69$, number of lateral roots $R^2 = 0.62$, dead plants $R^2 = 0.82$. Scots pine root length $R^2 = 0.90$, number of lateral roots $R^2 = 0.91$ and dead plants $R^2 = 0.84$

0.36–194.4 Gy, *A. thaliana* only) days after sowing. Such exposure levels are relevant for those found in contaminated areas, e.g. it was previously estimated that the first 2 weeks after the Chernobyl accident coniferous species in this area received a dose of 3.7 Gy (Fesenko et al. 2005). Recently, it was also reported that the calculated absorbed gamma dose in dead pine trees in this area was 80–100 Gy (Kashparova et al. 2018). Furthermore, exposure dose rates of seaweed and algae were estimated to 100 µGy h^{-1} and 633 µGy h^{-1}, respectively, one month after the Fukushima accident (Vives i Batlle et al. 2014). Also, aquatic plants from the southern Urals received a dose rate of 450 µGy h^{-1} after the Mayak accident (Kryshev et al. 1997). Overall, our work supports that plants demonstrate considerable morphological and functional variation in their response to different gamma radiation dose rates and doses, and that radiosensitivity varies significantly with species (Kalisz and Kramer 2007; Wright and Gaut 2005).

Although adverse effects of gamma exposure of conifer seeds on subsequent germination and seedling growth, as well as growth and cell anomalies in older plants in response to ionizing radiation have been reported (Yoschenko et al. 2017; Tulik 2001; Mergen and Strøm Johansen 1964; Rudolph 1971; Zelena et al. 2005), information about effects of gamma exposure of young conifer seedlings is limited. Our results show an evident dose–response relationship with significantly reduced seedling length (both shoots and roots) in Norway spruce and Scots pine after 144-h gamma exposure at dose rates ≥ 40 mGy h^{-1}, consistent with slightly less well-developed SAM at ≥ 40 mGy h^{-1} (Fig. 1). In *A. thaliana* seedlings the fresh weight of shoots and roots was previously shown to increase in response to gamma radiation for 14 days at dose rates from 22 to 86 mGy h^{-1} and total doses from 7 to 29 Gy (van de Walle et al. 2016). In our experiments, consistent with normal histology of the SAM for all dose rates (Fig. 2a), no visible effect on shoot size of *A. thaliana* seedlings after 144 and 360 h of gamma was observed. However, the number of lateral roots was reduced and their elongation consistently delayed after 144-h exposure to 290–540 mGy h^{-1} and after 360 h with 100–540 mGy h^{-1} (Fig. 2b–d), indicating reduced cell division activity in the pericycle cell layer in the primary root, from which lateral roots originates. Although lateral roots were not yet present even in the unexposed controls of the Norway spruce and Scots pine seedlings at the end of the gamma radiation, decreased number of lateral roots was observed 44 days post-irradiation at dose rates ≥ 40 mGy h^{-1} (Fig. 7). This indicates a negative effect impacting cell division activity in the pericycle also in these species, but at lower dose rates than in *A. thaliana*. Our results show similarities to the situation in maize seedlings, which showed decreased root and shoot length with increasing gamma dose after exposure of seeds to 100–1000 Gy (Marcu et al. 2013).

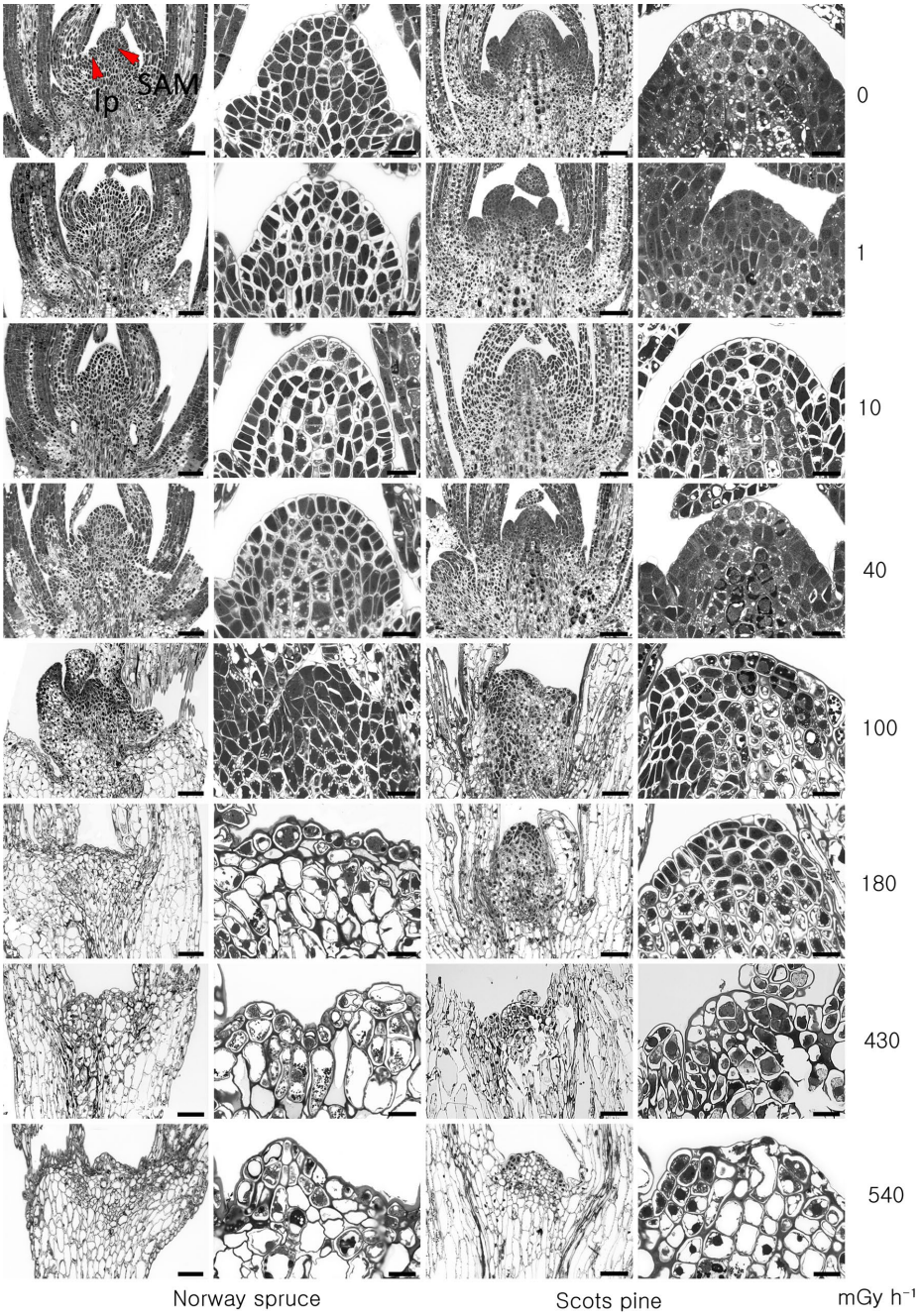

Fig. 8 Post-irradiation effect at day 44 (day 56 after sowing) after 144-h exposure to gamma radiation day 7–12 after sowing on histology of shoot apical meristems in seedlings of Norway spruce and Scots pine. For each species, the micrographs in the right panels are magnifications (scale bars 200 µm) of those to the left (scale bars 50 µm). *SAM* shoot apical meristem, *lp* leaf primordia. Six plants were investigated per treatment

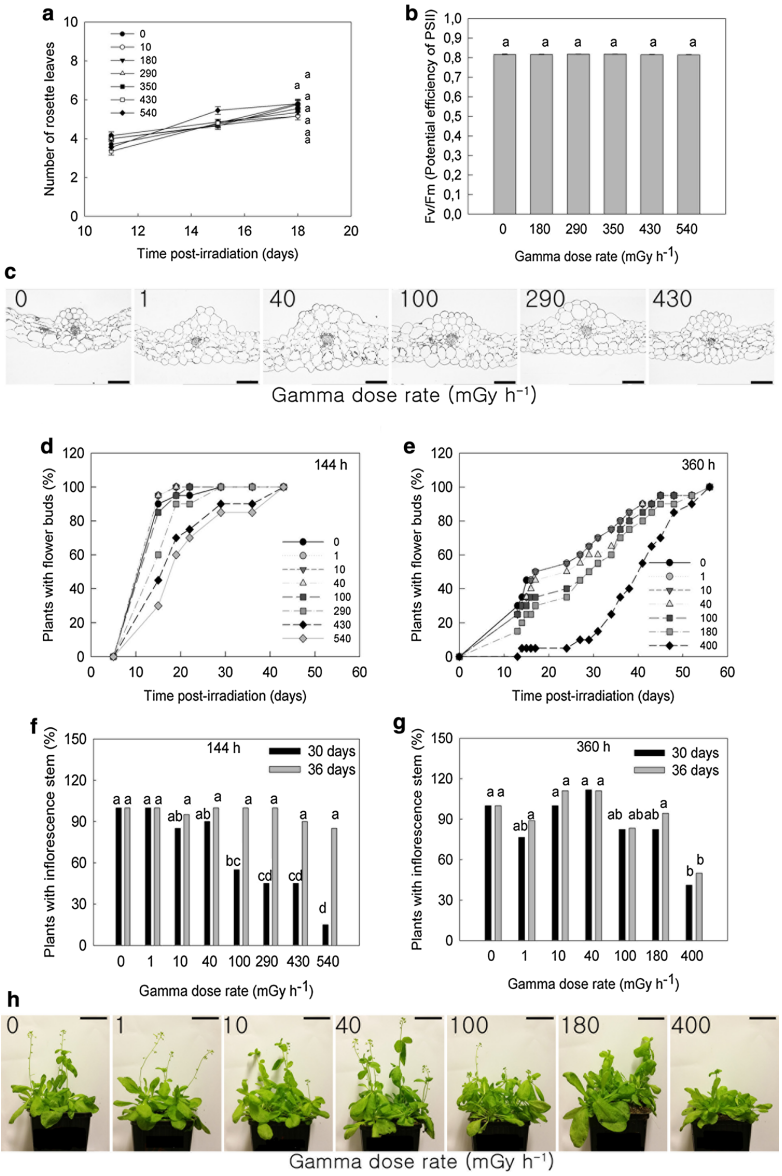

Fig. 9 Post-irradiation effects of gamma radiation in *Arabidopsis thaliana*. Post-irradiation effects of 144-h gamma exposure day 7–12 after sowing on **a** number of rosette leaves and **b** chlorophyll fluorescence (F_v/F_m) at day 28 post-irradiation (40 days after sowing). Results are mean of 20 plants ± SE for number of leaves and 35 plants ± SE for F_v/F_m. **c** Histology of rosette leaves at day 44 post-irradiation (56 days after sowing) after 360-h gamma day 7–21 after sowing. Scale bar: 100 µm. Percentage of plants with flower buds post-irradiation after exposure to **d** 144-h or **e** 360-h gamma. Percentage of plants with inflorescence stem post-irradiation after exposure to **f** 144-h, **g** or 360-h gamma. The results are mean ± SE of 10–20 plants per gamma dose rate per experiment, with results recorded in each of three and two experiments for 144-h and 360-h exposure. Regression analyses: plants with flower buds 144 h $R^2 = 0.51$ and 360 h $R^2 = 0.95$. Plants with inflorescence stem 144 h 30 days $R^2 = 0.91$ and 36 days $R^2 = 0.49$, 360 h 30 days $R^2 = 0.31$ and 36 days $R^2 = 0.26$. Different letters indicate significant differences within each graph ($p \leq 0.05$), based on analysis of variance followed by Tukey's test (for the last time point only for number of leaves). **h** Phenotype of plants at day 44 post-irradiation after 360-h gamma. Scale bars: 3 cm

The minimum dose at which morphologic effects occurred in the Chernobyl zone (reduction in the shoot growth of pine trees, appearance of morphoses in the year following the accidental one) was reported to be 0.43 Gy year^{-1} (Sidorov 1994). Although abnormal needle lengths of about 120 mm (maximum 260 mm) in contrast to the normal length of about 70 mm were observed in older Scots pine plants 1 year after the Chernobyl accident (Goltsova et al. 1991), no enhanced effect of gamma radiation on needle length was observed in Scots pine and Norway spruce seedlings in our study. In contrast, in our study needle length as well as shoot elongation and number of needles were reduced post-irradiation in a dose-rate dependent manner from 40 to 540 mGy h^{-1} (Fig. 6, Table 3, Supplementary Fig. S1). The reduced plant size in both conifer species in our study resembles more the situation with reduced lengths of auxiblast

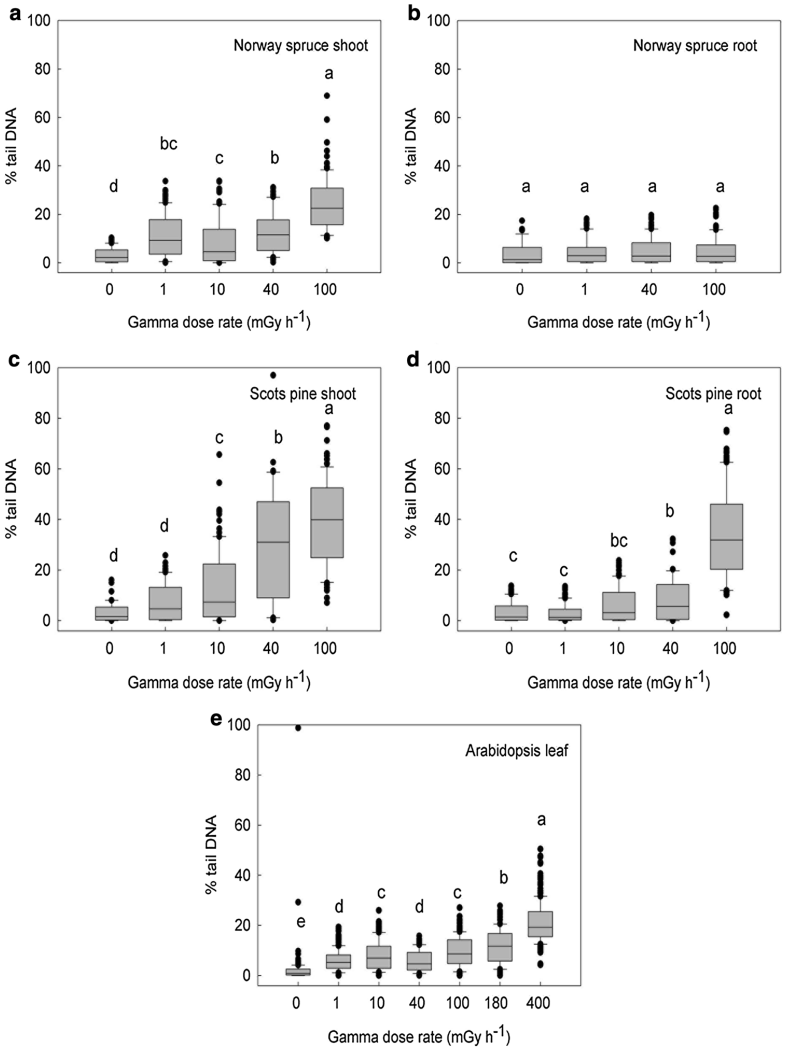

Fig. 10 Post-irradiation effect on DNA damage assessed by the COMET assay at day 44 post-irradiation (56 days after sowing) after 144-h gamma radiation day 7–12 after sowing in **a** Norway spruce shoot tips with young needles, **b** Norway spruce root tips, **c** Scots pine shoot tips with young needles and **d** Scots pine root tips. **e** DNA-damage in *A. thaliana* rosette leaves at day 44 post-irradiation after 360-h gamma day 7–21 after sowing. The results are mean ± SE of the median values for 3 biological replicates per dose rate with 3 technical replicates (gels) for each sample which 50–100 nuclei scored in each gel. Lower and upper box boundaries = 25 and 75% percentiles, error bars = 10 and 90% percentiles with data points outside these shown as dots. Regression analyses: Norway spruce shoot $R^2 = 0.74$ and root $R^2 = 0.45$, Scots pine shoot $R^2 = 0.88$ and root $R^2 = 0.62$, *A. thaliana* leaf $R^2 = 0.82$. Different letters within a species and plant part indicate significant differences ($p \leq 0.05$) based on analyses of variance followed by Tukey's test

shoots in older Scots pine plants in Chernobyl 1 year after the accident, i.e. with 5 cm auxiblasts in exposed plants receiving a total dose at 20 Gy in contrast to the normal length of about 24 cm (Goltsova et al. 1991).

Furthermore, within the dose rate range from 40 to 540 mGy h^{-1}, in the conifers we also observed increased visible damage and mortality post-irradiation with increasing dose rate. Previous work on older Scots pine plants that had grown more than 25 years in the Bryansk region of Russia that was contaminated during to the Chernobyl accident, reported increased frequency of necrotic needles with increasing level of radiation exposure ranging from 0.1 to 130 mGy $year^{-1}$ (calculated values for 2008) (Makarenko et al. 2016). However, the effects differed with year, and no clear relationship was observed between the length, the mass of needles and the radiation exposure. A high number of dead trees and different radiomorphoses were also observed after the Chernobyl accident with the effects depending on the absorbed dose (Tikhomirov and Shcheglov 1994; Arkhipov et al. 1994).

Although the SAM in Norway spruce and Scots pine seedlings after 144-h gamma exposure appeared slightly less well-developed at dose rates ≥ 40 mGy h^{-1}, clearly damaged and aberrant cells in the SAM and RAM were then not

observed. In contrast, 44 days post-irradiation after exposure to the highest tested dose rates (higher than 100 mGy h^{-1}/ totally 14.4 Gy) (Fig. 8), aberrant cells and malformed or virtually absent apical dome in the SAM were present. This implies that cellular damages were latent and took some time to be manifested. It is conceivable that inflicted DNA damage initially induces cell cycle arrest resulting in reduced growth. Such post-irradiation histological damage is consistent with the situation in 5-year-old *Pinus pinnae Pinus halepensis* exposed to gamma radiation (^{60}Co source) at rates of 2.6–18.8 R day^{-1} up to 1513 days. Such plants also showed different radiosensitivity among cells in the SAM and between the apical and sub-apical meristem. Particularly, cells of the apical initial zone and the central mother zone showed a greater radiosensitivity than the cells of the rib meristem and peripheral tissue zone (Donini 1967). In comparison, consistent with the lack of visible damage and no mortality in *A. thaliana* in our experiments, the SAM (after 360-h gamma) and leaves (44 days post-irradiation), showed no histological differences between the unexposed controls and the different dose rates.

Although no post-irradiation effects on leaf formation rate, leaf histology or chlorophyll fluorescence (F_v/F_m) were observed in *A. thaliana*, delayed development of flower buds and delayed inflorescence elongation were observed irrespective of gamma duration at dose rates of ≥ 400 mGy h^{-1} (Fig. 9). This effect of high gamma dose rates/doses is similar to previous results showing decreased inflorescence height after exposure of *A. thaliana* seedlings to a high gamma dose of 50 Gy (Wi et al. 2007). By contrast, Wi et al. 2005 reported slightly increased inflorescence height in response to a low dose of 1–2 Gy. No such effect was observed in our study. Also, consistent with high tolerance to gamma radiation, the delay in flower bud formation and inflorescence elongation in our study was transient only and eventually all plants flowered and obtained similar inflorescence lengths within 45–58 days after the radiation (depending on the duration of the exposure).

Ionizing radiation interacts with water molecules as a major target, resulting in formation of ionized water molecules (H_2O^+) and ROS. The ROS interact with DNA and cause oxidative damage such as base modifications and single and double strand breaks (Belli et al. 2002; Roldán-Arjona and Ariza 2009). When comparing the conifers and *A. thaliana* at the end of the gamma exposure, somewhat higher degree of DNA damage (double and single strand breaks (% tail DNA) as analysed by the COMET assay) was observed in conifers, particularly in Scots pine, but *A. thaliana* also showed clear dose-rate dependent, relatively high levels of DNA damage (Fig. 3). For *A. thaliana* this is in contrast to a previous study in which the COMET assay on *A. thaliana* exposed to ^{137}Cs gamma source with a dose rate range from 81 to 2336 µGy h^{-1} revealed no differential effect of gamma dose rates on DNA integrity (Vandenhove et al. 2010). The growing conditions and accession (ecotype) used differed between this and our study, and although not investigated, it cannot be excluded that these factors may potentially influence the susceptibility to DNA damage. Nevertheless, DNA damage in a dose-rate dependent manner, as assessed by the COMET assay has been reported in different plant species after gamma exposure from a ^{60}Co source. This was, e.g. the case in tobacco (*Nicotiana tabacuum*) exposed to 0.39 and 0.47 Gy min^{-1}, Lombardy poplar (*Populus nigra*) exposed to dose rates from 0.5 to 15 Gy h^{-1} for 20 h and rice (*Oryza sativa*) exposed to 25 and 50 Gy provided as 0.28 Gy min^{-1} or 50, 100 and 200 Gy given as 5.15 Gy min^{-1} (Macovei and Tuteja 2013).

A persistent high level of DNA damage was found 44 days post-irradiation in all three investigated plant species (Fig. 10). Consistent with the far more severe post-irradiation developmental effects and visible damage (chlorosis and necrosis), cellular damage of the apical meristems and mortality in the conifers, at this time point higher degree of DNA damage was still observed in the conifers than in *A. thaliana*, except for in Norway spruce roots. Again, the highest damage level (% tail DNA) occurred in Scots pine. In spite of no damage or mortality and only small, transient developmental post-irradiation effect on reproductive development observed in *A. thaliana*, the persistence of similar dose-rate-dependent DNA damage after 144 or 360 h of gamma exposure and 44 days post-irradiation, indicates higher tolerance to DNA damage compared to the conifers. It thus appears that DNA damage is not necessarily linked to mortality or reduced reproductive capacity or other adverse outcome and that at least plants like *A. thaliana* do not have to mount a massive DNA repair, at least in the somatic tissues, to grow, develop and reproduce normally. The post-irradiation DNA damage may possibly be due to gamma-induced genomic instability, involving mechanisms such as DNA repair defects and programmed cell death (Mothersill and Seymour 1998; Morgan et al. 1996; Hurem et al. 2017). Epigenetic mechanisms like altered DNA methylation and deficiency in the histone variant H2AX, which is important for proper DNA repair, may also be involved (Aypar et al. 2011; Bassing et al. 2002).

The genome size, the number of chromosomes and the degree of endoreplication have been suggested as factors explaining differences in radiosensitivity between species. Indeed, the genome size of *A. thaliana* is far smaller with its 135 Mbp than those of Scots pine and Norway spruce with their huge 23- and 20-Gbp genomes, respectively. However, since common duckweed (*Lemna minor*) with its 480-Mbp genome appears more sensitive than *A. thaliana* and more similarly sensitive to Scots pine and Norway spruce with respect to gamma dose rate resulting in growth inhibiting effect although with less visible damage/mortality (Van

Hoeck et al. 2015, 2017), the correlation between genome size and effect of gamma radiation in plants should be further studied. Furthermore, endoreplication in response to stress, which has been shown to be less common in gymnosperms than angiosperms, was previously suggested to possibly explain high resistance towards stress (De Veylder et al. 2011). However, in *L. minor* exposed to ionizing radiation significantly increased endoreplication was observed only in the plants exposed to the highest dose rate (1500 mGy h^{-1} for 7 days), which also resulted in strong growth inhibition (Van Hoeck et al. 2015). Thus, endoreplication cannot explain the higher tolerance to lower dose rates in this species. To evaluate the importance of endoreplication in resistance towards gamma radiation, further studies of different species are required. It should also be noted that due to the far shorter life cycle of *A. thaliana* than the long-lived conifers, they rapidly entered different growth stages after the gamma irradiation. Whereas *A. thaliana* enters the reproductive stage within a few weeks, the conifers normally stay vegetative for 20 years or more. In this sense, it may be argued that the conifers had less physiological time to recover after the gamma irradiation.

Although acute and chronic stress may lead to different responses, earlier studies have suggested similar responses of plants to acute radiation and other stressors, including immediate repair of the damage, activation of pro-survival mechanisms, and inhibition of cell division and cell differentiation (Kovalchuk et al. 2007). In *A. thaliana* the *CYCB1* gene, encoding a B type mitotic cyclin, was strongly induced after a gamma dose of 100 Gy provided during 8 h (Culligan et al. 2006). Similarly, our study showed upregulation *CYCB1;2* in *A. thaliana* between 40 and 400 mGy h^{-1} and Scots pine between 10 and 40 mGy h^{-1} (Fig. 4). Although this may suggest a role of such genes in response to gamma radiation, no such induction was observed in Norway spruce although this species show similar sensitivity towards gamma irradiation as Scots pine. However, although we analysed transcript levels of the gene orthologs with highest sequence similarity in the different species, it cannot be excluded that one or more other similar *CYC* genes could be affected by gamma radiation also in Norway spruce (and the other species). In contrast, *CYCD3;1* and *CDKB1:2* did not show any indication of upregulation at the transcript level in any of the species. The DNA repair genes *SOG1* and *RAD51* were shown to be induced in *A. thaliana* exposed to 100 Gy of gamma radiation during 8 h (Culligan et al. 2006; Yoshiyama et al. 2009). Similarly, the *RAD51* gene expression increased in *A. thaliana* from 180 to 400 mGy h^{-1} and Scots pine at 10 mGy h^{-1}, whereas no differences were observed in Norway spruce (Fig. 4). In comparison, in our study *SOG1* did not show any induction in any of the plant species after gamma radiation treatment.

Chronic exposure of *Arabidopsis* to gamma radiation from a ^{134}Cs source altered gene expression level involved in cell defence, stress response and detoxification in roots (Sahr et al. 2005). Furthermore (van de Walle et al. 2016) showed increased transcript levels of antioxidant genes and enzyme activity important for cell wall strengthening and stress resistance in different *A. thaliana* life stages in response to gamma irradiation at 22–457 mGy h^{-1} for 14 days of exposure. Consistent with this, *PX3* showed induction in Norway spruce at 180 and 400 mGy h^{-1} and Scots pine at 40 mGy h^{-1} (Fig. 5). However, no such upregulation was observed in *A. thaliana* and no increase in *CAT* and *SOD* transcript levels was observed in any of the species, except 100 mGy h^{-1} in Norway spruce. Two genes related to defence and cell wall strengthening, the class IV chitinase *CHI4* and *PAL* (typically used as stress defence induction indicators in Norway spruce) (Fossdal et al. 2012), did not exhibit any differences in expression between different dose rates in any of the species, except for *CHI4* in *A. thaliana* at 180 mGy h^{-1} (Fig. 5). Taken together, although increased transcript levels of specific genes in one or two species were observed in response to gamma radiation, there was no consistent differences that could help to explain the sensitivity difference to gamma radiation between the conifers and *A. thaliana*. Since the analysed genes generally are representatives of gene families, it cannot be excluded that other genes within these families may be affected by gamma-induced stress. Also, differences for specific genes between previous investigations and our study may possibly also be due to different exposure conditions, and concomitant different levels of radiation stress induced as well as different growing conditions and accession/ecotypes.

Conclusions

In conclusion, at the organismal as well as the cellular level, Scots pine and Norway spruce seedlings show relatively similar but far higher sensitivity to gamma radiation as compared to the radioresistant *A. thaliana*. These conifers showed dose-rate-dependent cell damage in the apical meristems and severe inhibition of shoot and root developmental parameters after 144-h exposure to $\geq$ 40 mGy h^{-1} and post-irradiation, including post-irradiation mortality. The two conifers appeared similarly sensitive to gamma radiation with respect to most of the recorded growth parameters and cellular damage. *A. thaliana* showed no cellular damage or mortality, only delayed lateral root formation after 144-h and 360-h exposure to $\geq$ 400 mGy h^{-1} and post-irradiation only slightly transiently delayed flower bud formation and inflorescence elongation. Similar dose-rate-dependent degree of DNA damage after the gamma exposure and 44 days post-irradiation, although at higher levels in Norway spruce than

A. thaliana and still higher levels in Scots pine, strongly indicates that the conifers are far less tolerant to persistent DNA-damage than *A. thaliana*. Thus, persistent DNA damage, which may be caused by genomic instability, is not necessarily linked to mortality or other adverse outcome in radioresistant plants like *A. thaliana*, in contrast to the radiosensitive conifers. Nevertheless, DNA damage was also present in the conifers at lower dose rates than those resulting in growth inhibition.

Author contribution statement JEO, DAB, OCL, BS, DB, KAS and YKL conceived and planned the study. DB, JEO, DAB and OCL conducted the gamma exposure experiments. DB prepared the plant materials, performed the phenotyping, post-irradiation experiments, collected samples and performed the qPCR analyses. IY and CGF aided in selection of genes and sequence comparisons. KAS supervised DB in the F_v/F_m measurements. YKL performed COMET assay and histological studies. DB performed the statistical analyses and wrote the manuscript under supervision of JEO, DAB and OCL, with additional input from BS, YKL, KAS, CGF and IY on a late version. All authors read and approved the final manuscript.

Acknowledgements The Norwegian Research Council through its Centre of Excellence funding scheme (Grant 223268/F50) and the Norwegian University of Life Sciences (among others PhD scholarship to DB) are acknowledged for financial support. Sincere thanks to Marit Siira and Ida K. Hagen for technical assistance in plant growing and Tone I. Melby and Dr. Marcos Viejo for advices in RT-qPCR analyses. Dr. Elisabeth L. Hansen is acknowledged for assistance in dosimetry work, and Dr. Gunnar Brunborg and staff members at the Norwegian Institute of Public Health for providing expertise and scoring facility for the COMET assay.

Compliance with ethical standards

Conflict of interest The authors declare that there is no conflict of interest.

References

Ahmad P, Jaleel CA, Salem MA, Nabi G, Sharma S (2010) Roles of enzymatic and nonenzymatic antioxidants in plants during abiotic stress. Crit Rev Biotechnol 30(3):161–175. https://doi.org/10.3109/07388550903524243

Amiro BD, Sheppard SC (1994) Effects of ionizing radiation on the boreal forest: Canada's FIG experiment, with implications for radionuclides. Sci Total Environ 157:371–382. https://doi.org/10.1016/0048-9697(94)90600-9

Apel K, Hirt H (2004) Reactive oxygen species: metabolism, oxidative stress, and signal transduction. Annu Rev Plant Biol 55(1):373–399. https://doi.org/10.1146/annurev.arplant.55.031903.141701

Arkhipov NP, Kuchma ND, Askbrant S, Pasternak PS, Musica VV (1994) Acute and long-term effects of irradiation on pine (*Pinus sylvestris*) stands post-Chernobyl. Sci Total Environ 157:383–386. https://doi.org/10.1016/0048-9697(94)90601-7

Averbeck D, Salomaa S, Bouffler S, Ottolenghi A, Smyth V, Sabatier L (2018) Progress in low dose health risk research: novel effects and new concepts in low dose radiobiology. Mutat Res 776:46–69. https://doi.org/10.1016/j.mrrev.2018.04.001

Aypar U, Morgan WF, Baulch JE (2011) Radiation-induced genomic instability: are epigenetic mechanisms the missing link? Int J Radiat Biol 87(2):179–191. https://doi.org/10.3109/09553002.2010.522686

Azzam EI, Jay-Gerin JP, Pain D (2012) Ionizing radiation-induced metabolic oxidative stress and prolonged cell injury. Cancer Lett 327:48–60. https://doi.org/10.1016/j.canlet.2011.12.012

Barescut J, Lariviere D, Stocki T, Vanhoudt N, Cuypers A, Vangronsveld J, Horemans N, Wannijn J, Van Hees M, Vandenhove H (2012) Study of biological effects and oxidative stress related responses in gamma irradiated *Arabidopsis thaliana* plants. Radioprotection 46(6):S401–S407. https://doi.org/10.1051/radiopro/20116510s

Bassing CH, Chua KF, Sekiguchi J, Suh H, Whitlow SR, Fleming JC, Monroe BC, Ciccone DN, Yan C, Vlasakova K, Livingston DM, Ferguson DO, Scully R, Alt FW (2002) Increased ionizing radiation sensitivity and genomic instability in the absence of histone H2AX. Proc Natl Acad Sci USA 99(12):8173–8178. https://doi.org/10.1073/pnas.122228699

Belli M, Sapora O, Tabocchini MA (2002) Molecular targets in cellular response to ionizing radiation and implications in space radiation protection. J Radiat Res 43(Suppl):S13–S19

Caplin N, Willey N (2018) Ionizing radiation, higher plants, and radioprotection: from acute high doses to chronic low doses. Front Plant Sci. https://doi.org/10.3389/fpls.2018.00847

Culligan KM, Robertson CE, Foreman J, Doerner P, Britt AB (2006) ATR and ATM play both distinct and additive roles in response to ionizing radiation. Plant J 48(6):947–961. https://doi.org/10.1111/j.1365-313X.2006.02931.x

De Micco V, Arena C, Pignalosa D, Durante M (2011) Effects of sparsely and densely ionizing radiation on plants. Radiat Environ Biophys 50(1):1–19. https://doi.org/10.1007/s00411-010-0343-8

De Veylder L, Larkin JC, Schnittger A (2011) Molecular control and function of endoreplication in development and physiology. Trends Plant Sci 16(11):624–634. https://doi.org/10.1016/j.tplants.2011.07.001

Deckbar D, Jeggo PA, Lobrich M (2011) Understanding the limitations of radiation-induced cell cycle checkpoints. Crit Rev Biotechnol 46(4):271–283. https://doi.org/10.3109/10409238.2011.575764

Deflorio G, Horgan G, Woodward S, Fossdal CG (2011) Gene expression profiles, phenolics and lignin of Sitka spruce bark and sapwood before and after wounding and inoculation with *Heterobasidion annosum*. Physiol Mol Plant Pathol 75(4):180–187. https://doi.org/10.1016/j.pmpp.2011.02.002

Donini B (1967) Effects of chronic gamma-irradiation on *Pinus pinea* and *Pinus halepensis*. Radiat Bot 7(3):183–192. https://doi.org/10.1016/S0033-7560(67)80018-8

Esnault M-A, Legue F, Chenal C (2010) Ionizing radiation: advances in plant response. Environ Exp Bot 68(3):231–237. https://doi.org/10.1016/j.envexpbot.2010.01.007

Fesenko SV, Alexakhin RM, Geras'kin SA, Sanzharova NI, Spirin YV, Spiridonov SI, Gontarenko IA, Strand P (2005) Comparative radiation impact on biota and man in the area affected by the accident at the Chernobyl nuclear power plant. J Environ Radioact 80(1):1–25. https://doi.org/10.1016/j.jenvrad.2004.08.011

Fossdal CG, Yaqoob N, Krokene P, Kvaalen H, Solheim H, Yakovlev IA (2012) Local and systemic changes in expression of

resistance genes, nb-lrr genes and their putative microRNAs in Norway spruce after wounding and inoculation with the pathogen *Ceratocystis polonica*. BMC Plant Biol 12:105. https://doi.org/10.1186/1471-2229-12-105

Gichner T, Patková Z, Kim JK (2003) DNA damage measured by the comet assay in eight agronomic plants. Biol Plant 47(2):185–188. https://doi.org/10.1023/B:BIOP.0000022249.86426.2a

Gill SS, Tuteja N (2010) Reactive oxygen species and antioxidant machinery in abiotic stress tolerance in crop plants. Plant Physiol Biochem 48(12):909–930. https://doi.org/10.1016/j.plaphy.2010.08.016

Goltsova N, Abaturov Y, Abaturov A, Melankholin P, Girbasova A, Rostova N (1991) Chernobyl radionuclide accident: effects on the shoot structure of *Pinus sylvestris*. Annales Botanici Fennici 28(1):1–13

Hansen EL, Lind OC, Oughton DH, Salbu B (2019) A framework for exposure characterization and gamma dosimetry at the NMBU FIGARO irradiation facility. Int J Radiat Biol 95(1):82–89. https://doi.org/10.1080/09553002.2018.1539878

Hurem S, Gomes T, Brede DA, Lindbo Hansen E, Mutoloki S, Fernandez C, Mothersill C, Salbu B, Kassaye YA, Olsen A-K, Oughton D, Alestrom P, Lyche JL (2017) Parental gamma irradiation induces reprotoxic effects accompanied by genomic instability in zebrafish (*Danio rerio*) embryos. Environ Res 159:564–578. https://doi.org/10.1016/j.envres.2017.07.053

Kalisz S, Kramer EM (2007) Variation and constraint in plant evolution and development. Heredity 100:171. https://doi.org/10.1038/sj.hdy.6800939

Kashparova E, Levchuk S, Morozova V, Kashparov V (2018) A dose rate causes no fluctuating asymmetry indexes changes in silver birch (*Betula pendula* (L.) Roth.) leaves and Scots pine (*Pinus sylvestris* L.) needles in the Chernobyl Exclusion Zone. J Environ Radioact. https://doi.org/10.1016/j.jenvrad.2018.05.015

Kawai T, Inoshita T (1965) Effects of gamma ray irradiation on growing rice plants—I: irradiations at four main developmental stages. Radiat Bot 5(3):233–255. https://doi.org/10.1016/S0033-7560(65)80121-1

Killion DD, Constantin MJ (1972) Gamma irradiation of corn plants: effects of exposure, exposure rate, and developmental stage on survival, height, and grain yield of two cultivars. Radiat Bot 12(3):159–164. https://doi.org/10.1016/S0033-7560(72)80061-9

Kim JH, Chung BY, Kim JS, Wi SG (2005) Effects of in Planta gamma-irradiation on growth, photosynthesis, and antioxidative capacity of red pepper (*Capsicum annuum* L.) plants. J Plant Biol 48(1):47–56. https://doi.org/10.1007/bf03030564

Kim DS, Kim JB, Goh EJ, Kim WJ, Kim SH, Seo YW, Jang CS, Kang SY (2011) Antioxidant response of *Arabidopsis* plants to gamma irradiation: genome-wide expression profiling of the ROS scavenging and signal transduction pathways. J Plant Physiol 168(16):1960–1971. https://doi.org/10.1016/j.jplph.2011.05.008

Koppen G, Azqueta A, Pourrut B, Brunborg G, Collins AR, Langie SAS (2017) The next three decades of the comet assay: a report of the 11th International Comet Assay Workshop. Mutagenesis 32(3):397–408

Kovalchuk O, Kovalchuk I, Titov V, Arkhipov A, Hohn B (1999) Radiation hazard caused by the Chernobyl accident in inhabited areas of Ukraine can be monitored by transgenic plants. Mutat Res Genetic Toxicol Environ Mutagen 446(1):49–55. https://doi.org/10.1016/S1383-5718(99)00147-3

Kovalchuk I, Molinier J, Yao Y, Arkhipov A, Kovalchuk O (2007) Transcriptome analysis reveals fundamental differences in plant response to acute and chronic exposure to ionizing radiation. Mutat Res Fund Mol Mech Mutagen 624(1–2):101–113. https://doi.org/10.1016/j.mrfmmm.2007.04.009

Kryshev II, Romanov GN, Isaeva LN, Kholina YB (1997) Radioecological state of lakes in the southern Ural impacted by radioactivity release of the 1957 radiation accident. J Environ Radioact 34(3):223–235. https://doi.org/10.1016/0265-931X(96)00033-1

Lee Y, Karunakaran C, Lahlali R, Liu X, Tanino KK, Olsen JE (2017) Photoperiodic Regulation of Growth-Dormancy Cycling through Induction of Multiple Bud-Shoot Barriers Preventing Water Transport into the Winter Buds of Norway Spruce. Front Plant Sci. https://doi.org/10.3389/fpls.2017.02109

Lind OC, Helen Oughton D, Salbu B (2018) The NMBU FIGARO low dose irradiation facility. Int J Radiat Biol. https://doi.org/10.1080/09553002.2018.1516906

Macovei A, Tuteja N (2013) Different expression of miRNAs targeting helicases in rice in response to low and high dose rate γ-ray treatments. Plant Signal Behav 8(8):e25128. https://doi.org/10.4161/psb.25128

Makarenko ES, Oudalova AA, Geraskin SA (2016) Study of needle morphometric indices in Scots pine in the remote period after the Chernobyl accident. Radioprotection 51(1):19–23

Marcu D, Damian G, Cosma C, Cristea V (2013) Gamma radiation effects on seed germination, growth and pigment content, and ESR study of induced free radicals in maize (Zea mays). J Biol Phys 39(4):625–634. https://doi.org/10.1007/s10867-013-9322-z

Maxwell K, Johnson GN (2000) Chlorophyll fluorescence—a practical guide. J Exp Bot 51(345):659–668. https://doi.org/10.1093/jexbot/51.345.659

Mergen F, Strøm Johansen T (1964) Effect of ionizing radiation on seed germination and seedling growth of *Pinus rigida* (mill). Radiat Bot 4(4):417–427. https://doi.org/10.1016/S0033-7560(64)80009-0

Mittler R, Vanderauwera S, Gollery M, Van Breusegem F (2004) Reactive oxygen gene network of plants. Trends Plant Sci 9(10):490–498. https://doi.org/10.1016/j.tplants.2004.08.009

Morgan WF, Day JP, Kaplan MI, McGhee EM, Limoli CL (1996) Genomic instability induced by ionizing radiation. Radiat Res 146(3):247–258. https://doi.org/10.2307/3579454

Mothersill C, Seymour CB (1998) Mechanisms and implications of genomic instability and other delayed effects of ionizing radiation exposure. Mutagenesis 13(5):421–426. https://doi.org/10.1093/mutage/13.5.421

Murashige T, Skoog F (1962) A revised medium for rapid growth and bio assays with tobacco tissue cultures. Physiol Plant 15(3):473–497. https://doi.org/10.1111/j.1399-3054.1962.tb08052.x

Nagata T, Todoriki S, Hayashi T, Shibata Y, Mori M, Kanegae H, Kikuchi S (1999) γ-Radiation induces leaf trichome formation in *Arabidopsis*. Plant Physiol 120(1):113–120

Olsen JE (2010) Light and temperature sensing and signaling in induction of bud dormancy in woody plants. Plant Mol Biol 73(1):37–47. https://doi.org/10.1007/s11103-010-9620-9

Paschoa AS (1998) Potential environmental and regulatory implications of naturally occurring radioactive materials (NORM). Appl Radiat Isot 49(3):189–196. https://doi.org/10.1016/S0969-8043(97)00239-X

Reisz JA, Bansal N, Qian J, Zhao W, Furdui CM (2014) Effects of ionizing radiation on biological molecules—mechanisms of damage and emerging methods of detection. Antioxid Redox Signal 21(2):260–292. https://doi.org/10.1089/ars.2013.5489

Roldán-Arjona T, Ariza RR (2009) Repair and tolerance of oxidative DNA damage in plants. Mutat Res 681(2):169–179. https://doi.org/10.1016/j.mrrev.2008.07.003

Rozen S, Skaletsky HJ (2000) Primer3 on the WWW for general users and for biologist programmers. Methods Mol Biol 132:365–386

Rudolph TD (1971) Gymnosperm seedling sensitivity to gamma radiation: its relation to seed radiosensitivity and nuclear variables. Radiat Bot 11(1):45–51. https://doi.org/10.1016/S0033-7560(71)91371-8

Sahr T, Voigt G, Schimmack W, Paretzke HG, Ernst D (2005) Low-level radiocaesium exposure alters gene expression in roots of *Arabidopsis*. New Phytol 168(1):141–148. https://doi.org/10.1111/j.1469-8137.2005.01485.x

Sidorov VP (1994) Cytogenetic effect in *Pinus sylvestris* needle cells as a result of the Chernobyl accident. Radiat Biol 34(6):847–851

Stalter R, Kincaid D (2009) Community development following gamma radiation at a pine–oak forest, Brookhaven National Laboratory, Long Island, New York1. Am J Bot 96(12):2206–2213. https://doi.org/10.3732/ajb.0800418

Tikhomirov FA, Shcheglov AI (1994) Main investigation results on the forest radioecology in the Kyshtym and Chernobyl accident zones. Sci Total Environ 157:45–57. https://doi.org/10.1016/0048-9697(94)90564-9

Tulik M (2001) Cambial history of Scots pine trees (*Pinus sylvestris*) prior and after the Chernobyl accident as encoded in the xylem. Environ Exp Bot 46(1):1–10. https://doi.org/10.1016/S0098-8472(01)00075-2

UNSCEAR (1996) Sources and effects of ionizing radiation. United Nations Scientific Commitee on the Effects of Atomic Radiation, New York

UNSCEAR (2017) Sources, effects and risks of ionizing radiation. United Nations Scientific Commitee on the Effects of Atomic Radiation, New York

van de Walle J, Horemans N, Saenen E, Van Hees M, Wannijn J, Nauts R, van Gompel A, Vangronsveld J, Vandenhove H, Cuypers A (2016) *Arabidopsis* plants exposed to gamma radiation in two successive generations show a different oxidative stress response. J Environ Radioact 165:270–279. https://doi.org/10.1016/j.jenvrad.2016.10.014

Van Hoeck A, Horemans N, Van Hees M, Nauts R, Knapen D, Vandenhove H, Blust R (2015) Characterizing dose response relationships: chronic gamma radiation in *Lemna minor* induces oxidative stress and altered polyploidy level. J Environ Radioact 150:195–202. https://doi.org/10.1016/j.jenvrad.2015.08.017

Van Hoeck A, Horemans N, Nauts R, Van Hees M, Vandenhove H, Blust R (2017) *Lemna minor* plants chronically exposed to ionising radiation: RNA-seq analysis indicates a dose rate dependent shift from acclimation to survival strategies. Plant Sci 257:84–95. https://doi.org/10.1016/j.plantsci.2017.01.010

Vandenhove H, Vanhoudt N, Cuypers A, van Hees M, Wannijn J, Horemans N (2010) Life-cycle chronic gamma exposure of *Arabidopsis thaliana* induces growth effects but no discernable effects on oxidative stress pathways. Plant Physiol Biochem 48(9):778–786. https://doi.org/10.1016/j.plaphy.2010.06.006

Vives i Batlle J, Aono T, Brown JE, Hosseini A, Garnier-Laplace J, Sazykina T, Steenhuisen F, Strand P (2014) The impact of the Fukushima nuclear accident on marine biota: retrospective assessment of the first year and perspectives. Sci Total Environ 487:143–153. https://doi.org/10.1016/j.scitotenv.2014.03.137

Watanabe Y, Se Ichikawa, Kubota M, Hoshino J, Kubota Y, Maruyama K, Fuma S, Kawaguchi I, Yoschenko VI, Yoshida S (2015) Morphological defects in native Japanese fir trees around the Fukushima Daiichi Nuclear Power Plant. Sci Rep 5:13232. https://doi.org/10.1038/srep13232

Wi SG, Chung BY, Kim JH, Baek MH, Yang DH, Lee JW, Kim JS (2005) Ultrastructural changes of cell organelles in *Arabidopsis* stems after gamma irradation. J Plant Biol 48(2):195–200. https://doi.org/10.1007/bf03030408

Wi SG, Chung BY, Kim J-S, Kim J-H, Baek M-H, Lee J-W, Kim YS (2007) Effects of gamma irradiation on morphological changes and biological responses in plants. Micron 38(6):553–564. https://doi.org/10.1016/j.micron.2006.11.002

Woodwell GM (1962) Effects of ionizing radiation on terrestrial ecosystems. Experiments show how ionizing radiation may alter normally stable patterns of ecosystem behavior. Science 138(3540):572–577. https://doi.org/10.1126/science.138.3540.572

Woodwell GM, Rebuck AL (1967) Effects of chronic gamma radiation on the structure and diversity of an oak-pine forest. Ecol Monogr 37(1):53–69. https://doi.org/10.2307/1948482

Wright SI, Gaut BS (2005) Molecular population genetics and the search for adaptive evolution in plants. Mol Biol Evol 22(3):506–519. https://doi.org/10.1093/molbev/msi035

Yoschenko V, Ohkubo T, Kashparov V (2017) Radioactive contaminated forests in Fukushima and Chernobyl. J For Res. https://doi.org/10.1080/13416979.2017.1356681

Yoshiyama K, Conklin PA, Huefner ND, Britt AB (2009) Suppressor of gamma response 1 (SOG1) encodes a putative transcription factor governing multiple responses to DNA damage. Proc Natl Acad Sci USA 106(31):12843–12848. https://doi.org/10.1073/pnas.0810304106

Yoshiyama KO, Sakaguchi K, Kimura S (2013) DNA damage response in plants: conserved and variable response compared to animals. Biology 2(4):1338–1356. https://doi.org/10.3390/biology2041338

Zelena L, Sorochinsky B, von Arnold S, van Zyl L, Clapham DH (2005) Indications of limited altered gene expression in *Pinus sylvestris* trees from the Chernobyl region. J Environ Radioact 84(3):363–373. https://doi.org/10.1016/j.jenvrad.2005.03.008

Supplementary material

Table S1. Oligonucleotide primer sequences used for RT-gPCR analyses of specific reference genes, DNA-repair-, antioxidant-, cell cycle- and defence-related-related genes in *A. thaliana* seedlings.

Gene	Accession number	Forward (5`->3`)	Reverse (3'->5')
ACT2	AT3G18780	TCAGATGCCCAGAAGTCTTGTTCC	CCGTACAGATCCTTCCTGATATCC
EF-1α	AT5G60390	CCCAGGCTGATTGTGCTGT	GGGTAGTGGCATCCATCTTGTT
RAD51	AT5G20850	GTGAGTTCCGCTCTGGAAAG	CCTGAATGTTCCCTCAGCAT
SOG1	AT1G25580	GTGAAAACCAACTGGGTGA	CTGTTGTGGCTGCTGGTAGA
SOD	AT1G08830	GGAACTGCCACCTTCACAAT	TCCAGTAGCCAGGCTGAGTT
CAT	AT4G35090	CGAGGTATGACCAGGTTCGT	CTCCAGGCTCCTTGAAGTTG
PX3	AT1G71695	AAGAAGTGCGGTCAAGTCGT	GCCAAGTGGGACAGCATAGT
CYCD3;1	AT4G34160	AACTACCAGTGGACCGCATC	TCGCTATTGAAAGGGTTTGC
CYCB1;1	AT4G37490	CCCATATGGACCAGCACTCT	CTTGTTGCTTCCATTGCTGA
CDKB1;2	AT2G38620	GCTCGAAATGGACGAAGAAG	TAACATGTTCGACGCAGAGG
Chi4	AT3G54420	TGAGATTGCAGCGTTCTTTG	GTTGCATTCTCGTCGCAGTA
PaL	AT3G53260	GTTCGTGAGGGAAGAGCTTG	TCCGTTCCATTCCTTGAGAC

Table S2. Oligonucleotide primer sequences used for RT-gPCR analyses of specific reference genes, DNA-repair-, antioxidant-, cell cycle- and defence-related-related genes in Norway spruce seedlings.

Gene	Accession number	Forward (5`->3`)	Reverse (3'->5')
ACT	AY961918	TGAGCTCCCTGATGGGCAGGTGA	TGGATACCAGCAGCTTCCATCCCAAT
EF-1α	X57980	GGATTGCCACACTTGCCACA	CTTGGGTTCCTTCTCCAGTTCC
RAD51	MA_93267g0010	ATCCCCGAGGAAGAAGAAAA	CAACAGCTTCTACCGTGCAA
SOG1	MA_8533126g0010	GATTTCGTGTGGCAACCTTT	TGCGACCATATTCAACTGGA
SOD	MA_10431443g0010	CACAGAGCTCAAGGGGTTTC	TCTCCTTCCTGGGTGAATTG
CAT	MA_10437148g0010	GGGAGGCAAACCTATGTGAA	TTGGTTGCATGACTGTGGTT
PX3	GT127236	ATGGTGGCGCTGTCAATTC	TGCTGTAGAACGTCCAAGAAAGAC
CYCD3;1	MA_17738g0010	GGCTTTTTGCCATCTGTTGT	TCACTTTCATGGCACTGAGC
CYCB1;1	MA_10431608g0020	AGGGTATCACGAGCCAACAC	CAGAGGTTTCCTCCCATTGA
CDKB1;2	MA_106416g0010	ATAAGCTCTGCCGTTCCAGA	GGATGTTGCAATGCCTTTTT
Chi4	MA_10427514g0010	TGGAGGGTTGTGCTACATCA	CCACGTCCATGGTAGCTCTT
PaL	MA_123220g0010	GTTATGAACGGGAAGCCTGA	TCCCGTCCAAGACATACTCC

Table S3. Oligonucleotide primer sequences used for RT-gPCR analyses of specific reference genes, DNA-repair-, antioxidant-, cell cycle- and defence-related-related genes in Scots pine seedlings.

Gene	Accession number	Forward (5`->3`)	Reverse (3'->5')
ACT	FN546174	TGACATGGAGAAGATTTGGC	CATACATAGCAGGCACATTG
GAPDH	L07501	CTGGTGTCTTCACCGACAAA	GGTGCTCATTAACCCCAACA
RAD51	EU513162.1	TATGGGGAATTTCGAACAGG	GTTCCCTCGGCATCAATAAA
SOG1	PITA_000080155-RA	ATGGAATCTGCTCTGCTCGT	GCGTTTACGGTTGCCTGTAT
SOD	AJ307586.1	AACCGTCATGCTGGTGATTT	CTGCCCTCCCAACTATTGAA
CAT	EU513163.1	GGGAGGCAAACCTATGTGAA	TGGTTGCATGACTGTGGTTT
PX3	PITA_000062937-RA	GTGATCTATGGAGGCGCTGT	GCCTGTGTGATGTCTGCACT
CYCD3;1	PITA_000011498-RA	TTCCCCTTCTCCTGGACTTT	ACAGGACTCATTCGCCATTC
CYCB1;1	PITA_000017697-RA	CTGCAGTCTACACCGCTCAA	GGAATGCCACCATCAGTCTT
CDKB1;2	PITA_000082194-RA	GGGAACGTATGGCAAAGTGT	GTGGGAGGAACTCCCTCTTC
Chi4	PITA_000043780-RA	ATCCCACCATCTCGTTCAAG	GGCTGTTGATGGCTTTGATT
PaL	PITA_000041078-RA	TTGTGTGTTTCGATGCCAAT	GATGGTGCTTCAGCTTGTGA

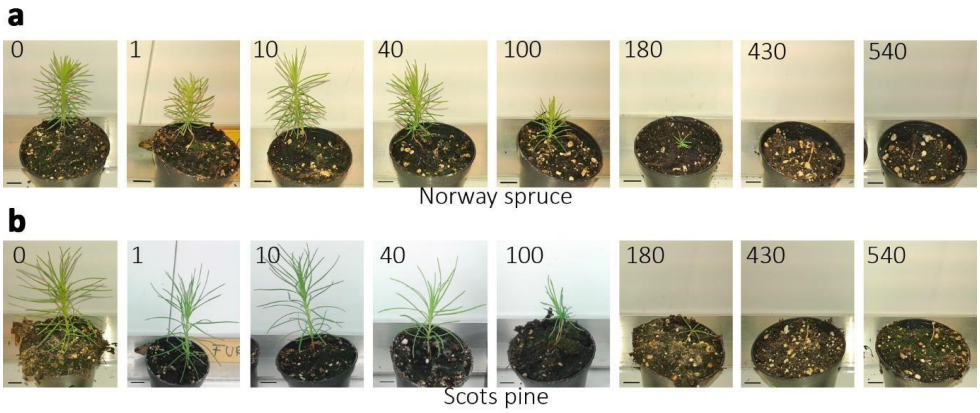

Fig. S1 Phenotype of seedlings of **a)** Norway spruce and **b)** Scots pine plants at day 44 postirradiation (day 56 after sowing) following exposure to gamma radiation at different dose rates (mGy h^{-1}) for 144 h 7-12 days after sowing.

Paper II

Photochemical & Photobiological Sciences

PAPER

Cite this: Photochem. Photobiol. Sci., 2019, 18, 1945

No evidence of a protective or cumulative negative effect of UV-B on growth inhibition induced by gamma radiation in Scots pine (*Pinus sylvestris*) seedlings†

Dajana Blagojevic,‡[a,b] YeonKyeong Lee,‡[a,b] Li Xie,[b,c] Dag A. Brede,[b,d] Line Nybakken,[b,d] Ole Christian Lind,[b,d] Knut Erik Tollefsen,[b,c] Brit Salbu,[b,d] Knut Asbjørn Solhaug[b,d] and Jorunn E. Olsen *[a,b]

Exposure to ambient UV-B radiation may prime protective responses towards various stressors in plants, though information about interactive effects of UV-B and gamma radiation is scarce. Here, we aimed to test whether UV-B exposure could prime acclimatisation mechanisms contributing to tolerance to low-moderate gamma radiation levels in Scots pine seedlings, and concurrently whether simultaneous UV-B and gamma exposure may have an additive adverse effect on seedlings that had previously not encountered either of these stressors. Responses to simultaneous UV-B (0.35 W m^{-2}) and gamma radiation (10.2–125 mGy h^{-1}) for 6 days with or without UV-B pre-exposure (0.35 W m^{-2}, 4 days) were studied across various levels of organisation, as compared to effects of either radiation type. In contrast to UV-B, and regardless of UV-B presence, gamma radiation at ≥42.9 mGy h^{-1} caused increased formation of reactive oxygen species and reduced shoot length, and reduced root length at 125 mGy h^{-1}. In all experiments there was a gamma dose rate-dependent increase in DNA damage at ≥10.8 mGy h^{-1}, generally with additional UV-B-induced damage. Gamma-induced growth inhibition and gamma- and UV-B-induced DNA damage were still visible 44 days post-irradiation, even at 20.7 mGy h^{-1}, probably due to genomic instability, but this was reversed after 8 months. In conclusion, there was no evidence of a protective effect of UV-B on gamma-induced growth inhibition and DNA damage in Scots pine, and no additive adverse effect of gamma and UV-B radiation on growth in spite of the additional UV-B-induced DNA damage.

Received 31st October 2018,
Accepted 6th July 2019

DOI: 10.1039/c8pp00491a

rsc.li/pps

1 Introduction

As sessile organisms, plants need to cope with a range of changing environmental conditions and stressors, including high energy radiation such as ionising radiation (IR) and UV-B (280–315 nm). In natural environments IR is ubiquitously present and includes cosmic radiation and radiation from radionuclide-containing bedrock, soils and sediments. Since the origin of life the average global IR level from geological sources has decreased by a factor of approximately 8, and the current global mean background dose rate is 2.5 mGy per year, which corresponds to about 0.29 μGy h^{-1}.[1] However, as in the past, many areas have naturally elevated IR due to high radionuclide content in the bedrock, such as Ihla Grande in Brazil, Ramsar in Iran and the Fen field in Norway, where dose rates have been measured at 14–15 μGy h^{-1}, 4.4 μGy h^{-1} and 8 μGy h^{-1} respectively.[1–3] Furthermore, elevated levels of IR in nature are also due to radionuclide release from anthropogenic activities, such as waste and accidental releases from nuclear power plants, nuclear weapon tests, and medical use.[1,4]

Of the different types of electromagnetic radiation, gamma radiation has the highest energy, and accordingly high penetration power. Low doses and dose rates of IR, such as gamma radiation, are currently defined as ≤100 mGy and ≤6 mGy h^{-1}, respectively.[5,6] It should be noted that these threshold values are largely related to health effects. On the basis of results from experiments and accidents, it has been generally noted

[a]Department of Plant Sciences, Faculty of Biosciences, Norwegian University of Life Sciences, P.O. Box 5003, N-1432 Ås, Norway. E-mail: jorunn.olsen@nmbu.no
[b]Centre of Environmental Radioactivity (CERAD), Norwegian University of Life Sciences, P.O. Box 5003, N-1432 Ås, Norway
[c]Norwegian Institute for Water Research (NIVA), Section of Ecotoxicology and Risk Assessment, Gaustadalléen 21, N-0349 Oslo, Norway
[d]Faculty of Environmental Sciences and Natural Resource Management, Norwegian University of Life Sciences, P.O. Box 5003, N-1432 Ås, Norway
†Electronic supplementary information (ESI) available. See DOI: 10.1039/c8pp00491a
‡These authors contributed similarly to the experimental data.

that acute high doses of IR between 10–1000 Gy can be lethal to plants, but that <10 mGy day^{-1} (about 0.42 mGy h^{-1}) probably have no detrimental effect on terrestrial plants in the field.[1,7] From this it follows that plants may tolerate much higher IR levels than the natural background levels. However, different organisms, including various plant species, may respond differently to specific IR or gamma radiation dose rates or total doses. This may be particularly true for low-moderate doses or dose rates, which are less well studied than higher doses and dose rates.[8–11] Significant variation in the effects of IR on plant morphology and physiology has been observed, with *e.g.* conifers being considered radiosensitive and *Arabidopsis thaliana* more radioresistant.[1,12–15] After the Chernobyl nuclear power plant accident in 1986, Scots pine (*Pinus sylvestris*) in particular showed high mortality close to the power plant zone.[16–18] It has been estimated that during the first two weeks after the accident conifers in this area received a dose of approximately 3.7 Gy.[19] Furthermore, under chronic IR exposure, loss of the apical dominance was observed in young populations of Scots pine in the Chernobyl exclusion zone as well as in Japanese red pine (*Pinus densiflora*) and Japanese fir (*Abies firma*) in the contaminated Fukushima power plant zone after the 2011 accident.[20,21]

UV-B has the highest energy of the solar UV radiation reaching the ground, and the levels vary with time of the day and year, latitude, altitude and cloud cover. To illustrate this, in a coastal area at 60°N (Helsinki, Finland) the UV-B in early June (2011) was measured at 1.2 W m^{-2} under photosynthetically active radiation (PAR) of ~1600 μmol m^{-2} s^{-1}.[22] A considerable number of studies have described harmful effects of UV-B in a wide range of living organisms, including plants.[23,24] However, many earlier plant studies were performed with high UV-B levels under low light conditions, which has been shown to aggravate many UV effects.[25] In recent years, more realistic UV-B exposure conditions have been shown to rarely result in accumulation of UV-B-related damage.[26,27] It appears that UV-B radiation stress only becomes significant when plants are either challenged by other stressors, exposed to a high ratio of UV-B to PAR or exposed to very high UV-B levels in general.[26] Drought, nutrient deficiency and extreme climatic conditions are examples of stressors shown to result in aggravated UV stress.[28–30]

On the other hand, there is substantial evidence that UV-B at a moderate level acts as an important signal for induction of stress protection, as well as a morphogenic signal.[31–33] UV radiation has also been shown to induce cross-tolerance to stressors such as drought, cold, salt stress, wounding and pathogens.[34–42] Although such a relationship is not always clear, it has been shown that the negative effects of simultaneous exposure to UV-B and Cadmium on photosynthesis were minimized by pre-exposure to either of these.[43] Thus, cross-tolerance is apparently due to acclimation.

Exposure to elevated IR results in production of reactive oxygen species (ROS) due to the radiolysis of water.[1] UV-B may also induce ROS formation, with the degree of ROS accumulation depending on the UV-B level.[44] ROS may interact rapidly with proteins, lipids and nucleic acids, resulting in damage and genotoxicity.[45] In addition, IR can cause direct ionisation of biomolecules, causing additional damage.[1] DNA damage may cause persistent mutations, which in turn can reduce plant genome stability and growth.[46,47] However, depending on the duration and level of irradiation, signals that activate DNA repair mechanisms may be triggered, in which cell cycle regulatory proteins and antioxidant genes also play a major role.[1,48–50]

To counteract ROS-induced oxidative stress, plants can modulate their antioxidative defence systems, which include ROS scavenging enzymes and non-enzymatic antioxidant metabolites. This enables plants to avoid cellular damage while still allowing ROS-dependent signalling that is known to be an integrated part of defence responses.[47,51,52] Induction of antioxidants and genes encoding antioxidant enzymes in gamma-irradiated plants has been reported for a number of plant species.[47,48,53,54] UV-B is also well known to induce production of a range of phenolic compounds, including flavonoids, which protect against damage through their UV-B screening ability and by serving as ROS scavengers, thereby neutralizing free radicals before they damage the cells.[31,55] Information about whether gamma radiation may also induce such phenolic compounds is limited. Furthermore, although UV-priming of plant defence systems may afford the plant protection against different stressors, information about whether this may apply for low to moderate levels of gamma radiation is not available. It may be suggested that the ubiquitous presence of IR in nature, and the higher IR levels in the past, may have helped to drive the evolution of DNA repair and protection towards oxidative stress as well as regulatory responses.[1] If so, cross-protection against oxidative stress generated by UV-B and low-moderate levels of gamma radiation may well be possible.

The overall aim of this work was to study interactive effects of UV-B and gamma radiation across various levels of organisation in Scots pine seedlings, using gamma doses realistic to those at different distances to accidental realeases like in Chernobyl. The specific aims were to test (1) whether UV-B has the potential to prime stress acclimatisation mechanisms, thereby conferring some tolerance to low-moderate gamma radiation levels and producing Scots pine seedlings with better physiological sufficiency and growth than they would otherwise have had without UV-B radiation; (2) whether UV-B radiation exposure applied simultaneously with gamma radiation will have an additive adverse effect on plants that have not previously encountered either of these two radiation types; and (3) whether there is a dose-dependent response of Scots pine to gamma radiation with an interactive effect of this response with exposure to UV-B radiation.

2 Materials and methods

2.1 Plant materials and pre-growing conditions

Seeds of the Scots pine (*Pinus sylvestris* L.) provenance CØ1 from Halden, Norway (59°N latitude, 0–149 m altitude, seed

lot 5632, Skogfrøverket, Hamar, Norway), were surface sterilized in 1% sodium hypochlorite for 5 min, rinsed five times in sterile, distilled water and dried on a sterile filter paper. The seeds were evenly sown on $\frac{1}{2}$ strength MS medium[56] (Duchefa Biochemie, Harleem, Netherland) with 0.8% agar (Plant agar, Sigma-Aldrich, St Louis, Mo, USA) in Petri dishes of 5 cm diameter with 15–20 seeds per dish (germination rate of approximately 50–60%). The seeds were germinated for 6 days in a growth chamber at 20 °C under a photon irradiance of 30 μmol m^{-2} s^{-1} at 400–700 nm (TL-D 58W/840 lamps Phillips, Eindhoven, The Netherlands) and a 16 h photoperiod. As the plastic lids of the Petri dishes were not UV-B-transparent, all lids were replaced with UV-B-transparent cling film at the start of the experimental treatments.

2.2 Experimental growing conditions, gamma and UV-B radiation sources and dosimetry

During the experiments (the treatments are described in the chapter below), which started when the seedlings were six days old, the Petri dishes with seedlings were kept in two identical growth chambers (without metal in the front and end walls; manufactured by the Norwegian University of Life Sciences (NMBU), Ås, Norway). The chambers were maintained at 20 °C, with a 12 h photoperiod and a photon irradiance of 200 μmol m^{-2} s^{-1} at 400–700 nm. Light was provided by white light emitting diode panels (PCB1E 5000K, Evolys, Oslo, Norway) and incandescent lamps (Osram, Munchen, Germany). The irradiance was measured at the top of the Petri dishes with a quantum sensor (Model LI-190 LI-COR, Lincoln, NE, USA). The red : far red (R : FR) ratio was 1.9, as measured by a 660/730 nm sensor (Skye Instruments, Powys, Wales, UK). The relative air humidity (RH) of the chambers was adjusted to 78%, corresponding to a water vapour deficit of 0.5 kPa.

The plants in one of the growth chambers were exposed to constant gamma radiation for six days (144 h), with the exception of 10–15 min in the middle of each experiment when the Petri dishes were rotated. Gamma radiation was provided using the FIGARO UV and low dose rate gamma (^{60}Co; 1173.2 and 1332.5 keV γ-rays) irradiation facility at the Norwegian University of Life Sciences (NMBU), Norway.[57] The growth chamber was placed in front of the collimator containing the ^{60}Co source, while the other growth chamber was kept outside the irradiation sector behind gamma radiation-shielding lead walls.

The gamma dosimetry of the exposed plants followed an established protocol.[58] Petri dishes with plants were positioned at different distances from the gamma source to obtain the intended average air kerma rates (Table 1). For each air kerma rate there were eight Petri dishes with plants, four side by side, with four others immediately behind these. To obtain similar gamma exposure, the front and back Petri dishes were interchanged, and all dishes rotated 180° in the middle of the experiment. Each average air kerma rate was calculated from measurements of the dose rates in front of and behind the two Petri dish rows per kerma rate, using four nanodot dosimeter measurements in each case (microStar, Landauer Inc., Greenwood, IL, USA), and taking the rotation of the Petri dishes into account. On the basis of the air kerma rates, the average, minimum and maximum dose rates to water were estimated according to Hansen *et al.* (2019),[58] and the average was used as a proxy for the dose rates provided to the plants (Table 1). The total doses and dose intervals were calculated from the estimated absorbed dose rates to water (mGy h^{-1}), multiplied by total exposure time (h).

In each growth chamber UV-B was provided for 10 h daily from two UV-B fluorescent tubes (UVB-313, Q-Panel Co., Cleveland, OH, USA) mounted in the ceiling of the growth chamber. The UV-B radiation started 1 h after the light was turned on and ended 1 h before the light was turned off. To block UV-wavelengths below 290 nm in the UV-B treatments, cellulose diacetate foil (0.13 mm, Jürgen Rachow, Hamburg, Germany) was placed on top of half of the Petri dishes in each growth chamber. UV-blocking polycarbonate filters were placed on top of the rest of the Petri dishes to provide non-UV-B-exposed controls.

Table 1 The gamma radiation dose rates and total doses applied in the experiments with 6 days gamma exposure of young seedlings of Scots pine using a ^{60}Co source. The minimum and maximum values represent the dose rates and total doses behind and in front of the Petri dishes with the seedlings. Dose rates to water, which were used as proxies for the dose rates received by the seedlings, were calculated from the measured dose rate air kerma values

Average dose rate air kerma[a] (mGy h^{-1})	Dose rate air kerma interval (mGy h^{-1})		Average dose rate to water (mGy h^{-1})	Dose rate to water interval (mGy h^{-1})		Average total dose (Gy) 144 h (6 days) exposure	Total dose interval[b] 144 h (6 days) exposure (Gy)	
	Minimum	Maximum		Minimum	Maximum		Minimum	Maximum
112[c]	102.3	131.7	125	113.7	146.5	18.01	17.29	18.73
38.5	35.6	41.5	42.9	39.6	46.1	6.17	5.93	6.41
18.6	17.6	19.6	20.7	19.6	21.8	2.98	2.86	3.10
9.7	9.2	10.2	10.8	10.2	11.4	1.55	1.49	1.61
0.004[d]	0.005	0.003	0.005	0.006	0.004	0.00072	0.0009	0.0006

[a] Air kerma rates represent the averages of four nanodot measurements per treatment. [b] The interval represents the weighted minimum and maximum dose rates taking into account rotation of the samples. [c] Measured between the two rows of Petri dishes. [d] Dose rate in lead-shielded control zone.

The UV-B irradiance was measured at the top of the Petri dishes (under the filters) with a broadband UV-B sensor (SKU340, Skye Instruments, Powys, UK). Based on a calibration factor obtained from simultaneous measurement of UV-B with an Optronic model 756 spectroradiometer (Optronic laboratories, Orlando, FL, USA) and the broadband UV-B sensor, the absolute UV-B irradiation was calculated to 0.35 W m^{-2} (corresponding to 0.9 μmol m^{-2} s^{-1}; calculated according to Aphalo *et al.* (2012)[22]). Using the Green weighting function,[59] which is based on relating the DNA damage at different wavelengths to the DNA damage at 300 nm (set to 1), the biologically effective UV-B ($UV\text{-}B_{BE}$) was calculated to 0.18 W m^{-2} (corresponding to 0.45 μmol m^{-2} s^{-1}).

2.3 The specific UV-B and gamma radiation treatments and experiments

To test whether UV-B combined with different dose rates of gamma radiation would have a cumulative negative effect on plants that have not previously encountered either of these radiation types, six repeated experiments including simultaneous UV-B and gamma exposure (without UV-B pre-treatment) were performed (Table 2). In each of these, eight subsets of plants (four Petri dishes per subset) were exposed to different treatments as follows: in one growth chamber six subsets of plants (four Petri dishes per subset) were exposed to gamma radiation at dose rates of either 20.7, 42.9 or 125 mGy h^{-1} for six days (144 h), either in the presence (denoted "UV-B+gamma") or absence (denoted "gamma") of UV-B at 0.35 W m^{-2} for 10 h daily (as described in the chapter above). The reason for selecting relatively high UV-B to PAR ratios was that conifers like Scots pine are highly tolerant to UV-B due to efficient screening in the epidermis.[60–62] In the growth chamber outside the gamma radiation sector, another subset of plants was exposed to UV-B only (denoted "UV-B" (no gamma)), and still another plant subset was not exposed to UV-B (denoted "control" (no UV-B, no gamma).

To test whether UV-B has the potential to prime stress acclimatisation mechanisms contributing to tolerance to low-moderate gamma radiation levels, three further experiments including UV-B pre-treatment prior to irradiation with different gamma dose rates and UV-B were conducted (Table 2). In these experiments, eight subsets of plants were exposed to the different treatments described above (UV-B+gamma, gamma, UV-B and control), but prior to the UV-B+gamma and UV-B treatments, these plants were pre-treated with UV-B at 0.35 W m^{-2} for 10 h daily for four days (with cellulose acetate on top of the Petri dishes) in the growth chamber outside the gamma radiation sector. To study the effect of a lower gamma dose rate, 10.8, 20.7 and 42.9 mGy h^{-1} were used. Due to the limited length of the growth chamber, 125 mGy h^{-1} could not be included in these experiments. The UV-B pre-treatments started when the plants were six days old, and the plants not receiving UV-B were kept in the same growth chamber under UV-B blocking polycarbonate filters.

In an additional UV-B pre-treatment experiment the plants received the same treatments, except that 0.52 W m^{-2} UV-B (1.3 μmol m^{-2} s^{-1}), corresponding to a $UV\text{-}B_{BE}$ 0.26 W m^{-2} (0.65 μmol m^{-2} s^{-1}), was provided during the UV-B pre-treatment. This was done to test whether a higher UV-B level would make any difference since no significant UV-B effect on growth was observed at 0.35 W m^{-2}.

2.4 Growth parameter recordings at the end of the UV-B and gamma irradiation

At the end of the treatments, seedlings were placed between two transparent plastic sheaths with mm paper on top and scanned. The shoot and root lengths of the scanned seedlings were measured using the ImageJ software (US National Institutes of Health, Bethesda, MD, USA; http:/imagej.nih.gov/ij/). Eight-15 seedlings per treatment were measured in each of the six repeated experiments with simultaneous UV-B+gamma radiation without UV-B pre-treatment, as well as 9–17 seedlings per treatment in each of the three repeated UV-B pre-treatment experiments (Table 2). In the experiment with 0.52 W m^{-2} UV-B pre-treatment, 10 seedlings were measured per treatment.

2.5 Post-irradiation growing conditions

Since the negative effects of gamma-related stress may take some time to be fully manifested, and the potential recovery from growth-inhibition and DNA damage may also take time,[63,64] the after-effects of the UV-B and gamma treatments on the growth parameters and DNA damage were investigated. For this purpose, seedlings (number of experiments and plants per treatment described below and in Table 2) were transferred to pots (5 cm diameter and 5 cm height) filled with S-soil (45% low moist peat, 25% high moist peat, 25% perlite and 5% sand; Hasselfors Garden AS, Örebro, Sweden) with one plant per pot. The seedlings were then grown in growth chambers (manufactured by NMBU; different from those under the UV-B-gamma exposure) at temperature and RH the same as during the UV-B-gamma irradiation. A 24 h photoperiod was given with the 12 h main light period at a photon irradiance of 180 μmol m^{-2} s^{-1} and a R : FR ratio of 1.7, using metal halide lamps (HPI-T Plus 250 W, Phillips, Eindhoven, Netherlands) and incandescent lamps (Osram). This was followed by 12 h day extension with low-intensity light from the incandescence lamps only (8–10 μmol m^{-2} s^{-1}). Since the sensitivity to photoperiod in woody species increases after the first period following germination, and the length of the photoperiod sustaining growth increases with increasing northern origin, such long days were used to ensure growth of the northern ecotype used in the experiments.[65]

To assess more long-term effects of the irradiation treatments on growth and DNA-damage, plants from one UV-B pre-treatment experiment with 0.35 W m^{-2} and one with 0.52 W m^{-2} UV-B were transferred to a greenhouse compartment at NMBU, Ås, Norway (59°39′N, 10°47′E). The plants were transferred in the end of March and April 2018 after two months in the post-irradiation growth conditions described above and were grown for an additional six or five months, respectively. A greenhouse compartment was used as the growth chambers

Table 2 Overview of the treatments and recorded parameters/analyses in the gamma- and UV-B irradiation experiments without (totally six repeated experiments) or with UV-B pre-treatment (totally three repeated experiments). For growth measurements the number of plants per treatment is shown. For other parameters the number of samples per treatment is shown with the number of plants per sample in brackets. For DNA damage analysis the second number in the brackets refers to the number of technical replicates (gels) with 50–100 nuclei scored in each

		UV-B+gamma			UV-B pre-treatment → UV-B+gamma		
		Experimental factors			Experimental factors		
Chamber	Treatment	UV-B pre-treatment	Gamma	UV-B	UV-B pre-treatment	Gamma	UV-B
1	Control	–	–	–	–	–	–
	UV-B	–	–	+	+	–	+
2	Gamma	–	+	–	–	+	–
	UV-B+gamma	–	+	+	+	+	+
Treatment levels		–	0, 20.7, 42.9, 125 mGy h^{-1}	0.35 W m^{-2}	0.35 W m^{-2}	0, 10.8, 20.7, 42.9 mGy h^{-1}	0.35 W m^{-2}
Treatment duration (days)		–	6	6	4	6	6

		UV-B+gamma			UV-B pre-treatment → UV-B+gamma		
Time point	Parameter	Number of experiments	Number of replicates per treatment per experiment	Total number of replicates per treatment (total all exp.)	Number of experiments	Number of replicates per treatment per experiment	Total number replicates per treatment (total all exp.)
At the end of irradiation	Shoot and root length	6	8–15	48–90	3	9–17	27–51
	Histology	1	5	5	—	—	—
	DNA damage	2	3 (3 : 3)	6	2	3 (3 : 3)	6
	ROS	2	4	8	1	4	4
	Antioxidant capacity	1 (seedlings) 1 (shoots only)	4 (1 : 3) 3 (3 : 3)	4 3	—	—	—
	Phenolic compounds	—	—	—	1	8 (7–8)	8
Post-irradiation (44 days if otherwise not mentioned)	Growth parameters	2	12	24	2 1 (8 months)	10–15 6–10	20–30 6–10
	Histology	1	5	5	—	—	—
	DNA damage	2	3 (3 : 3)	6	1 1 (8 months)	3 (3 : 3) 3 (3 : 3)	3 3

were no longer available. The greenhouse had UV-blocking acrylic plastic walls and UV-B-blocking glass roof. In addition to the natural light, supplementary light at 165 μmol m^{-2} s^{-1} was provided 16 h daily from HQI (Powerstar HQI-T 400 W, Osram) and high-pressure sodium (HPS 400 W Master PIA, Phillips) lamps (1 : 1 ratio). The temperature was set to 21 °C and RH to 75%.

2.6 Post-irradiation growth parameter recordings

After the transfer of seedlings to pots in the growth chambers, plant height, number of needles and plant diameter of 10–15 plants per treatment were recorded over time, from 9–44 days post-irradiation. This was performed in two experiments with simultaneous UV-B+gamma irradiation without UV-B pre-treatment, and two experiments including also UV-B pre-treatment (0.35 W m^{-2}; Table 2). Plant height was measured from the rim of the pot to the shoot apical meristem (SAM), and the cumulative growth was calculated. The average shoot diameter from needle tip to needle tip across the plant at the shoot apex was calculated from two perpendicular measurements per plant. Pant height and shoot diameter were also measured eight months post-irradiation in 6–10 plants per treatment in one UV-B pre-treatment experiment (0.35 W m^{-2}) (Table 2).

2.7 Plant tissue preparation and histological studies by microscopy

Histological studies of shoot and root tips were performed according to Lee *et al.* (2017)[66] in experiments with simultaneous UV-B-gamma exposure without UV-B pre-treatment (Table 2). Three millimetres of shoot tips were harvested at the end of the irradiation, and 3 mm of shoot tips, 3 mm of root tips and 3 mm of the middle part of expanded needles were harvested 44 days post-irradiation from each of 5 plants per treatment. The samples were immediately fixed in 4% formaldehyde and 0.025% glutaraldehyde in sodium phosphate buffer (PBS, pH 7.0), vacuum infiltrated at room temperature for 1 h and thereafter kept at 4 °C overnight. The fixed samples were then washed with PBS, dehydrated in a graded ethanol series, infiltrated in a progressively increasing ratio of LR White resin (London Resin Company, London, UK) to ethanol and finally embedded in the resin. Thereafter 1 μm thick sections of the embedded plant materials were made using an Ultracut Leica EM UC6 microtome (Leica, Mannheim, Germany), stained with toluidine blue O for visualisation of the cells[67] (Sigma-Aldrich) and examined using a Leica DM6B light microscope (Leica).

2.8 COMET assay for analysis of DNA damage

To quantify the DNA damage (single and double strand breaks) in response to the gamma and UV-B treatments a COMET assay was performed according to the method described in Gichner *et al.* (2003)[68] (with some modifications). The assay is based on the principle that damaged DNA moves out of the cell nucleus during electrophoresis of lysed cells/cell nuclei in an agarose gel, and visualisation of this is possible by fluorescence microscopy. DNA breaks are quantified on the basis of the intensity and length of the elongated cell nucleus ("COMET") due to damaged DNA, relative to the head. The COMET analyses were performed at the end of the treatments (on shoot tips; two repeated experiments without and two with 0.35 W m^{-2} UV-B pre-treatment; Table 2). To test for persistence of the DNA damage, such analyses were also performed 44 days (on shoot and root tips; two repeated experiments without UV-B pre-treatment), and eight and seven months post-irradiation (on shoot tips; experiments with UV-B-pre-treatment with 0.35 W m^{-2} (Table 2) and 0.52 W m^{-2}, respectively). Three replicate biological samples per treatment (per experiment), each consisting of 3–4 mm of shoot tips or root tips from three plants, were investigated individually for DNA damage. For each sample, three technical replicates (gels) were analysed with 500–100 nuclei scored in each. As recommended by Koppen *et al.* (2017),[69] the median value for each biological sample was calculated, followed by calculation of the average of these values for the three biological replicates.

To avoid light-induced ROS formation resulting in DNA damage, the COMET assay was performed under inactinic red light. The plant materials were placed in 400 μl cold extraction buffer (PBS, pH 7.0 and 200 mM EDTA) in a 9 cm Petri dish. Cells/cell nuclei were isolated by chopping the plant materials vigorously for 30 s with a razor blade and the nuclei solution without plant debris was collected. The nuclear suspension (75 μl) and 1% low melting point agarose (50 μl) (NuSieve GTG Agarose, Lonza, Basel, Switzerland) prepared in distilled water at 40 °C, were gently mixed and 10 μl aliquots placed on microscope slides pre-coated with 1% low melting point agarose. To unwind DNA prior to electrophoresis, the slides (gels) were placed on ice for 1 min, followed by 10 min in a horizontal gel electrophoresis tank containing freshly prepared cold electrophoresis buffer (1 mM Na_2EDTA and 300 mM NaOH, pH 13). Electrophoresis was performed at 20 V (300 mA) for 5 min at 4 °C, and after electrophoresis, the slides were washed with distilled water and neutralised in PBS buffer for 10 min. The slides were then washed with distilled water, fixed in 95% ethanol and dried overnight before staining with Syber Gold (Life Technologies Ltd, Paisley, UK; dilution 1 : 5000) for 20 min and washing in distilled water three times for 5 min each. "COMETS" were scored using Comet IV (Perceptive Instruments Ltd, Bury St Edmunds, UK) and an Olympus BX51 fluorescence microscope with a CCD camera (Olympus, Tokyo, Japan).

2.9 Analyses of the reactive oxygen species H_2O_2

The level of the reactive oxygen species H_2O_2 was quantified using 2′,7′-dichlorofluorescein diacetate (H_2DCFDA) (Molecular Probes Inc., Eugene, OR, USA), which upon oxidation is de-esterified to the highly fluorescent 2′,7-dichlorofluorescein (H_2DCFD). A 50 mM stock solution of H_2DCFDA was prepared in DMSO and stored at −18 °C until use. After UV-B and gamma treatments in two repeated experiments without, and one experiment with UV-B pre-treatment (0.35 W m^{-2}) (Table 2), four plants per treatment were randomly selected and washed with PBS (PBS tablet, Thermo Fisher

Scientific Inc., Waltham, MA, USA) to remove any remaining agarose gel. After gentle drying with tissue paper, the plants were weighed with a microbalance, chopped individually into small pieces (0.5 cm) with a razor blade, and immersed in 100 μM H_2DCFDA in PBS for 3 h. The materials were then rinsed with PBS to remove excess probe, transferred to a 24-well microplate with 2 ml PBS per well, and the H_2DCFD fluorescent signal for each of the four samples was measured by a microplate reader (Fluoroskan Ascent FL, Thermo, Vantaa, Finland) with excitation and emission wavelengths of 480 nm and 530 nm, respectively.[70,71] The background fluorescence (without presence of plant materials) was also analysed and the resulting fluorescence subtracted from the values for the samples. The relative fluorescence obtained was normalised by weight, and the results were presented as fold difference relative to the unexposed control (no gamma, no UV-B).

2.10 Analyses of total antioxidant capacity

After UV-B and gamma exposure (without UV-B pre-exposure; Table 2), total antioxidant capacity was determined using the OxiSelect Ferric Reducing Antioxidant Power (FRAP) Assay Kit (Cell Biolabs, San Diego, USA). In one experiment, four samples of individual, entire seedlings were analysed, while in another experiment, analyses were performed on four samples consisting of pooled shoots from three plants per sample (Table 2). The analysis was done according to the manufacturer's protocol (https://www.cellbiolabs.com/sites/default/files/STA-859-frap-assay-kit.pdf). Approximately 10 mg plant tissue was homogenised in 1 ml cold 1× Assay buffer and centrifuged at 12 000 rpm for 15 min at 4 °C and the supernatant collected. Thereafter, a 1 mM iron(II) standard solution, diluted from a freshly made 36 mM stock solution, was used to prepare a series of standards according to the manufacturer's recommendations. For the assay, in each well of a 96 well microplate, 100 μl of the reaction reagent was added to 100 μl sample or standard solution, mixed by pipetting and incubated for 10 min at room temperature. Three technical replicates were used per sample. Immediately after the incubation, the absorbance was detected in a microplate reader (Biochrom Asys UVM 340 with KIM, UK) at a wavelength of 540 nm. The average absorbance values were determined for each sample and standard, and the net absorbance calculated by subtracting the zero-standard value. The sample results were determined on basis of the standard curve and normalised by weight.

2.11 Analyses of phenolic compounds

After the UV-B and gamma exposure in two experiments including UV-B-pre-treatment, plant materials were collected, divided into shoots and roots and freeze dried for 24 h to examine phenolic compounds. In each experiment, eight shoot samples per treatment were analysed. In one experiment (0.35 W m^{-2} UV-B pre-treatment), each sample consisted of shoots from 7–8 plants (Table 2), whereas in another experiment (0.52 W m^{-2} UV-B pre-treatment) shoots from 15–20 plants were pooled per sample.

The samples were transferred to 2 ml vials, each containing 600 μl MeOH and a stainless-steel bead (5 mm in diameter) and homogenised for 30 s in a centrifuge at 6500 rpm (Retsch, Haan, Germany). The vials were placed in an ice bath for 15 min and thereafter centrifuged for 3 min at 15 000 rpm, followed by transfer of the supernatant from each sample to a 10 ml vial. The procedure was then repeated four times (without ice bath incubation), leaving the pellet colourless. The MeOH was evaporated using a SpeedVac (SAVANT SC210A, Thermo Scientific, Weaverville NC, USA) vacuum centrifuge, and the dried extracts were re-dissolved in 200 μl MeOH using an ultrasound bath, and diluted with 200 μl Millipore-water. The extracts were then transferred to a 1.5 ml Eppendorf vial and centrifuged, followed by transfer to HPLC vials and analysis by HPLC (Agilent, Series 1100, Germany). The different metabolites were separated by use of a 50 × 4.6 mm ODS Hypersil column (Thermo Fisher Scientific Inc., Waltham, MA, USA). The samples were eluted (flow rate 2 ml min^{-1}) using a MeOH: water gradient according to Nybakken *et al.* (2012).[72] The injection volume was 20 μl, and the column temperature was 30 °C. The identification of the phenolic compounds was based on their retention times and UV spectra as compared with those of commercial standards. The chromatogram peak areas were used to quantify phenolic acids and flavonoid compounds.

2.12 Statistical analyses

In experiments with and without UV-B pre-treatment (summarised in Table 2), the effects of UV-B and gamma radiation on growth parameters (shoot and root length, post-irradiation cumulative shoot elongation, plant diameter and number of needles), DNA damage, H_2O_2 levels, antioxidant capacity and content of phenolic compounds were assessed by two-way analyses of variance (ANOVA) in the general linear model mode and by regression analysis using the Minitab statistical software (Minitab 18, Minitab Inc., PA, USA) ($p \leq 0.05$). For the post-irradiation growth parameters, the results from the final time point when the differences between the treatments were the largest were analysed. To test for differences between means, Tukey's *post hoc* test was used. When results from repeated experiments were available, the final statistical analyses included all these results. These individual experiments were first analysed separately to confirm equal responses.

3 Results

3.1 Effect of gamma radiation but no effect of UV-B on elongation growth

Exposure to UV-B radiation (0.35 W m^{-2}; provided separately or in combination with gamma radiation, with or without UV-B pre-treatment) did not affect the shoot or root length or the SAM histology (Fig. 1 and Fig. S1†). On the other hand, exposure to gamma radiation decreased the shoot length from

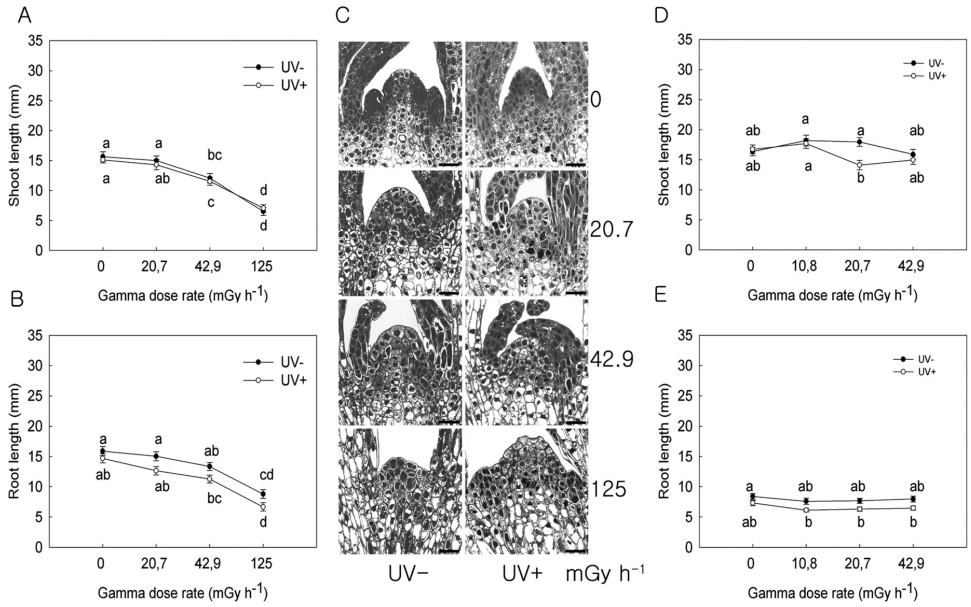

Fig. 1 Effect of 6 days of gamma irradiation without (UV–) or with (UV+) UV-B (0.35 W m^{-2}) in Scots pine seedlings; (A) shoot (regression analysis value (R^2): UV– and UV+: 0.98) and (B) root length (R^2: UV– and UV+: 0.99). Mean ± SE of 48–90 plants per treatment. (C) Histology of shoot apical meristems. 5 plants analysed per treatment. Scale bars: 100 μm. (D) Shoot (R^2: UV–: 0.12; UV+: 0.40) and (E) root length (R^2: UV–: 0.08; UV+: 0.23) in experiments including also 4 days UV-B (0.35 W m^{-2}) pre-treatment of the UV-B exposed plants. Mean ± SE of 27–51 plants per treatment. The treatments started when plants were 6 days old. Different letters within a plant part indicate significant differences ($p \leq 0.05$) based on analysis of variance followed by Tukey's test.

16 mm in the control plants to 12 mm at 42.9 mGy h^{-1} and 7 mm at 125 mGy h^{-1}: a reduction of 25% and 56% respectively. Likewise, our gamma-radiation treatments reduced root length from 16 mm in the controls to 9 mm at 125 mGy h^{-1}: a reduction of 44% (Fig. 1A, B and Fig. S1A, B†). Histological analysis revealed slightly impaired SAM development at 125 mGy h^{-1} (Fig. 1C). However, in another series of experiments (including UV-B pre-treatment (0.35 W m^{-2})), there was no effect of exposure to gamma radiation at 42.9 mGy h^{-1} (the highest tested gamma dose rate) on shoot and root length (Fig. 1D, E and Fig. S1C, D†). Pre-treatment with a higher UV-B level (0.52 W m^{-2}) was also tested but no effect on shoot or root length was observed (Fig. S1E–H†).

3.2 Gamma and UV-B radiation-induced DNA damage

All our gamma radiation and UV-B treatments increased DNA damage in both experiments with and without the UV-B pre-treatments (Fig. 2 and Fig. S2†). Exposure to UV-B radiation (0.35 W m^{-2}, without UV-B pre-treatment) resulted in 10% DNA in the COMET tail: a 10 fold increase compared with the treatment without UV-B which had only 1% tail DNA in the COMET tail (Fig. 2A and Fig. S2A†). This compares with 5% tail DNA with UV-B exposure and 0.08% tail-DNA without UV-B (a 63% change) in the equivalent treatments for plants in the 0.35 W m^{-2} UV-B pre-treatment experiments (Fig. 2B and Fig. S2B†). Seedlings exposed only to gamma radiation had DNA tails of 9% (20.7 mGy h^{-1}), 14% (42.9 mGy h^{-1}) and 19% (125 mGy h^{-1}); whereas after the gamma plus UV-B irradiation (without UV-B pre-treatment) the DNA tails were 17% (42.9 mGy h^{-1}) and 26% (125 mGy h^{-1}). This represents an increase for each of these dose rates of 21% and 37% additional DNA damage when the two types of radiation were given together (Fig. 2A and Fig. S2A†). This compares with DNA tails of 7% (10.8 mGy h^{-1}), 11% (20.7 mGy h^{-1}) and 17% (42.9 mGy h^{-1}) in the gamma only treatments in the experiments including 0.35 W m^{-2} UV-B pre-treatment (Fig. 2B and Fig. S2B†). Here the UV-B plus gamma treatments produced DNA tails of 11% (10.8 mGy h^{-1}) and 14% (20.7 mGy h^{-1}): an increase of 57% and 27%, respectively, as compared to the gamma only treatment (Fig. 2B and Fig. S2B†).

The higher-dosage UV-B pre-treatment of 0.52 W m^{-2} produced similar results to the lower-dosage UV-B pre-treatment described above. Here, the UV-B exposed plants had a 10% tail-DNA compared with 0.3% in the no UV-B controls: corresponding to a 33-fold increase (Fig. S2C and D). The plants exposed to gamma radiation had DNA-tails of 11% (10.8 mGy h^{-1}), 14% (20.7 mGy h^{-1}) and 17% (42.9 mGy h^{-1}), whereas those exposed to UV-B and gamma radiation had 14%, 17%

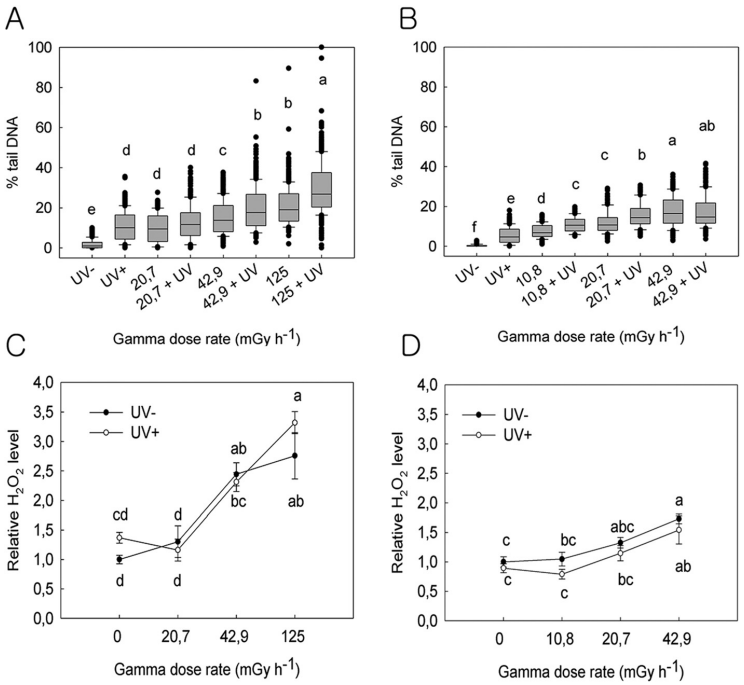

Fig. 2 Effect of 6 days of gamma irradiation without (UV–) or with (UV+) UV-B (0.35 W m^{-2}) in Scots pine seedlings; (A) DNA damage (COMET assay) in shoot tips (regression analysis value (R^2): 0.92). (B) DNA damage in shoot tips (R^2: 0.91) in experiments including also 4 days UV-B (0.35 W m^{-2}) pre-treatment of the UV-B exposed plants. The line in each box = mean of median values for 6 samples per treatment with 3 technical replicates (gels) per sample with 50–100 nuclei scored per gel. Lower and upper box boundaries = 25 and 75% percentiles, error bars = 10 and 90% percentiles with data points outside shown as dots. (C) Reactive oxygen species (ROS; *i.e.* H_2O_2) in experiments without UV-B pre-treatment (R^2: UV–: 0.84; UV+: 0.94). Mean ± SE of 8 samples per treatment. (D) ROS in experiment with UV-B pre-treatment (R^2: UV–: 0.97; UV+: 0.87). Mean ± SE of 4 samples per treatment. The treatments started when plants were 6 days old. Different letters within a parameter indicate significant differences ($p \leq 0.05$) based on analysis of variance followed by Tukey's test.

and 26% DNA-tails at the same gamma dose rates, respectively. This represents an increase in DNA damage of 27%, 21% and 53% for the respective gamma radiation dose rates when combined with the UV-B treatment (Fig. S2C and D†).

3.3 Effect of gamma radiation but no effect of UV-B on level of H_2O_2

There was no significant effect of UV-B on the H_2O_2 levels (Fig. 2C and D). On the other hand, compared to the unexposed control, significantly increased levels of H_2O_2 were observed in response to gamma radiation at 42.9 (an average of 96% and 48% in experiments without and with UV-B pre-treatment, respectively) and 125 mGy h^{-1} (154% increase; analysed in experiments without UV-B pre-treatment); (Fig. 2C and D).

Analyses of total antioxidant capacity using the FRAP assay (analysed in experiments without UV-B pre-treatment) revealed no significant effect of UV-B or gamma radiation when analysing entire seedlings or shoots only (Fig. S3†).

3.4 UV-B-induction of phenolic compounds but no effect of gamma radiation

There was no significant effect of gamma radiation on the levels of any of the phenolic compounds analysed in shoot tissue (analysed in experiments with 0.35 W m^{-2} UV-B pre-treatment; Fig. 3). On the contrary, UV-B-induction of some components was observed. Chlorogenic acid derivatives showed significant increase in shoots in response to UV-B in the no gamma control and at 20.7 mGy h^{-1}, whereas for the other gamma treatments there were no significant differences (Fig. 3A). Quercetins showed no significant difference between UV-B-gamma and gamma only-treated plants in shoots, except at 20.7 mGy h^{-1} (Fig. 3B). However, the levels of kaempferols increased significantly in response to UV-B as compared to the no gamma radiation (no UV-B) control and all gamma only-treated plants (Fig. 3C). Whereas stilbenes were not affected by UV-B, MeOH-soluble condensed tannins showed significant increases in response to UV-B in the no gamma control and at 10.8 mGy h^{-1} gamma only (Fig. 3D and E).

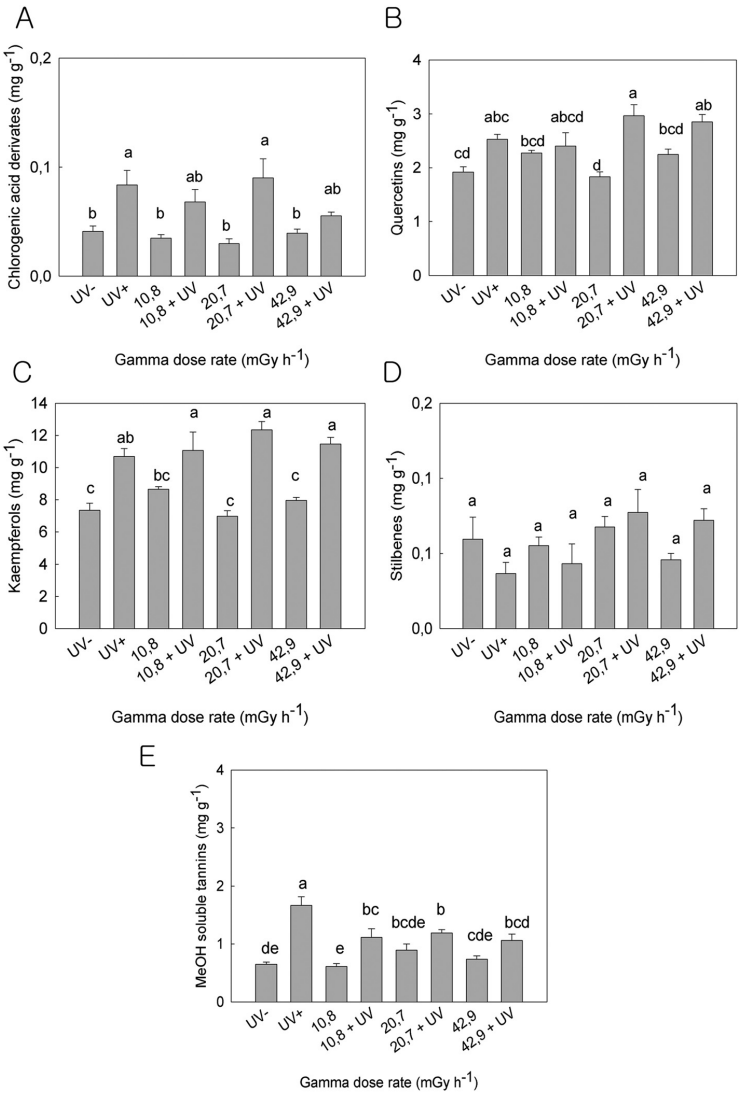

Fig. 3 Effect of 6 days of gamma irradiation without (UV–) or with (UV+) UV-B (0.35 W m^{-2}), including also 4 days UV-B (0.35 W m^{-2}) pre-treatment of UV-B exposed plants, on levels of phenolic compounds in shoots of Scots pine seedlings; (A) chlorogenic acid derivates, (B) quercetins, (C) kaempferols, (D) stilbenes and (E) MeOH-soluble tannins. Mean ± SE of 8 samples per treatment (shoots from 7–8 plants per sample). UV-B pre-treatment started when plants were 6 days old. Different letters within a parameter indicate significant differences ($p \leq 0.05$) based on analysis of variance followed by Tukey's test.

3.5 Post-irradiation effect of gamma radiation on growth but no such effect of UV-B

There was no post-irradiation effect of the UV-B treatments on the cumulative shoot elongation, shoot diameter (from needle tip to needle tip) or number of needles (Fig. 4 and Fig. S4†). However, compared to the unexposed control plants (no gamma, no UV-B), the cumulative elongation growth was significantly reduced by exposure to gamma radiation (Fig. 4 and Fig. S4†). In the first series of experiments (without UV-B pre-treatment) the cumulative elongation growth was reduced by an average of 67%, 78% and 93%, respectively, 44 days after

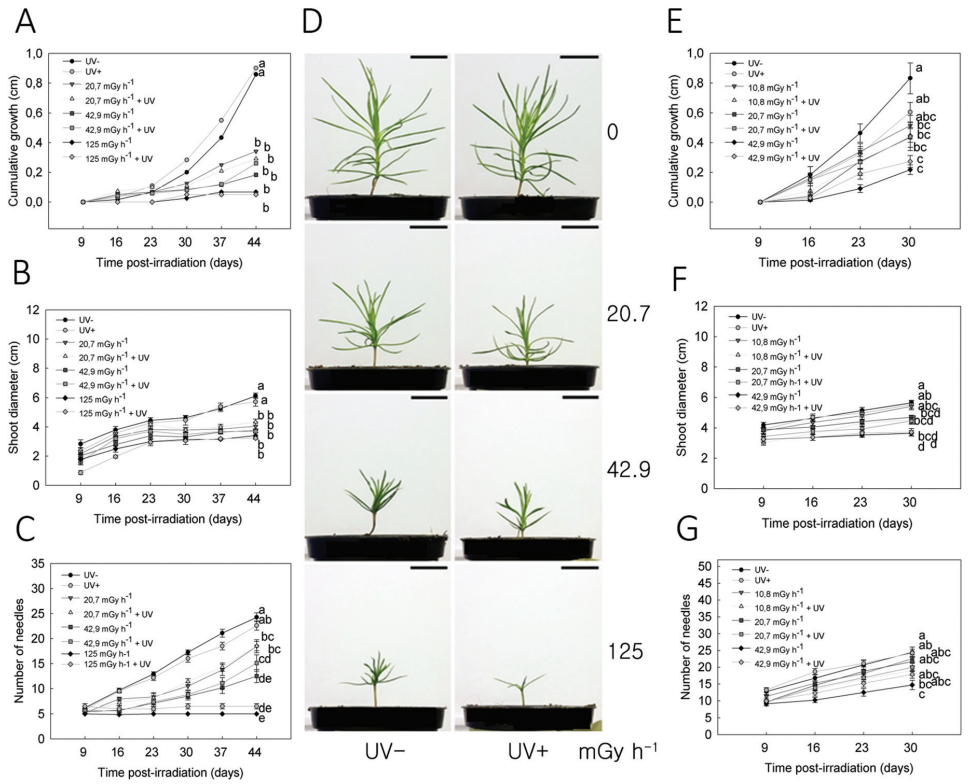

Fig. 4 Post-irradiation effects of 6 days of gamma irradiation without (UV–) or with (UV+) UV-B (0.35 W m^{-2}) in Scots pine seedlings; (A) cumulative shoot elongation, (B) shoot diameter (needle tip to needle tip), (C) number of needles and (D) phenotype 44 days post-irradiation. (E) Cumulative shoot elongation, (F) shoot diameter and (G) number of needles in experiments including also 4 days UV-B (0.35 W m^{-2}) pre-treatment of the UV-B exposed plants. The irradiation treatments started when the seedlings were 6 days old, and time 0 corresponds to the day the irradiation treatments ended. The results are mean ± SE of 24 plants per treatment. Different letters within a parameter indicate significant differences ($p \leq 0.05$) based on analysis of variance followed by Tukey's test. Regression analysis values (R^2): Without UV-B-pre-treatment for 0, 20.7, 42.9, 125 mGy h^{-1}; cumulative shoot elongation UV–: 0.83, 0.93, 0.94, 0.77 and UV+: 0.89, 0.94, 0.84, 0.83, shoot diameter UV–: 0.99, 0.96, 0.90, 0.17 and UV+: 0.99, 0.93, 0.95, 0.15, number of needles UV–: 0.97, 0.70, 0.84, 0.78 and UV+: 0.96, 0.72, 0.60, 0.84. With UV-B pre-treatment: for 0, 10.8, 20.7, 42.9, mGy h^{-1}; cumulative shoot elongation UV–: 0.98, 0.99, 0.97, 0.89 and UV+: 0.98, 0.97, 0.97, 0.94, shoot diameter UV–: 0.99, 0.99, 0.98, 0.99 and UV+: 0.99, 0.97, 0.96, 0.95, number of needles UV–: 0.99, 0.99, 0.98, 0.97 and UV+: 0.97, 0.99, 0.60, 0.99.

exposure to 20.7, 42.9 and 125 mGy h^{-1} gamma radiation (from 0.9 cm growth in the control to 0.3, 0.2 and 0.06 cm at 20.7, 42.9 and 125 mGy h^{-1}) (Fig. 4A and Fig. S4A†). Shoot diameter showed a significant reduction by 34%, 39% and 44% after exposure to 20.7, 42.9 and 125 mGy h^{-1} (from 6.1 cm shoot diameter in the control to 4, 3.7 and 3.4 cm at 20.7, 42.9 and 125 mGy h^{-1}; Fig. 4B and Fig. S4B†). The number of needles was also reduced by approximately 21% and 46% after exposure to 20.7 and 42.9 mGy h^{-1}, respectively (from 24 needles in the control to 19 and 13 needles at 20.7 and 42.9 mGy h^{-1}; Fig. 4C and Fig. S4C†). After the highest dose rate (125 mGy h^{-1}) no or only very few new needles had developed (Fig. 4C, D and Fig. S4C†). In the second series of experiments (with UV-B pre-treatment), the cumulative elongation growth was significantly reduced by 50% and 75%, respectively, 30 days after exposure to 20.7 and 42.9 mGy h^{-1} (from 0.8 cm growth in the control to 0.4 and 0.2 cm at 20.7 and 42.9 mGy h^{-1}). Shoot diameter was reduced by 18% and 37% after 20.7 and 42.9 mGy h^{-1} (from 5.7 cm shoot diameter in the control to 4.7 and 3.6 cm at 20.7 and 42.9 mGy h^{-1}), and the number of needles was reduced by 42% after 42.9 mGy h^{-1} (from 26 needles in the control to 15 needles at 42.9 mGy h^{-1}; Fig. 4E–G and Fig. S4D, F†).

Histological studies of shoot apical meristems and needles 44 days post-irradiation (experiment without UV-B pre-treatment), showed no visible cellular changes in any of the irradiation treatments compared to the unexposed controls (Fig. 5).

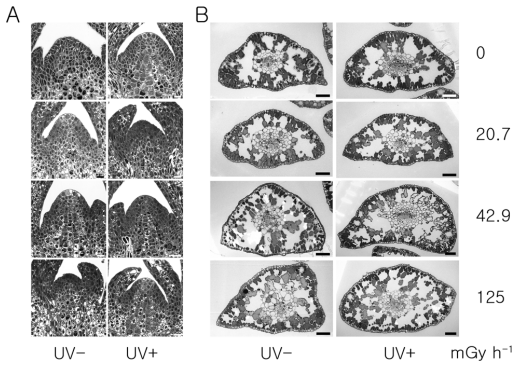

Fig. 5 Post-irradiation effect 44 days after 6 days of gamma irradiation without (UV–) or with (UV+) UV-B (0.35 W m^{-2}) on histology of (A) shoot apical meristems and (B) needles in seedlings of Scots pine. The irradiation treatments started when the seedlings were 6 days old. Five plants were analysed per treatment. Scale bar: 25 μm.

3.6 Persistent UV-B and gamma radiation-induced DNA damage 44 days post-irradiation

In shoot and root tips, a significant dose rate-dependent increase in % tail DNA values was observed with increased gamma dose rate, as recorded 44 days post-irradiation (Fig. 6 and Fig. S5†). In shoots there was 3%, 11% and 15% tail DNA after 20.7, 42.9 and 125 mGy h^{-1}, and in roots the corresponding values were 2%, 3%, 8% (Fig. 6A and Fig. S5A†). No significant effect of the UV-B only-exposure on DNA damage in shoot and root tips was observed at this time point. However, as compared to the gamma radiation only, seedlings co-exposed to UV-B and 42.9 mGy h^{-1} (16% tail DNA) or 125 mGy h^{-1} (22% tail DNA) showed 45% and 47% additional increase in DNA damage in shoot tissue, respectively. In root tissue, co-exposure with UV-B resulted in 100% and 38% additional increase in DNA damage for 20.7 (4% tail DNA) or 125 mGy h^{-1} (11% tail DNA), respectively (Fig. 6B and Fig. S5B†).

3.7 Long-term growth post-irradiation eliminates DNA damage and normalises the phenotype

At eight months post-irradiation a normal phenotype was more or less restored (Fig. 7). Although some plants at the highest dose rate (42.9 mGy h^{-1}) were still slightly shorter compared to the controls (Fig. 7A), there were no overall significant differences in shoot diameter (needle tip to needle tip) or plant height (Fig. 7B and C). Moreover, the COMET assay analysis revealed that there was no longer any significant DNA damage in the gamma and UV-B-exposed plants as compared to the unexposed controls (Fig. 7D and Fig. S6A;† analysed in experiments with 0.35 W m^{-2} UV-B pre-treatment).

Although some gamma-exposed plants were still smaller (plant height) than the unexposed controls in the experiment with 0.52 W m^{-2} UV-B-pre-treatment seven months post-irradiation, growth generally appeared rather normal (Fig. S6B†). Analyses of DNA damage showed that there was a slight, but significantly higher degree of DNA damage in the UV-B only-exposed plants compared to the unexposed controls (no gamma-no UV-B) as well as in plants co-exposed to UV-B and 10.8 mGy h^{-1} compared to 10.8 mGy h^{-1} only (Fig. S6C and D†). Furthermore, in this experiment all gamma-irradiated plants except the ones exposed to 10.8 mGy h^{-1} without UV-B, still had slightly, but significantly more DNA damage than the no gamma-no UV-B control plants.

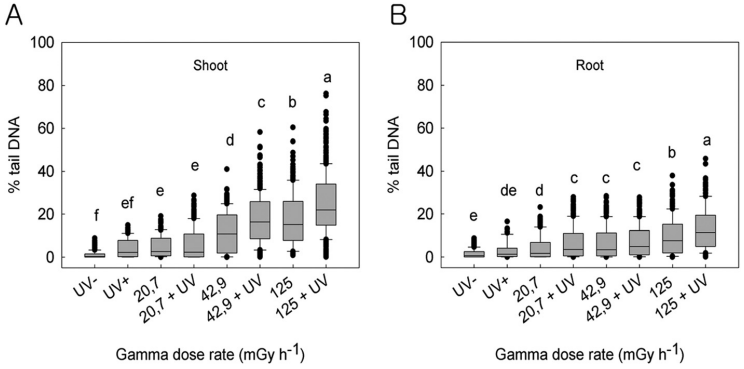

Fig. 6 Post-irradiation effect 44 days after 6 days of gamma irradiation without (UV–) or with (UV+) UV-B (0.35 W m^{-2}) on DNA damage (COMET assay) in (A) shoot (regression analysis value (R^2): 0.90) and (B) root tips (R^2: 0.87) of Scots pine seedlings. The irradiation treatments started when plants were 6 days old. The line in each box = the mean of median values for 6 samples per treatment with 3 technical replicates (gels) per sample with 50–100 nuclei scored per gel. Lower and upper box boundaries = 25 and 75% percentiles, error bars = 10 and 90% percentiles with data points outside shown as dots. Different letters within a plant part indicate significant differences ($p \leq 0.05$) based on analysis of variance followed by Tukey's test.

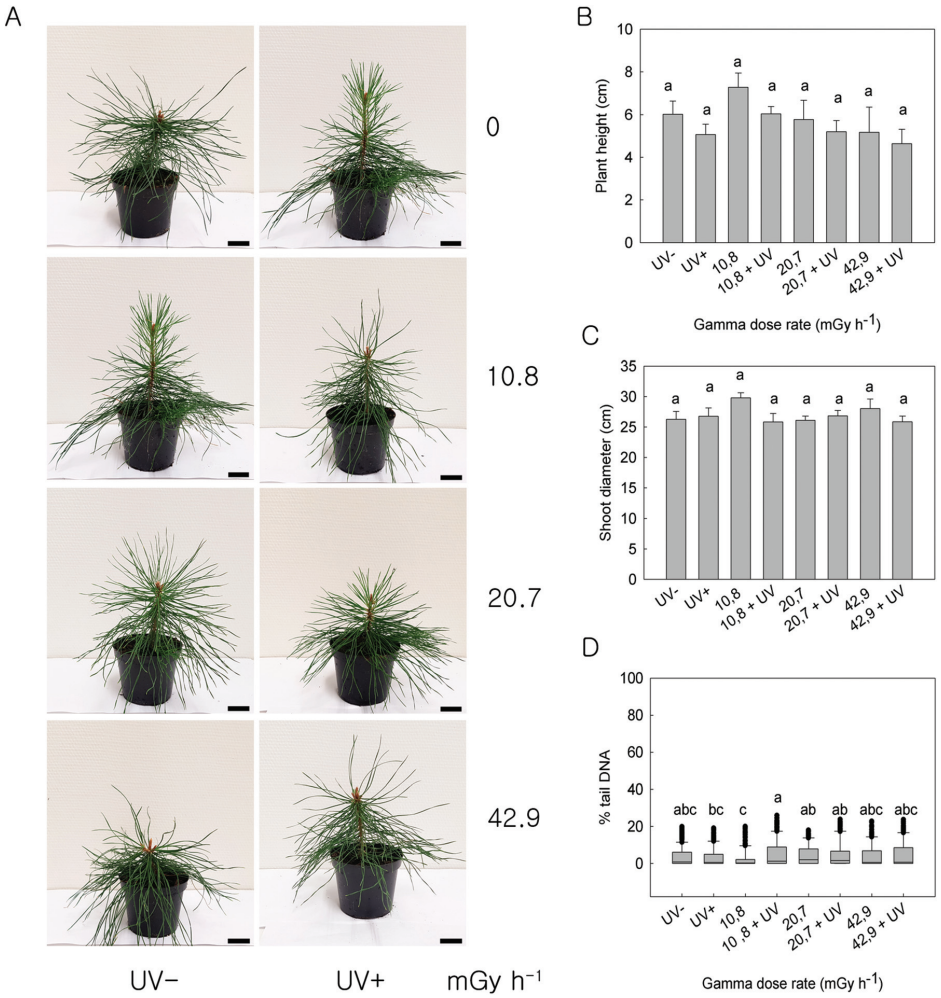

Fig. 7 Post-irradiation effect 8 months after 6 days of gamma irradiation without (UV–) or with (UV+) UV-B (0.35 W m^{-2}) in Scots pine, including also 4 days UV-B (0.35 W m^{-2}) pre-treatment of UV-B exposed plants. The irradiation treatments started when the seedlings were 6 days old. (A) Phenotype. (B) Plant height and (C) shoot diameter (needle tip to needle tip). Mean ± SE of 6–10 plants. (D) DNA damage (COMET assay) in shoot tips (R^2: 0.27). The line in each box = the mean of the median values for 3 repeated samples per treatment with 3 technical replicates (gels) per sample with 50–100 nuclei scored per gel. Lower and upper box boundaries = 25 and 75% percentiles, error bars = 10 and 90% percentiles with data points outside these shown as dots. Different letters within each parameter indicate significant differences ($p \leq 0.05$) based on analysis of variance followed by Tukey's test.

4 Discussion

In their natural environments plants are normally exposed to low, non-damaging background levels of IR such as gamma radiation, but some areas have elevated, potentially harmful levels particularly due to releases from anthropogenic activities and accidents.[1] Although high levels of UV-B radiation may be stressful to plants, ambient UV-B levels have been suggested to prime defence mechanisms towards different stressors.[34–42] However, information about interactive effects of UV-B and gamma radiation is scarce. In experiments with or without UV-B pre-treatment prior to simultaneous UV-B and gamma irradiation, we tested whether UV-B can prime mechanisms contributing to tolerance to low-moderate gamma radiation levels in seedlings of Scots pine, and whether simultaneous UV-B and gamma radiation may have an additive adverse effect on plants not previously exposed to either of these radiation types.

Our results revealed no additive adverse effect of six days of simultaneous gamma and UV-B irradiation on shoot or root elongation, only growth inhibition in response to the gamma dose rates of 42.9 (25%) and 125 mGy h^{-1} (56%) in shoots and 125 mGy h^{-1} in roots (44%) (Fig. 1A, B and Fig. S1†). On the other hand, in experiments including UV-B pre-treatment for four days prior to the six days of simultaneous UV-B-gamma exposure, no growth inhibition was observed after 42.9 mGy h^{-1} (highest dose rate tested). However, this applied also to the gamma only treatment and was accordingly not due to priming by UV-B pre-treatment. The reason for the difference in effect of 42.9 mGy h^{-1} between the experimental series remains elusive. Growth inhibition in response to elevated levels of ionising radiation is well known in plants, although the sensitivity may vary with species and developmental stage, with Scots pine considered relatively sensitive.[1] Nevertheless, it could be noted that elongation growth was not affected by exposure to 20.7 and 10.8 mGy h^{-1}, which are far higher dose rates than the natural background levels.[1] This demonstrates that even this species is resistant to gamma radiation levels far higher than the background levels currently found in the natural environment.

Although UV-B has been shown to reduce shoot elongation and leaf expansion in a wide range of experiments with different plant species,[31,32,73–76] we did not detect any significant effect of UV-B on shoot and root elongation after the 6 or 10 days of UV-B exposure (Fig. 1 and Fig. S1†). This lack of effect of UV-B on elongation growth even at the relatively high UV-B to PAR ratio(s) used (0.35 W m^{-2} UV-B for 6 or 10 days or 0.52 W m^{-2} for 4 days followed by 0.35 W m^{-2} for 6 days, all under a PAR of 200 μmol m^{-2} s^{-1}), may be due to the efficient UV-screening in the epidermis of such evergreen conifers.[60–62]

Gamma radiation is well known to induce production of ROS, including H_2O_2, which in high amounts results in damage to macromolecules like lipids, proteins and DNA.[46,47] Indeed, the negative effect of 42.9 and 125 mGy h^{-1} gamma radiation on elongation growth in the experiments without UV-B pre-treatment, correlated with significantly increased H_2O_2 levels compared to the unexposed control and lower gamma dose rates (Fig. 2C). The lack of growth inhibition after 42.9 mGy h^{-1} in the experiments including UV-B pre-treatment may be at least partially explained by the overall lower increase in H_2O_2 (on average 48%) in these experiments compared to the same dose rate in the experiments without UV-B pre-treatment (an average of 96% increase) (Fig. 2D). UV-B has an energy level that may induce ROS formation,[77] but consistent with the lack of effect of UV-B on elongation growth and efficient UV-B screening in the epidermis of conifers like Scots pine,[60–62] no significant effect of UV-B on H_2O_2 levels was detected (Fig. 2C and D).

Furthermore, consistent with the increasing ROS levels with increasing gamma dose rate, the gamma irradiation resulted in a dose rate-dependent increase in DNA damage (Fig. 2A, B and Fig. S2A, B†), as expected.[1,46,47] This was the case in the experiments without, as well as with, UV-B pre-treatment in spite of effect on elongation growth in the first type of experiment only. Additionally, UV-B exposure, which did not affect H_2O_2 levels or elongation growth, resulted in increased DNA damage. Thus, although a relationship between DNA damage and growth inhibition may be expected, the results demonstrate tolerance to some degree of DNA damage since DNA damage also occurs in other conditions than those affecting growth. It should be noted that although the DNA damage levels in the controls were always low, there was some variation between experiments (ranging from 0.08% to 1% tail DNA). This made the difference in DNA damage between the exposed and control seedlings appear larger in experiments with the lowest control values. Nevertheless, the DNA damage levels (% tail DNA) were generally relatively similar for specific gamma dose rates and increased as expected with increasing dose rate. The reason for the variation in the controls remains elusive since action was taken during the sample processing to avoid light-induced ROS production which may induce DNA damage.

UV-inducible phenolic compounds including flavonoids, which act as antioxidants, are important in protection against ROS generated by exposure to UV-B.[31,55] It may be hypothesised that their antioxidant activity may also protect against ROS formed in response to gamma radiation, and that they may be induced by low-moderate gamma radiation levels. The results demonstrate that gamma radiation does not induce production of any of the phenolic compounds analysed in the Scots pine seedlings (Fig. 3). In contrast, consistent with previous studies,[78–81] general UV-B-induction of specific flavonoids was observed, *i.e.* glycosides of the flavonoid kaempferol. A significant increase in chlorogenic acid and methanol-soluble tannins in response to UV-B was also observed, but only when UV-B was provided separately or in combination with gamma dose rates not affecting elongation growth. However, the induction of phenolic compounds by UV-B did not protect against a negative effect of gamma radiation on growth, since gamma-induced growth inhibition at the highest dose rates was similar in the presence and absence of UV-B. Surprisingly, although both gamma radiation and UV-B are well known to induce the formation of different groups of antioxidants,[31,47,51,52,82] no significant effect of the irradiation treatments on total antioxidant capacity could be detected when entire seedlings or shoots only were analysed (Fig. S3†). The reason for this remains elusive.

To test whether damage resulting from the irradiation treatments may possibly take some time to be recovered from, or even fully manifested as shown in some other studies,[63,64] growth parameters and DNA damage were also assessed post-irradiation. Indeed, although the shoot apical meristems and needle anatomy appeared normal at all dose rates 44 days post-irradiation (Fig. 5), gamma-induced growth inhibition was generally visible at lower dose rates post-irradiation than at the end of the gamma exposure (Fig. 4 and Fig. S4†). In contrast to findings from the end of the gamma exposure, growth parameters were negatively affected post-irradiation by 20.7 mGy h^{-1} in all experiments, and by 42.9 mGy h^{-1} in the experiments with UV-B pre-treatment. On the other hand, consistent with lack of significant effect of UV-B at the end of the

irradiation treatments, there were no after-effects of UV-B on growth parameters.

At day 44 post-irradiation, the gamma dose rate-dependent and UV-B-induced DNA damage was quite similar to what was found at the end of the six days of gamma exposure (Fig. 6 and Fig. S5†). The growth-inhibition at even lower dose rates post-irradiation than that found at the end of the gamma exposure may suggest that the effect of DNA damage on growth may take some time to be fully realised. The post-irradiation DNA damage even in the UV-B-exposed plants may be due to the type of damage induced, *e.g.* possibly double strand breaks rather than photo-repairable UV-B-induced lesions,[83,84] or because of damage generated post-irradiation. Consistent with the latter, (at least for the gamma-exposed plants), genomic instability induced by IR has been shown in other organisms.[63,64,85] This may involve mechanisms such as DNA repair defects due to mutations and programmed cell death. Genomic instability may also be related to epigenetic mechanisms such as changes in DNA methylation and deficiency in the histone variant H2AX, which is important for proper DNA repair.[86,87] However, seven and eight months post-irradiation, the DNA-damage was either fully or nearly recovered, consistent with a normalised phenotype with formation of long needles like in the unexposed control plants, and no significant overall difference in plant height or shoot diameter between the treatments (Fig. 7 and Fig. S6†).

5 Conclusions

In conclusion, our results showed no evidence of a protective effect of UV-B on growth inhibition and DNA damage induced by low doses of gamma radiation (given as moderate to high dose rates) in Scots pine seedlings. There was also no additive adverse effect of UV-B and gamma radiation on growth. Gamma radiation negatively affected growth parameters and resulted in increased ROS-production and DNA damage in a dose rate-dependent manner. In spite of additional DNA damage in response to UV-B, UV-B did not affect ROS production or the growth of shoots and roots. The DNA damage after the gamma and UV-B irradiation was long-lasting and may have been due to induction of genomic instability. Nevertheless, growth inhibition post-irradiation was observed only in response to gamma radiation, in a dose rate-dependent manner, suggesting tolerance to low levels of DNA damage.

Conflicts of interest

There are no conflicts of interest to declare.

Acknowledgements

The Norwegian Research Council through its Centre of Excellence funding scheme (Grant 223268/F50) and the Norwegian University of Life Sciences are acknowledged for financial support. Thanks to Camilo Chiang, Marit Siira and Ida K Hagen for technical assistance in the plant growth experiments and to Sheona Innes for language revision.

References

1 N. Caplin and N. Willey, Ionizing Radiation, Higher Plants, and Radioprotection: From Acute High Doses to Chronic Low Doses, *Front. Plant Sci.*, 2018, **9**, 847.
2 A. C. Freitas and A. S. Alencar, Gamma dose rates and distribution of natural radionuclides in sand beaches—Ilha Grande, Southeastern Brazil, *J. Environ. Radioact.*, 2004, **75**, 211–223.
3 J. Mrdakovic Popic, C. Raj Bhatt, B. Salbu and L. Skipperud, Outdoor 220Rn, 222Rn and terrestrial gamma radiation levels: investigation study in the thorium rich Fen Complex, Norway, *J. Environ. Monit.*, 2012, **14**, 193–201.
4 UNSCEAR, *Summary of low-dose radiation effects on health*, United Nations Scientific Commitee on the Effects of Atomic Radiation, New York, 2010.
5 D. Averbeck, S. Salomaa, S. Bouffler, A. Ottolenghi, V. Smyth and L. Sabatier, Progress in low dose health risk research: Novel effects and new concepts in low dose radiobiology, *Mutat. Res./Rev. Mutat. Res.*, 2018, **776**, 46–69.
6 UNSCEAR, *Sources, effects and risks of ionizing radiation*, United Nations Scientific Commitee on the Effects of Atomic Radiation, New York, 2017.
7 UNSCEAR, *Sources and effects of ionizing radiation*, United Nations Scientific Commitee on the Effects of Atomic Radiation, New York, 1996.
8 G. M. Woodwell and A. L. Rebuck, Effects of Chronic Gamma Radiation on the Structure and Diversity of an Oak-Pine Forest, *Ecol. Monogr.*, 1967, **37**, 53–69.
9 C. L. Ballare, A. L. Scopel, A. E. Stapleton and M. J. Yanovsky, Solar Ultraviolet-B Radiation Affects Seedling Emergence, DNA Integrity, Plant Morphology, Growth Rate, and Attractiveness to Herbivore Insects in Datura ferox, *Plant Physiol.*, 1996, **112**, 161–170.
10 S. A.-H.-. Mackerness, Plant responses to ultraviolet-B (UV-B: 280–320 nm) stress: What are the key regulators?, *Plant Growth Regul.*, 2000, **32**, 27–39.
11 H. Frohnmeyer and D. Staiger, Ultraviolet-B Radiation-Mediated Responses in Plants. Balancing Damage and Protection, *Plant Physiol.*, 2003, **133**, 1420–1428.
12 G. M. Woodwell, Effects of Ionizing Radiation on Terrestrial Ecosystems, Experiments show how ionizing radiation may alter normally stable patterns of ecosystem behavior, *Science*, 1962, **138**, 572–577.
13 T. Kawai and T. Inoshita, Effects of gamma ray irradiation on growing rice plants—I: Irradiations at four main developmental stages, *Radiat. Bot.*, 1965, **5**, 233–255.
14 D. D. Killion and M. J. Constantin, Gamma irradiation of corn plants: Effects of exposure, exposure rate, and developmental stage on survival, height, and grain yield of two cultivars, *Radiat. Bot.*, 1972, **12**, 159–164.

15 S. G. Wi, B. Y. Chung, J.-S. Kim, J.-H. Kim, M.-H. Baek, J.-W. Lee and Y. S. Kim, Effects of gamma irradiation on morphological changes and biological responses in plants, *Micron*, 2007, **38**, 553–564.
16 M. Tulik, Cambial history of Scots pine trees (Pinus Sylvestris) prior and after the Chernobyl accident as encoded in the xylem, *Environ. Exp. Bot.*, 2001, **46**, 1–10.
17 L. Zelena, B. Sorochinsky, S. von Arnold, L. van Zyl and D. H. Clapham, Indications of limited altered gene expression in Pinus sylvestris trees from the Chernobyl region, *J. Environ. Radioact.*, 2005, **84**, 363–373.
18 V. Yoschenko, T. Ohkubo and V. Kashparov, Radioactive contaminated forests in Fukushima and Chernobyl, *J. For. Res.*, 2018, **23**, 3–14.
19 S. V. Fesenko, R. M. Alexakhin, S. A. Geras'kin, N. I. Sanzharova, Y. V. Spirin, S. I. Spiridonov, I. A. Gontarenko and P. Strand, Comparative radiation impact on biota and man in the area affected by the accident at the Chernobyl nuclear power plant, *J. Environ. Radioact.*, 2005, **80**, 1–25.
20 Y. Watanabe, S. e. Ichikawa, M. Kubota, J. Hoshino, Y. Kubota, K. Maruyama, S. Fuma, I. Kawaguchi, V. I. Yoschenko and S. Yoshida, Morphological defects in native Japanese fir trees around the Fukushima Daiichi Nuclear Power Plant, *Sci. Rep.*, 2015, **5**, 1–7.
21 N. Goltsova, Y. Abaturov, A. Abaturov, P. Melankholin, A. Girbasova and N. Rostova, Chernobyl radionuclide accident: Effects on the shoot structure of Pinus sylvestris, *Ann. Bot. Fenn.*, 1991, **28**, 1–13.
22 P. J. Aphalo, A. Albert, L. O. Björn, A. R. McLeod, T. M. Robson and E. Rosenqvist, *Beyond the visible: A handbook of best practice in plant UV photobiology*, Division of Plant Biology, Helsinki, 2012.
23 J. Rozema, J. van de Staaij, L. O. Björn and M. Caldwell, UV-B as an environmental factor in plant life: stress and regulation, *Trends Ecol. Evol.*, 1997, **12**, 22–28.
24 M. A. K. Jansen, V. Gaba and B. M. Greenberg, Higher plants and UV-B radiation: balancing damage, repair and acclimation, *Trends Plant Sci.*, 1998, **3**, 131–135.
25 L. O. Björn, On the history of phyto-photo UV science (not to be left in skoto toto and silence), *Plant Physiol. Biochem.*, 2015, **93**, 3–8.
26 A. Coffey and M. A. K. Jansen, Effects of natural solar UV-B radiation on three Arabidopsis accessions are strongly affected by seasonal weather conditions, *Plant Physiol. Biochem.*, 2019, **134**, 64–72.
27 M. A. K. Jansen, *Ultraviolet-B Radiation: Stressor and Regulatory Signal*, Pondicherry, India, 2017.
28 T. S. L. Lau, E. Eno, G. Goldstein, C. Smith and D. A. Christopher, Ambient levels of UV-B in Hawaii combined with nutrient deficiency decrease photosynthesis in near-isogenic maize lines varying in leaf flavonoids: Flavonoids decrease photoinhibition in plants exposed to UV-B, *Photosynthetica*, 2006, **44**, 394–403.
29 J. Belnap, S. L. Phillips, S. Flint, J. Money and M. Caldwell, Global change and biological soil crusts: effects of ultraviolet augmentation under altered precipitation regimes and nitrogen additions, *Global Change Biol.*, 2008, **14**, 670–686.
30 K. R. Albert, T. N. Mikkelsen, H. Ro-Poulsen, M. F. Arndal and A. Michelsen, Ambient UV-B radiation reduces PSII performance and net photosynthesis in high Arctic Salix arctica, *Environ. Exp. Bot.*, 2011, **73**, 10–18.
31 M. A. K. Jansen and J. F. Bornman, UV-B radiation: from generic stressor to specific regulator, *Physiol. Plant.*, 2012, **145**, 501–504.
32 T. M. Robson, K. Klem, O. Urban and M. A. K. Jansen, Re-interpreting plant morphological responses to UV-B radiation, *Plant, Cell Environ.*, 2015, **38**, 856–866.
33 M. Dotto and P. Casati, Developmental reprogramming by UV-B radiation in plants, *Plant Sci.*, 2017, **264**, 96–101.
34 S. Nogués and N. R. Baker, Effects of drought on photosynthesis in Mediterranean plants grown under enhanced UV-B radiation, *J. Exp. Bot.*, 2000, **51**, 1309–1317.
35 V. Alexieva, I. Sergiev, S. Mapelli and E. Karanov, The effect of drought and ultraviolet radiation on growth and stress markers in pea and wheat, *Plant, Cell Environ.*, 2001, **24**, 1337–1344.
36 J. Stratmann, Ultraviolet-B radiation co-opts defense signaling pathways, *Trends Plant Sci.*, 2003, **8**, 526–533.
37 C. Ouhibi, H. Attia, F. Rebah, N. Msilini, M. Chebbi, J. Aarrouf, L. Urban and M. Lachaal, Salt stress mitigation by seed priming with UV-C in lettuce plants: Growth, antioxidant activity and phenolic compounds, *Plant Physiol. Biochem.*, 2014, **83**, 126–133.
38 Y. Manetas, Y. Petropoulou, K. Stamatakis, D. Nikolopoulos, E. Levizou, G. Psaras and G. Karabourniotis, in *UV-B and Biosphere*, ed. J. Rozema, W. W. C. Gieskes, S. C. Van De Geijn, C. Nolan and H. De Boois, Springer Netherlands, Dordrecht, 1997, pp. 100–108, DOI: 10.1007/978-94-011-5718-6_9.
39 A.-M. Schmidt, D. P. Ormrod, N. J. Livingston and S. Misra, The Interaction of Ultraviolet-B Radiation and Water Deficit in Two Arabidopsis thaliana Genotypes, *Ann. Bot.*, 2000, **85**, 571–575.
40 L. Chalker-Scott and J. D. Scott, Elevated Ultraviolet-B Radiation Induces Cross-protection to Cold in Leaves of Rhododendron Under Field Conditions, *Photochem. Photobiol.*, 2004, **79**, 199–204.
41 M. E. Poulson, M. R. T. Boeger and R. A. Donahue, Response of photosynthesis to high light and drought for Arabidopsis thaliana grown under a UV-B enhanced light regime, *Photosynth. Res.*, 2006, **90**, 79.
42 T. M. Robson, S. M. Hartikainen and P. J. Aphalo, How does solar ultraviolet-B radiation improve drought tolerance of silver birch (Betula pendula Roth.) seedlings?, *Plant, Cell Environ.*, 2015, **38**, 953–967.
43 X. Li, L. Zhang, Y. Li, L. Ma, N. Bu and C. Ma, Changes in photosynthesis, antioxidant enzymes and lipid peroxidation in soybean seedlings exposed to UV-B radiation and/or Cd, *Plant Soil*, 2012, **352**, 377–387.
44 É. Hideg, M. A. K. Jansen and Å. Strid, UV-B exposure, ROS, and stress: inseparable companions or loosely linked associates?, *Trends Plant Sci.*, 2013, **18**, 107–115.

45 J. A. Reisz, N. Bansal, J. Qian, W. Zhao and C. M. Furdui, Effects of Ionizing Radiation on Biological Molecules—Mechanisms of Damage and Emerging Methods of Detection, *Antioxid. Redox Signaling*, 2014, **21**, 260–292.

46 S. Biedermann, S. Mooney and H. Hellmann, *Recognition and Repair Pathways of Damaged DNA in Higher Plants*, 2011.

47 S. S. Gill and N. Tuteja, Reactive oxygen species and antioxidant machinery in abiotic stress tolerance in crop plants, *Plant Physiol. Biochem.*, 2010, **48**, 909–930.

48 J. van de Walle, N. Horemans, E. Saenen, M. Van Hees, J. Wannijn, R. Nauts, A. van Gompel, J. Vangronsveld, H. Vandenhove and A. Cuypers, Arabidopsis plants exposed to gamma radiation in two successive generations show a different oxidative stress response, *J. Environ. Radioact.*, 2016, **165**, 270–279.

49 K. O. Yoshiyama, K. Sakaguchi and S. Kimura, DNA Damage Response in Plants: Conserved and Variable Response Compared to Animals, *Biology*, 2013, **2**, 1338–1356.

50 A. Van Hoeck, N. Horemans, R. Nauts, M. Van Hees, H. Vandenhove and R. Blust, Lemna minor plants chronically exposed to ionising radiation: RNA-seq analysis indicates a dose rate dependent shift from acclimation to survival strategies, *Plant Sci.*, 2017, **257**, 84–95.

51 R. Mittler, S. Vanderauwera, M. Gollery and F. Van Breusegem, Reactive oxygen gene network of plants, *Trends Plant Sci.*, 2004, **9**, 490–498.

52 P. Ahmad, C. A. Jaleel, M. A. Salem, G. Nabi and S. Sharma, Roles of enzymatic and nonenzymatic antioxidants in plants during abiotic stress, *Crit. Rev. Biotechnol.*, 2010, **30**, 161–175.

53 H. Vandenhove, N. Vanhoudt, A. Cuypers, M. van Hees, J. Wannijn and N. Horemans, Life-cycle chronic gamma exposure of Arabidopsis thaliana induces growth effects but no discernable effects on oxidative stress pathways, *Plant Physiol. Biochem.*, 2010, **48**, 778–786.

54 N. Vanhoudt, N. Horemans, J. Wannijn, R. Nauts, M. Van Hees and H. Vandenhove, Primary stress responses in Arabidopsis thaliana exposed to gamma radiation, *J. Environ. Radioact.*, 2014, **129**, 1–6.

55 T. Løvdal, K. M. Olsen, R. Slimestad, M. Verheul and C. Lillo, Synergetic effects of nitrogen depletion, temperature, and light on the content of phenolic compounds and gene expression in leaves of tomato, *Phytochemistry*, 2010, **71**, 605–613.

56 T. Murashige and F. Skoog, A Revised Medium for Rapid Growth and Bio Assays with Tobacco Tissue Cultures, *Physiol. Plant.*, 1962, **15**, 473–497.

57 O. C. Lind, D. Helen Oughton and B. Salbu, The NMBU FIGARO low dose irradiation facility, *Int. J. Radiat. Biol.*, 2019, **95**, 76–81.

58 E. L. Hansen, O. C. Lind, D. H. Oughton and B. Salbu, A framework for exposure characterization and gamma dosimetry at the NMBU FIGARO irradiation facility, *Int. J. Radiat. Biol.*, 2019, **95**, 82–89.

59 A. E. S. Green, T. Sawada and E. P. Shettle, The middle ultraviolet reaching the ground*, *Photochem. Photobiol.*, 1974, **19**, 251–259.

60 T. A. Day, T. C. Vogelmann and E. H. DeLucia, Are some plant life forms more effective than others in screening out ultraviolet-B radiation?, *Oecologia*, 1992, **92**, 513–519.

61 T. A. Day, Relating UV-B radiation screening effectiveness of foliage to absorbing-compound concentration and anatomical characteristics in a diverse group of plants, *Oecologia*, 1993, **95**, 542–550.

62 R. J. Fischbaher, B. Kossman, H. Panten, R. Steinbrecher, W. Heller, H. K. Seidlitz, H. Sandermann, N. Hertkorn and J.-P. Schnitzler, Seasonal accumulation of ultraviolet-B screening pigments in needles of Norway spruce (Picea abies (L.) Karst.), *Plant, Cell Environ.*, 1999, **22**, 27–37.

63 W. F. Morgan, J. P. Day, M. I. Kaplan, E. M. McGhee and C. L. Limoli, Genomic Instability Induced by Ionizing Radiation, *Radiat. Res.*, 1996, **146**, 247–258.

64 C. Mothersill and C. B. Seymour, Mechanisms and implications of genomic instability and other delayed effects of ionizing radiation exposure, *Mutagenesis*, 1998, **13**, 421–426.

65 J. E. Olsen, Light and temperature sensing and signaling in induction of bud dormancy in woody plants, *Plant Mol. Biol.*, 2010, **73**, 37–47.

66 Y. Lee, C. Karunakaran, R. Lahlali, X. Liu, K. K. Tanino and J. E. Olsen, Photoperiodic Regulation of Growth-Dormancy Cycling through Induction of Multiple Bud–Shoot Barriers Preventing Water Transport into the Winter Buds of Norway Spruce, *Front. Plant Sci.*, 2017, **8**, 2109.

67 R. Arora, L. Rowland and K. Tanino, *Induction and Release of Bud Dormancy in Woody Perennials: A Science Comes of Age*, 1953.

68 T. Gichner, Z. Patková and J. K. Kim, DNA Damage Measured by the Comet Assay in Eight Agronomic Plants, *Biol. Plant.*, 2003, **47**, 185–188.

69 G. Koppen, A. Azqueta, B. Pourrut, G. Brunborg, A. R. Collins and S. A. S. Langie, The next three decades of the comet assay: a report of the 11th International Comet Assay Workshop, *Mutagenesis*, 2017, **32**, 397–408.

70 L. Xie, T. Gomes, K. A. Solhaug, Y. Song and K. E. Tollefsen, Linking mode of action of the model respiratory and photosynthesis uncoupler 3,5-dichlorophenol to adverse outcomes in Lemna minor, *Aquat. Toxicol.*, 2018, **197**, 98–108.

71 J. Razinger, L. Drinovec and A. Zrimec, Real-time visualization of oxidative stress in a floating macrophyte Lemna minor L. exposed to cadmium, copper, menadione, and AAPH, *Environ. Toxicol.*, 2010, **25**, 573–580.

72 L. Nybakken, R. Hörkkä and R. Julkunen-Tiitto, Combined enhancements of temperature and UVB influence growth and phenolics in clones of the sexually dimorphic Salix myrsinifolia, *Physiol. Plant.*, 2012, **145**, 551–564.

73 M. M. Caldwell, J. F. Bornman, C. L. Ballaré, S. D. Flint and G. Kulandaivelu, Terrestrial ecosystems, increased solar ultraviolet radiation, and interactions with other climate change factors, *Photochem. Photobiol. Sci.*, 2007, **6**, 252–266.

74 K. Hectors, E. Prinsen, W. De Coen, M. A. K. Jansen and Y. Guisez, Arabidopsis thaliana plants acclimated to low dose rates of ultraviolet B radiation show specific changes in morphology and gene expression in the absence of stress symptoms, *New Phytol.*, 2007, **175**, 255–270.
75 A. G. Roro, S. A. F. Dukker, T. I. Melby, K. A. Solhaug, S. Torre and J. E. Olsen, UV-B-induced Inhibition of Stem Elongation and Leaf Expansion in Pea Depends on Modulation of Gibberellin Metabolism and Intact Gibberellin Signalling, *J. Plant Growth Regul.*, 2017, **36**, 680–690.
76 M. A. K. Jansen, Ultraviolet-B radiation effects on plants: induction of morphogenic responses, *Physiol. Plant.*, 2002, **116**, 423–429.
77 G. I. Jenkins, Signal Transduction in Responses to UV-B Radiation, *Annu. Rev. Plant Biol.*, 2009, **60**, 407–431.
78 Y.-P. Cen and J. F. Bornman, The effect of exposure to enhanced UV-B radiation on the penetration of monochromatic and polychromatic UV-B radiation in leaves of Brassica napus, *Physiol. Plant.*, 1993, **87**, 249–255.
79 S. Reuber, J. F. Bornman and G. Weissenbock, A flavonoid mutant of barley (Hordeum vulgare L.) exhibits increased sensitivity to UV-B radiation in the primary leaf, *Plant, Cell Environ.*, 1996, **19**, 593–601.
80 L. C. Olsson, M. Veit, G. Weissenböck and J. F. Bornman, Differential flavonoid response to enhanced uv-b radiation in brassica napus, *Phytochemistry*, 1998, **49**, 1021–1028.
81 J.-P. Schnitzler, T.P. Jungblut, C. Feicht, M. Köfferlein, C. Langebartels, W. Heller and H. Sandermann Jr., UV-B induction of flavonoid biosynthesis in Scots pine (Pinus sylvestris L.) seedlings, *Trees*, 1997, **11**, 162–168.
82 A. K. Hahlbrock and D. Scheel, Physiology and Molecular Biology of Phenylpropanoid Metabolism, *Annu. Rev. Plant Physiol. Plant Mol. Biol.*, 1989, **40**, 347–369.
83 A. B. Britt, Repair of DNA Damage Induced by Solar UV, *Photosynth. Res.*, 2004, **81**, 105–112.
84 R. P. Rastogi, Richa, A. Kumar, M. B. Tyagi and R. P. Sinha, Molecular Mechanisms of Ultraviolet Radiation-Induced DNA Damage and Repair, *J. Nucleic Acids*, 2010, **2010**, 592980.
85 S. Hurem, T. Gomes, D. A. Brede, E. Lindbo Hansen, S. Mutoloki, C. Fernandez, C. Mothersill, B. Salbu, Y. A. Kassaye, A.-K. Olsen, D. Oughton, P. Alestrom and J. L. Lyche, Parental gamma irradiation induces reprotoxic effects accompanied by genomic instability in zebrafish (Danio rerio) embryos, *Environ. Res.*, 2017, **159**, 564–578.
86 U. Aypar, W. F. Morgan and J. E. Baulch, Radiation-induced genomic instability: Are epigenetic mechanisms the missing link?, *Int. J. Radiat. Biol.*, 2011, **87**, 179–191.
87 C. H. Bassing, K. F. Chua, J. Sekiguchi, H. Suh, S. R. Whitlow, J. C. Fleming, B. C. Monroe, D. N. Ciccone, C. Yan, K. Vlasakova, D. M. Livingston, D. O. Ferguson, R. Scully and F. W. Alt, Increased ionizing radiation sensitivity and genomic instability in the absence of histone H2AX, *Proc. Natl. Acad. Sci. U. S. A.*, 2002, **99**, 8173–8178.

Supplementary Figure Legends

Fig. S1 Effect of 6 days of gamma irradiation without (UV-) or with (UV+) UV-B (0.35 W m^{-2}) in Scots pine seedlings; A) Shoot and B) root length relative to the unexposed control. Mean of 48-90 plants per treatment. C) Shoot and D) root length relative to the unexposed control in experiments including also 4 days UV-B at 0.35 W m^{-2} pre-treatment of the UV-B exposed plants. Mean of 27-51 plants per treatment. (The actual shoot and root lengths shown in Fig. 1). Relative E) shoot and F) root length and actual G) shoot (regression analysis values (R^2): UV-: 0.84; UV+: 0.20).and H) root length (R^2: UV-: 0.91; UV+: 0.05) in an experiment including 4 days UV-B pre-treatment at 0.52 W m^{-2}. Mean ± SE of 10 plants per treatment. The treatments started when plants were 6 days old. Different letters within a plant part indicate significant differences ($p \leq 0.05$) based on analysis of variance followed by Tukey`s test.

Fig. S2 Effect of 6 days of gamma irradiation without (UV-) or with (UV+) UV-B (0.35 W m^{-2}) in Scots pine seedlings; A) DNA damage (COMET assay) in shoot tips relative to the unexposed control. B) DNA damage in shoot tips relative to the unexposed control in experiments including also 4 days UV-B (0.35 W m^{-2}) pre-treatment of the UV-B exposed plants. (The actual DNA damage values shown in Fig. 2). C) Relative and D) actual DNA damage (COMET assay) (regression analysis value (R^2): 0.87) in shoot tips in an experiment including 4 days UV-B pre-treatment at 0.52 W m^{-2}. Mean of 6 (A, B) or 3 (C, D) samples per treatment with 3 technical replicates (gels) per sample with 50-100 nuclei scored per gel. The treatments started when plants were 6 days old. Different letters indicate significant differences ($p \leq 0.05$) based on analysis of variance followed by Tukey`s test.

Fig. S3 Effect of 6 days gamma irradiation with (UV+) or without (UV-) UV-B (0.35 W m^{-2}) on total antioxidant capacity (Ferric reducing antioxidant power (FRAP) assay) in A) entire Scots pine seedlings (mean ± SE of 4 samples) or B) shoots only (mean ± SE of 3 samples). Three technical replicates were

analysed per sample. The treatments started when the seedlings were 6 days old. Different letters within a diagram indicate significant differences ($p \leq 0.05$) based on analysis of variance followed by Tukey`s test.

Fig. S4 Post-irradiation effects of 6 days of gamma irradiation without (UV-) or with (UV+) UV-B (0.35 W m^{-2}) in Scots pine seedlings; A) Cumulative shoot elongation, B) shoot diameter (needle tip to needle tip) and C) number of needles relative to the unexposed control. D) Cumulative shoot elongation, E) shoot diameter and F) number of needles relative to the unexposed control in experiments including also 4 days UV-B (0.35 W m^{-2}) pre-treatment of the UV-B exposed plants. (The actual values are shown in Fig. 4). The irradiation treatments started when the seedlings were 6 days old, and time 0 corresponds to the day the irradiation treatments ended. The results are mean ± SE of 24 plants per treatment.

Fig. S5 Post-irradiation effect 44 days after 6 days of gamma irradiation without (UV-) or with (UV+) UV-B (0.35 W m^{-2}) on DNA damage (COMET assay) relative to the unexposed control in A) shoot and B) root tips of Scots pine seedlings. The irradiation treatments started when plants were 6 days old. The results are mean of 6 samples per treatment with 3 technical replicates (gels) per sample with 50-100 nuclei scored per gel.

Fig. S6 Post-irradiation effect 7 months after 6 days of gamma irradiation without (UV-) or with (UV+) UV-B (0.35 W m^{-2}) in Scots pine seedlings, including also 4 days UV-B (0.52 W m^{-2}) pre-treatment of UV-B exposed seedlings. A) Plant phenotype. DNA damage in shoot tips B) relative to the unexposed control and C) actual DNA damage values (regression analysis value R^2: 0.33). The line in each box = the mean of the median values for 3 repeated samples per treatment with 3 technical replicates (gels) per sample with 50-100 nuclei scored per gel. Lower and upper box boundaries = 25 and 75% percentiles,

error bars = 10 and 90% percentiles with data points outside these shown as dots. Different letters indicate significant differences ($p \leq 0.05$) based on analysis of variance followed by Tukey`s test.

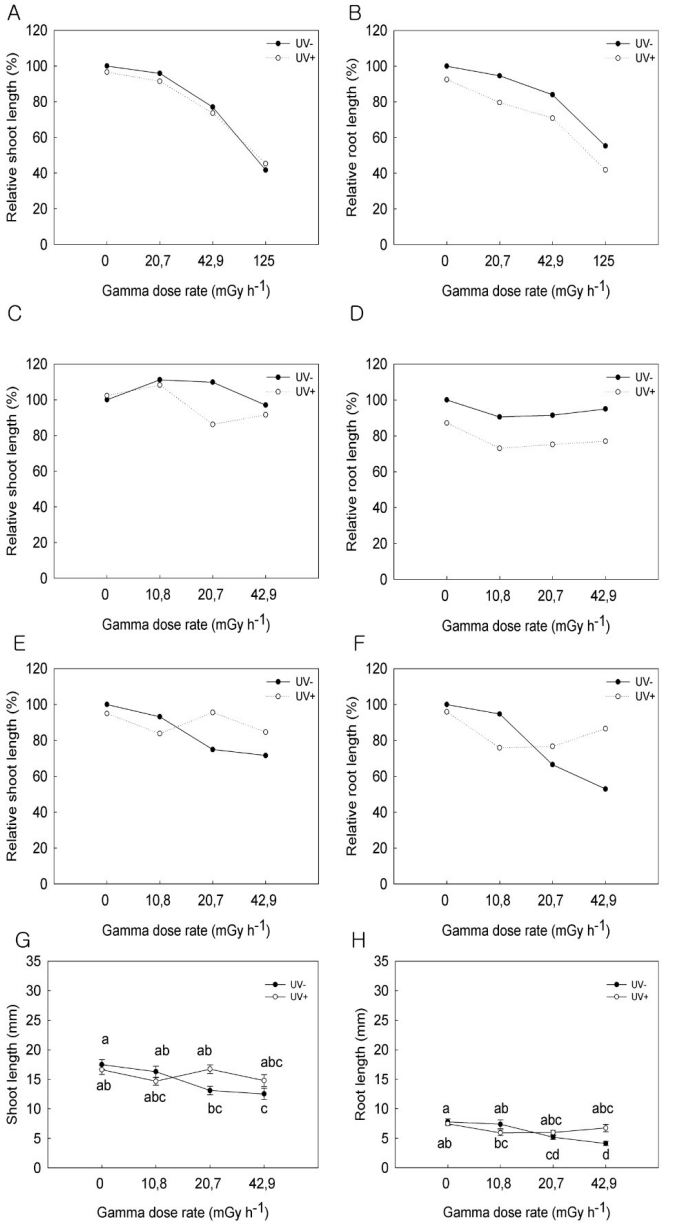
A
B
C
D
E
F
G
H
Relative shoot length (%)
Relative root length (%)
Shoot length (mm)
Root length (mm)
UV-
UV+
0
20
40
60
80
100
120
0
5
10
15
20
25
30
35
0
20,7
42,9
125
10,8
Gamma dose rate (mGy h-1)
a
ab
abc
bc
c
cd
d

Fig. S1

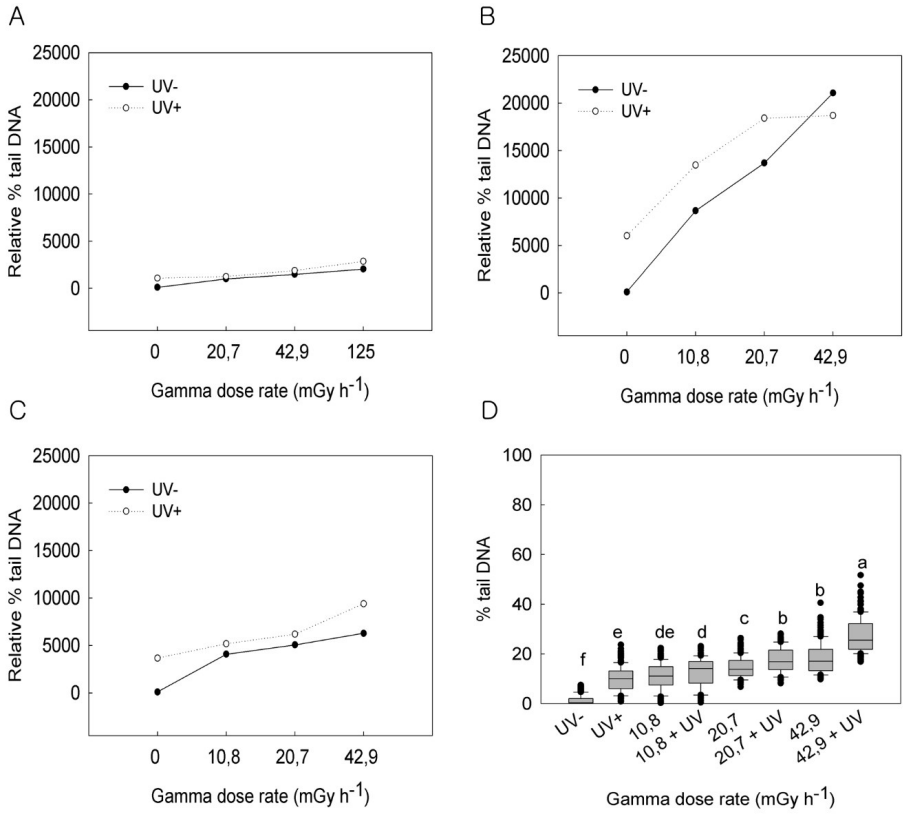
A
B
C
D
Relative % tail DNA
% tail DNA
UV-
UV+
0
5000
10000
15000
20000
25000
0
20,7
42,9
125
10,8
Gamma dose rate (mGy h-1)
20
40
60
80
100
a
b
c
d
de
e
f
UV-
UV+
10,8
10,8 + UV
20,7
20,7 + UV
42,9
42,9 + UV

Fig. S2

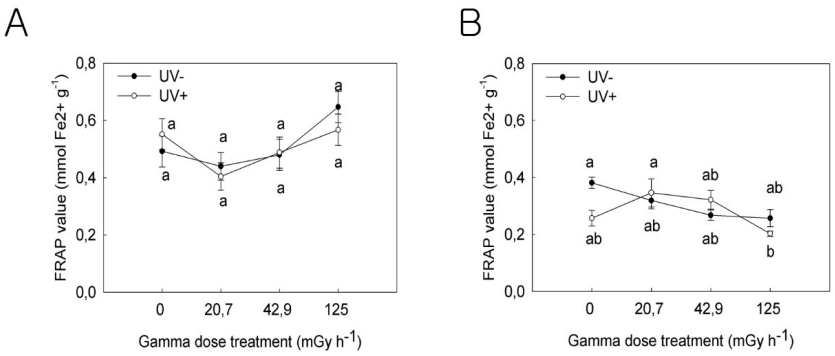
A
B
UV-
UV+
FRAP value (mmol Fe2+ g-1)
0,0
0,2
0,4
0,6
0,8
0
20,7
42,9
125
Gamma dose treatment (mGy h-1)
a
a
a
a
a
a
a
a
ab
ab
ab
ab
ab
b

Fig. S3

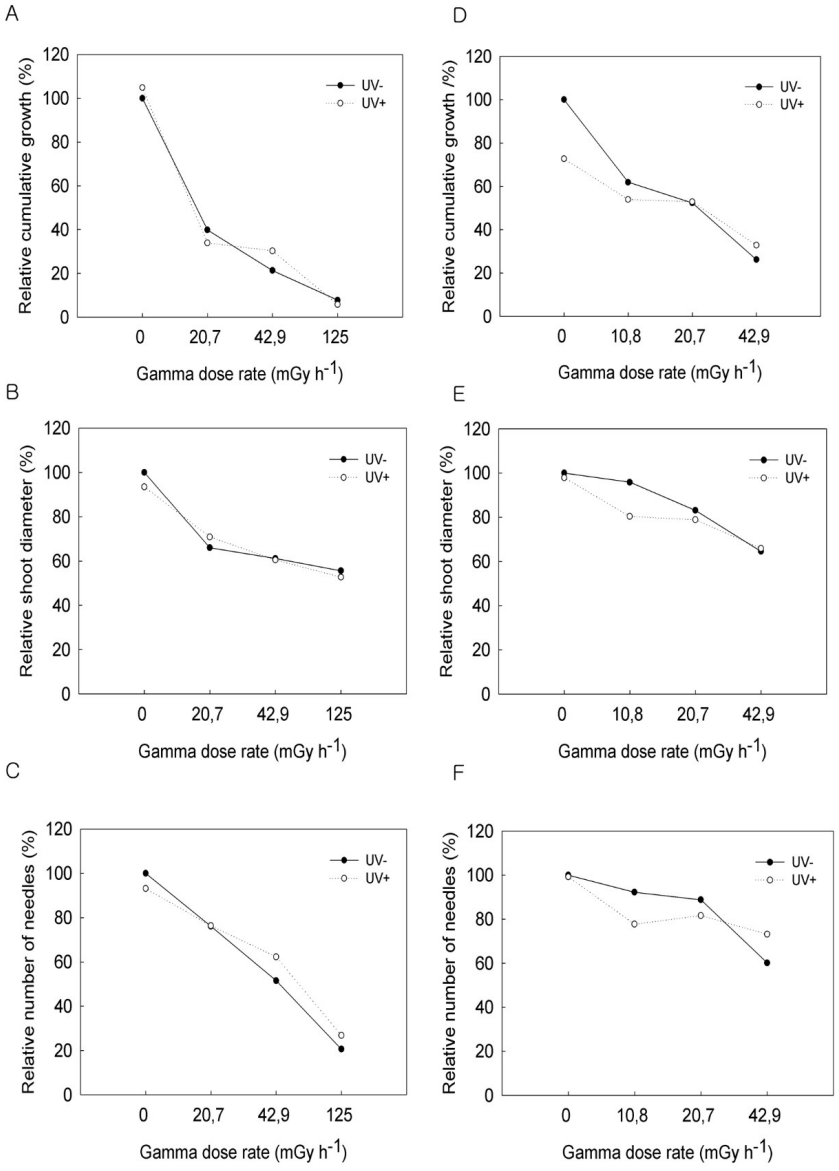
A
D
B
E
C
F
Relative cumulative growth (%)
Relative cumulative growth /%)
Relative shoot diameter (%)
Relative number of needles (%)
UV-
UV+
0
20
40
60
80
100
120
0
20,7
42,9
125
10,8
Gamma dose rate (mGy h-1)

Fig. S4

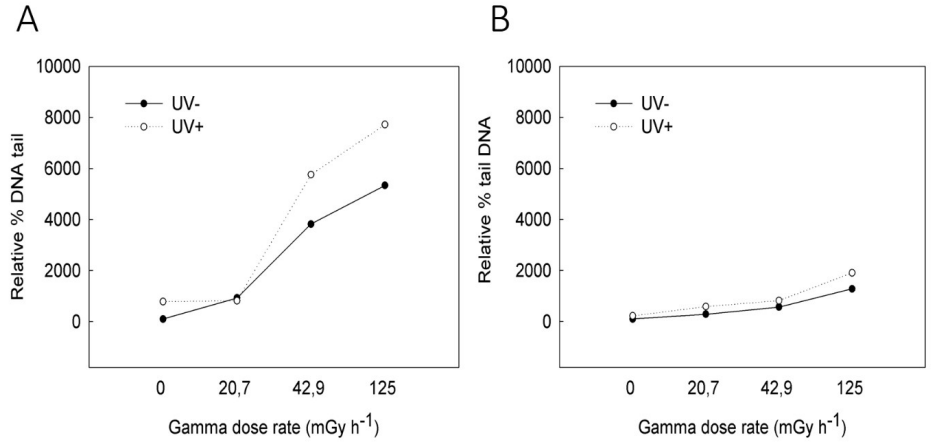
A
B
10000
8000
6000
4000
2000
0
UV-
UV+
Relative % DNA tail
Relative % tail DNA
0
20,7
42,9
125
Gamma dose rate (mGy h-1)

Fig. S5

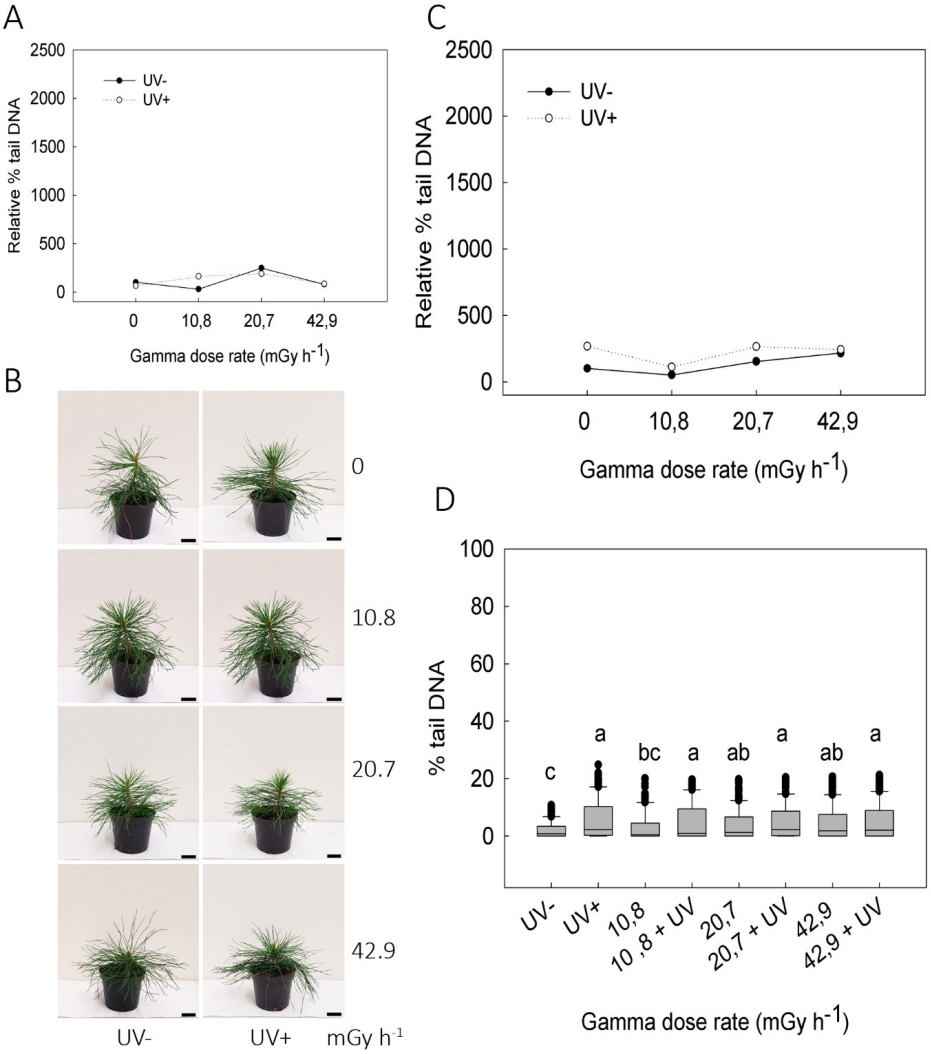

Fig. S6

Paper III

Transcriptomic responses associated with gamma radiation damage in seedlings of the radiosensitive conifer species Norway spruce

Dajana Blagojevic[1,2], Payel Bhattacharjee[1,2], YeonKyeong Lee[1,2], Lars Grønvold[3], Gareth Benjamin Gillard[4], Torgeir Rhoden Hvidsten[4], Simen Rød Sandve[3], Brit Salbu[2,5], Dag Anders Brede[2,5], Jorunn E. Olsen[1,2]

Addresses

[1] *Department of Plant Sciences, Faculty of Biosciences, Norwegian University of Life Sciences, P.O. Box 5003, N-1432 Ås, Norway*

[2] *Centre of Environmental Radioactivity (CERAD), Norwegian University of Life Sciences, P.O. Box 5003, N-1432 Ås, Norway*

[3] *Centre for Integrative Genetics (CIGENE), Department of Animal Science, Faculty of Biosciences, Norwegian University of Life Sciences, P.O. Box 5003, N-1432 Ås, Norway*

[4]*Faculty of Chemistry, Biotechnology and Food science, Norwegian University of Life Sciences, P.O. Box 5003, N-1432 Ås, Norway*

[5]*Faculty of Environmental Sciences and Natural Resource Management, Norwegian University of Life Sciences, P.O. Box 5003, N-1432 Ås, Norway*

Abstract

Conifer species are considered among the most radiosensitive plants species, and a previous study demonstrated similar sensitivity to gamma radiation in Norway spruce and Scots pine seedlings with progressive growth inhibition and mortality at dose rates ≥40 mGy h^{-1} provided for 144 h. Using an RNA sequencing approach and concomitant analyses of DNA damage and growth, we here aimed to assess early molecular events in response to gamma radiation, and to establish a dose response connection to adverse phenotypic effects in Norway spruce seedlings. After 48 h exposure to gamma radiation, increased, dose rate-dependent DNA damage was observed at all tested dose rates. However, RNA seq analyses (0, 1, 10, 40, 100 mGy h^{-1}) showed that only gamma radiation dose rates ≥40 mGy h^{-1} resulted in comprehensively altered gene expression with overall upregulation of genes related to energy-metabolism, protein degradation, DNA repair and specific antioxidants and downregulation of genes associated with plant hormone biosynthesis/signalling/transport (growth stimulating hormones; auxin, gibberellin, brassinosteroid, cytokinin), cell division control, nitrogen metabolism, and lipid biosynthesis. Consistent with reduced growth at 100 mGy h^{-1}, including post-irradiation, genes related to photosynthesis were massively downregulated at this but not lower dose rates. In conclusion, only minor changes in gene expression occurred in response to 1 and 10 mGy h^{-1} despite significantly increased DNA damage, whereas higher dose rates, which resulted in progressively increased DNA damage and eventually reduced growth, caused a massive shift in gene expression from photosynthesis and growth to energy-requiring mobilisation of protection and repair mechanisms.

Keywords DNA damage, ionizing radiation, growth inhibition, *Picea abies*, DNA repair, RNA sequencing

Introduction

As sessile organisms, plants are constantly exposed to different abiotic stress factors, including ionizing radiation. The natural background of ionizing radiation due to cosmic radiation and radiation from radionuclides in bedrock, soils and sediments may vary, but dose rates of up to 15 μGy h^{-1} has been measured, and the current global mean background dose rate has been estimated to 2.5 mGy $year^{-1}$, corresponding to about 0.29 μGy h^{-1} (Caplin & Willey 2018). Anthropogenic activities such as accidental radioactive release from nuclear power plants have resulted in areas with elevated levels of ionizing radiation. It has been calculated that the absorbed gamma dose was 80-100 Gy in the needles of dead pine trees in heavily contaminated sites in Chernobyl (Kashparova et al. 2018). Generally, acute high doses of ionizing radiation between 10-1000 Gy can be lethal to plants, but <0.42 mGy h^{-1} does probably not result in damage to terrestrial plants in the field (Caplin & Willey 2018; UNSCEAR 1996).

Elevated levels of ionizing radiation may cause adverse biological responses such as DNA damage, oxidative stress, growth reduction, reproduction impairment and morphological alterations (Blagojevic et al. 2019a; Blagojevic et al. 2019b; Reisz et al. 2014). The extent to which ionizing radiation induces adverse effects depends on several factors such as exposure duration (acute or chronic), exposure dose rate level and total dose, species, life stage of exposure and the co-occurrence of contaminants or environmental conditions affecting sensitivity to ionizing radiation (Garnier-Laplace et al. 2013; Kovalchuk et al. 2007). Effects of low to moderate levels of ionizing radiation in plants have been less studied than high levels. Although the threshold values are largely based on health consequences and has varied through the years, low doses and dose rates of ionizing radiation are currently defined as ≤100 mGy and ≤6 mGy h^{-1}, respectively (Averbeck et al. 2018; UNSCEAR 2017).

However, the International Commission on Radiological Protection (ICRP) define Derived Consideration Reference Levels (DCRLs) for environmental protection for pine trees from 0.1 to 1 mGy d^{-1}, which corresponds to 0.0041-0.041 mGy h^{-1} (Pentreath et al. 2014).

In the first years after the Chernobyl nuclear power plant accident in 1986, plant populations, especially Scots pine trees (*Pinus sylvestris*), in the Chernobyl exclusion zone showed highly elevated mutation rates (Geras'kin et al. 2008). Furthermore, several studies in this area indicated

that the radiosensitivity of Norway spruce (*Picea abies*) trees was greater than that of pines (Kozubov & Taskaev 2007). Conversely, our recent comparative study of seedlings of these species exposed to gamma radiation under controlled conditions indicated relatively similar sensitivity (Blagojevic et al. 2019a). In this study, growth inhibition was observed after 144 h at 40 mGy h^{-1} and higher dose rates, including post-irradiation. In another study of Scots pine seedlings, reduced growth during the post-irradiation period was also observed after exposure to a gamma dose rate of 20 mGy h^{-1} for 144 h (Blagojevic et al. 2019b). Compared to other plant species like the herbaceous *Arabidopsis thaliana* and lichens, conifers are less tolerant to radiation exposure (Blagojevic et al. 2019a; Geraskin & Sarapul`sev 1995; IAEA 1992; Vanhoudt et al. 2014).

Ionizing radiation may cause adverse effects directly, via ionization or excitation of specific biomolecules, or indirectly through production of reactive oxygen species (ROS) (Gill & Tuteja 2010). ROS and other oxidants are balanced against the antioxidative defence system, including enzymes like catalases (CAT), superoxide dismutases (SOD) and peroxidases (PX) as well as metabolites such as ascorbate (AsA) and glutathione (GSH) (Foyer & Noctor 2003; Vandenhove et al. 2009). Thus, the action of such metabolites and enzymes makes up the cell`s antioxidative power that maintains the cellular homeostasis within certain limits (Foyer & Noctor 2003). The antioxidative defence in response to ionizing radiation has been relatively well studied in *Arabidopsis thaliana* and some other species. This revealed increased activity and gene expression of antioxidants such as SOD and ascorbate peroxidase (APX) (Alothman et al. 2009; van de Walle et al. 2016; Vandenhove et al. 2009; Vanhoudt et al. 2014).

In DNA molecules, ionizing radiation may cause single or double strand breaks in plant and animal cells (Yoshiyama et al. 2013b). However, DNA damage triggers biochemical signals that activate different DNA repair mechanisms, playing a crucial role in recovering DNA strands from damage (Bray & West 2005; Britt 2002; Hays 2002; Kunz et al. 2005). The RADIATION 51 (RAD51) protein, which is involved in homologous recombination, were induced in *A. thaliana* following gamma exposure (Kim et al. 2013; Yoshiyama et al. 2013b). Furthermore, several genes in the DNA repair pathways are modulated through SUPRESSOR OF GAMMA RESPONSE 1 (SOG1), which consecutively activate canonical pathways involved in DNA repair, programmed cell death and endoreduplication (Yoshiyama et al. 2013b). Also, the induction of the DNA ligase

enzyme LIG4 and interaction with a homolog of the X-RAY REPAIR CROSS COMPLEMENTING 4 (XRCC4) protein in *A. thaliana* after gamma radiation, indicates increased DNA damage repair of both single- and double-strand breaks during replication and recombination (West et al. 2000).

The cell cycle checkpoints are essential for plants to ensure proper DNA repair. This is achieved by activation of the cell cycle checkpoints that target the cyclin (CYC)/cyclin-dependent kinase (CDK)-complex that normally promotes cell cycle progression (Belli et al. 2002; Deckbar et al. 2011). In cases where DNA damage does not get repaired, permanent cell cycle arrest or programmed cell death is induced to eliminate severely damaged cells (Belli et al. 2002).

A. thaliana exposed to gamma radiation showed induction of *CYCB1;1* and suppression of *CDKB2;1* 1.5 h after 100 Gy provided during 2 days (Culligan et al. 2006; Yoshiyama et al. 2009). In Scots pine seedlings exposed to gamma radiation dose rates of 10 or 40 mGy h^{-1} for 144 h, *CYCB1;2* was upregulated whereas no such induction was observed at ≥100 mGy h^{-1} (Blagojevic et al. 2019a). No such effect of gamma radiation was observed in Norway spruce seedlings, but in *A. thaliana* induction of the *CYCB1;2* gene was observed at ≥40 mGy h^{-1} (Blagojevic et al. 2019a).

It appears that plants mount profoundly different gene expression responses to chronic or acute irradiation (Kovalchuk et al. 2007; Kovalchuk et al. 1999). An RNA-sequencing study of *A. thaliana* plants revealed that two thirds of the differentially expressed genes were similarly regulated 2 and 24 h after acute gamma irradiation (external ^{60}Co exposure; 90 000 mGy h^{-1} for 40 sec; total dose 1 Gy), while less than 10% of the up- and down-regulated genes showed different expression 2 and 24 h after chronic gamma irradiation (internal ^{137}CsCl (about 24% of the total radiation) and external ^{60}Co (about 76%) exposure; 2 mGy h^{-1} for 21 days; total dose 0.93 Gy) (Kovalchuk et al. 2007). A recent study of the transcriptome of *Lemna minor* exposed for 7 days to gamma doses from 53 to 423 mGy h^{-1} showed differentially expressed genes e.g. related to antioxidative defence systems, DNA repair, photosynthesis, hormones and the cell cycle (Van Hoeck et al. 2017). The gene expression pattern indicated that increasing levels of chronic ionizing radiation exposures forced *L. minor* from an acclimation response (eustress) towards a survival response (distress) (Van Hoeck et al. 2017). A transcriptome study of gamma-exposed *A. thaliana* also indicated strong induction of antioxidants and genes related to signal transduction (Kim et al.

2011). This work employed very high gamma doses from 100-2000 Gy (24 h exposure from a ^{60}Co source) during vegetative and reproductive developmental stages.

There is limited information about the molecular mechanisms underlying the responses of radiosensitive conifers exposed to low to moderate levels of ionizing radiation, and detailed transcriptome data from standardized exposure under controlled conditions is to our knowledge not available. By employing an RNA sequencing approach and concomitant analyses of DNA damage and growth, we here aimed to assess the early molecular events in response to gamma radiation and to establish a dose response connection to adverse phenotypic effects.

Material and methods

Plant materials and pre-growing conditions

Seeds of Norway spruce (*Picea abies* L. H. Karst), from the provenance CØ1 from Halden, Norway (59°N latitude, seed lot 98063, Skogfrøverket, Hamar, Norway (www.skogfroverket.no), were surface sterilized in 1% sodium hypochlorite for 5 min. The seeds were subsequently rinsed five times in distilled water and placed on a sterile filter paper for drying. All seeds were evenly sown on ½ MS medium ((Murashige & Skoog 1962); Duchefa Biochemie, Harleem, Netherland) with 0.8% agar (Plant agar, Sigma-Aldrich, St. Louis, MO, USA) in Petri dishes of 5 cm diameter. About 20-30 seeds were sown per plate, and the germination rate was about 50-60%. The seeds were then germinated for 6 days at 20 °C under a photon flux density of 30 µmol m^{-2} s^{-1} at 400-700 nm (TL-D 58W/840 lamps, Philips, Eindhoven, The Netherlands) in a 16 h photoperiod.

Exposure of seedlings to gamma radiation using a ^{60}Co source and growing conditions during the exposure

Six days old seedlings of Norway spruce were exposed to gamma radiation for 48 h using the FIGARO low dose gamma irradiation facility (^{60}Co; 1173.2 and 1332.5 keV γ-rays) at Norwegian University of Life Sciences (Lind et al. 2018). The dosimetry of the exposed seedlings followed an established protocol (Hansen et al. 2019). Petri dishes with seedlings were placed at different distances from the gamma source to obtain the average dose rates to water 1, 10, 40, 100 and 290 mGy h^{-1} (Table 1). The dose rates to water and dose rate intervals (in front and back of the petri

dishes) were calculated from air kerma rate for each position obtained from 4 nanodot dosimeter measurements per position (MicroStar, Landauer Inc. Greenwood, IL, USA), taking into account that the petri dishes were rotated 180° in the middle of the experiment (after 24 h) to obtain more even irradiation throughout each Petri dish. The total doses (0.048-13.9 Gy; Table 1) were calculated from the estimated absorbed dose rates to water, multiplied by total exposure time (48 h). Petri dishes with control samples not exposed to gamma radiation were also placed in the same room (same temperature and light conditions), but outside the radiation sector, shielded by lead walls. Two repeated gamma irradiation experiments were performed. During the gamma radiation treatment, the room temperature was 20 ˚C±1 °C, and the plants were exposed to a 12 h photoperiod. An irradiance of 55 μmol m^{-2} s^{-1} from high pressure metal halide lamps (HPI-T Plus 250W lamps, Philips, Eindhoven, The Netherlands) was measured at the top of the petri dishes with a Li-Cor Quantum/Radiometer/Photometer (model LI-250, LI-COR, Lincoln, NE, USA). The red:far red (R:FR) ratio was measured to 3.5 using a 660/730 nm sensor (Skye Instruments, Powys, Wales, UK).

Post-irradiation growing conditions

To assess post-irradiation effects of the 48 h of gamma irradiation, gamma-exposed plants were transferred to pots (5 cm diameter, 5 cm height, one plant per pot) filled with S-soil (45% low moist peat, 25% high moist peat, 25% perlite and 5% sand; Hasselfors Garden AS, Örebro, Sweden). The plants were then grown in a growth chamber (manufactured by Norwegian University of Life Sciences) at 20˚C under a 12 h main light period provided by metal halide lamps (HPI-T Plus 250W, Philips) with the R:FR-ratio adjusted to 1.7 with incandescent lamps (Osram, Munich, Germany). The photon irradiance was gradually increased from 50 to 180 μmol m^{-2} s^{-1} during 7 days. The photoperiod was extended to 24 h with the incandescent lamps only to ensure a photoperiod longer than the critical one for growth in the northern provenance used. The relative air humidity (RH) was adjusted to 78%, corresponding to 0.5 kPa water vapour pressure deficiency.

Growth parameter recordings after the gamma exposure and post-irradiation

After the gamma irradiation, seedlings were placed between two transparent plastic sheaths with mm paper on top and scanned. The shoot and root lengths of the scanned seedlings were measured using Image J (US National Institutes of Health, Bethesda, MD, USA; http:/imagej.nih.gov/ij/). The lengths of totally 28-37 plants were measured per gamma dose rate.

Post-irradiation, shoot elongation, the number of needles and plant diameter were recorded in 11-22 plants per treatment in a time course up of 59 days. Plant height was measured from the shoot apical meristem to the rim of the pot, and the cumulative shoot elongation calculated. The plant diameter was calculated from two perpendicular measurements from needle tip to needle tip across the plant at the shoot apex.

Histological studies of shoot tips

Histological studies of shoot apical meristems at the end of the gamma irradiation were performed according to (Lee et al. 2017). After the 48 h of gamma irradiation, shoot tips were immediately fixed in 4% paraformaldehyde and 0.025% glutaraldehyde in phosphate buffered saline (PBS, pH 7.0) and vacuum infiltrated for 1 h at room temperature and stored at 4 °C overnight. The fixed tissues were then washed with PBS solution for 30 min and dehydrated in a graded ethanol solution. After dehydration, approximately 3 mm of the shoot tips of each of 5 plants per treatment were infiltrated and embedded in LR White (London Resin Company, London, UK). After polymerisation 1 µm thick sections were made using an Ultracut Leica EM UC6 microtome (Leica, Mannheim, Germany), and the sections were stained with toluidine blue O to visualize the cells (del Cerro et al. 1980). The stained sections were inspected using a light microscope with bright field optics (Leica DM6).

The COMET assay for analysis of DNA damage

Single and double strand DNA breaks were quantified in response to gamma treatments at the end of the gamma irradiation and 77 days post-irradiation, using the COMET assay ((Gichner et al. 2003) with some modifications (Blagojevic et al. 2019a; Blagojevic et al. 2019b)). Right after the

gamma exposure, three biological replicates per dose rate, each consisting of 3-4 mm of shoot tips from 3 plants, were used to identify DNA damage.

The analyses were performed under inactinic red light in order to avoid light-induced DNA damage. In a 9 cm Petri dish with 400 µl cold extraction buffer (PBS, pH 7.0 and 200 mM EDTA), approximately 200 mg plant material per treatment was chopped for 30 s with a razor blade. Thereafter the nuclei solution without plant debris was collected and 75 µl of the nuclei solution was gently mixed with 1% low melting point agarose (50 µl), prepared in advance in distilled water at 40 °C, and 10 µl aliquots was placed on microscope slides pre-coated with 1% low melting point agarose. Three gels (technical replicates) were made per biological sample. The slides were then placed on ice for 1 min to unwind DNA prior to electrophoresis, which was performed for 10 min in a horizontal gel tank with freshly prepared cold electrophoresis buffer (1 mM Na_2EDTA and 300 mM NaOH, pH 13) at 20 V (300 mA) for 5 min at 4 °C. The slides were washed right after the electrophoresis with distilled water and neutralized in PBS buffer for 10 min. Then slides were again washed with distilled water, fixed in 95 % ethanol and dried overnight before staining with Syber Gold (Life Technologies Ltd, Paisley, UK; dilution 1:5000) for 20 min and washing in distilled water 3 times for 5 min each. To score the COMETS (elongated cell nuclei as a consequence of DNA damage), COMET IV (Perceptive Instruments Ltd, Bury St. Edmunds, UK) and an Olympus BX51 fluorescence microscope with a CDD camera (Olympus, Tokyo, Japan) were used. For each of the three biological replicates per dose rate, totally 200 cell nuclei were scored at the end of the irradiation and day 77 post-irradiation, with 60-70 nuclei, scored in each technical replicate (gel). The median values were calculated for each biological replicate per treatment, followed by calculation of the average value for the three biological replicates, as recommended by (Koppen et al. 2017).

Statistical analyses of the growth parameter- and DNA damage data

The effect of the gamma radiation treatments on DNA damage, shoot and root length at the end of the irradiation as well as the post-irradiation cumulative growth, plant diameter and number of needles as well as DNA damage 77 days post-irradiation were assessed by one-way analyses of variance in the general linear model mode and by regression analyses using the Minitab 18 software (Minitab Inc., PA, USA). For the post-irradiation growth data, only the results from the

final time point when the differences were largest, were analysed (day 58 or 59). Tukey`s post hoc test was used to test for differences between means.

RNA extraction and sequencing

At the end of the 48 h of gamma exposure, four samples, each consisting of 4 shoots, were harvested in liquid nitrogen per gamma dose rate (0, 1, 10, 40, 100 mGy h^{-1}) and stored at -80°C until analyses. Total RNA was extracted using the Masterpure Complete DNA and RNA Purification Kit (Epicenter, Madison, WI, USA) following the manufacturer`s instructions except that 0.5% polyvinylpyrrolidone (PVP, mw 360 000, Sigma Aldrich, Steinheim, Germany) was added to the extraction buffer and that 3 µl beta-mercaptoethanol per sample replaced the 1.4-dithiothreitol (DTT) in the manufacturer`s protocol. Evaluation of RNA quality was done using an Agilent 2100 Bioanalyzer with an RNA 144000 NanoKit (Agilent technologies, Palo Alto, CA, USA), while RNA quantity was measured by a NanoDrop ND-1000 Spectrophotometer (Thermo Scientific, Wilmington, DE, USA).

The transcriptomes of the shoots were sequenced on an Illumina HiSeq4000 platform at the Norwegian Sequencing Centre (Ullevål University Hospital, Oslo, Norway) using the Strand specific 20xTruseqTM RNA library preparation (paired end; read length 150 bp) as recommended by the manufacturer (Illumina, San Diego, CA, USA). All samples were sequenced in 2 repeated lanes on the HiSeq 4000. The raw sequence data were submitted to the ArrayExpress under the accession number E-MTAB-8081 (stored in the European Nucleotide Archive).

Differential expression analyses

The transcript abundances were estimated with Salmon read mapping software (Patro et al. 2017) using the Norway spruce genome (*Picea abies* 1.0 assembly) (Nystedt et al. 2013) downloaded from http://congenie.org/ as a reference. Differential expression (DE) analysis was performed using DESeq2 (version 1.18.1) using default parameters, which includes shrinkage estimation of fold changes (Love et al. 2014). The samples from each of the dose rate levels were compared with the control samples. Genes were classified as differentially expressed genes (DEGs) if the False Discovery Rate (Benjamini & Hochberg correction) adjusted P-values were < 0.05.

Functional annotations were downloaded from ftp://plantgenie.org/Data/ConGenIE/Picea_abies/v1.0/Annotation/. From this site we obtained gene ontology (GO) annotations from the file Pabies1.0-gene_go_concat and the best matching *Arabidopsis thaliana* orthologs to Norway spruce genes from the file piabi_artha_BEST_DIAMOND (under BEST DIAMOND under Best BLAST at ftp://plantgenie.org/Data/ConGenIE/Picea_abies/v1.0/Annotation/). Enrichment of GO terms in sets of DEGs was performed using topGO (version 2.34.0), and enrichment of KEGG (Kyoto Encyclopedia of Genes and Genomes) pathways was performed using the kegga function from the limma package (version 3.38.2). The *Arabidopsis* orthologs were used to associate the Norway spruce genes with KEGG pathways. In addition, since only 20% of the genes in Norway spruce currently have a GO annotation, gene function assignment of selected DEG were manually curated based on relevant literature and GO terms from the RNAseq analyses.

Results

Phenotype, growth, histology and DNA damage in response to gamma irradiation

After 48 h of exposure to gamma radiation there was no significant difference in shoot length between seedlings exposed to 1, 10 and 40 mGy h^{-1} and the unexposed control (Figure 1a). In comparison, at 100 and 290 mGy h^{-1} shoot length was significantly reduced, but no significant difference in shoot length was detected between these two dose rates. Root length did not exhibit any significant difference among the different dose rates and the unexposed control (Figure 1b). Inspection of shoot apical meristems by light microscopy did not reveal any visible difference between any of the dose rates and the control (Figure 1c). Assessment of DNA damage by the COMET assay revealed a dose-response relationship with generally increasing DNA damage with increasing dose rate (Figure 1d). Significantly increased DNA damage was observed even at 1 mGy h^{-1} and 10 mGy h^{-1} with 6% and 8% tail DNA, respectively. At 40, 100 and 290 mGy h^{-1} 10, 14 and 24 % tail DNA were observed, and these differed significantly from each other, the lower dose rates and the control, which had 1% tail DNA.

At day 59 post-irradiation there was no significant difference in cumulative growth between the different gamma dose rates (Figure 2a, Table S1). However, the shoot diameter and number of

needles were significantly reduced at 100 and 290 mGy h^{-1} compared to control, 1, 10 and 40 mGy h^{-1} (Figure 2b-c, Table S1; day 58). Analyses of DNA damage at day 77 post-irradiation showed significantly increased DNA damage for all gamma dose rates compared to the unexposed control plants but with generally lower levels than at the end of the gamma irradiation (Figure 2d). At this time point growth appeared rather normalized for all dose rates (Figure 2e).

DEGs in gamma-exposed seedlings

RNAseq analyses of the Norway spruce seedlings showed a total of 66 069 predicted genes were expressed, of which 37542 (57%) had an *A. thaliana* homolog. Of the total expressed genes, we found 5326 individual differentially expressed genes (DEGs) (8.1%) between any level of gamma exposure (1, 10, 40, 100 mGy h^{-1}) and the unexposed control plants, with 587 genes differentially expressed at multiple dose rates (Figure 3a). Of the DEGs, 3894 (73%) had an *A. thaliana* ortholog and 1890 (35%) had a GO annotation. There were 38 DEGs in 1 mGy h^{-1} (18 ↑, 20 ↓), 43 DEGs in 10 mGy h^{-1} (35 ↑, 8 ↓), 822 DEGs in 40 mGy h^{-1} (509 ↑, 313 ↓), and 5047 DEGs 100 mGy h^{-1} (2332 ↑, 2715 ↓) (Figure 3a). Thus, the number of DEGS in 100 mGy h^{-1} were 133 and 117-fold higher than in 1 and 10 mGy h^{-1}, respectively, but only 6-fold higher than in 40 mGy h^{-1}. The 40 mGy h^{-1} had 19 and 22-fold higher number of DEGs than 1 and 10 mGy h^{-1}, respectively. Differential expression was highly correlated between the different dose rates, especially for the higher dose rate (DEG fold change correlation was 0.86 between 40 mGy h^{-1} and 100 mGy h^{-1}) (Figure 3b). Multiple DEGs found at a given dose rate were also differentially expressed at a higher dose rate, as seen in the overlap of DEGs (Figure 3c).

GO and KEGG ortholog enrichment analyses

GO term enrichment analyses of biological processes revealed very few GO terms enriched at 10 mGy h^{-1} and these stress- and developmental-related GO terms commonly had only one single upregulated DEG in each, which was in most cases not affected at higher dose rates (Figure 4). The higher gamma dose rates resulted in regulatory changes in a wide range of GO terms, particularly terms related to energy metabolism, lipid biosynthesis, protein degradation and misfolding, stress-responses and defence-related secondary metabolism, signalling, cell cycle and

protein synthesis (translation), DNA-repair, epigenetics, auxin transport, photosynthesis and light-responses (Figure 4).

Significantly enriched GO terms related to energy metabolism were observed for upregulated DEGs at 40 mGy h^{-1}; the tricarboxylic acid (TCA,) cycle (also denoted Krebs cycle), mitochondrial electron transport and the glyoxylate cycle (Figure 4). Of these, the TCA cycle and glyoxylate cycle GO terms were also highly enriched at 100 mGy h^{-1}. At this dose rate other energy-metabolism related catabolic GO terms were also enriched in upregulated DEGs, i.e. glycolytic processes, gluconeogenesis, cellular respiration and fatty acid beta-oxidation, whereas the anabolic pentose phosphate pathway was enriched in downregulated DEGs at this dose rate (Figure 4).

GO terms associated with lipid biosynthesis were enriched in downregulated DEGs at the two highest dose rates (40 mGy h^{-1} and 100 mGy h^{-1}), i.e. very long chain fatty acid metabolic- and biosynthetic-process, fatty acid biosynthetic process, suberin biosynthetic process, cuticle development (Figure 4).

The GO term response to misfolded protein was enriched in upregulated DEGs at both 40 and 100 mGy h^{-1} and protein degradation related GO terms at 100 mGy h^{-1} only, i.e. proteasome-mediated ubiquitin-dependent and ubiquitin-dependent protein catabolic process as well as proteasome core complex assembly (Figure 4).

A range of GO terms associated with stress responses and secondary metabolism (defence) was affected. Of these, response to gamma radiation was enriched in upregulated DEGs at both 40 and 100 mGy h^{-1}, and hyperosmotic response, response to temperature stimulus and regulation of flavonoid biosynthetic processes at 100 mGy h^{-1} only (Figure 4). Downregulated DEGs were enriched at 40 mGy h^{-1} only for terpenoid biosynthetic process, cellular ion homeostasis and response to water, an anthocyanin-accumulation-related GO term and response to ozone at both 40 and 100 mGy h^{-1}, and isopentenyl diphosphate biosynthetic process at 100 mGy h^{-1} only (Figure 4).

Signalling-related GO terms were affected, with guanosine-containing compound metabolic process and GTPase-mediated signal transduction being enriched in upregulated DEGs, respectively, at 40 mGy h^{-1} and both 40 and 100 mGy h^{-1}, whereas regulation of protein dephosphorylation was enriched in downregulated DEGs at 100 mGy h^{-1} only (Figure 4).

GO terms related to the cell cycle and protein synthesis, i.e. anaphase, regulation of G2/M transition of mitotic cell cycle, DNA replication initiation, regulation of DNA replication, DNA

endoreduplication and translation, were enriched in upregulated DEGs at 40 mGy h^{-1} only, while the GO terms cell proliferation and DNA replication showed enrichment in upregulated DEGs at both 40 and 100 mGy h^{-1} (Figure 4). Genes within purine ribonucleotide metabolic process and regulation of nucleobase-containing process were enriched in upregulated DEGs at 100 mGy h^{-1} only (Figure 4).

DNA repair was enriched in upregulated DEGs with the GO term double strand break repair via HR enriched at both 40 and 100 mGy h^{-1} (Figure 4).

Epigenetics-related GO terms were affected, including DNA methylation, histone H3K9 methylation and RNA methylation that were enriched in upregulated DEGs at 40 mGy h^{-1} only, and ncRNA metabolic process that was enriched in downregulated DEGs at 100 mGy h^{-1} only (Figure 4).

GO terms associated with basipetal and acropetal transport and efflux of the plant hormone auxin were enriched in downregulated DEGs at 40 mGy h^{-1} (Figure 4). Starch catabolic process was enriched in downregulated DEGs at both 40 and 100 mGy h^{-1}, but other photosynthesis- and light response-related genes were enriched in downregulated DEGs at 100 mGy h^{-1} only and included genes within the GO terms chlorophyll and carotenoid biosynthesis, thylakoid membrane organization, photosystem II assembly, photosynthetic electron transport, stomatal complex morphogenesis, chloroplast relocation and response to far red and red light (Figure 4).

KEGG pathway enrichment analysis was also performed to provide additional information about the pathways affected by gamma radiation (Figure 5). This revealed that energy metabolism-related pathways were enriched in upregulated DEGs; i.e. the pentose phosphate pathway at 10 mGy h^{-1} only, the glycolysis/gluconeogenesis at 10 and 40 mGy h^{-1}, the TCA cycle, glyoxylate and dicarboxylate metabolism, pyruvate metabolism and carbon metabolism at 40 and 100 mGy h^{-1}, and fatty acid degradation and fructose and mannose metabolism at 100 mGy h^{-1} only (Figure 5).

Lipid biosynthesis/metabolism was generally enriched in downregulated DEGs, with sphingolipid metabolism and glycosphingolipid metabolism at 40 mGy h^{-1} only, and fatty acid elongation, glycerolipid metabolism as well as cutin, suberin and wax biosynthesis at both 40 and 100 mGy h^{-1} (Figure 5). Furthermore, nitrogen metabolism was downregulated at 100 mGy h^{-1}.

Protein-degradation through the proteasome pathway was enriched for upregulated DEGs at 40 and 100 mGy h^{-1}, and general degradation pathways, i.e. the phagosome and the SNARE interactions in vesicular transport pathway, at 100 mGy h^{-1} only (Figure 5).

Stress-related secondary metabolism and signalling was affected; flavonoid biosynthesis as well as stilbenoid, diarylheptanoid and gingerol metabolism were enriched in upregulated DEGs at 100 mGy h^{-1} only, while terpenoid backbone biosynthesis was enriched in downregulated DEGs at 40 and 100 mGy h^{-1} and flavone and flavonol biosynthesis and well as the MAPK signalling pathway at 100 mGy h^{-1} only (Figure 5).

DNA repair genes involved in base excision repair were enriched in upregulated DEGs at 40 mGy h^{-1} only, whereas mismatch repair, nucleotide excision repair, non-homologous end joining and homologous recombination were at both 40 and 100 mGy h^{-1} (Figure 5).

Of pathways related to cell division, transcription and protein synthesis; ribosome and biosynthesis of amino acids were enriched in upregulated DEGs at 40 mGy h^{-1} only, DNA replication at 40 and 100 mGy h^{-1}, and RNA transport and protein processing in endoplasmatic reticulum at 100 mGy h^{-1} only (Figure 5).

Plant hormone signal transduction as well as photosynthesis-related pathways; i.e. porphyrin and chlorophyll metabolism, photosynthesis, photosynthesis-antenna proteins and carotenoid biosynthesis were enriched in downregulated DEGs at 100 mGy h^{-1} only (Figure 5). However, carbon fixation in photosynthetic organism was enriched in upregulated DEGs at 40 mGy h^{-1} and in both up- and downregulated DEGs at 100 mGy h^{-1}.

Inspection of expression of genes in specific categories in gamma-irradiated seedlings

Since only 20% of the genes in Norway spruce has been ascribed a GO term, the entire gene expression data set was also manually inspected with respect to specific genes selected on basis of the observed phenotype and previous knowledge in addition to gene categories identified in the GO term and KEGG pathway analyses (Table 2, 3, 4, Table S2, entire data set in Table S3).

The expression levels of genes of different DNA repair pathways were mostly upregulated in response to gamma irradiation but there were also some examples of down-regulated ones (Table 2). Genes involved in nucleotide excision repair (NER) were upregulated; The *GAMMA RESPONSE GENE 1* (*GR1*), which is also involved in homologous recombination (HR), was

highly induced at 10, 40 and 100 mGy h^{-1} and *RAD4* was upregulated at 100 mGy h^{-1}. Base excision repair (BER) showed upregulated transcript levels of *POLY(ADP-RIBOSE) POLYMERASE 1* (*PARP1*) at 100 mGy h^{-1} and *POLY(ADP-RIBOSE) POLYMERASE 2* (*PARP2*) and *FLAP ENDONUCLEASE I* (*FEN1*) at 40 and 100 mGy h^{-1}. DNA mismatch repair (MMR) genes were upregulated; *MUTL HOMOLOG 1 and 3* (*MLH1*, *MLH3*), *MUTS HOMOLOG 2* and 3 (*MSH2, MSH3)* at 100 mGy h^{-1} and *MSH 7* at 40 and 100 mGy h^{-1}. A *PROLIFERATING CELLULAR NUCELAR ANTIGEN* (*PCNA*) gene involved in NER, BER and MMR was upregulated at 40 and 100 mGy h^{-1}, but another *PCNA* ortholog was downregulated at 100 mGy h^{-1}. The *POLYMERASE DELTA 4* (*POLD4*) gene involved in NER, BER, MMR and HR was upregulated at 40 and 100 mGy h^{-1}. Key genes in HR such as *XRCC2* and *XRCC3* were upregulated at 100 mGy h^{-1} and *MRE11* at 40 and 100 mGy h^{-1} (the two latter also involved in MMR and non-homologous end-joining (NHEJ)). NHEJ genes in general showed only upregulation with *ATP-DEPENDENT DNA HELICASE 2 SUBUNIT KU80* (*KU80)* and *DNA REPAIR AND MEIOSIS PROTEIN 11* (*MRE11*) being inducted at 40 and 100 mGy h^{-1} and *DNA LIGASE 4* (*LIG4*) at 100 mGy h^{-1} only.

Of the cell-division controlling genes, the cyclin genes *CYCA1;1*, *CYCA2;2*, *CYCD1;1*, *CYCB1;1*, *CYCB1;2* and *CYCU2-1* were downregulated at 100 mGy h^{-1}, whereas *CDKB2;2* and *CYCB2;3* genes were upregulated at 40 mGy h^{-1} (Table 3). The *WEE1* gene, which encodes a protein involved in DNA-repair-related inhibition of cell division (De Schutter et al. 2007) was upregulated at 40 and 100 mGy h^{-1}, and *SOG1* at 100 mGy h^{-1} only (Table 3).

At the highest dose rate, up- and downregulation were observed for genes related to ROS scavenging enzymes (Table 4). At 100 mGy h^{-1} four peroxidase (*PX*) genes were significantly up-regulated while 11 were downregulated (one also at 40 mGy h^{-1}). Six glutathione S-transferase genes were upregulated at 100 mGy h^{-1} only, two at 40 and 100 mGy h^{-1} and one at 10, 40 and 100 mGy h^{-1}, whereas one was down-regulated at 100 mGy h^{-1}. Two ascorbate peroxidase (*APX*) genes, which encode central enzymes of the ascorbate-glutathione (ASC-GSH) cycle, were upregulated at 100 mGy h^{-1} (Table 4).

Also, genes related to biosynthesis of phenolics like flavonoids and lignin were affected (Table S2a). Two flavonoid biosynthesis *CHALCONE SYNTHASE* (*CHS*) orthologs were upregulated at 100 mGy h^{-1}, but another was downregulated. Orthologs of lignin biosynthesis genes were DEGs at 100 mGy h^{-1}; *CINNAMYL ALCOHOL DEHYDROGENASE 9* (*CAD9*), two

LACCASE (*LAC11*) (one also at 40 mGy h^{-1}), *LAC5* and *PHENYL ALANINE AMONIA LYASE 4* (*PAL4*) were downregulated while another *LAC5* and *LAC12* were upregulated. Several other *LAC* gene orthologs (*LAC 2, 3, 6*), showed no significant difference (Table S3).

Proteasome-related genes and genes associated with ubiquitin labelling of proteins for degradation and the unfolded protein response (UPR) were upregulated particularly at 100 mGy $h^{-1,}$ but some also at 40 mGy h^{-1}, and a few of the latter type also at 10 mGy h^{-1} (Table S2b-c). However, there were also some examples of such genes showing downregulation at 100 mGy h^{-1} and one gene at 40 mGy h^{-1} (Table S2b-c). Also, genes encoding senescence and cell death-related genes were affected at 100 mGy h^{-1}, like the senescence-related *P85* gene and two *ACELLERATED GELL DEATH 11* (*ACD11*) genes that were upregulated (one also at 40 mGy h^{-1}), and another senescence-related gene, *ARABIDOPSIS A-FIFTEEN* (*AAF*), that was downregulated (Table S2d).

Furthermore, a wide range of histone- and epigenetics-related genes were DEGs (Table S2e). Histone biosynthesis genes that were upregulated at 100 mGy h^{-1} included *HISTONE H2A, HISTONE H4* (one ortholog was downregulated at 100 mGy h^{-1}) and a putative *HISTONE H2A.7* (*HTA6*). On the other hand, an *HTA7* ortholog encoding H2A was downregulated at 100 mGy^{-1} and a H2A3-encoding gene *HTA2, H1.2* and *H2B.* Some genes involved in histone modifications resulting in transcriptional repression, were downregulated at 100 mGy h^{-1}, like histone-binding protein *MSI1* and the *HISTONE METHYL TRANSFERASE* gene *EFS* (H3-K4 and H3-K36 specific methylation), while *HISTONE DEACETYLASE 6* (*HDA6*) showed upregulation at 100 mGy h^{-1}. However, there were also some examples of *HISTONE METHYL TRANSFERASE* genes, such as *SUVH4, SUVR4 and SUVR5* that were upregulated at this dose rate.

A substantial number of genes related to growth-promoting plant hormones were DEGs (Table S2f). A multitude of auxin response genes were down-regulated at 40 mGy h^{-1} and even more commonly so at 100 mGy h^{-1}, like *AUXIN RESPONSE FACTOR 6* and *19 (ARF6, ARF19*; 4 orthologs of each), several *INDOLE 3-ACETIC ACID INDUCIBLE* genes (*IAA9, IAA14, IAA16, IAA26, IAA27*) and *SMALL AUXIN-UPREGULATED 10* (*SAUR 10*). Several genes involved in auxin transport were also downregulated at 100 mGy h^{-1}, like *AUXIN RESISTANT 1* (*AUX1*) gene encoding an auxin influx transporter and the auxin efflux regulators *PIN-FORMED 3* and *4* (*PIN3, PIN4*). Only a couple of *SAUR* orthologs were upregulated at 100 mGy h^{-1}. Also, some gibberellin-regulated genes were downregulated in response to 100 mGy h^{-1}, like *GAST 1 PROTEIN HOMOLOG 5* and *11* (*GASA5, GASA11*). At this dose rate the brassinosteroid biosynthesis gene

CYTOCHROME P450 90A1 (*CYP90A1*) gene was significantly downregulated and one ortholog of the brassinolide inactivation gene (*CYP734A1*) was upregulated whereas another was downregulated. Furthermore, several genes related to the cell division-stimulating hormone cytokinin were affected by gamma irradiation. Downregulation at 100 mGy h^{-1} only was observed for the cytokinin biosynthesis gene (*CYP735A2*), two orthologs each of the cytokinin activation gene *LONELY GUY 8* (*LOG8*, involved in hydrolysis of N-glucosyl cytokinin conjugates) and the cytokinin receptor gene *ARABIDOPSIS HISTIDINE KINASE 3*; (*AHK3).* The cytokinin-inactivation genes *CYTOKININ OXIDASE/ DEHYDROGENASE 1* (*CKK1*) and *CYTOKININ OXIDASE 7* (*CKX7*), were also downregulated at this dose rate, and another *CYP735A2* homolog was upregulated.

Genes related to plant hormones involved in growth inhibition and defence were also affected by the gamma exposure, but only at 100 mGy h^{-1} (Table S2f). The *CYP707A3* gene involved in abscisic acid (ABA) catabolism was downregulated and the ABA receptor gene *PYR 1-LIKE 4* (*PYL4*) upregulated. Also, a number of ethylene-response related genes responsible for senescence of vegetative tissues and defence signalling were down-regulated, including the ethylene-responsive transcription factor/signalling genes *ERF016* (2 orthologs), *ERF022*, *ERF039*, *AINTEGUMENTA (ANT), RELATED TO AP2 11* (*RAP2-11*), *TARGET OF EARLY ACTIVATION TAGGED 3* (*TOE3*) and *ETHYLENE INSENSITIVE 3-LIKE 1 (EIL1).* The jasmonate regulated gene *JRG21* was downregulated at 100 mGy h^{-1}, while salicylic acid-related genes did not show any significant difference compared to the untreated control (Table S3).

Furthermore, multiple photosynthesis-related genes were downregulated at 100 mGy h^{-1} (Table S1g), including genes related to the photosystem I and II reaction centre, the oxygen-evolving complex, RuBisCo and other components involved in electron transport. Specific embryogenesis-related genes showed up- or downregulation mostly at 100 mGy h^{-1} including, some genes encoding LATE EMBRYOGENSIS RELATED (LEA) proteins of which one was also upregulated at 40 mGy h^{-1} (Table S2h).

Discussion

In the present study, Norway spruce seedlings exposed to gamma radiation for 48 h were assessed for phenotypic and genotoxic effects (1, 10, 40, 100 and 290 mGy h^{-1}), combined with an RNA

seq analysis (1, 10, 40 and 100 mGy h^{-1}) to identify molecular mechanisms related to adverse outcome. Assessment of growth showed no significant difference in root length but a significant reduction in shoot length was evident at 100 and 290 mGy h^{-1} even at such short-term gamma exposure (Figure 1a-b). In a previous study we have shown that growth inhibition of Norway spruce increased with increasing dose rate at ≥ 40 mGy h^{-1} when irradiation was provided for 144 h (Blagojevic et al. 2019a). Furthermore, in the former study late effects (post-irradiation) developed progressively at dose rates ≥ 40 mGy h^{-1} and eventually caused mortality and growth-inhibition post-irradiation (Blagojevic et al. 2019a). Growth inhibition after 48 h of gamma exposure (Fig. 1a) and reduced shoot elongation and number of needles post-irradiation (Figure 2b-c) only at 100 and 290 mGy h^{-1} in the current study illustrate that adverse effects on growth also depend on the total dose. Previous field studies of Scots pine showed abnormal needle length or increased frequency of necrotic needles in response to ionizing radiation (Gotsova et al 1991, Makarenko et al 2016).

Gamma radiation is a potent genotoxic agent (Caplin & Willey 2018). The COMET analysis showed significant DNA damage even at 1, 10 and 40 mGy h^{-1} when growth inhibition was not observed (Figure 1d). Like previously shown for 144 h gamma exposure, the Norway spruce plants tolerate some DNA damage without necessarily showing any signs of growth-inhibition or visible cellular damage (Blagojevic et al. 2019a; Blagojevic et al. 2019b). Although inhibition of shoot growth was only observed at 100 and 290 mGy h^{-1} after the 48 h-gamma exposure, the degree of DNA damage at the different gamma dose rates was relatively similar to the previous 144 h-study. In the current study histological analysis showed apparently normal cells and meristems at the end of the 48 h-irradiation even at the dose rates inhibiting growth (Figure 1c). However, although the 48-h irradiation did not cause visible cellular damage or mortality, the current study demonstrates the existence of persistent DNA damage at ≥1 mGy h^{-1} even 77 days after gamma radiation (Figure 2d). This implies long-term effects from short-term exposures.

Comparison of the genes that were differentially expressed in each of the four gamma treatments analysed (1, 10, 40 and 100 mGy h^{-1}) showed that only five genes were upregulated in all four gamma treatments and none downregulated (Figure 3c). These genes are involved in response to gamma radiation, endoreduplication, DNA repair and photorespiration. Given that there were few DEGs at 1 (38) and 10 (43) mGy h^{-1} (Fig. 3a), it is not surprising that there was so little overlap between all four dose rates. However, large number of DEGs were shared only by 40

mGy h^{-1} and 100 mGy h^{-1}; 326 specific genes were upregulated and 209 downregulated at these dose rates only (Figure 3c).

Consistent with growth-inhibition after 48 h exposure to a gamma dose rate of 100 mGy h^{-1}, a multitude of genes related to biosynthesis/activation of growth-promoting plant hormones (cytokinin, brassinosteroid), hormone signalling/response (auxin, GA, cytokinin) and transport (auxin) were downregulated and hormone inactivation (brassinosteroid, cytokinin) genes upregulated (Figure 4, 5, Table S2f). This is consistent with previous studies showing downregulation of growth-stimulating hormones under stressful conditions (Verma et al. 2016). Among hormones known to be involved in stress responses, senescence and defence against pathogens and pests (Verma et al. 2016), jasmonic acid and ethylene response/signalling genes were downregulated whereas no genes related to another such hormone; salicylic acid were differentially expressed. In contrast, the levels and response to the plant hormone ABA, which is known to increase in response to different stressors (Verma et al. 2016), may probably have been increased since ABA catabolism genes and signalling genes were upregulated (Table S2f).

Also, photosynthesis-related genes of the light energy harvesting reactions were massively downregulated (Figure 4, 5, Table S2g). Decrease in photosynthetic efficiency in response to gamma irradiation was previously observed in the green algae *Chlamydomonas reinhardtii* (Gomes et al. 2016). On the other hand, chronic gamma exposure of *Lemna minor* (7 days exposure from a ^{137}Cs gamma source; dose rates from 53 to 423 mGy h^{-1}) resulted in upregulation of photosynthesis-related genes (cytochrome b6, RuBisCo, photosystem II and electron transport chain) (Van Hoeck et al. 2017). *A. thaliana* also showed upregulation of photosynthesis-related genes after chronic exposure to about 2 mGy h^{-1} for 21 days and after 7 days of exposure to gamma dose rates up to 350 mGy h^{-1} (Kovalchuk et al. 2007; Vanhoudt et al. 2014). In contrast, exposure of *A. thaliana* to 4 h at 50 Gy h^{-1} showed decreased photosynthesis activity (Kim et al. 2011). This illustrates that the photosynthetic apparatus responds differently to different irradiation dose rates/doses and that the response differs among plant species, possibly due to differences in antioxidant protection or differences in repair of photosynthesis-related components like the D1 protein of photosystem II.

A common consequence of gamma radiation is DNA damage, and two important pathways in DNA repair are ATM and ATR, which are mainly activated by double-strand breaks (DSB) and single-strand breaks (SSB), respectively. Previous studies of *A. thaliana* have shown high

sensitivity of *atm* and *atr* mutants to agents (ionizing radiation or methyl methane sulphonate) inducing DNA damage (Culligan et al. 2004; Culligan et al. 2006; Garcia et al. 2003). Also, *Lemna minor*, exposed to gamma dose rates of 53-423 mGy h^{-1}, showed upregulation of ATM-related genes (Van Hoeck et al. 2017). By contrast, our results did not show any induction of ATM and ATR (Table 2, Table S2).

SOG1 is required for multiple plant responses to DNA damage, including transcriptional response, suppression of genes regulating the cell cycle progression, and death of stem cells (Preuss & Britt 2003; Yoshiyama et al. 2009; Yoshiyama et al. 2013a), A *SOG1* gene was upregulated at 100 mGy h^{-1} in our study (Table 3). Furthermore, in the presence of DNA damage, cell cycle checkpoints occur at the G1/S, (preventing replication), and G2/M (preventing segregation of chromosomes) transitions. The gene encoding *CYCD3;1* which mediates the G1-S transition, was shown to be upregulated after UV-B stress in *A. thaliana* (Ali et al. 2015), but showed no induction in our study (Table 3). In *A. thaliana* the transcript of *CYCB1;1* is rapidly upregulated in response to ionizing radiation (Culligan et al. 2006). An earlier study showed upregulation of *CYCB1;2* in Scots pine and *A. thaliana* exposed 144 h to gamma radiation, but not in Norway spruce in spite of similar DNA damage levels (Blagojevic et al. 2019a). However, in this study both *CYCB1;1* and *CYCB1;2* showed downregulation at 100 mGy h^{-1}. Furthermore, *CDKB2;2* and *CYCB2;3* showed upregulation but only at 40 mGy h^{-1}. Similar to in *A. thaliana* (De Schutter et al. 2007), the *WEE1* gene, which encodes a protein involved in the DNA replication checkpoint, was upregulated in our study at 40 and 100 mGy h^{-1}. Taken together, in spite of upregulation of specific cell cycle genes at 40 mGy h^{-1} (Table 2, Figure 4 and 5), these results indicate overall downregulation of cell division at the highest dose rate, consistent with the inhibition of shoot growth observed at 100 mGy h^{-1}.

In *A. thaliana* the DNA repair mechanism employing HR involves the RAD51 like proteins RAD51B, RAD51C, RAD51D, XRCC2 and XRCC3 and the regulatory proteins BRCA1 and BRCA2 (Bleuyard et al. 2005; Culligan et al. 2006; Lafarge & Montané 2003; McIlwraith et al. 2000; Rieger & Chu 2004). By contrast, our previous qPCR-based analyses showed no induction of *RAD51* in Norway spruce (0-400 mGy h^{-1}, (Blagojevic et al. 2019a)). In this study, *RAD51B* and *BRCA2* were also not significantly different from the control (Table S2). However, *XRCC2* and *XRCC3* was upregulated at 100 mGy h^{-1}, while *BRCA1* was up- and downregulated at 40 and 100 mGy h^{-1} (Table 2).

Furthermore, in NHEJ the initial recognition of the double strand break, may be mediated by a complex of *Ku70* and *Ku80* (Bray & West 2005; Friesner & Britt 2003). Ku proteins have additional roles in eukaryotes in maintaining telomeres, providing a link between DNA-damage-related DSBs and naturally occurring chromosome ends (Gallego et al. 2003; Riha et al. 2002). The *Ku70* gene was not affected by gamma radiation, but *Ku80* was up-regulated at 100 mGy h^{-1} (Table 2, Table S2). In contrast, Van Hoeck et al 2017 showed downregulation of *Ku70* and *Ku80* in response to gamma radiation in *Lemna minor*. Moreover, in NHEJ, the DNA ends may then be processed (possibly by the MRN complex) to make them suitable substrates for DNA ligase. Ligation is catalysed by a complex of DNA ligase enzymes (West et al. 2000). In this study, *LIG4* was induced at 100 mGy h^{-1} (Table 2), while *XRCC4* did not exhibit any induction (Table S2). Interestingly, we found protein gamma response 1 (*GR1*) to be highly up regulated at 10, 40 and 100 mGy h^{-1} (Table 2).

MSH proteins play a role in DNA repair, recognising mismatches in replicating DNA to prevent the establishment of mutations in the genome (Bray & West 2005; de Wind & Hays 2001). Among genes encoding MSH proteins, *MSH7*, which is unique to plants (Tam et al. 2009), showed high upregulation at 40 and 100 mGy h^{-1} (Table 2), together with *MSH2* and *MSH3* which were upregulated at 100 mGy h^{-1} only (Table 2). Also *MRE11*, a subunit of the MRN complex, involved in recognising damage and generating single-stranded DNA (Daoudal-Cotterell et al. 2002), showed high upregulation at 40 and 100 mGy h^{-1} (Table 2). Other genes such as those encoding the PARP1 and PARP2 proteins, which recognise DNA damage (Doucet-Chabeaud et al. 2001; Lepiniec et al. 1995) and RPA1A, which stabilises ssDNA (Chang et al. 2009; Ishibashi et al. 2005), were upregulated; *PARP1* at 40 mGy h^{-1} and *PARP2* and *RPA1A* at both 40 and 100 mGy h^{-1} (Table 2). Collectively, the data on DNA repair genes, including the GO term enrichment and KEGG analyses (Figure 4 and 5), demonstrate substantial mobilisation of DNA repair at 40 and 100 mGy h^{-1} but not at lower dose rates.

A. thaliana plants exposed to ionizing radiation (20-day-old plants) showed increased expression of the epigenetic regulators *MET1*, *CMT3* and *SUVH5* (Sidler et al. 2015). In this study, the DNA methyl transferase gene *CMT3* was upregulated at 40 mGy h^{-1} while the histone-lysine -methyltransferase gene *SUVH5* was not significantly different from the control but *SUVH4* was upregulated at 100 mGy h^{-1} (Table S2e, Table S3). Another study showed DNA hyper-methylation

in *P. sylvestris* trees exposed to high doses post Chernobyl, a mechanism suggested to stabilise the genome (Kovalchuk et al. 2003).

Specific antioxidant genes were induced in response to the gamma irradiation. However, we did not find any *SOD* gene being induced after radiation, but different *PX* genes were either up- or downregulated (Table 4, Table S3). In contrast, a comparative study employing qPCR analysis showed upregulation of *SOD* in Norway spruce exposed for 144 h to 100 mGy h^{-1}, but no induction of *PX* (Blagojevic et al 2019a). This study showed upregulation of different glutathione S-transferase family genes from 10-100 mGy h^{-1}. (Vanhoudt et al. 2014) measured ROS-scavenging enzymes in *A. thaliana* and found increased activities of SOD and APX but decreased activities of catalase (CAT), syringaldazine peroxidase (SPX) and guaiacol peroxidase (GPX) in roots, while leaves showed increased GPX capacity. In gamma-radiation exposed *Lemna mino*r upregulation was found for CAT, SOD, APX (also denoted APOD) and other peroxidases (PX), suggesting oxidative stress (Van Hoeck et al. 2017). In our study two *APOD* genes, which encodes a central enzyme of the ascorbate-glutathione (ASC-GSH) cycle involved in the scavenging of ROS in plants (Van Hoeck et al. 2017), were upregulated at 100 mGy h^{-1} (Table 4). Also, flavonoid metabolism which includes secondary metabolites with multiple phenolic groups which have ROS scavenging activities, showed either up- or downregulation of different *CHS* orthologs and *PAL4* downregulation at 100 mGy h^{-1} (Table S2a).

Protein degradation through the ubiquitin–26S proteasome pathway has been associated with hormone signalling, photomorphogenesis, and stress-triggered responses in plants (Rodrigues et al. 2014). Consistent with this, massive upregulation of genes related to the proteasome, ubiquitin-labelling of proteins for degradation and the UPR response were observed at 40 and 100 mGy h^{-1} in our study (Figure 4, 5, Table S2b-c). Several plant species, including *A. thaliana*, exposed to different abiotic stressors such as drought, wounding, cold, salt, UV, and heat have shown activation of MAPK signalling cascades (Sinha et al. 2011), but in this study MAPK signalling pathways were downregulated at 100 mGy h^{-1} (Figure 5). In this respect and on a general basis, it could be noted that differences in expression of specific genes between this study and other studies may be due to different exposure conditions, different radiation levels and growth conditions in addition to possible differences between species and developmental stages.

Conclusions

This study shows that a profound transcriptomic change occurs in Norway spruce seedlings exposed to gamma radiation dose rates of 40 and 100 mGy h^{-1} for 48 h, while only surprisingly few genes were affected at lower dose rates (1 and 10 mGy h^{-1}). A substantial number of DEGs at 40 and 100 mGy h^{-1} were consistent with the observed adverse effects. The high levels of DNA damage and reduced shoot growth were associated with overall increased expression of energy metabolism and plant defence-related genes, including DNA repair, cell cycle arrest, synthesis of antioxidants and flavonoids as well as reduced expression of genes involved in growth hormone biosynthesis, signalling and transport, lipid biosynthesis, nitrogen metabolism and photosynthesis.

Acknowledgements The Norwegian Research Council through its Centre of Excellence funding scheme (Grant 223268/F50) and the Norwegian University of Life Sciences (NMBU) are acknowledged for financial support. Sincere thanks to Marit Siira for technical assistance in plant growing, Dr. Ole Christian Lind (NMBU) and Dr. Elisabeth L Hansen (Norwegian Radiation and Nuclear Safety authority) for assistance in the dosimetry work, and the Norwegian Institute of Public health for providing advices and the scoring facility for the COMET assay.

References

Ali, H., Ghori, Z., Sheikh, S. & Gul, A. (2015). Effects of gamma radiation on crop production. In Hakeem, K. R. (ed.) *Crop production and global environmental issues*, pp. 27-78. Cham: Springer International Publishing.

Alothman, M., Bhat, R. & Karim, A. A. (2009). Effects of radiation processing on phytochemicals and antioxidants in plant produce. *Trends in Food Science & Technology*, 20 (5): 201-212.

Averbeck, D., Salomaa, S., Bouffler, S., Ottolenghi, A., Smyth, V. & Sabatier, L. (2018). Progress in low dose health risk research: Novel effects and new concepts in low dose radiobiology. *Mutation Research/Reviews in Mutation Research*, 776: 46-69.

Belli, M., Sapora, O. & Tabocchini, M. A. (2002). Molecular targets in cellular response to ionizing radiation and implications in space radiation protection. *J Radiat Res*, 43 Suppl: 13-9.

Blagojevic, D., Lee, Y., Brede, D., Lind, O. C., Salbu, B., Solhaug, K. A., Nybakken, L. & Olsen, J. (2019a). Comparative toxicity assessment of ionizing radiation in Scots pine, Norway spruce and *Arabidopsis thaliana*. *Planta*.

Blagojevic, D., Lee, Y., Xie, L., Brede, D. A., Nybakken, L., Lind, O. C., Tollefsen, K. E., Salbu, B., Solhaug, K. A. & Olsen, J. E. (2019b). No evidence of a protective or cumulative negative effect of UV-B on growth inhibition induced by gamma radiation in Scots pine (*Pinus sylvestris*) seedlings. *Photochemical & Photobiological Sciences*, 18 (8): 1945-1962.

Bleuyard, J.-Y., Gallego, M. E., Savigny, F. & White, C. I. (2005). Differing requirements for the *Arabidopsis* Rad51 paralogs in meiosis and DNA repair. *The Plant Journal*, 41 (4): 533-545.

Bray, C. M. & West, C. E. (2005). DNA repair mechanisms in plants: crucial sensors and effectors for the maintenance of genome integrity. *New Phytologist*, 168 (3): 511-528.

Britt, A. (2002). *Repair of damaged bases*. American Society of Plant Biologists: American Society of Plant Biologists. 13 pp.

Caplin, N. & Willey, N. (2018). Ionizing radiation, higher plants, and radioprotection: From acute high doses to chronic low doses. *Frontiers in Plant Science*, 9.

Chang, Y., Gong, L., Yuan, W., Li, X., Chen, G., Li, X., Zhang, Q. & Wu, C. (2009). Replication protein A (RPA1a) is required for meiotic and somatic DNA repair but is dispensable for DNA replication and homologous recombination in rice. *Plant physiology*, 151 (4): 2162-2173.

Culligan, K., Tissier, A. & Britt, A. (2004). ATR regulates a G2-phase cell-cycle checkpoint in *Arabidopsis thaliana*. *The Plant Cell*, 16 (5): 1091.

Culligan, K. M., Robertson, C. E., Foreman, J., Doerner, P. & Britt, A. B. (2006). ATR and ATM play both distinct and additive roles in response to ionizing radiation. *The Plant Journal*, 48 (6): 947-961.

Daoudal-Cotterell, S., Gallego, M. E. & White, C. I. (2002). The plant Rad50–Mre11 protein complex. *FEBS Letters*, 516 (1-3): 164-166.

De Schutter, K., Joubès, J., Cools, T., Verkest, A., Corellou, F., Babiychuk, E., Van Der Schueren, E., Beeckman, T., Kushnir, S., Inzé, D., et al. (2007). Arabidopsis WEE1 kinase controls cell cycle arrest in response to activation of the DNA integrity checkpoint. *The Plant Cell*, 19 (1): 211-225.

de Wind, N. & Hays, J. B. (2001). Mismatch repair: praying for genome stability. *Current Biology*, 11 (14): R545-R548.

Deckbar, D., Jeggo, P. A. & Lobrich, M. (2011). Understanding the limitations of radiation-induced cell cycle checkpoints. *Critical Reviews in Biochemistry and Molecular Biology*, 46 (4): 271-283.

del Cerro, M., Cogen, J. & del Cerro, C. (1980). Stevenel's Blue, an excellent stain for optical microscopical study of plastic embedded tissues. *Microsc Acta.*, 83 (2): 117-121.

Doucet-Chabeaud, G., Godon, C., Brutesco, C., de Murcia, G. & Kazmaier, M. (2001). Ionising radiation induces the expression of PARP-1 and PARP-2 genes in *Arabidopsis*. *Molecular Genetics and Genomics*, 265 (6): 954-963.

Foyer, C. H. & Noctor, G. (2003). Redox sensing and signalling associated with reactive oxygen in chloroplasts, peroxisomes and mitochondria. *Physiologia Plantarum*, 119 (3): 355-364.

Friesner, J. & Britt, A. B. (2003). Ku80- and DNA ligase IV-deficient plants are sensitive to ionizing radiation and defective in T-DNA integration. *The Plant Journal*, 34 (4): 427-440.

Gallego, M. E., Bleuyard, J. Y., Daoudal-Cotterell, S., Jallut, N. & White, C. I. (2003). Ku80 plays a role in non-homologous recombination but is not required for T-DNA integration in *Arabidopsis*. *The Plant Journal*, 35 (5): 557-565.

Garcia, V., Bruchet, H., Camescasse, D., Granier, F., Bouchez, D. & Tissier, A. (2003). AtATM is essential for meiosis and the somatic response to DNA damage in plants. *The Plant Cell*, 15 (1): 119-132.

Garnier-Laplace, J., Geras'kin, S., Della-Vedova, C., Beaugelin-Seiller, K., Hinton, T. G., Real, A. & Oudalova, A. (2013). Are radiosensitivity data derived from natural field conditions consistent with data from controlled exposures? A case study of Chernobyl wildlife chronically exposed to low dose rates. *Journal of Environmental Radioactivity*, 121: 12-21.

Geras'kin, S., Fesenko, S. & M Alexakhin, R. (2008). *Effects of non-human species irradiation after the Chernobyl NPP accident*, vol. 34. 880-97 pp.

Geraskin, S. A. & Sarapul`sev, B. I. (1995). A stochastic model of induced genome instability. 35 (4): 451-462.

Gichner, T., Patková, Z. & Kim, J. K. (2003). DNA damage measured by the comet assay in eight agronomic plants. *Biologia Plantarum*, 47 (2): 185-188.

Gill, S. S. & Tuteja, N. (2010). Reactive oxygen species and antioxidant machinery in abiotic stress tolerance in crop plants. *Plant Physiology and Biochemistry*, 48 (12): 909-930.

Gomes, T., Xie, L., Brede, D., Lind, O. C., Solhaug, K. A., Salbu, B. & Tollefsen, K. E. (2016). Sensitivity of the green algae Chlamydomonas reinhardtii to gamma radiation: Photosynthetic performance and ROS formation. *Aquatic Toxicology*, 183.

Hansen, E. L., Lind, O. C., Oughton, D. H. & Salbu, B. (2019). A framework for exposure characterization and gamma dosimetry at the NMBU FIGARO irradiation facility. *International Journal of Radiation Biology*, 95 (1): 82-89.

Hays, J. B. (2002). *Arabidopsis thaliana*, a versatile model system for study of eukaryotic genome-maintenance functions. *DNA Repair*, 1 (8): 579-600.

IAEA. (1992). Effects of ionizng radiation on plants and animals at levels implied by current radiation protection standards 88.

Ishibashi, T., Koga, A., Yamamoto, T., Uchiyama, Y., Mori, Y., Hashimoto, J., Kimura, S. & Sakaguchi, K. (2005). Two types of replication protein A in seed plants. *The FEBS Journal*, 272 (13): 3270-3281.

Kashparova, E., Levchuk, S., Morozova, V. & Kashparov, V. (2018). A dose rate causes no fluctuating asymmetry indexes changes in silver birch (*Betula pendula* (L.) Roth.) leaves and Scots pine (*Pinus sylvestris* L.) needles in the Chernobyl Exclusion Zone. *Journal of Environmental Radioactivity*: 105731.

Kim, D. S., Kim, J.-B., Goh, E. J., Kim, W.-J., Kim, S. H., Seo, Y. W., Jang, C. S. & Kang, S.-Y. (2011). Antioxidant response of *Arabidopsis* plants to gamma irradiation: Genome-wide expression profiling of the ROS scavenging and signal transduction pathways. *Journal of Plant Physiology*, 168 (16): 1960-1971.

Kim, J.-H., Kim, J. E., Lee, M. H., Lee, S. W., Cho, E. J. & Chung, B. Y. (2013). Integrated analysis of diverse transcriptomic data from Arabidopsis reveals genetic markers that reliably and reproducibly respond to ionizing radiation. *Gene*, 518 (2): 273-279.

Koppen, G., Azqueta, A., Pourrut, B., Brunborg, G., Collins, A. R. & Langie, S. A. S. (2017). The next three decades of the comet assay: a report of the 11th international comet assay workshop. *Mutagenesis*, 32 (3): 397-408.

Kovalchuk, I., Molinier, J., Yao, Y., Arkhipov, A. & Kovalchuk, O. (2007). Transcriptome analysis reveals fundamental differences in plant response to acute and chronic exposure to ionizing radiation. *Mutation Research/Fundamental and Molecular Mechanisms of Mutagenesis*, 624 (1–2): 101-113.

Kovalchuk, O., Kovalchuk, I., Titov, V., Arkhipov, A. & Hohn, B. (1999). Radiation hazard caused by the Chernobyl accident in inhabited areas of Ukraine can be monitored by transgenic plants. *Mutation Research/Genetic Toxicology and Environmental Mutagenesis*, 446 (1): 49-55.

Kovalchuk, O., Burke, P., Arkhipov, A., Kuchma, N., James, S. J., Kovalchuk, I. & Pogribny, I. (2003). Genome hypermethylation in Pinus silvestris of Chernobyl—a mechanism for radiation adaptation? *Mutation Research/Fundamental and Molecular Mechanisms of Mutagenesis*, 529 (1): 13-20.

Kozubov, M. G. & Taskaev, I. A. (2007). *[Characteristics of morphogenesis and growth processes of conifers in the Chernobyl nuclear accident zone]*, vol. 47. 204-23 pp.

Kunz, B. A., Anderson, H. J., Osmond, M. J. & Vonarx, E. J. (2005). Components of nucleotide excision repair and DNA damage tolerance in *Arabidopsis thaliana*. *Environmental and Molecular Mutagenesis*, 45 (2-3): 115-127.

Lafarge, S. & Montané, M. H. (2003). Characterization of *Arabidopsis thaliana* ortholog of the human breast cancer susceptibility gene 1: AtBRCA1, strongly induced by gamma rays. *Nucleic acids research*, 31 (4): 1148-1155.

Lee, Y., Karunakaran, C., Lahlali, R., Liu, X., Tanino, K. K. & Olsen, J. E. (2017). Photoperiodic regulation of growth-dormancy cycling through induction of multiple bud–shoot barriers preventing water transport into the winter buds of Norway spruce. *Frontiers in Plant Science*, 8 (2109).

Lepiniec, L. c., Babiychuk, E., Kushnir, S., Van Montagu, M. & Inze´, D. (1995). Characterization of an *Arabidopsis thaliana* cDNA homologue to animal poly(ADP-ribose) polymerase. *FEBS Letters*, 364 (2): 103-108.

Lind, O. C., Helen Oughton, D. & Salbu, B. (2018). The NMBU FIGARO low dose irradiation facility. *International Journal of Radiation Biology*: 1-6.

Love, M. I., Huber, W. & Anders, S. (2014). Moderated estimation of fold change and dispersion for RNA-seq data with DESeq2. *Genome biology*, 15 (12): 550-550.

McIlwraith, M. J., Van Dyck, E., Masson, J.-Y., Stasiak, A. Z., Stasiak, A. & West, S. C. (2000). Reconstitution of the strand invasion step of double-strand break repair using human Rad51 Rad52 and RPA proteins11. *Journal of Molecular Biology*, 304 (2): 151-164.

Murashige, T. & Skoog, F. (1962). A revised medium for rapid growth and bio assays with tobacco tissue cultures. *Physiologia Plantarum*, 15 (3): 473-497.

Nystedt, B., Street, N. R., Wetterbom, A., Zuccolo, A., Lin, Y.-C., Scofield, D. G., Vezzi, F., Delhomme, N., Giacomello, S., Alexeyenko, A., et al. (2013). The Norway spruce genome sequence and conifer genome evolution. *Nature*, 497: 579.

Patro, R., Duggal, G., Love, M. I., Irizarry, R. A. & Kingsford, C. (2017). Salmon provides fast and bias-aware quantification of transcript expression. *Nature methods*, 14 (4): 417-419.

Pentreath, R. J., Lochard, J., Larsson, C.-M., Cool, D. A., Strand, P., Simmonds, J., Copplestone, D., Oughton, D. & Lazo, E. (2014). Protection of the Environment under Different Exposure Situations. *Ann ICRP.*, 43 (1): 1-58.

Preuss, S. B. & Britt, A. B. (2003). A DNA-damage-induced cell cycle checkpoint in *Arabidopsis*. *Genetics*, 164 (1): 323-334.

Reisz, J. A., Bansal, N., Qian, J., Zhao, W. & Furdui, C. M. (2014). Effects of ionizing radiation on biological molecules—mechanisms of damage and emerging methods of detection. *Antioxidants & Redox Signaling*, 21 (2): 260-292.

Rieger, K. E. & Chu, G. (2004). Portrait of transcriptional responses to ultraviolet and ionizing radiation in human cells. *Nucleic Acids Research*, 32 (16): 4786-4803.

Riha, K., Watson, J. M., Parkey, J. & Shippen, D. E. (2002). Telomere length deregulation and enhanced sensitivity to genotoxic stress in *Arabidopsis* mutants deficient in Ku70. *The EMBO Journal*, 21 (11): 2819.

Rodrigues, M. A., Bianchetti, R. E. & Freschi, L. (2014). Shedding light on ethylene metabolism in higher plants. 5 (665).

Sidler, C., Li, D., Kovalchuk, O. & Kovalchuk, I. (2015). Development-dependent expression of DNA repair genes and epigenetic regulators in *Arabidopsis* plants exposed to ionizing radiation. *Radiation Research*: 219-232.

Sinha, A. K., Jaggi, M., Raghuram, B. & Tuteja, N. (2011). Mitogen-activated protein kinase signaling in plants under abiotic stress. *Plant signaling & behavior*, 6 (2): 196-203.

Tam, S. M., Samipak, S., Britt, A. & Chetelat, R. T. (2009). Characterization and comparative sequence analysis of the DNA mismatch repair MSH2 and MSH7 genes from tomato. *Genetica*, 137 (3): 341-354.

UNSCEAR. (1996). Sources and effects of ionizing radiation. *United Nations Scientific Commitee on the Effects of Atomic Radiation*.

UNSCEAR. (2017). Sources, effects and risks of ionizing radiation. *United Nations Scientific Commitee on the Effects of Atomic Radiation*.

van de Walle, J., Horemans, N., Saenen, E., Van Hees, M., Wannijn, J., Nauts, R., van Gompel, A., Vangronsveld, J., Vandenhove, H. & Cuypers, A. (2016). Arabidopsis plants exposed to gamma radiation in two successive generations show a different oxidative stress response. *Journal of Environmental Radioactivity*, 165: 270-279.

Van Hoeck, A., Horemans, N., Nauts, R., Van Hees, M., Vandenhove, H. & Blust, R. (2017). *Lemna minor* plants chronically exposed to ionising radiation: RNA-seq analysis indicates a dose rate dependent shift from acclimation to survival strategies. *Plant Science*, 257: 84-95.

Vandenhove, H., Vanhoudt, N., Wannijn, J., Van Hees, M. & Cuypers, A. (2009). Effect of low-dose chronic gamma exposure on growth and oxidative stress related responses in *Arabidopsis thaliana*. *Radioprotection*, 44 (5): 487-491.

Vanhoudt, N., Horemans, N., Wannijn, J., Nauts, R., Van Hees, M. & Vandenhove, H. (2014). Primary stress responses in *Arabidopsis thaliana* exposed to gamma radiation. *Journal of Environmental Radioactivity*, 129: 1-6.

Verma, V., Ravindran, P. & Kumar, P. P. (2016). Plant hormone-mediated regulation of stress responses. *BMC Plant Biology*, 16 (1): 86.

West, C. E., Waterworth, W. M., Jiang, Q. & Bray, C. M. (2000). *Arabidopsis* DNA ligase IV is induced by γ-irradiation and interacts with an *Arabidopsis* homologue of the double strand break repair protein XRCC4. *The Plant Journal*, 24 (1): 67-78.

Yoshiyama, K., Conklin, P. A., Huefner, N. D. & Britt, A. B. (2009). Suppressor of gamma response 1 (SOG1) encodes a putative transcription factor governing multiple responses to DNA damage. *Proceedings of the National Academy of Sciences of the United States of America*, 106 (31): 12843-12848.

Yoshiyama, K. O., Kobayashi, J., Ogita, N., Ueda, M., Kimura, S., Maki, H. & Umeda, M. (2013a). ATM-mediated phosphorylation of SOG1 is essential for the DNA damage response in *Arabidopsis*. *EMBO Reports*, 14 (9): 817-822.

Yoshiyama, K. O., Sakaguchi, K. & Kimura, S. (2013b). DNA damage response in plants: Conserved and variable response compared to animals. *Biology*, 2 (4): 1338-1356.

Table and figure legends

Table 1. The gamma radiation dose rates and total doses applied in experiments with 48 h exposure of seedlings of Norway spruce day 7 and 8 after sowing, using a ^{60}Co source.

Table 2. DNA repair genes with significantly altered expression shown as log2 fold change (lfc) in seedlings of Norway spruce after 48 h of gamma irradiation day 7 and 8 after sowing as compared to unexposed control plants. Blue = downregulated, red = upregulated, black rectangles = significant difference ($p < 0.05$) from unexposed control. BER = base excision repair, NER = nucleotide excision repair, MMR = mismatch repair, HR = homologous repair, NHEJ = non-homologous end joining.

Table 3. Antioxidant genes with significantly altered expression shown as log2 fold change (lfc) in seedlings of Norway spruce after 48 h of gamma irradiation day 7 and 8 after sowing as compared to unexposed control plants. Blue = downregulated, red = upregulated, black rectangles = significant difference ($p < 0.05$) from unexposed control.

Table 4. Cell cycle genes with significantly altered expression shown as log2 fold change (lfc) in seedlings of Norway spruce after 48 h of gamma irradiation day 7 and 8 after sowing as compared to unexposed control plants. Blue = downregulated, red = upregulated, black rectangles = significant difference ($p < 0.05$) from unexposed control.

Figure 1. Effect of 48 h of gamma irradiation day 7 and 8 after sowing on seedlings of Norway spruce. A) Shoot (regression analysis value R^2: 0.92) and B) root length (R^2: 0.46). The results are mean ± SE of 28-37 plants per dose rate. C) Histology of shoot apical meristems. D) DNA damage analysed by the COMET assay (R^2: 0.91). The line in each box represents the mean of the median values for 3 repeated biological samples per dose rate (each consisting of 3 pooled plants) with 3 technical replicates (gels) for each sample. Totally 200 nuclei were scored per biological sample (60-70 nuclei per gel). Lower and upper box boundaries = 25 and 75% percentiles, error bars = 10

and 90% percentiles with data points outside these shown as dots. Different letters within each figure indicate significant difference ($p \leq 0.05$) based on analysis of variance followed by Tukey`s test.

Figure 2. Post-irradiation effects of 48 h of gamma irradiation day 7 and 8 after sowing on Norway spruce seedlings. A) Cumulative growth and B) shoot diameter and C) number of needles (Regression analyses (R^2) values in Table S1. The results are mean ± SE of 11-22 plants per dose rate. D) DNA damage (COMET assay; R^2: 0.71) at day 77 post-irradiation. The line in each box represents the mean of the median values for 3 repeated biological samples per dose rate (each consisting of 3 pooled plants) with 3 technical replicates (gels) for each sample. Totally 200 nuclei were scored per biological sample (60-70 nuclei pr. gel). Lower and upper box boundaries = 25 and 75% percentiles, error bars = 10 and 90% percentiles with data points outside these shown as dots. E) Phenotype day 77 post-irradiation. Different letters within each figure indicate significant difference ($p \leq 0.05$) based on analysis of variance followed by Tukey`s test (only the final time point analysed for growth data).

Figure 3. Differentially expressed genes (DEGs) in Norway spruce seedlings exposed to gamma radiation for 48 h day 7 and 8 after sowing. A) Number of DEGs for the different dose rates compared to the unexposed control (False discovery rate (FDR) <0.05). Up- and downregulation of genes are indicated as positive and negative values on the y-axis, respectively. The colour indicates the level of log2 fold change. B) Correlation of expression fold change values between pairs of dose rates, for the DEGs shared between the different dose rates. C) Venn diagram showing the number of DEGs and up- (red numbers) or down- (blue numbers) regulated genes that overlap between the different gamma dose rates.

Figure 4. Gene ontology (GO) enrichment analysis for biological processes between different gamma dose rates compared to the unexposed control in Norway spruce seedlings exposed to gamma radiation for 48 h day 7 and 8 after sowing.

Figure 5 KEGG pathway analysis for different gamma dose rates compared to the unexposed control in Norway spruce seedlings exposed to gamma radiation for 48 h day 7 and 8 after sowing.

Supplementary materials

Table S1. Regression analysis (R^2) for post-irradiation effects on cumulative growth (day 59), shoot diameter and number of needles (both day 58) in Norway spruce seedlings following gamma irradiation for 48 h day 7 and 8 after sowing as compared to unexposed control plants.

Table S2. Differentially expressed genes in seedlings of Norway spruce after 48 h of gamma irradiation day 7 and 8 after sowing as compared to unexposed control plants. Genes related to a) phenolics (flavonoids, lignin) b) the proteasome, c) unfolded protein response (UPR), d) senescence e) epigenetics, protein modification, f) plant hormones, g) photosynthesis, h) embryogenesis.

Table S3. Gene expression (all predicted genes) in seedlings of Norway spruce after 48 h of gamma irradiation day 7 and 8 after sowing as compared to unexposed control plants. NA = not applied; when gene expression was too low to be tested (see DESeq2 documentation). In the log2 fold change (lfc) columns, red or blue colour denote higher or lower transcript levels than in the unexposed control. In the false discovery rate adjusted p-value (padj) columns, red letters denote significant difference (padj < 0.05) relative to the unexposed control.

Table 1.

Dose rate ($mGy\ h^{-1}$)	Dose rate interval ($mGy\ h^{-1}$)		Total dose (Gy) after 48 h exposure	Total dose interval (Gy) after 48 h exposure)	
	Minimum	Maximum		Minimum	Maximum
290	255	325	13.9	12.2	15.6
100	88	112	4.8	4.3	5.4
40	35	45	1.9	1.69	2.15
10	8,8	11,2	0.48	0.41	0.55
1	0,88	1,12	0.048	0.041	0.055
0	-	-	0	-	-

Table 2.

		Gamma dose rate (mGy h^{-1})					
Pathway	**geneID**	**G1.lfc**	**G10.lfc**	**G40.lfc**	**G100.lfc**	**At name**	**At description**
BER	MA_10436358g0010	-0,12	0,70	0,41	1,20	PARP1	Poly [ADP-ribose] polymerase 1
	MA_10260775g0010	0,12	1,12	1,63	2,15	PARP2	Poly [ADP-ribose] polymerase 2
	MA_10434805g0020	0,06	0,42	0,72	0,85	PCNA*	Proliferating cellular nuclear antigen 1
	MA_83835g0010	0,18	-0,37	0,11	-1,24	PCNA*	Proliferating cellular nuclear antigen 1
	MA_9716862g0010	0,00	0,61	0,71	0,98	FEN1	Flap endonuclease 1
	MA_9971131g0010	0,31	0,46	0,86	0,76	FEN1	Flap endonuclease 1
	MA_402253g0010	0,13	0,50	0,62	0,44	OGG1	8-oxoguanine-DNA glycosylase 1
	MA_202491g0010	-0,01	0,89	1,33	1,52	POLD4*	Polymerase delta 4
NER	MA_185929g0010	-0,13	0,08	0,17	0,44	RAD4	DNA repair protein RAD4
	MA_50946g0010	0,18	1,64	1,99	2,72	GR1	Protein gamma response 1
MMR	MA_10425989g0010	0,13	0,26	0,34	0,66	MLH1	DNA mismatch repair protein MLH1
	MA_10187354g0010	0,02	0,42	0,26	0,88	MLH3	MUTL protein homolog 3
	MA_59360g0010	0,23	0,11	0,49	0,59	MSH2	DNA mismatch repair protein MSH2
	MA_540053g0010	0,11	0,35	0,46	0,70	MSH3	DNA mismatch repair protein MSH3
	MA_199995g0010	0,40	0,12	1,18	0,98	MSH7	DNA mismatch repair protein MSH7
	MA_214705g0010	0,24	0,47	1,13	0,83	MSH7	DNA mismatch repair protein MSH7
HR	MA_10426539g0010	0,07	0,65	0,67	1,04	MRE11	DNA repair and meiosis protein (Mre11)
	MA_12220g0020	0,39	-0,42	0,62	-0,80	ATBARD1	Breast cancer associated ring 1
	MA_5849g0010	0,11	0,94	0,50	1,18	ATBARD1	Breast cancer associated ring 1
	MA_217423g0010	0,02	0,78	1,10	1,72	RPA1A	Replication protein A 70 kDa DNA-binding subunit A
	MA_10435430g0020	-0,03	0,20	0,75	1,04	XRCC3	DNA repair protein XRCC3 homolog
	MA_7323292g0010	0,80	0,82	0,91	1,00	XRCC2	homolog of X-ray repair cross complementing 2 (XRCC2)

	MA_50946g0010	0,18	1,64	1,99	2,72	GR1*	Protein gamma response 1
NHEJ	MA_159677g0010	0,31	0,44	0,87	0,85	KU80	ATP-dependent DNA helicase 2 subunit KU80
	MA_10426539g0010	0,07	0,65	0,67	1,04	MRE11	DNA repair and meiosis protein (Mre11)
	MA_10434317g0010	0,15	0,40	0,28	0,83	LIG4	DNA ligase 4

*POLD4 genes is involved in BER, NER, MMR and HR. PCNA gene is involved in NER and MMR. GR1 gene is involved in NER and HR

Table 3.

	Gamma dose rate (mGy h^{-1})					
geneID	**G1.lfc**	**G10.lfc**	**G40.lfc**	**G100.lfc**	**At name**	**At description**
MA_98008g0010	-0,11	0,61	0,75	1,06	SOG1*	Suppressor of gamma response 1
MA_9923120g0010	-0,45	-0,75	-1,07	-1,13	NA	Rhodanese/Cell cycle control phosphatase superfamily protein
MA_3364g0010	0,13	-0,15	-0,39	-0,68	NA	Rhodanese/Cell cycle control phosphatase superfamily protein
MA_10429701g0010	0,22	-0,19	-0,07	-0,68	CYCB1-1	Cyclin-B1-1
MA_84856g0010	0,28	-0,16	0,13	-0,54	CYCB1-2	Cyclin-B1-2
MA_10433093g0020	0,43	-0,35	1,02	-0,22	CYCB2-3	Cyclin-B2-3
MA_94639g0010	0,04	-0,31	-1,05	-1,49	CYCD1-1	Cyclin-D1-1
MA_8772g0010	-0,20	-0,17	-0,33	-0,43	CYCU2-1	Cyclin
MA_858g0010	0,21	1,28	2,11	2,38	WEE1	Wee1-like protein kinase
MA_6619g0010	0,13	-0,21	0,40	-0,65	CYCA1-1	Cyclin A1;1
MA_88982g0010	0,29	-0,35	0,77	-0,73	CYCA2-2	Cyclin-A2-2
MA_920994g0010	0,330128	-0,15995	0,879904	-0,17715	CDKB2-2	Cyclin-dependent kinase B2-2

*SOG1 is involved in DNA repair pathway

Table 4.

		Gamma dose rate (mGy h^{-1})					
Pathway	**geneID**	**G1.lfc**	**G10.lfc**	**G40.lfc**	**G100.lfc**	**At name**	**At description**
L-ascorbate peroxidase	MA_1920881g0010	0,14	0,17	0,30	0,56	APX3	L-ascorbate peroxidase 3
	MA_20242g0010	0,10	0,40	0,41	0,58	APX3	L-ascorbate peroxidase 3
Hydroxyacylglutathione hydrolase	MA_10428814g0010	0,11	0,41	0,50	0,54	GLX2-2	Hydroxyacylglutathione hydrolase cytoplasmic
Glutathione S-transferase	MA_137828g0010	-0,38	-0,02	-0,17	-0,96	GSTF10	Glutathione S-transferase F10
	MA_10145917g0010	0,47	0,21	0,28	0,43	GSTL2	Glutathione S-transferase L2, chloroplastic
	MA_10429044g0010	0,36	0,43	0,34	0,49	GSTL3	Glutathione S-transferase L3
	MA_55125g0010	-0,02	0,34	1,37	0,94	GSTL3	Glutathione S-transferase L3
	MA_8443026g0010	0,51	1,00	1,32	1,11	GSTU11	Glutathione S-transferase U11
	MA_10434037g0020	0,53	1,19	0,70	1,23	GSTU18	Glutathione S-transferase U18
	MA_406744g0010	-0,14	0,88	0,56	1,05	GSTU18	Glutathione S-transferase U18
	MA_8194534g0010	-0,42	0,67	0,40	0,93	GSTU18	Glutathione S-transferase U18
	MA_8315329g0010	1,02	1,35	1,13	1,61	GSTU18	Glutathione S-transferase U18
	MA_5806734g0010	0,78	0,64	1,48	0,69	GSTU23	Glutathione S-transferase U23
Peroxidase	MA_10431963g0010	0,01	-0,07	-0,20	-0,46	NA	Acid phosphatase/vanadium-dependent haloperoxidase-related protein
	MA_8841968g0010	0,09	-0,46	-0,79	-1,77	PER15	Peroxidase 15
	MA_412995g0010	0,07	0,80	0,57	1,03	PER3	Peroxidase
	MA_41416g0010	0,00	-0,88	-0,63	-0,94	PER3	Peroxidase
	MA_444g0010	0,73	0,94	0,53	0,94	PER3	Peroxidase
	MA_941794g0010	-0,44	-0,33	-1,13	-1,08	PER51	Peroxidase 51
	MA_9110627g0010	-0,09	0,42	-0,88	-1,18	PER51	Peroxidase 51
	MA_207021g0010	-0,31	-0,23	-0,78	-1,02	PER52	Peroxidase 52

MA_73697g0020	-0,58	-0,42	-0,45	-0,60	PER52	Peroxidase 52
MA_96757g0010	-0,22	1,03	0,11	1,10	PER52	Peroxidase 52
MA_10g0010	0,70	0,84	0,53	1,13	PER65	Peroxidase 65
MA_644225g0010	-0,68	-0,18	-0,15	-0,95	PER66	Peroxidase 66
MA_103352g0010	0,18	0,15	-0,32	-0,74	PER72	Peroxidase
MA_166754g0010	0,24	-0,32	-0,86	-1,61	PER72	Peroxidase
MA_195775g0010	0,30	-0,48	-0,76	-1,24	PER9	Peroxidase 9

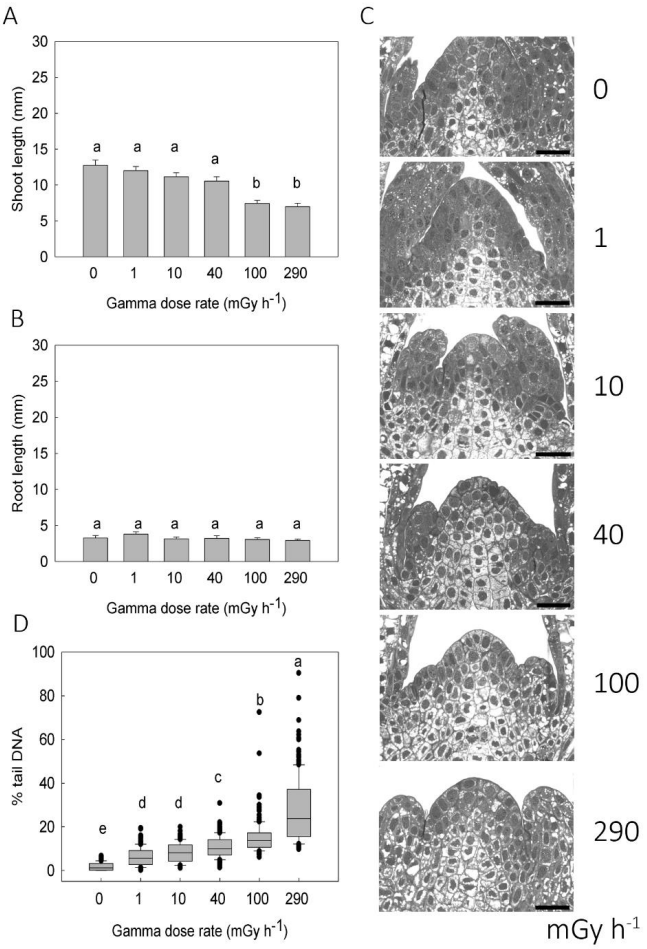
A
Shoot length (mm)
30
25
20
15
10
5
0
a a a a b b
0 1 10 40 100 290
Gamma dose rate (mGy h-1)
B
Root length (mm)
30
25
20
15
10
5
0
a a a a a a
0 1 10 40 100 290
Gamma dose rate (mGy h-1)
D
% tail DNA
100
80
60
40
20
0
e d d c b a
0 1 10 40 100 290
Gamma dose rate (mGy h-1)
C
0
1
10
40
100
290
mGy h-1

Figure 1.

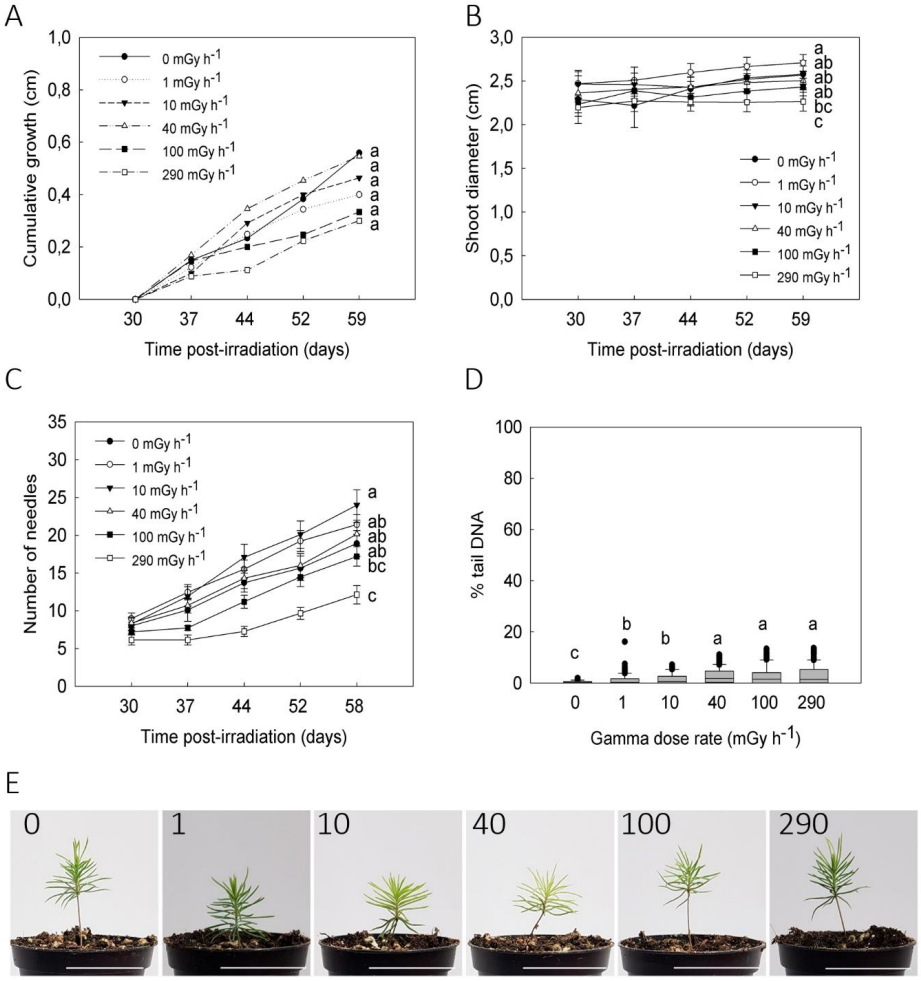
A
Cumulative growth (cm)
Time post-irradiation (days)
0 mGy h-1
1 mGy h-1
10 mGy h-1
40 mGy h-1
100 mGy h-1
290 mGy h-1
B
Shoot diameter (cm)
Time post-irradiation (days)
C
Number of needles
Time post-irradiation (days)
D
% tail DNA
Gamma dose rate (mGy h-1)
E
0
1
10
40
100
290

Figure 2.

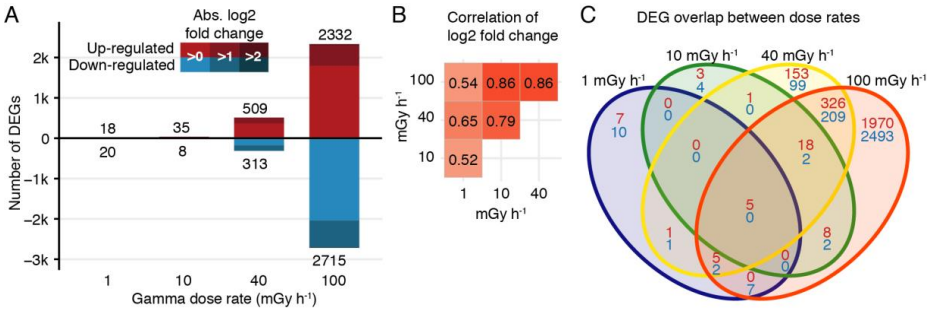
A
Abs. log2 fold change
Up-regulated
Down-regulated
>0
>1
>2
Number of DEGs
2k
1k
0
−1k
−2k
−3k
18
20
35
8
509
313
2332
2715
1
10
40
100
Gamma dose rate (mGy h⁻¹)
B
Correlation of log2 fold change
100
40
10
mGy h⁻¹
0.54
0.86
0.86
0.65
0.79
0.52
1
10
40
mGy h⁻¹
C
DEG overlap between dose rates
1 mGy h⁻¹
10 mGy h⁻¹
40 mGy h⁻¹
100 mGy h⁻¹
7
10
3
4
153
99
326
209
1970
2493
0
0
1
0
0
0
18
2
5
0
1
1
8
2
5
2
0
0
0
7

Figure 3.


Gamma dose rate (mGy h-1)
10
40
100
GO biological process (total genes) [GO ID]
positive regulation of flower development (29 genes) [GO:0009911]
respiratory burst involved in defense response (30 genes) [GO:0002679]
para−aminobenzoic acid metabolic process (27 genes) [GO:0046482]
response to arsenic−containing substance (14 genes) [GO:0046685]
mRNA polyadenylation (7 genes) [GO:0006378]
regulation of pollen tube growth (16 genes) [GO:0080092]
pollen tube guidance (7 genes) [GO:0010183]
regulation of nucleobase−containing compound metabolic process (668 genes) [GO:0019219]
sulfur compound metabolic process (337 genes) [GO:0006790]
cellular respiration (49 genes) [GO:0045333]
hyperosmotic response (95 genes) [GO:0006972]
response to temperature stimulus (401 genes) [GO:0009266]
ubiquitin−dependent protein catabolic process (168 genes) [GO:0006511]
purine ribonucleotide metabolic process (202 genes) [GO:0009150]
D−xylose metabolic process (19 genes) [GO:0042732]
proteasome−mediated ubiquitin−dependent protein catabolic process (66 genes) [GO:0043161]
glycolytic process (106 genes) [GO:0006096]
regulation of flavonoid biosynthetic process (40 genes) [GO:0009962]
gluconeogenesis (92 genes) [GO:0006094]
small GTPase mediated signal transduction (49 genes) [GO:0007264]
tricarboxylic acid cycle (20 genes) [GO:0006099]
response to misfolded protein (82 genes) [GO:0051788]
photorespiration (61 genes) [GO:0009853]
proteasome core complex assembly (64 genes) [GO:0080129]
fatty acid beta−oxidation (92 genes) [GO:0006635]
cell proliferation (113 genes) [GO:0008283]
double−strand break repair via homologous recombination (28 genes) [GO:0000724]
DNA replication (174 genes) [GO:0006260]
DNA endoreduplication (58 genes) [GO:0042023]
reciprocal meiotic recombination (64 genes) [GO:0007131]
mitochondrial electron transport, cytochrome c to oxygen (5 genes) [GO:0006123]
guanosine−containing compound metabolic process (5 genes) [GO:1901068]
response to gamma radiation (31 genes) [GO:0010332]
glyoxylate cycle (6 genes) [GO:0006097]
somatic cell DNA recombination (8 genes) [GO:0016444]
mitotic cell cycle (148 genes) [GO:0000278]
DNA methylation (67 genes) [GO:0006306]
DNA replication initiation (34 genes) [GO:0006270]
histone H3−K9 methylation (75 genes) [GO:0051567]
regulation of G2/M transition of mitotic cell cycle (23 genes) [GO:0010389]
anaphase (52 genes) [GO:0051322]
regulation of DNA replication (59 genes) [GO:0006275]
RNA methylation (62 genes) [GO:0001510]
translation (303 genes) [GO:0006412]
Gamma dose rate (mGy h-1)
40
100
GO biological process (total genes) [GO ID]
regulation of biological process (2085 genes) [GO:0050789]
very long−chain fatty acid metabolic process (35 genes) [GO:0000038]
suberin biosynthetic process (21 genes) [GO:0010345]
anthocyanin accumulation in tissues in response to UV light (53 genes) [GO:0043481]
very long−chain fatty acid biosynthetic process (20 genes) [GO:0042761]
response to ozone (18 genes) [GO:0010193]
cuticle development (12 genes) [GO:0042335]
starch catabolic process (20 genes) [GO:0005983]
cellular ion homeostasis (106 genes) [GO:0006873]
purine nucleobase transport (19 genes) [GO:0006863]
response to water (143 genes) [GO:0009415]
microsporocyte differentiation (7 genes) [GO:0010480]
regulation of meristem structural organization (15 genes) [GO:0009934]
metabolic process (5244 genes) [GO:0008152]
basipetal auxin transport (18 genes) [GO:0010540]
multicellular organism development (1611 genes) [GO:0007275]
acropetal auxin transport (15 genes) [GO:0010541]
auxin efflux (15 genes) [GO:0010315]
terpenoid biosynthetic process (99 genes) [GO:0016114]
multicellular organismal process (1741 genes) [GO:0032501]
regulation of protein dephosphorylation (38 genes) [GO:0035304]
ncRNA metabolic process (200 genes) [GO:0034660]
plastid transcription (40 genes) [GO:0042793]
photosynthesis (161 genes) [GO:0015979]
response to far red light (37 genes) [GO:0010218]
iron−sulfur cluster assembly (55 genes) [GO:0016226]
response to red light (41 genes) [GO:0010114]
positive regulation of transcription, DNA−templated (159 genes) [GO:0045893]
unsaturated fatty acid biosynthetic process (34 genes) [GO:0006636]
maltose metabolic process (84 genes) [GO:0000023]
carotenoid biosynthetic process (59 genes) [GO:0016117]
stomatal complex morphogenesis (85 genes) [GO:0010103]
photosynthetic electron transport in photosystem I (25 genes) [GO:0009773]
pentose−phosphate shunt (100 genes) [GO:0006098]
photosystem II assembly (63 genes) [GO:0010207]
chloroplast relocation (66 genes) [GO:0009902]
isopentenyl diphosphate biosynthetic process, methylerythritol 4−phosphate pathway (109 genes) [GO:0019288]
rRNA processing (120 genes) [GO:0006364]
chlorophyll biosynthetic process (57 genes) [GO:0015995]
thylakoid membrane organization (118 genes) [GO:0010027]
DEGs in pathway
Ratio
Enriched
Regulation
up
down
both

Figure 4.

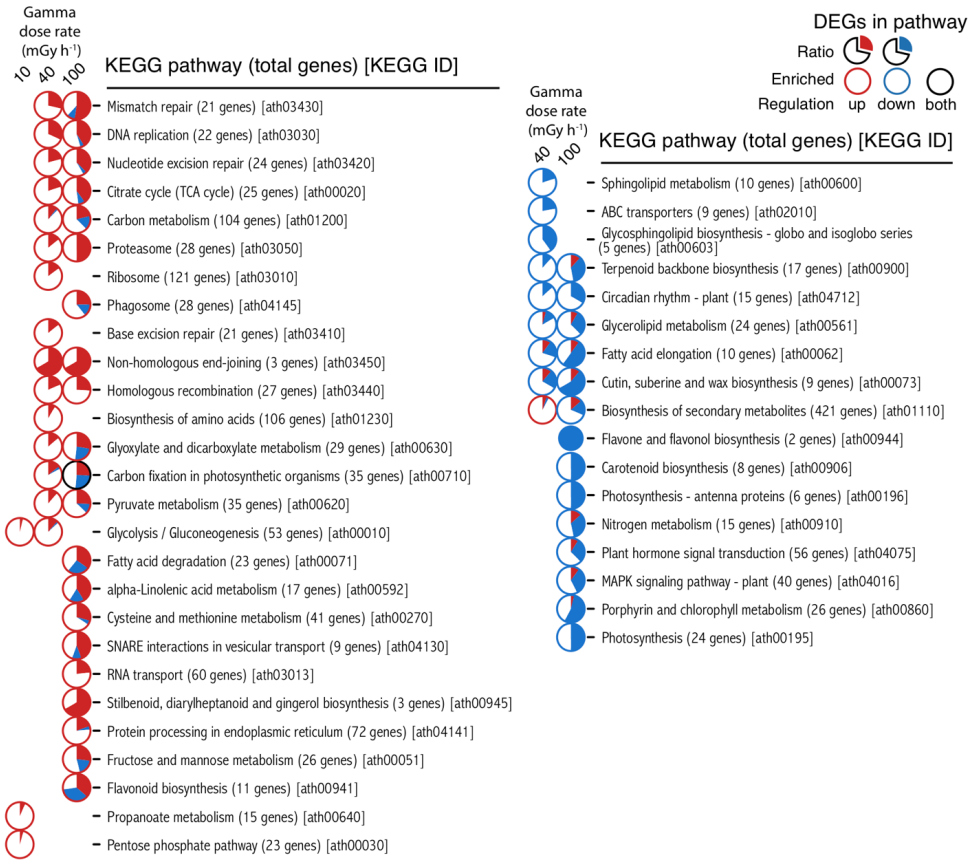
Gamma dose rate (mGy h-1)
10
40
100
KEGG pathway (total genes) [KEGG ID]
Mismatch repair (21 genes) [ath03430]
DNA replication (22 genes) [ath03030]
Nucleotide excision repair (24 genes) [ath03420]
Citrate cycle (TCA cycle) (25 genes) [ath00020]
Carbon metabolism (104 genes) [ath01200]
Proteasome (28 genes) [ath03050]
Ribosome (121 genes) [ath03010]
Phagosome (28 genes) [ath04145]
Base excision repair (21 genes) [ath03410]
Non-homologous end-joining (3 genes) [ath03450]
Homologous recombination (27 genes) [ath03440]
Biosynthesis of amino acids (106 genes) [ath01230]
Glyoxylate and dicarboxylate metabolism (29 genes) [ath00630]
Carbon fixation in photosynthetic organisms (35 genes) [ath00710]
Pyruvate metabolism (35 genes) [ath00620]
Glycolysis / Gluconeogenesis (53 genes) [ath00010]
Fatty acid degradation (23 genes) [ath00071]
alpha-Linolenic acid metabolism (17 genes) [ath00592]
Cysteine and methionine metabolism (41 genes) [ath00270]
SNARE interactions in vesicular transport (9 genes) [ath04130]
RNA transport (60 genes) [ath03013]
Stilbenoid, diarylheptanoid and gingerol biosynthesis (3 genes) [ath00945]
Protein processing in endoplasmic reticulum (72 genes) [ath04141]
Fructose and mannose metabolism (26 genes) [ath00051]
Flavonoid biosynthesis (11 genes) [ath00941]
Propanoate metabolism (15 genes) [ath00640]
Pentose phosphate pathway (23 genes) [ath00030]
DEGs in pathway
Ratio
Enriched
Regulation
up
down
both
Gamma dose rate (mGy h-1)
40
100
KEGG pathway (total genes) [KEGG ID]
Sphingolipid metabolism (10 genes) [ath00600]
ABC transporters (9 genes) [ath02010]
Glycosphingolipid biosynthesis - globo and isoglobo series (5 genes) [ath00603]
Terpenoid backbone biosynthesis (17 genes) [ath00900]
Circadian rhythm - plant (15 genes) [ath04712]
Glycerolipid metabolism (24 genes) [ath00561]
Fatty acid elongation (10 genes) [ath00062]
Cutin, suberine and wax biosynthesis (9 genes) [ath00073]
Biosynthesis of secondary metabolites (421 genes) [ath01110]
Flavone and flavonol biosynthesis (2 genes) [ath00944]
Carotenoid biosynthesis (8 genes) [ath00906]
Photosynthesis - antenna proteins (6 genes) [ath00196]
Nitrogen metabolism (15 genes) [ath00910]
Plant hormone signal transduction (56 genes) [ath04075]
MAPK signaling pathway - plant (40 genes) [ath04016]
Porphyrin and chlorophyll metabolism (26 genes) [ath00860]
Photosynthesis (24 genes) [ath00195]

Figure 5.

Table S1.

Parameter	Figure	Gamma dose rate (mGy h^{-1})/ R^2 value					
		0	**1**	**10**	**40**	**100**	**290**
Cumulative shoot elongation	2A	0.98	0.97	0.97	0.97	0.94	0.97
Shoot diameter	2B	0.85	0.98	0.60	0.99	0.63	0.40
Number of needles	2C	0.98	0.99	0.99	0.98	0.96	0.90

Table S2a. Phenolics

		Gamma dose rate (mGy h^{-1})					
Pathway	**geneID**	**G1.lfc**	**G10.lfc**	**G40.lfc**	**G100.lfc**	**At name**	**At description**
Phenylalanine ammonia lyase	MA_632036g0010	-0,78	-0,54	-0,59	-1,48	PAL4	Phenylalanine ammonia-lyase 4
	MA_954115g0010	0,27	-0,21	0,82	-0,09	NA	Chalcone-flavonone isomerase family protein
Chalcone synthase	MA_20764g0010	0,10	0,23	0,12	0,67	CHS	Chalcone synthase family protein
	MA_219828g0010	0,16	0,59	0,45	0,69	CHS	Chalcone synthase family protein
	MA_84838g0010	-0,23	-0,23	-0,63	-1,20	CHS	Chalcone synthase family protein
Lignin	MA_423264g0010	0,03	-0,07	-0,15	-0,58	CAD9	Probable cinnamyl alcohol dehydrogenase 9
	MA_10434090g0010	0,60	1,09	0,59	1,14	LAC12	Laccase-12
	MA_10434084g0010	-0,17	-0,36	-0,52	-0,68	LAC11	Laccase-11
	MA_28768g0010	-0,19	-0,47	-1,52	-2,57	LAC11	Laccase-11
	MA_10435226g0010	-0,80	-0,93	-0,81	-1,11	LAC5	Laccase-5
	MA_63042g0010	-0,20	0,74	0,45	1,09	LAC5	Laccase-5

Table S2b. Proteasome

	Gamma dose rate (mGy h^{-1})					
geneID	**G1.lfc**	**G10.lfc**	**G40.lfc**	**G100.lfc**	**At name**	**At description**
MA_10435598g0010	0,09	0,16	0,14	0,25	EMB2107	26S proteasome regulatory subunit, putative (RPN5)
MA_406151g0010	0,21	0,07	0,36	0,29	RPN6	26S proteasome non-ATPase regulatory subunit 11 homolog
MA_10428103g0010	0,11	0,18	0,22	0,36	RPN7	26S proteasome non-ATPase regulatory subunit 6 homolog
MA_14467g0010	0,31	0,35	0,57	0,49	RPN8A	26S proteasome non-ATPase regulatory subunit 7 homolog A
MA_2117g0010	0,19	0,35	0,42	0,49	RPN8A	26S proteasome non-ATPase regulatory subunit 7 homolog A
MA_38368g0010	0,19	0,10	0,32	0,52	RPN8B	26S proteasome non-ATPase regulatory subunit 7 homolog B
MA_10426728g0010	0,23	0,03	0,18	0,38	NA	Proteasome component (PCI) domain protein
MA_10426083g0010	0,28	0,10	0,26	0,51	RPN11	26S proteasome non-ATPase regulatory subunit 14 homolog
MA_10428869g0010	0,00	0,29	0,31	0,52	RPN11	26S proteasome non-ATPase regulatory subunit 14 homolog
MA_10426182g0010	0,16	0,09	0,27	0,37	RPN12A	REGULATORY PARTICLE NON-ATPASE 12A
MA_17736g0010	0,17	0,31	0,41	0,48	RPN12A	REGULATORY PARTICLE NON-ATPASE 12A
MA_6189g0010	0,11	0,20	0,30	0,36	RPN1A	26S proteasome non-ATPase regulatory subunit 2 homolog
MA_13350g0010	0,06	0,25	0,33	0,33	RPT3	REGULATORY PARTICLE TRIPLE-A ATPASE 3
MA_479907g0010	-0,28	-0,32	-0,76	-1,10	RPT3	Root phototropism protein 3
MA_90165g0010	-0,45	-0,11	-0,67	-0,94	RPT3	Root phototropism protein 3
MA_9950020g0020	-0,57	-0,19	-0,68	-1,27	RPT3	Root phototropism protein 3
MA_10434108g0010	0,08	0,31	0,45	0,79	NA	Probable proteasome inhibitor

Table S2c. UPR

	Gamma dose rate (mGy h^{-1})					
geneID	**G1.lfc**	**G10.lfc**	**G40.lfc**	**G100.lfc**	**At name**	**At description**
MA_10426928g0010	-0,01	0,69	0,72	0,86	HSP17.6	17.6 kDa class II heat shock protein
MA_128588g0010	0,40	0,29	0,93	1,17	HSP17.6	17.6 kDa class II heat shock protein
MA_104614g0010	0,41	0,36	1,07	1,02	HSP17.7	17.7 kDa class II heat shock protein
MA_103104g0010	0,06	0,50	0,63	1,04	HSP17.7	17.7 kDa class II heat shock protein
MA_7016698g0010	-0,21	0,43	0,45	0,85	HSP17.7	17.7 kDa class II heat shock protein
MA_106449g0010	0,12	0,26	0,36	0,56	HSP22.0	22.0 kDa heat shock protein
MA_15211g0010	-0,11	0,07	0,07	0,24	CAM7	Calmodulin 7
MA_10434871g0010	0,11	0,24	0,23	0,48	CAMTA2	Calmodulin-binding transcription activator 2
MA_139086g0010	-0,26	-0,09	-0,46	-0,58	CRT3	Calreticulin-3
MA_10433768g0010	0,02	-0,16	-0,17	-0,37	CNX2	COFACTOR OF NITRATE REDUCTASE AND XANTHINE DEHYDROGENASE 2
MA_10008335g0010	0,04	0,35	0,09	0,68	CNX3	Cyclic pyranopterin monophosphate synthase, mitochondrial
MA_107468g0010	0,03	0,16	0,25	0,58	NA	E3 ubiquitin-protein ligase
MA_135987g0010	-0,10	0,27	0,10	0,60	NA	E3 ubiquitin-protein ligase
MA_932090g0010	0,11	0,36	0,41	1,00	ATL6	E3 ubiquitin-protein ligase ATL6
MA_10428833g0020	-0,13	0,40	0,42	1,19	BAH1	E3 ubiquitin-protein ligase BAH1
MA_10425980g0010	-0,05	-0,30	-0,27	-0,38	HUB2	E3 ubiquitin-protein ligase BRE1-like 2
MA_65484g0010	0,12	-0,31	-0,20	-0,44	KEG	E3 ubiquitin-protein ligase KEG
MA_754688g0010	-0,56	-0,54	-0,66	-1,41	RHA2A	E3 ubiquitin-protein ligase RHA2A
MA_9308767g0010	0,21	0,34	0,39	0,50	UPL1	E3 ubiquitin-protein ligase UPL1

MA_10429426g0020	-0,32	-0,57	-0,66	-0,78	HSP90-1	Heat shock protein 90-1
MA_605776g0010	-0,13	0,49	0,52	0,83	HSP21	HEAT SHOCK PROTEIN 21
MA_10436974g0010	0,15	-0,44	-0,02	-0,95	HSP21	HEAT SHOCK PROTEIN 21
MA_10436974g0020	0,28	-0,37	-0,06	-1,04	HSP21	HEAT SHOCK PROTEIN 21
MA_10430708g0010	0,06	0,17	0,20	0,49	AMC4	Metacaspase-4
MA_162400g0010	-0,11	0,13	0,04	0,44	CNX7	Molybdopterin synthase sulfur carrier subunit
MA_10434284g0010	0,11	0,15	0,28	0,32	PDIL5-1	PDI-LIKE 5-1
MA_14427g0010	0,00	0,30	0,07	0,31	UBQ14	Polyubiquitin 14
MA_46617g0010	-0,45	0,87	1,27	1,43	UBQ14	Polyubiquitin 14
MA_93495g0010	-0,46	-0,39	-0,35	-0,49	UBQ10	Polyubiquitin 10
MA_54183g0010	-0,24	0,33	0,28	0,89	RF178	Probable E3 ubiquitin-protein ligase BAH1-like
MA_132866g0010	-0,08	-0,13	-0,22	-0,49	UBC16	Probable ubiquitin-conjugating enzyme E2 16
MA_194786g0010	0,11	0,12	0,46	0,46	UBC16	Probable ubiquitin-conjugating enzyme E2 16
MA_306852g0010	-0,23	0,62	0,38	0,91	UBC18	Probable ubiquitin-conjugating enzyme E2 18
MA_11973g0010	0,06	0,19	0,04	0,31	UBC24	Probable ubiquitin-conjugating enzyme E2 24
MA_16445g0010	-0,18	-0,03	-0,13	-0,29	PERK1	Proline-rich receptor-like protein kinase PERK1
MA_96038g0010	0,24	0,13	0,30	0,56	PDIL1-1	Protein disulfide isomerase-like 1-1
MA_40499g0010	0,07	0,42	0,37	0,69	PDIL1-2	Protein disulfide isomerase-like 1-2
MA_101402g0010	0,18	0,19	0,21	0,43	PDIL1-4	Protein disulfide-isomerase
MA_10211138g0010	0,20	0,32	0,26	0,54	VCL1	Protein VACUOLELESS1
MA_10426600g0010	0,11	0,13	0,30	0,41	XBAT31	Putative E3 ubiquitin-protein ligase XBAT31
MA_955355g0020	-0,06	0,06	-0,05	0,55	SKIP15	SKP1-interacting partner 15
MA_82940g0020	-0,03	0,35	0,21	0,43	SKP1A	SKP1-like protein 1A

MA_571079g0010	0,28	0,47	0,40	0,41	KEU	SNARE-interacting protein KEULE
MA_100977g0010	0,15	0,21	0,25	0,41	YKT61	SNARE-like superfamily protein
MA_10426927g0010	0,11	0,41	0,32	0,50	UBP14	Ubiquitin carboxyl-terminal hydrolase 14
MA_16290g0010	-0,28	-0,43	-0,52	-0,86	UBP18	Ubiquitin carboxyl-terminal hydrolase 18
MA_132593g0020	0,16	0,28	0,46	0,81	UBP23	Ubiquitin carboxyl-terminal hydrolase 23
MA_10437015g0010	0,03	0,25	0,22	0,45	UBP3	Ubiquitin carboxyl-terminal hydrolase 3
MA_96084g0010	0,23	0,33	0,16	0,81	UCH3	Ubiquitin carboxyl-terminal hydrolase 3
MA_102108g0010	0,09	-0,10	0,23	0,39	NA	Ubiquitin system component Cue protein
MA_9129425g0010	0,07	0,31	0,61	0,41	RPL40B	Ubiquitin-60S ribosomal protein L40-1
MA_10432468g0010	0,31	1,07	1,21	1,90	UBC15	Ubiquitin-conjugating enzyme 15
MA_10138732g0010	0,02	0,26	0,24	0,47	UBC36	Ubiquitin-conjugating enzyme 36
MA_1787g0020	-0,23	1,31	1,70	2,22	UBC37	Ubiquitin-conjugating enzyme 37
MA_194g0030	0,04	0,30	0,25	0,65	UBC11	Ubiquitin-conjugating enzyme E2 11
MA_65542g0010	0,12	0,11	0,06	0,45	NA	Ubiquitin-fold modifier 1
MA_10427922g0010	0,09	0,21	0,22	0,60	NA	Ubiquitin-like modifier-activating enzyme 5
MA_10431959g0010	0,26	0,20	0,43	0,42	NA	Ubiquitin-like modifier-activating enzyme 5
MA_10425939g0010	0,08	0,49	0,65	0,81	NA	Ubiquitin-like superfamily protein

Table S2d. Senescence

	Gamma dose rate (mGy h^{-1})					
geneID	**G1.lfc**	**G10.lfc**	**G40.lfc**	**G100.lfc**	**At name**	**At description**
MA_10428194g0010	-0,02	-0,14	-0,19	-0,61	AAF	Senescence-associated protein AAF, chlorolplastic
MA_10434212g0010	-0,01	0,30	0,19	0,77	P85	Senescence/dehydration-associated protein At4g35985, chloroplastic
MA_10427262g0010	0,03	0,27	0,19	0,48	ACD11	Accelerated cell death 11
MA_952115g0010	0,49	0,48	0,72	0,68	ACD11	Accelerated cell death 11

Table S2e. Epigenetics

	Gamma dose rate (mGy h^{-1})					
geneID	**G1.lfc**	**G10.lfc**	**G40.lfc**	**G100.lfc**	**At name**	**At description**
MA_10436985g0010	0,25	0,19	0,41	0,54	DMT1	DNA (cytosine-5)-methyltransferase 1
MA_173651g0010	0,36	-0,01	0,82	-0,45	CMT3	DNA (cytosine-5)-methyltransferase CMT3
MA_5243726g0010	-0,33	-0,09	-0,44	-0,83	HIS1-3	HIS1-3
MA_16730g0010	0,25	0,35	0,93	0,52	ASF1B	Histone chaperone ASF1B
MA_102457g0010	0,11	-0,44	-0,17	-1,04	NA	Histone H1.1
MA_877599g0010	0,07	-0,29	-0,05	-1,28	HIS1-3	HISTONE H1-3
MA_6409g0010	-0,25	-0,24	-0,38	-0,47	HIS1-3	HISTONE H1-3
MA_5243726g0010	-0,33	-0,09	-0,44	-0,83	HIS1-3	HISTONE H1-3
MA_500183g0010	-0,18	-0,23	-0,23	-0,73	HIS1-3	HISTONE H1-3
MA_173054g0010	-0,07	-0,30	-0,13	-0,94	HIS1-3	HISTONE H1-3
MA_93628g0020	-0,21	-0,04	-0,43	-0,74	HTA7	Histone H2A
MA_9379473g0010	0,45	0,82	0,61	1,15	HTA5	Histone H2A
MA_323386g0010	0,44	0,93	0,91	1,24	H2AV	Histone H2A
MA_234535g0010	-0,36	0,38	0,25	0,94	NA	Histone H4
MA_116904g0010	-0,22	-0,12	-0,30	-0,44	NA	Histone H4
MA_12995g0010	-0,23	0,52	0,77	1,02	NA	Histone H4
MA_10435143g0020	-0,34	-0,09	-0,65	-1,19	EFS	Histone methyltransferases (H3-K4 specific);histone methyltransferases (H3-K36 specific)
MA_259842g0010	-0,03	0,17	0,21	0,41	NA	Histone superfamily protein
MA_219390g0010	0,14	0,70	0,38	1,19	NA	Histone superfamily protein

MA_10294952g0020	-1,14	-0,66	-1,66	-0,65	NA	Histone superfamily protein
MA_8946159g0010	-0,10	-0,43	-0,47	-0,74	MSI1	Histone-binding protein MSI1
MA_10434820g0010	0,40	-0,39	0,24	-0,87	MSI1	Histone-binding protein MSI1
MA_10432677g0010	0,14	-0,56	-0,14	-1,26	MSI1	Histone-binding protein MSI1
MA_116780g0010	0,06	0,58	0,40	0,58	SUVR4	Histone-lysine N-methyltransferase SUVR4
MA_10428226g0010	0,07	0,09	0,05	0,46	SUVR5	Histone-lysine N-methyltransferase SUVR5
MA_604033g0010	-0,13	0,24	0,35	0,66	SUVR5	Histone-lysine N-methyltransferase SUVR5
MA_839575g0010	0,14	0,48	0,63	0,91	SUVH4	Histone-lysine N-methyltransferase, H3 lysine-9 specific SUVH4
MA_10426818g0010	-0,09	-0,11	-0,36	-0,37	NA	Methyltransferase
MA_323386g0010	0,44	0,93	0,91	1,24	NA	Methyltransferase
MA_191819g0010	-0,58	-0,25	-0,48	-0,60	HTA2	Probable histone H2A.3
MA_7320190g0010	-0,07	0,18	0,04	0,35	HTA6	Probable histone H2A.7
MA_100568g0010	-0,01	0,10	0,15	0,34	NA	Probable methyltransferase PMT13
MA_9992039g0010	-0,13	-0,33	-0,74	-1,20	NA	Probable methyltransferase PMT17
MA_10430553g0010	0,13	0,10	0,15	0,26	ERD3	Probable methyltransferase PMT21
MA_304552g0020	0,09	0,28	0,08	0,63	NA	Probable methyltransferase PMT9
MA_10267018g0010	0,20	0,46	0,54	0,96	NA	Putative methyltransferase family protein
MA_10436213g0010	0,11	0,35	0,39	1,02	NA	S-adenosyl-L-methionine-dependent methyltransferases superfamily protein
MA_10437275g0010	-0,05	-0,32	-0,10	-0,50	NA	S-adenosyl-L-methionine-dependent methyltransferases superfamily protein
MA_10428312g0010	0,19	0,26	0,12	0,53	NA	S-adenosyl-L-methionine-dependent methyltransferases superfamily protein
MA_63056g0010	0,22	0,65	0,48	1,32	CCoAOMT1	S-adenosyl-L-methionine-dependent methyltransferases superfamily protein
MA_10429464g0010	0,05	0,15	0,25	0,43	TYW1	S-adenosyl-L-methionine-dependent tRNA 4-demethylwyosine synthase
MA_10427274g0010	0,34	0,22	0,39	0,54	HDA6	HISTONE DEACETYLASE 6

Table S2f. Hormones

		Gamma dose rate (mGy h^{-1})					
Pathway	**geneID**	**G1.lfc**	**G10.lfc**	**G40.lfc**	**G100.lfc**	**At name**	**At description**
Brassinosteroids	MA_6685g0010	0,04	-0,15	-0,13	-0,50	CYP90A1	CONSTITUTIVE PHOTOMORPHOGENIC DWARF
	MA_36763g0010	0,25	1,03	0,43	0,88	CYP734A1	PHYB ACTIVATION TAGGED SUPPRESSOR 1
	MA_65486g0010	-0,53	0,09	-0,51	-0,94	CYP734A1	PHYB ACTIVATION TAGGED SUPPRESSOR 1
Abscisic acid	MA_202815g0010	-0,33	-0,01	-0,65	-1,04	CYP707A3	Abscisic acid 8'-hydroxylase 3
	MA_43111g0010	-0,04	0,08	0,34	0,64	PYL4	Abscisic acid receptor PYL4
Auxin	MA_10431695g0010	-0,34	-0,46	-0,82	-1,35	ARF19	Auxin response factor 19
	MA_122218g0010	-0,26	-0,59	-0,80	-1,12	ARF19	Auxin response factor 19
	MA_85955g0010	-0,21	-0,20	-0,37	-0,65	ARF19	Auxin response factor 19
	MA_85955g0020	-0,07	-0,38	-0,49	-0,57	ARF19	Auxin response factor 19
	MA_10022392g0010	0,01	-0,44	-0,47	-0,52	ARF6	Auxin response factor 6
	MA_10121946g0020	0,01	-0,32	-0,44	-0,57	ARF6	Auxin response factor 6
	MA_103763g0010	-0,13	-0,15	-0,33	-0,48	ARF6	Auxin response factor 6
	MA_55076g0010	-0,02	-0,17	-0,18	-0,29	ARF6	Auxin response factor 6
	MA_73460g0010	-0,03	0,08	0,18	0,37	ARF6	Auxin response factor 6
	MA_10429195g0010	-0,04	-0,36	-0,18	-0,63	AUX1	Auxin transporter protein 1
	MA_10430843g0010	-0,58	-0,09	-0,51	-1,00	IAA14	Indole-3-acetic acid inducible 14
	MA_12760g0020	-0,37	-0,14	-0,56	-1,04	IAA16	Auxin-responsive protein IAA16
	MA_123046g0010	-0,27	-0,41	-0,67	-1,02	IAA26	Auxin-responsive protein IAA26
	MA_10431093g0030	-0,15	-0,24	-0,38	-0,89	IAA27	Auxin-responsive protein IAA27

	MA_53529g0010	-0,32	-0,36	-0,30	-0,67	IAA27	Auxin-responsive protein IAA27
	MA_203952g0010	-0,07	-0,12	-0,15	-0,45	IAA9	Auxin-responsive protein IAA9
	MA_38g0010	-0,06	-0,21	-0,12	-0,46	IAA9	Auxin-responsive protein IAA9
	MA_61553g0010	-0,31	-0,18	-0,35	-0,51	PIN3	Auxin efflux carrier component 3
	MA_100472g0010	-0,33	-0,48	-0,56	-0,75	PIN4	Auxin efflux carrier component
	MA_10431380g0010	0,04	-0,10	-0,09	-1,21	SAUR10	Protein SMALL AUXIN UP-REGULATED RNA 10
	MA_66756g0010	-0,02	0,12	0,00	-0,02	SAUR71	Auxin-responsive protein SAUR71
	MA_139427g0010	0,34	0,70	0,97	0,97	SAUR72	Auxin-responsive protein SAUR72
	MA_245557g0010	-0,01	0,40	0,08	0,63	SAUR76	Auxin-responsive protein SAUR76
Cytokinins	MA_17212g0010	-0,05	-0,09	-0,93	-1,15	ATCKX1	cytokinin oxidase/dehydrogenase 1
	MA_31778g0010	0,05	-0,14	-0,06	-0,22	CKX7	Cytokinin dehydrogenase 7
	MA_407719g0010	-0,36	-0,23	-0,35	-1,12	CYP735A2	Cytokinin hydroxylase
	MA_6136648g0010	1,01	0,16	0,77	0,86	CYP735A2	Cytokinin hydroxylase
	MA_10432368g0020	-0,14	-0,11	-0,19	-0,33	LOG8	Cytokinin riboside 5'-monophosphate phosphoribohydrolase
	MA_47673g0010	-0,11	-0,23	-0,30	-0,40	LOG8	Cytokinin riboside 5'-monophosphate phosphoribohydrolase
	MA_101803g0010	0,01	-0,23	-0,25	-0,44	AHK3	HISTIDINE KINASE 3
	MA_10430235g0010	-0,07	-0,89	-0,72	-1,21	AHK3	HISTIDINE KINASE 3
Ethylene	MA_5629699g0010	-0,43	-0,25	-0,46	-0,75	ERF016	Ethylene-responsive transcription factor ERF016
	MA_774017g0010	0,32	-0,48	0,21	-0,99	ERF016	Ethylene-responsive transcription factor ERF016
	MA_8384767g0010	0,11	-0,01	0,05	-0,62	ERF022	Ethylene-responsive transcription factor ERF022
	MA_446533g0010	0,04	0,10	-0,46	-1,10	ERF039	Ethylene-responsive transcription factor ERF039
	MA_121578g0010	-0,34	-0,14	-0,69	-0,95	ANT	AP2-like ethylene-responsive transcription factor ANT
	MA_132897g0010	-0,08	-0,10	-0,22	-0,35	EIL1	ETHYLENE INSENSITIVE 3-like 1 protein

	MA_65190g0010	-0,66	-0,54	-0,57	-1,10	RAP2-11	Ethylene-responsive transcription factor RAP2-11
	MA_10434312g0010	-0,18	-0,41	-0,40	-0,72	TOE3	AP2-like ethylene-responsive transcription factor TOE3
Gibberellins	MA_23745g0010	-0,11	-0,68	-0,37	-1,15	GASA11	Gibberellin-regulated protein 11
	MA_24001g0010	-0,15	-0,28	-0,18	-0,67	GASA5	Gibberellin-regulated protein 5
	MA_10086937g0010	-0,01	0,65	0,63	0,85	NA	Gibberellin-regulated protein 8
	MA_7575249g0010	-0,50	-0,33	-0,45	-0,82	NA	Gibberellin-regulated family protein
Jasmonate	MA_8668831g0010	-0,22	-0,32	-0,59	-1,01	JRG21	JASMONATE-INDUCED OXYGENASE3
Salicilic acid	MA_14282g0010	0,05	-0,05	-0,11	-0,14	NPR1	Regulatory protein NPR1

Table S2g. Photosynthesis

		Gamma dose rate (mGy h^{-1})					
Pathway	**Gene ID**	**G1.lfc**	**G10.lfc**	**G40.lfc**	**G100.lfc**	**At name**	**At description**
Photosystem I	MA_100910g0020	-0,37	-0,07	-0,49	-0,85	PsaG	Photosystem I reaction center subunit V, chloroplastic
	MA_16054g0010	-0,47	-0,24	-0,47	-0,72	PsaK	Photosystem I reaction center subunit psaK, chloroplastic
	MA_348255g0010	-0,37	-0,09	-0,36	-0,65	PsaN	Photosystem I reaction center subunit PSI-N, chloroplast, putative / PSI-N, putative (PSAN)
	MA_893g0010	-0,20	-0,09	-0,39	-0,73	PsaO	Photosystem I subunit O
Photosystem II	MA_3005g0010	-0,37	-0,07	-0,37	-0,55	PsbP1	Oxygen-evolving enhancer protein 2-1, chloroplastic
	MA_575444g0010	-0,23	-0,05	-0,23	-0,58	PsbS	Photosystem II 22 kDa protein, chloroplastic
	MA_10431532g0010	-0,34	-0,11	-0,33	-0,54	PsbW	Photosystem II reaction center W
	MA_18349g0010	-0,05	-0,01	-0,19	-0,49	Psb28	Photosystem II reaction center Psb28 protein
Cytochrome b6/f complex	MA_32523g0010	-0,22	0,09	-0,35	-0,54	PETC	Cytochrome b6-f complex iron-sulfur subunit, chloroplastic
	MA_733845g0010	-0,09	-0,10	-0,48	-0,67	PETC	Cytochrome b6-f complex iron-sulfur subunit, chloroplastic
Photosynthetic electron transport	MA_10427889g0020	-0,31	-0,12	-0,29	-0,60	PETE1	Plastocyanin 1
F-type ATPase	MA_10744g0010	-0,19	-0,16	-0,25	-0,67	ATPD	ATP SYNTHASE DELTA-SUBUNIT GENE
	MA_657g0010	-0,21	-0,01	-0,44	-0,84	ATPD	ATP SYNTHASE DELTA-SUBUNIT GENE
	MA_80944g0010	-0,25	-0,34	-0,36	-1,05	ATPD	ATP SYNTHASE DELTA-SUBUNIT GENE
RuBisCo	MA_184421g0020	0,19	-0,13	-0,15	-0,67	RAF1.1	Rubisco accumulation factor 1.1, chloroplastic

MA_10425789g0020	-0,09	-0,33	-0,29	-0,56	NA	Rubisco methyltransferase family protein
MA_482451g0010	-0,15	-0,05	-0,04	-0,51	NA	Rubisco methyltransferase family protein

Table S2h. Embryogenesis

	Gamma dose rate (mGy h^{-1})					
Gene ID	**G1.lfc**	**G10.lfc**	**G40.lfc**	**G100.lfc**	**At name**	**At description**
MA_137741g0010	0,34	0,30	0,42	0,82	emb1381	Embryo defective 1381
MA_77759g0010	-0,18	0,07	0,36	0,62	EMB514	Protein EMBRYO DEFECTIVE 514
MA_2116g0010	0,15	0,18	0,51	0,94	EMF1	Protein EMBRYONIC FLOWER 1
MA_10427267g0020	0,22	-0,32	-0,32	-0,59	EMF1	Protein EMBRYONIC FLOWER 1
MA_17597g0010	0,02	0,49	1,36	1,10	NA	Late embryogenesis abundant protein (LEA) family protein
MA_41035g0010	-0,11	0,49	1,10	1,07	NA	Late embryogenesis abundant protein (LEA) family protein
MA_9339426g0010	-0,57	0,05	0,65	1,21	UNE15	Late embryogenesis abundant protein (LEA) family protein
MA_5069103g0010	-0,13	-0,48	-0,45	-1,04	NA	Maternal effect embryo arrest protein
MA_97456g0010	-0,05	-0,45	-0,35	-0,83	NA	Maternal effect embryo arrest protein

ISBN: 978-82-575-1664-2
ISSN: 1894-6402

Norwegian University
of Life Sciences

Postboks 5003
NO-1432 Ås, Norway
+47 67 23 00 00
www.nmbu.no

105554 / ANDVORDGRAFISK.NO